Titre: Title:	Upstream geomineralurgical characterization of a sedimentary phosphate deposit for mine waste sustainable management and valorization purposes
Auteur: Author:	Safa Chlahbi
Date:	2024
Type:	Mémoire ou thèse / Dissertation or Thesis
Référence: Citation:	Chlahbi, S. (2024). Upstream geomineralurgical characterization of a sedimentary phosphate deposit for mine waste sustainable management and valorization purposes [Thèse de doctorat, Polytechnique Montréal]. PolyPublie. https://publications.polymtl.ca/59464/

URL de PolyPublie: PolyPublie URL:	https://publications.polymtl.ca/59464/
Directeurs de recherche: Advisors:	Tikou Belem, Abdellatif E. L. G. H. A. LI, & Mostafa Benzaazoua
Programme: Program:	Génie minéral

POLYTECHNIQUE MONTRÉAL

Affiliée à l'Université de Montréal

et

Université du Québec en Abitibi-Témiscamingue

MOHAMMED VI POLYTECHNIC UNIVERSITY

Upstream geomineralurgical characterization of a sedimentary phosphate deposit for mine waste sustainable management and valorization purposes

SAFA CHLAHBI

Département des génies civil, géologique et des mines

Polytechnique Montréal

et

Geology & sustainable mining institute

Mohammed VI Polytechnic University

Thèse en cotutelle présentée en vue de l'obtention du diplôme de *Philosophiae Doctor*

Génie minéral

Septembre 2024

POLYTECHNIQUE MONTRÉAL

Affiliée à l'Université de Montréal

et

Université du Québec en Abitibi-Témiscamingue

MOHAMMED VI POLYTECHNIC UNIVERSITY

Cette thèse intitulée:

Upstream geomineralurgical characterization of a sedimentary phosphate deposit for mine waste sustainable management and valorization purposes

Présentée par **Safa CHLAHBI**

en vue de l'obtention du diplôme de *Philosophiae Doctor*

a été dûment acceptée par le jury d'examen constitué de :

Azzouz KCHIKACH, président et membre
Tikou BELEM, membre et directeur de recherche
Abdellatif ELGHALI, membre et directeur de recherche
Mostafa BENZAAZOUA, membre et codirecteur de recherche
Lucie COUDERT, membre interne
Mariam EL ADNANI, membre externe
Mustapha MOUFLIH, membre externe
Rachid HAKKOU, membre examinateur

DEDICATION

To my parents Mohammed and Aicha,

To my husband Ayoub,

To my brother Oussama and my sisters: Najlae and Maryem,

To all my family and friends.

ACKNOWLEDGEMENTS

Alhamdulillah, praise Allah for helping me throughout my life, particularly during my thesis project. Without His guidance, this work would not have been possible. I want to express my gratitude to Allah for giving me the courage to step out of my comfort zone and the patience to overcome the numerous challenges I have faced on this remarkable journey.

I am extremely thankful for the efforts of the Geology and Sustainable Mining Institute **(GSMI-Mohammed VI Polytechnic University)** and the Research Institute on Mines and the Environment **(RIME-Université du Québec en Abitibi-Témiscamingue, Canada)** for the establishment of this jointly supervised Ph.D.

I would like to express my heartfelt gratitude to all the individuals I have encountered throughout my years of study, as they have played an instrumental role in supporting and assisting me on this educational journey. Foremost, I would like to extend my deepest appreciation to my thesis supervisors: **Abdellatif Elghali, Tikou Belem,** and **Mostafa Benzaazoua**, for granting me the invaluable opportunity to undertake this doctoral project under the optimal circumstances. Their unwavering guidance, profound scientific insights, unwavering commitment, constant availability, and unwavering support throughout the entirety of my thesis have been truly indispensable. I am fully aware that this work would not have come to fruition without their exceptional assistance. Their expertise and dedication have driven my academic success, and I am eternally grateful for their unwavering belief in my abilities. I extend my deepest gratitude to them for their unwavering support and guidance.

I would like to express my gratitude and acknowledgements for the funding support from the **OCP Group** (Benguerir mine) and the **experimental mine** in Morocco for their support in the framework of project RE04. I would like to extend my warmest thanks to **Nor eddine El Allam**, El **Houssine EL Mahfoudi**, **Essaid Zerouali**, **Saloua Belhabchia**, **Hanane El Korchi**, **Abdelmajid El Alami**, and **Hicham Aggadi** for their help and support during my thesis work.

The thesis is also teamwork! Thus, I would like to express my sincere gratitude to the **GSMI and RIME teams** for their unwavering support throughout my research. The laboratory work I conducted was made possible by the exceptional collaboration and assistance of the staff at both GSMI and RIME, and I am truly grateful for their contributions.

- **Team of GSMI-UM6P**: I would like to sincerely thank **Samia Rochdane** for her availability, suggestion, and coordination with the OCP group within the framework of the RE04 project. Additionally, I am deeply appreciative of **Otmane Raji** for the opportunity to visit the COX laboratory to carry out XRF core-scanning tests. Furthermore, I would like to express my gratitude to **Omar Inabi, Khalil Abdessamad, Elghorfi Mustapha, Jean Louis Bodinier, Abdelhadi Khaldoune, Yassine Taha**, **Rachid Hakkou**, **Youness Belmamouni, Ouabid Mahammed, Kissai Jamal** and **Soulaimani Saad** for their help and support during my thesis work. I would like also to express my grateful thanks to the GeoAnalytical Lab staff (**Bassou** and **Abdelmalek**) and Green Geomaterials Lab staff (**Elmahdi** and **Abdelhak**) for their support with materials testing the great help concerning the sampling, and the characterization. I would like to thank, **Fouzia, Ouafa Najat** and **Najib** for their administrative support.
- **Team of RIME-UQAT**: I would like to extend my warmest thanks to **Alain Perreault**, whose guidance and support were invaluable during my leaching tests (MLT). Additionally, I am deeply appreciative of **Melinda Gervais** for her assistance with my static tests (TCLP and SPLP). Furthermore, I would like to express my gratitude to **Akué-Sylvette Awoh, Roch Lamothe, Lilas Côté, Mathieu Villeneuve** and **Joël Beauregard** for their support and contributions to my research. Their dedication and involvement have been invaluable, and I am truly thankful for their assistance. Overall, the collaborative efforts of the entire RIME team have significantly enhanced the quality of my laboratory work, and I am indebted to each and every one of them for their valuable contributions, I should mention all your names. Many thanks.

I would like to express my thanks to the **public testing and study laboratory** for their invaluable collaboration and assistance in carrying out the core drilling. Additionally, I am immensely grateful to the **XPS laboratory** in Sudbury, Canada for their generous help in conducting the QEMSCAN analysis. Lastly, I would like to extend my sincere appreciation to **COX Analytical Systems** in Mölndal, Sweden for their invaluable assistance in conducting the XRF corescanning tests.

I would like to express my heartfelt gratitude to my friends **Aaron**, **Ahchech**, and **Nouhaila** for their invaluable assistance during the sample preparation phase. I would also like to extend my thanks to **Hssan Youssef Mehdaoui** and **Youssef Toubri** for their generous help in sending my samples for analysis. Moreover, I am deeply indebted to **Benjamin De Castro** for his extensive training on the optical microscope. Additionally, I would like to acknowledge the invaluable advice

and recommendations provided by **Yassine Ait Khouya**, **Nadia**, **Meriam** and **Yane**. Their insights and suggestions have significantly contributed to the refinement of my work.

Furthermore, I would like to express my gratitude to all my friends and colleagues who have supported me throughout my PhD thesis. Special mentions go to **Nezha, Wijdane, Oumaima, Abdessalem, Marie, Meryam, Noureddine, Khadija, Fatima, Hajar, Malak, Hicham, Cheikh, Redouane, Anas, Laila, Ricot, Mahya, Hajar, and Jamila**. Their encouragement, collaboration, and camaraderie have made this experience more fulfilling and enjoyable. To those I may have unintentionally omitted, my apologies, but please know that you are not forgotten in my thoughts.

I would like to express my heartfelt gratitude and give special thanks to my husband, **Ayoub Aqazddammou**, for his unwavering support, continuous encouragement, and immense effort in helping me make significant progress in my thesis work.

Finally, I would like to express my heartfelt gratitude to my incredible family who have been my pillars of strength throughout my thesis project. Their unwavering belief in me, constant support, and unconditional love have played an instrumental role in shaping the person I am today.

RÉSUMÉ

L'industrie minière au Maroc joue un rôle primordial dans l'économie du pays, notamment grâce à l'extraction de minéraux tels que le phosphate, l'argent, l'or, le zinc, le cuivre, le cobalt, la fluorite, et la barite. Toutefois, cette industrie génère d'importantes quantités de déchets miniers qui doivent être gérés efficacement. Les déchets miniers comprennent des matériaux tels que les résidus, les roches stériles, les boues, les eaux minières et les produits chimiques qui restent après l'extraction des minéraux. Ce projet de thèse se focalise sur l'industrie minière des phosphates, un secteur connu pour produire des quantités substantielles de stériles rocheux des phosphates (SRP). Ces stériles, sous-produits de l'extraction du phosphate, sont souvent mélangés et stockés en surface sous forme de grandes haldes de stériles, ce qui les rend difficiles à réhabiliter. Les stériles sont principalement des couvertures et des intercalaires, composés essentiellement de carbonates, d'argiles, de marnes et de silex.

L'objectif principal du présent travail est de s'orienter vers l'étude des SRP en amont de la chaîne minière dans la mine de Benguerir, au Maroc, afin de caractériser chaque lithologie séparément. Cette approche vise à fournir une compréhension détaillée et complète de la composition, des caractéristiques et des applications potentielles des stériles, facilitant ainsi l'identification des opportunités de réutilisation ou de valorisation efficace de ces sous-produits. En conséquence, trois objectifs spécifiques ont été définis : i) comprendre les propriétés géologiques et géomécaniques des SRP en vue de leurs potentielles applications dans le domaine génie civil ; ii) évaluer la géochimie et le comportement environnemental des SRP ; iii) adopter une approche intégrée de l'utilisation durable des SRP (p. ex. remblais routiers). Trois hypothèses ont été formulées dans cette thèse : i) la caractérisation géominéralurgique en amont permet d'explorer les possibilités de valorisation des SRP, ii) la réalisation d'une évaluation géo-environnementale complète en amont des SRP permet d'identifier les risques potentiels et d'explorer les possibilités de récupération des ressources, et iii) la proposition de lignes directrices pour la valorisation des SRP permettra de les transformer en ressources précieuses, contribuant ainsi à la gestion durable des déchets et à l'utilisation efficace des ressources.

Pour atteindre ces objectifs, l'approche méthodologique a débuté par une étude bibliographique approfondie qui a servi de base aux étapes suivantes. Cette première phase a été suivie par des missions sur le terrain portant sur le carottage et la collecte d'échantillons. Une stratégie

d'échantillonnage méticuleuse a été élaborée, combinant des méthodes aléatoires et ciblées afin de garantir un processus de collecte de données complet. Les échantillons prélevés ont ensuite fait l'objet de divers tests de caractérisation et d'analyses portant sur les aspects géologiques, géomécaniques, pétrographiques, minéralogiques, chimiques et environnementaux. Ces analyses ont permis d'obtenir une compréhension globale de la composition et des propriétés des intercalaires. L'intégration des paramètres géologiques (lithologie et épaisseur) dans un cadre de géomodélisation a permis d'estimer les volumes mais aussi de mettre en évidence la distribution du gisement. Enfin, cette approche méthodologique a permis de réaliser une analyse approfondie et multidimensionnelle essentielle à la prise de décision en matière de gestion des ressources et de conservation de l'environnement, en proposant des lignes directrices pour les voies de valorisation. Les résultats de chaque partie sont résumés dans ce qui suit.

Les résultats de la caractérisation géologique obtenus grâce aux descriptions lithologiques et à l'analyse structurale ont révélé la présence de neuf couches de phosphate et huit intercalaires, en plus de la découverture. En outre, quatre catégories de SRP ont été identifiées : carbonate, siliceuse, argile/marne et phosphate. L'évaluation géomécanique des échantillons de sols a montré un indice de plasticité (IP) moyen de 50% et une valeur de bleu de méthylène (VBM) de 7,1, les classant ainsi dans la classification A3-A4 qui correspond à des sols marneux plastiques et argileux. D'autre part, les échantillons de roche présentent des propriétés mécaniques remarquables, en particulier en termes de résistance à la compression uniaxiale (UCS), de la valeur d'abrasion de Los Angeles (LA) et de valeur de micro-Deval (MD). Notamment, les valeurs moyennes de résistance à la compression sont de 104 MPa pour le silex, 35 MPa pour le silex phosphaté, 32 MPa pour la silexite, 26 MPa pour le calcaire, 11 MPa pour le phosphate induré et 8 MPa pour le calcaire marneux.

Les résultats de l'évaluation géochimique et environnementale des SRP ont révélé une composition principalement constituée de calcite, de dolomite, d'apatite et de quartz, avec la présence de phases mineures supplémentaires telles que des minéraux argileux. D'un point de vue chimique, les SRP sont dominés par les principaux oxydes suivants : CaO et MgO, SiO_2 et P_2O_5. Les éléments traces présents dans les échantillons ont été classés en trois groupes distincts en fonction de leurs concentrations : un groupe comprenant Zn et Cr avec des concentrations supérieures à 150 ppm, un groupe contenant Ba, V, Ni, Zr, Y, U, Cu, Cd et Co avec des concentrations comprises entre 10 et 150 ppm, et un groupe d'éléments traces avec des concentrations relativement plus faibles (< 10

ppm), comprenant Rb, Pb, As, Mo, Se, Sc, Ga, Nb, Th, Hf, Sb, et Cs. Sur le plan environnemental, les résultats des tests de lixiviation ont indiqué que les lixiviats présentaient un pH neutre à alcalin de 6±0,6 à 9,1±0.3 pour tous les échantillons, ce qui indique un potentiel de neutralisation élevé de 38 à 991 kg $CaCO_3$/t. En outre, la libération des éléments majeurs (Ca, Mg, K, Si, Sr et P) et des éléments traces (As, Ba, Cd, Cr, Se et U) est restée dans les limites des normes internationales, à savoir la réglementation de l'Agence américaine pour la protection de l'environnement (USEPA) et la norme universelle de traitement (UTS) ; ce qui confirme la nature non dangereuse des stériles phosphatés. Par conséquent, les SRP étudié peuvent être considéré comme matière première naturelle viable convenant à diverses applications civiles.

L'étude de la valorisation potentielle des SRP, en particulier les lithologies d'argile marneuse et de calcaire marneux dans les remblais routiers, une étude à multiples facettes qui combine l'expérimentation, l'analyse de la stabilité et l'évaluation économique. Une caractérisation détaillée a révélé que les échantillons sont principalement composés de CaO, SiO_2 et MgO, avec des phases minérales dominantes comprenant du quartz, de la calcite, de la dolomite, de l'apatite et des minéraux argileux. Les évaluations environnementales ont classé les matériaux comme des déchets non dangereux, ouvrant ainsi la voie à leur utilisation en toute sécurité. L'analyse géotechnique a classé le calcaire marneux et l'argile marneuse comme appartenant à des catégories spécifiques, ce qui indique qu'ils conviennent comme matériaux de remblai durables. En outre, l'analyse de la stabilité a confirmé ce fait en déterminant que des remblais d'une hauteur maximale de 10 mètres utilisant de l'argile marneuse sont réalisables avec des facteurs de sécurité satisfaisants. Pour le calcaire marneux, un soutien supplémentaire, tel qu'un banc d'enrochement, peut permettre des remblais de hauteur similaire avec des marges de sécurité adéquates. En outre, une évaluation économique a souligné la rentabilité de l'utilisation des matériaux SRP dans un rayon de 28 km autour du site minier, ce qui en fait une alternative viable aux matériaux traditionnels pour les projets de construction.

Les résultats géomécaniques, géochimiques, minéralogiques et environnementaux ont révélé que les SRP présentent un potentiel important de réutilisation bénéfique. Les résultats suggèrent que les SRP peuvent être efficacement réutilisés dans des secteurs tels que le génie civil, l'industrie du ciment, la construction de routes, la récupération du phosphate résiduel et la neutralisation du drainage minier acide. Un guide structuré des voies de valorisation des SRP a été proposé, offrant un cadre structuré pour l'exploration des voies de valorisation potentielles des stériles phosphatés.

Le présent projet a permis de faire progresser les connaissances sur les déchets des mines de phosphate en amont et de mettre en évidence l'importance des pratiques durables et de l'optimisation des ressources dans diverses applications industrielles.

ABSTRACT

The mining industry in Morocco plays a crucial role in the country's economy, mainly through the extraction of minerals like phosphate, silver, gold, zinc, copper, cobalt, fluorite, barite, etc. However, this industry generates substantial quantities of mining waste that must be effectively managed. Mining waste includes materials such as tailings, rock, sludge, and mine water left over after the extraction of minerals. This thesis project focuses on the phosphate mining industry, a sector notorious for producing substantial amounts of phosphate waste rock (PWR). This waste rock, a byproduct of phosphate extraction, is often mixed and stored on the surface as large waste rock piles (WRPs), which makes it difficult to rehabilitate. The PWRs are mainly overburden and interburdens, primarily composed of carbonates, clays, marls, and flints.

The main aim of the present work is to provide a detailed and comprehensive understanding of the waste rock's composition, characteristics, and potential applications from phosphate exploitation, facilitating the identification of opportunities for effectively reusing or valorizing these by-products. Accordingly, three specified objectives were defined: i) understanding the geological and geomechanical properties of PWR given their potential civil applications, ii) assess the geochemistry and environmental behavior of PWR, and iii) Integrated approach to sustainable utilization of PWR in road embankments. Three hypotheses were drawn in the thesis: i) upstream geomineralurgical characterization allows exploring opportunities for PWR valorization, ii) conducted a comprehensive upstream geo-environmental assessment of PWR allows for the identification of potential hazards and exploration opportunities for resource recovery, and iii) proposing guidelines for the valorization of PWR will successfully convert it from a previously discarded by-product into a valuable resource, contributing to sustainable waste management and resource efficiency.

To achieve these objectives, the methodological approach began with an extensive bibliographic study that laid the foundation for subsequent steps. This initial phase was followed by field missions focused on core drilling and sample collection. The sampling strategy consisted of combining random and targeted methods to ensure a comprehensive data collection process. Various characterization tests and analyses were then conducted on the collected samples, encompassing geological, geomechanical, petrographic, mineralogical, chemical, and environmental aspects. These analyses provided a global understanding of the interburdens

composition and properties. The integration of the geological parameters (lithology and thickness) into a geomodeling framework allowed for volume estimations but also illuminated deposit distribution. Finally, this methodological approach ensured a thorough, multidimensional analysis essential for informed decision-making in resource management and environmental conservation by proposing guidelines for valorization pathways. The results of each part are summarized in the following.

The geological characterization results obtained through lithological descriptions and structural analysis have revealed the presence of nine phosphate layers in addition to the overburdens and eight interburdens in the studied area. Furthermore, four distinct types of PWR have been identified: carbonate, siliceous, marly clay, and phosphate. The geomechanical assessment of soil-like samples has shown an average plasticity index (PI) of 50% and a methylene blue value (MBV) of 7.1, thus categorizing them within the A3–A4 classification as plastic and clayey marl soils. On the other hand, the hard rock samples exhibit remarkable mechanical properties, particularly in terms of their uniaxial compressive strength (UCS), Los Angeles abrasion value (LA), and micro-Deval value (MD). Notably, the average compressive strength values stand at 104 MPa for flint, 35 MPa for phosphate flint, 32 MPa for silexite, 26 MPa for limestone, 11 MPa for indurated phosphate, and 8 MPa for marly limestone, showcasing the diverse mechanical characteristics of the rock formations present in the studied area.

The results of the geochemical and environmental assessment of PWR revealed a composition primarily comprised of calcite, dolomite, apatite, and quartz, with additional minor phases like clay minerals. Chemically, the PWRs are dominated by the following major oxides: CaO, MgO, SiO_2 and P_2O_5. Trace elements within the samples were categorized into three distinct groups based on their concentrations: a group including Zn, and Cr with concentrations exceeding 150 ppm, a group containing Ba, V, Ni, Zr, Y, U, Cu, Cd, and Co with concentrations ranging between 10 to 150 ppm, and a group of trace elements with relatively lower concentrations (< 10 ppm), including Rb, Pb, As, Mo, Se, Sc, Ga, Nb, Th, Hf, Sb, and Cs. Environmentally, the leachates exhibited a neutral to alkaline pH range of 6±0.6 to 9.1±0.3 across all samples, indicating a high neutralizing potential of 38 to 991 kg $CaCO_3$/t. Furthermore, the leaching test results indicated that the release of major (Ca, Mg, K, Si, Sr, and P) and trace (As, Ba, Cd, Cr, Se, and U) elements remained within international standard limits such as the United States Environmental Protection Agency (USEPA) regulations and the universal treatment standard (UTS); this is confirming the non-hazardous nature

of the PWR. Consequently, the studied PWR is a viable natural raw material suitable for various civil applications.

The investigation into the potential use of PWR, particularly marly clay and marly limestone lithologies in road embankments, is a multi-faceted study that combines experimentation, stability analysis, and economic evaluation. Detailed characterization revealed that the samples are primarily composed of CaO, SiO_2, and MgO, with dominant mineral phases including quartz, calcite, dolomite, apatite, and clay minerals. Environmental assessments categorized the materials as non-hazardous waste, paving the way for their safe utilization. Geotechnical analysis classified marly limestone and marly clay as belonging to specific categories, indicating their suitability as embankment materials. Furthermore, the stability analysis supported this by determining that embankments up to 10 meters in height using marly clay are feasible with satisfactory safety factors. For marly limestone, additional support, such as a rock-fill bench, can allow for embankments of similar height with adequate safety margins. Moreover, an economic evaluation underscored the cost-effectiveness of using PWR materials within a radius of 28 km from the mine site, making them a viable alternative to traditional materials for construction projects.

Through the geomechanical, geochemical, mineralogical, and environmental findings, it has been revealed that PWR holds significant potential for beneficial reuse. The findings suggest that PWR can be effectively repurposed in sectors like civil engineering, cement industry, road construction, phosphate recovery, and acid mine drainage neutralization. A structured guideline of the valorization pathways of PWR was proposed, offering a structured framework for exploring the potential valorization avenues of PWR. The present project progressed the knowledge of upstream characterization of phosphate mine waste and set up promising underscores the importance of sustainable practices and resource optimization in various industrial applications.

ملخص

تلعب صناعة التعدين في المغرب دورا أساسيا في اقتصاد البلاد، ويتجلى هذا من خلال استخراج عدة معادن مثل الفوسفات والفضة والذهب والزنك والنحاس والكوبالت والفلوريت والباريت، إلخ. ومع ذلك، فإن هذه الصناعة تخلف نفايات تعدين مهمة تستوجب إدارتها بفعالية. تشمل نفايات التعدين مواد مثل مخلفات المعامل والصخور والرواسب والمواد الكيميائية المتبقية بعد استخراج المعادن. يركز مشروع هذه الأطروحة على صناعة تعدين الفوسفات، وهو قطاع يتسم بإنتاج كميات كبيرة من صخور نفايات الفوسفات. وغالبًا ما يتم خلط هذه النفايات الصخرية، وهي منتج ثانوي لاستخراج الفوسفات، وتخزينها على السطح كأكوام كبيرة من نفايات الصخور، مما يجعل من الصعب إعادة تأهيلها. وتتكون صخور نفايات الفوسفات بشكل أساسي من غطاء ترابي وطبقات بينية، وتتكون بشكل أساسي من الكربونات والطين والمارل والصوان. ومع ذلك، تواجه صناعة الفوسفات تحديات بيئية متزايدة، بما في ذلك تلك المرتبطة بإدارة نفايات التعدين.

يتمثل الهدف الرئيسي من هذا البحث في التوجه نحو دراسة صخور نفايات الفوسفات في المراحل الأولى من سلسلة التعدين في منجم بن جرير بالمغرب لتوصيف كل صخور نفايات الفوسفات على حدة. يهدف هذا النهج إلى توفير فهم مفصل وشامل لتركيب صخور النفايات وخصائصها واستخداماتها المحتملة، مما يسهل تحديد فرص إعادة استخدام هذه النفايات أو تثمينها بشكل فعال. وبناءً على ذلك، تم تحديد ثلاثة أهداف محددة: '1' التوصيف الجيولوجي والجيوميكانيكي لصخور نفايات الفوسفات في ضوء تطبيقاتها المدنية المحتملة؛ '2' والتقييم الجيوكيمياء والبيئي لصخور نفايات الفوسفات؛ '3' إعادة الاستخدام المستدام لصخور نفايات الفوسفات (مثل سدود الطرق). ولتحقيق هذه الأهداف، استُهلّ النهج المنهجي بدراسة بليوغرافية موسعة أرست الأساس للخطوات اللاحقة. وأعقبت هذه المرحلة الأولية بعثات ميدانية ركزت على الحفر الجوفي وجمع العينات. ووضعت استراتيجية دقيقة لأخذ العينات، تجمع بين الطرق العشوائية والمستهدفة لضمان عملية شاملة لجمع البيانات. ثم أُجريت اختبارات وتحليلات توصيف مختلفة على العينات التي تم جمعها، شملت الجوانب الجيولوجية والجيوميكانيكية والبتروغرافية والمعدنية والكيميائية والبيئية. ووفرت هذه التحليلات فهماً شاملاً لتكوين الطبقات البينية وخصائصها. كما سمح دمج العوامل الجيولوجية (التركيب الصخري والسماكة) في إطار النمذجة الجيولوجية بتقدير الحجم، وقد سلط الضوء على توزيع الرواسب. أخيراً، ضمنت هذه المقاربة المنهجية تحليلاً شاملاً ومتعدد الأبعاد لاتخاذ قرارات سليمة في إدارة الموارد والحفاظ على البيئة من خلال اقتراح إرشادات لمسارات التثمين. وفيما يلي ملخص لنتائج كل جزء من الأجزاء.

كشفت نتائج التوصيف الجيولوجي التي تم الحصول عليها من خلال الأوصاف الصخرية والتحليل البنيوي عن وجود تسع طبقات فوسفاتية بالإضافة إلى الطبقات الترابية وثماني طبقات بينية في المنطقة المدروسة. بالإضافة إلى ذلك، تم تحديد أربعة أنواع متميزة من طبقات الفوسفات البينية: الكربونات والسيليسية والطين المارلي والفوسفات. وقد أظهر التقييم الجيوميكانيكي للعينات الشبيهة بالتربة أن متوسط مؤشر اللمرونة يبلغ 50% وقيمة الميثيلين الأزرق 7.1، وبالتالي تصنيفها ضمن التصنيف ٣أ-٤أ كتربة طينية بلاستيكية وطينية مارلية. ومن ناحية أخرى، تُظهر عينات الصخور الصلبة خواص ميكانيكية ملحوظة، خاصةً من حيث قوة الانضغاط أحادية المحور، وقيمة التآكل في لوس أنجلوس وقيمة الديفال الجزئي. وتجدر الإشارة إلى أن متوسط قيم قوة الانضغاط تبلغ 104 ميجا باسكال للصوان، و35 ميجا باسكال للصوان الفوسفاتي، و32 ميجا باسكال للسيلكسيت، و26 ميجا باسكال للحجر الجيري، و11 ميجا باسكال للفوسفات الصلب، و8 ميجا باسكال للحجر الجيري المارلي، مما يوضح الخصائص الميكانيكية المتنوعة للتكوينات الصخرية الموجودة في المنطقة المدروسة.

كشفت نتائج التقييم الجيوكيميائي والبيئي لصخور نفايات الفوسفات عن تركيبة تتكون في المقام الأول من الكالسيت والدولوميت والأباتيت والكوارتز، مع وجود معادن ثانوية إضافية مثل المعادن الطينية. ومن الناحية الكيميائية، تهيمن الأكاسيد الرئيسية التالية على صخور نفايات الفوسفات: أكسيد الكالسيوم وأكسيد المغنيسيوم، وثاني أكسيد السيليكون وخماسي أكسيد الفوسفاط. صُنّفت العناصر النادرة داخل العينات إلى ثلاث مجموعات متميزة بناءً على تركيزاتها: مجموعة تشمل الزنك والكروم بتركيزات تتجاوز 150 جزء من المليون، ومجموعة تحتوي على الباريوم الفاناديوم والنيكل والزركونيوم والأيتريوم واليورانيوم والنحاس والكادميوم والكوبالت بتركيزات تتراوح بين 10 إلى 150 جزء من المليون، ومجموعة من العناصر النادرة بتركيزات أقل نسبيًا (أقل من 10 جزء من المليون)، بما في ذلك الروبيوم و الرصاص و الأرسونيك و الموليبدينيت و السيلينيوم و السكانديوم و الغاليوم و النيوبيوم و الطوريوم و الهافنيوم و الأنطموان و السيزيوم. ومن الناحية البيئية، أظهرت المواد الناتجة عن عملية الرشح درجة حموضة متعادلة إلى قلوية تتراوح بين 6±0.6 إلى 9.3 في جميع العينات، مما يشير إلى قدرة عالية على المعادلة تتراوح بين 38 إلى 991 كجم من ثاني أكسيد الكربون/طن. وعلاوة على ذلك، أشارت نتائج اختبار الرشح إلى أن إطلاق العناصر الرئيسية (الكالسيوم والمغنيزيوم والبوتاسيوم والسيليكون والسرانسيوم والفوسفات) والعناصر النادرة (الأرسونيك، والباريوم، والكادميوم، والكروم، والسيلينيوم، واليورانيوم) ظلت ضمن الحدود القياسية الدولية (لوائح وكالة حماية

البيئة الأمريكية ومعيار المعالجة الشاملة)، مما يؤكد الطبيعة غير الخطرة لصخور نفايات الفوسفات. وبالتالي، فإن صخور الفوسفات المدروسة هي مادة خام طبيعية قابلة للتطبيق ومناسبة لمختلف التطبيقات المدنية.

إن دراسة إمكانية استخدام صخور نفايات الفوسفات، وخاصةً الطين المارلي والحجر الجيري المارلي في سدود الطرق، هي دراسة متعددة الجوانب تجمع بين التجريب وتحليل الاستقرار والتقييم الاقتصادي. كشف التوصيف التفصيلي أن العينات تتكون في المقام الأول من أكسيد الكالسيوم وثاني أكسيد السيليكون وأكسيد المغنيسيوم، مع وجود بعض المعادن بما في ذلك الكوارتز والكالسيت والدولوميت والأباتيت والمعادن الطينية. وصنفت التقييمات البيئية المواد على أنها نفايات غير خطرة، مما يمهد الطريق لاستخدامها الآمن. وصنف التحليل الجيوتقني الحجر الجيري المارلي والطين المارلي على أنهما ينتميان إلى فئات محددة، مما يشير إلى ملاءمتهما كمواد سدود مستدامة. وعلاوة على ذلك، دعم تحليل الثبات هذا الأمر من خلال تحديد أن السدود التي يصل ارتفاعها إلى 10 أمتار باستخدام الطين المارلي قابلة للاستخدام مع عوامل أمان مرضية. بالنسبة للحجر الجيري المارلي، يمكن أن يسمح الدعم الإضافي، مثل مقعد الحشو الصخري، بسدود بارتفاع مماثل مع هوامش أمان كافية. وعلاوة على ذلك، أكد تقييم اقتصادي على فعالية تكلفة استخدام صخور نفايات الفوسفات في دائرة نصف قطرها 28 كم من موقع المنجم، مما يجعلها بديلاً عملياً للمواد التقليدية لمشاريع البناء.

ومن خلال النتائج الجيوميكانيكية والجيوكيميائية والمعدنية والبيئية، تم الكشف عن أن هذا المعدن يتمتع على إمكانات كبيرة لإعادة الاستخدام المفيد. وتشير النتائج إلى أنه يمكن إعادة استخدامها بفعالية في قطاعات مثل الهندسة المدنية، وصناعة الأسمنت، وبناء الطرق، واستخلاص الفوسفات، وعمليات المعادلة. وقد تم اقتراح دليل إرشادي منظم لمسارات التثمين، مما يوفر إطارًا منظمًا لاستكشاف سبل التثمين المحتملة لصخور نفايات الفوسفات. وقد حقق المشروع الحالي تقدمًا في المعرفة بمخلفات مناجم الفوسفات في المراحل الأولى من عملية الاستخراج، كما أنه يؤكد على أهمية الممارسات المستدامة والاستخدام الأمثل للموارد في مختلف التطبيقات الصناعية.

TABLE OF CONTENTS

LIST OF TABLES

LIST OF FIGURES

LIST OF SYMBOLS AND ABBREVIATIONS

A3	Class code “Clays and marly clays, very plastic silts”
A3m	Subclass code of A3 “3 < IBI ≤ 10”
ABA	Acid-Base Accounting
AG	Analyse granulométrique
AMD	Acidic mine drainage
AP	Acid generation potential
BF	Bone fragment
BPL	Bone Phosphate Lime
c’	Effective cohesion or cohesive strength, in MPa
C0/SA	Interburden code
C3/C2	Interburden code
CAPEX	Capital expenditure
CBR	California bearing ratio
CD	Consolidated-drained
CE	Expansion coefficient
CG	Coated grain
CLR	Centered log ratio
Cop	Coprolite
D_{85}	The diameter for which the passing distribution is equal to 85 %, in mm
D.L	Detection limit
D_{max}	Maximal particle size, in mm
DE-XRT	Dual-energy X-ray transmission
DTM	Digital terrain model

Dol	Dolomite
EC	Electrical conductivity
EDS	Energy dispersive spectrometry
Eh	Redox potential
EPMA	Electron probe microanalysis
FR	Coefficient de fragmentabilité
FS	Fine sand
GDP	Gross domestic product
GRE	Guide for Road Earthworks
Gt	Gigatons (metric gigatons)
H	Height of embankment, in meter
HCl	Chloridric acid
IBI	Immediate Bearing Index
ICP-AES	Inductively Coupled Plasma-Atomic Emission Spectrometry
ICP-MS	Inductively coupled plasma- mass spectrometry
kg	Kilogram
km	Kilometer
km^2	Square kilometer
KMO	Kaiser-Meyer-Olkin
L	Width of surface layer
LA	Los Angeles Abrasion value
LC	Low content
LL	Liquid limit
LOI	Loss on ignition

LPEE	Laboratoire Public d'Essais et d'Études
m	Mètre (meter)
Ma	Million d'années
MAD	Moroccan dirhams
MBV	Methylene blue test value
MC	Medium content
MD	Micro-Deval abrasiveness value
MDCT	Million dry and commercial tons
MLT	Monolithic leaching test
Mm^3	Million cubic meters
mm	Millimètre/millimeter
MMDH	Milliards de dirhams marocains
MMSD	Mining, minerals, and sustainable development
MPa	Mégapascal
Mt	Million tons
MTSM	Millions de tonnes sèches et commerciales
NP	Neutralization potential
NNP	Net neutralization potential
NPAG	Non-potentially acid generating
OCP	Office Chérifien des Phosphates
OP	Other prices (implementation, extraction, loading…)
P	Peloids
Pu	Purchase of materials
P (m)	Depth

PAG	Potentially acid generating
PCA	Principal Component Analysis
PCSW	Phosphate coarse solids waste
PSD	Particle size distribution
PI	Plasticity index
PG	Phosphogypsum
PL	Plastic limit
PM	Profit margin
PPL	Plane Polarized Light
Ppm	Partie par million / part per million
PTE	Potentially toxic elements
PWR	Phosphate waste rocks
QAM	Quantitative automated mineralogical
QEMSCAN	Quantitative Evaluation of Minerals by SCANning electron microscope
Qtz	Quartz.
R33	Subclass code of R3 “Marly rock: low fragmentability, low degradable”
R	Radius of profitability
R^2	Coefficient de détermination
RIME	Research Institute on Mines and the Environment
Rc	Résistance à la compression, en MPa
REE	Rare earth elements
REG	Road earthwork guide
Rg	Ratio du gisement
RQD	Rock Quality Designation

SCM	Supplementary cement materials
SE	Sand equivalent
SF	Safety factor
Silic	Siliceous
SP	Sale price
SPLP	Synthetic Precipitation Leaching Procedure
SRP	Stériles rocheux de phosphate
t	Tonne
T	Cost of transport
TC	Total carbon
TE	Trace elements
TCLP	Toxicity Characteristic Leaching Procedure
TCR	Total Core Recovery
TS	Total sulfur
TSFs	Tailings storage facilities
TLM	Test de lixiviation en monolithe
UCS	Uniaxial compressive strength, in MPa
USEPA	United states environmental protection agency
UTS	Universal treatment standard
VLC	Very low content
w_{opn}	Proctor optimum moisture content
WDS	Wavelength-dispersive X-ray spectrometers
WR	Waste rock
WRP	Waste rock pile

XPL	Cross Polarized Light
XPS	Expert process solutions
φ'	Effective friction angle
α	Slope of the embankment
$\gamma_{d\text{-}max}$	Maximum dry density
3D	Trois dimensions

LIST OF APPENDICES

CHAPTER 1 INTRODUCTION

Mining activities have been an essential part of human civilization for centuries, providing essential minerals and resources for industries and communities worldwide. It is one of the most critical sectors in several countries' economies. In Morocco, this sector is essential in developing the national economy due to a favorable geological context, thus guaranteeing the diversity and abundance of mineral resources. Many minerals are exploited including phosphate, silver, gold, zinc, copper, cobalt, fluorite, and barite. The mining sector contributes 10% to Morocco's gross domestic product (GDP), with 90% coming from the phosphate industry in 2014 (Mehahad & Bounar, 2020). In 2019, total production reached 54.81 million tons (Mt), including 35.20 Mt of raw phosphate, 16.70 Mt of processed products (P_2O_5 and fertilizers), and 2.90 Mt for other mining products, with a turnover of 61.30 billion dirhams (MMDH) (Ministre de la Transition Energétique et du Développement Durable, 2021). Morocco has 70% of the world's phosphate reserves, with a reserve of 50 billion tons (USGS, 2021). It is the second-largest producer of phosphate rock after China (USGS, 2018). The OCP Group, created in 1920, formerly the Cherifian Phosphate Office, is responsible for the extraction, processing, valorization, and export of phosphate. Moroccan phosphates are sedimentary of marine origin and rich in biogenic elements (Boujo, 1976; Mouflih, 2015; Pufahl & Groat, 2017; Wadjinny, 1979). Phosphorus, for the fertilizer industry, is essential for modern agriculture to feed the world's population (Cissé & Mrabet, 2004). However, this industry is increasingly facing environmental challenges, including those linked to managing mining waste.

Mine waste is a byproduct of mining activities, which is generated during the extraction, beneficiation, and processing of ores and minerals. The geological material below the cut-off grade that is produced during mining operations is known as mine waste (Scoble et al., 2003). The type of generated waste depends on the mineral being extracted, the extraction method used, and the processing techniques employed. There are several types of mine waste, including tailings, waste rock, contaminated mine water, and sludge (Bian et al., 2010; Ledin & Pedersen, 1996). Tailings are the finely ground rock particles that are produced during mineral processing at the treatment plant. These tailings can contain harmful chemicals, which can contaminate surrounding water sources. Sludge is a byproduct of various mining processes. It is a semi-solid slurry composed of water, minerals, and residual chemicals. Sludge can be challenging to manage due to its high

moisture content and potential for containing toxic substances. Waste rock can be generated from various types of mining operations, including underground and open-pit mining, and can range in size from small stones to large blocks (Skierszkan et al., 2016). This rock can contain metals, which can leach into the surrounding soil and water.

The environmental impact of mine waste can be significant, causing soil and water pollution, habitat destruction, and health problems for humans and wildlife (Ukaogo et al., 2020). Therefore, it is crucial to manage and dispose of mine waste properly and implement measures to prevent contamination of the environment. On the other hand, mining activities have also provided economic benefits such as job creation and revenue generation for local communities. Therefore, managing mine waste is an environmental, social, and economic emergency within large companies today. It allows for preserving natural resources and liberating spaces dedicated to storing waste products. The valorization of industrial waste is an international challenge with economic and environmental interests.

The phosphate industry in Morocco generates significant quantities of waste (waste rock, sludge, and tailings). These mine wastes are generally stored on the surface in the form of waste rock piles or dumps for rocks or in the form of dams for sludge. In our case, we are interested in the mine waste rock. After open-air stripping operations, large quantities of waste rock are generated to access the phosphate layers. These phosphate waste rocks (PWR) are stored in piles on the surface and around the mines.

The management of waste rock is essential to minimize its impact on the environment. Proper management of waste rock includes measures such as engineering controls, monitoring, and remediation of altered areas. To mitigate the potential environmental risks associated with mine waste, mining companies must develop and implement effective waste management strategies, such as backfilling, reclamation, and proper storage and containment, to minimize the amount of waste rock and to prevent the release of harmful contaminants into the environment (Adiansyah et al., 2015; Krishna et al., 2020).

The main waste rock practices inside mining sites involve two key methods: cemented mine backfill and the construction of roads and dikes (Hakkou et al., 2016). These practices are implemented to effectively manage and handle the waste rock generated during mining operations. However, when it comes to the reuse of waste rock outside of mining sites, the opportunities remain

limited, as highlighted by Hakkou et al. (2016). It is worth noting that certain types of mine waste possess characteristics that make them suitable for various applications, such as civil engineering or ceramic manufacturing (Amrani et al., 2019; Bayoussef et al., 2021b; Hakkou et al., 2016; Segui et al., 2023; Taha et al., 2021). In particular, PWR holds potential as a secondary or alternative raw material, capable of supplying other industries like the civil engineering sector (Taha et al., 2021). By promoting the reuse of PWR in different industries, we can reduce waste generation, conserve natural resources, and foster sustainable practices. Previous studies have made significant strides in suggesting valorizing or reusing PWR as a secondary raw material. This proposal not only aims to conserve natural resources in the construction sector but also aims to reduce the environmental impact resulting from the disposal of such waste rock on the surface. While these studies have laid the groundwork for such initiatives, it is crucial to note that they have primarily focused on mixed waste rock.

In this research project, the focus shifts towards studying PWR upstream of the mining chain to characterize each PWR rock lithology separately. This targeted approach allows for a more nuanced understanding of the waste rock's composition, properties, and potential for reuse or valorization. By examining the waste rock from different lithologies individually, we can gain valuable insights into the specific challenges and opportunities associated with each type of waste rock. The specific objectives of this thesis are i) understanding the geological and geomechanical properties of PWR because of their potential civil applications, ii) assessing the geochemistry and environmental behavior of PWR, and iii) an integrated approach to sustainable utilization of PWR in road embankments. Three hypotheses were drawn in the thesis: i) upstream geomineralurgical characterization allows exploring opportunities for PWR valorization, ii) conducted a comprehensive upstream geo-environmental assessment of PWR allows for the identification of potential hazards and exploration opportunities for resource recovery, and iii) proposing guidelines for the valorization of PWR will successfully convert it from a previously discarded by-product into a valuable resource, contributing to sustainable waste management and resource efficiency. This research project holds great promise in contributing to sustainable practices within the mining industry and paving the way for more efficient utilization of PWR.

This thesis is presented in articles and is structured into eight chapters. This structure aims to provide a comprehensive overview of the research topic and present the findings in a logical and organized manner. The first two chapters, the introduction, and the literature review, set the stage

for the research by providing background information, outlining the research problem, and reviewing relevant literature. These chapters help the reader understand the context and significance of the research. The literature review chapter is structured into five sections. The first section provides a comprehensive overview of scientific knowledge and advances in the distribution, description, and characterization of phosphate deposits worldwide and in Morocco. The second section presents the study site (Benguerir mine, Morocco), its geographical, geological, stratigraphic, mining context, and mining methods. The third section describes the sedimentary rocks' petrographic, mineralogical, geochemical, and geomechanical properties. The fourth section focuses on the state-of-the-art of valorization pathways for PWR.

Chapter 3 presents the global methodology adopted in this thesis work, providing a comprehensive overview of the research process. Additionally, the raw materials, as well as the characterization techniques employed in this project, are explained, highlighting the tools and methods utilized to analyze and evaluate the materials under investigation.

The body of the thesis consists of three scientific articles, each corresponding to a specific chapter. This format allows for a more focused and in-depth analysis of the research findings. Each article presents the various results and scientific advances in the research field. Chapter 4 discusses the potential valorization of PWR. The study analyzes the geological and geomechanical properties of different PWR lithologies, including carbonate, siliceous, marly-clay, and phosphate, in view of their potential applications. The purpose of Chapter 5 is to evaluate the environmental behavior of PWR upstream of the extraction chain. To do this, various core drilling specimens and data from various lithologies and depths were collected to forecast the environmental profile and establish the mobility of the investigated chemical species. These samples were used for static leaching tests: toxicity characteristic leaching procedure (TCLP) and synthetic precipitation leaching procedure (SPLP), semi-dynamic test: monolithic leaching test (MLT), and chemical and mineralogical investigations. Finally, Chapter 6 assesses the possibilities for using specific lithologies (Marly limestone and Marly clayey) that were collected upstream of the mining chain as an alternative material for road embankment. The investigation has comprised evaluating their geotechnical and physical characteristics. The study also investigated the environmental effects of employing these materials, including the possibility of leaching, as well as chemical and mineralogical analysis.

The last two chapters of the thesis are dedicated to discussion, general conclusions, research recommendations, and prospects.

The following papers/communication have been published / in progress during this thesis project:

- **Papers**

Chlahbi, S., Belem, T., Elghali, A., Rochdane, S., Zerouali, E., Inabi, O., & Benzaazoua, M. **(2023)**. Geological and Geomechanical Characterization of Phosphate Mine Waste Rock in View of Their Potential Civil Applications: A Case Study of the Benguerir Mine Site, Morocco. Minerals, 13(10), 1291. https://www.mdpi.com/2075-163X/13/10/1291

Chlahbi, S., Benzaazoua, M., Elghali, A., Rochdane, S., Zerouali, E., Belem, T., **(2024)**. An upstream geo-environmental assessment of sedimentary phosphate waste rock. (Submitted to the Journal of Environmental Management on 20 May 2024).

Chlahbi, S., Elghali, A., Inabi O., Belem, T., Benzaazoua, M., **(2024)**. Integrated approach to sustainable utilization of phosphate waste rock in road embankments: experimental insights, stability analysis, and preliminary economic evaluation. Case Studies in Construction Materials 20 (2024) e03222. https://doi.org/10.1016/j.cscm.2024.e03222

- **Oral communications**

Chlahbi, S., Benzaazoua, M., Elghali, A., Belem, T. **(2023)**. Leaching tests for the assessment of the environmental behavior of phosphate waste rock. Euro-Mediterranean Conference for Environmental Integration (EMCEI), 02–05 October 2023, Rende (Cozenza), Italy.

Chlahbi, S., Benzaazoua, M., Elghali, A., Belem, T., **(2023)**. Assessment of the environmental behavior of phosphate waste rock: a case study of the Benguerir Mine Site, Morocco UM6P Interdisciplinary Doctoral Day, Université Mohammed VI Polytechnique, 25-27 September 2023, Benguerir, Morocco.

Chlahbi, S., Elghali, A., Benzaazoua, M., Belem, T. **(2022)**. Assessment of the environmental behavior of extraction waste rock: case study of the Benguerir Mine Site, Morocco. Mediterranean Geosciences Union (MedGU), 27–30 November 2022, Marrakech, Morocco.

- **Posters**

Chlahbi, S., Benzaazoua, M., Rochdane, S., Elghali, A., Belem, T., Zerouali, E. **(2021).** Geotechnical characterization of phosphate extraction waste rock for potential applications. Symposium Virtual sur les mines et l'environnement, Université du Québec en Abitibi-Témiscamingue (UQAT), 14-16 June 2021, Rouyn-Noranda, Canada.

Chlahbi, S., Benzaazoua, M., Rochdane, S., Elghali, A., Belem, T., Zerouali, E. **(2021).** Geological and geotechnical characterization of phosphate extraction waste rock for potential applications. UM6P Interdisciplinary Doctoral Day, Université Mohammed VI Polytechnique, 28 June 2021, Benguerir, Morocco.

Chlahbi, S., Benzaazoua, M., Rochdane, S. **(2020).** Valorization guide for phosphate extraction waste rock (Benguerir slabs and interlayers). UM6P Phosphate Days "Young Researchers Days: To Meet Technology Transfer Challenges ", Université Mohammed VI Polytechnique, 13-14 October 2020, Benguerir, Morocco.

CHAPTER 2 LITERATURE REVIEW

Phosphate generally refers to rock, mineral, or salt containing a sufficient concentration of phosphate minerals (phosphorus) (Jacob et al., 1990). Phosphate can be used directly or after enrichment to manufacture phosphate products (e.g., fertilizers and chemical products). There are three types of phosphate deposits in the world: sedimentary origin, igneous origin, and Guanos type deposits (Slansky, 1980). Among these, deposits of sedimentary origin hold the utmost importance due to their abundance and high P_2O_5 content, which often exceeds 28% (Slansky, 1980). These sedimentary deposits have been recognized as a reliable and substantial source of phosphate for various industrial applications.

2.1 Phosphate deposits in the world

Phosphate deposits are widely distributed across the globe's continents and the stratigraphic scale (Mouflih, 2015). The largest phosphate deposits are located in the South Tethyan phosphogenic province, which extends from North Africa to the Middle East over approximately 5500 km (El Bamiki, 2020a). These deposits represent more than 85% of the world's phosphate reserves (Jasinski, 2020). The oldest phosphate deposits in the stratigraphic scale are the Precambrian phosphates (Joosu et al., 2015). The spatial distribution and their abundance are summarized in Figure 2-1.

Currently, the regions with active phosphogenesis are located on the accidental borders of the continents, at tropical and subtropical latitudes, in the trade wind zone with generally desert to semi-arid climates: California, Peru, Chile, South-West Africa, Moroccan Sahara, Western Australia (Mouflih, 2015).

According to the United States Geological Survey (USGS, 2018), Morocco has 70% of the world's reserves. The OCP Group is responsible for its extraction, transformation, valorization, and export. Indeed, world reserves of phosphates are estimated at 70 billion tons, and it turns out that 50 billion tons are concentrated in Morocco, followed by 3.3 billion tons in China.

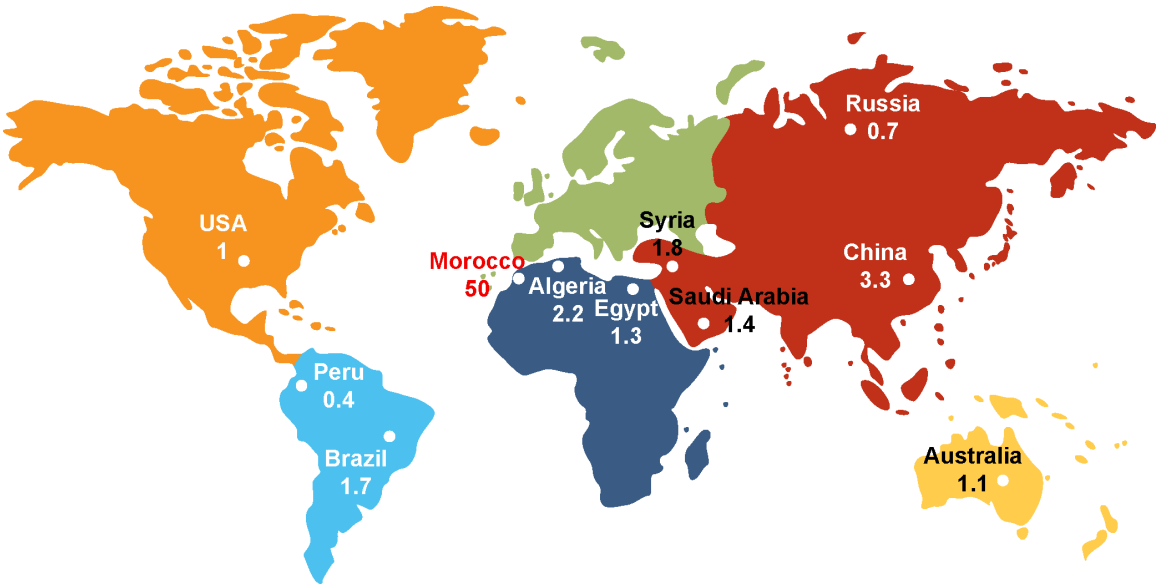

Figure 2-1: Situation of the main phosphate deposits in the world (reserves in billion tons) (USGS, 2018)

2.2 Phosphogenesis in sedimentary environment

Phosphogenesis is the set of physicochemical and/or biological processes leading to the formation of phosphate deposits. Phosphate formation is a multi-phase phenomenon transforming dissolved phosphorus molecules in seawater into phosphate accumulation (El Bamiki, 2020a). Phosphogenesis in sedimentary environments depends on several processes, particularly a sufficient source of phosphorus, favorable conditions for the formation of apatite in sediments, and favorable conditions to the concentration and accumulation of phosphate minerals (El Haddi, 2014). The possible sources of phosphorus can be subdivided into two: sources linked to the theory of direct supply from the continent and the other with supply from oceanic inputs (El Haddi, 2014).

Direct supply from the continent is explained by continental weathering, which releases phosphorus transported by rivers to the seas (Keyser & Cook, 1972; Peaver, 1966). An example is the Volga River in Russia, which discharges each year into the Caspian Sea 6000 tons of phosphorus in the form of phosphate mineral in solution and twice as much phosphorus in organic form (Slansky, 1980). The accumulation of such a contribution can give rise to a phosphate deposit in a few million years (Mouflih, 2015).

Supply from oceanic inputs is envisaged by a mechanism of supply of phosphate sedimentation from deep reserves (Mouflih, 2015); the average content of phosphate in solution in the oceans is

from 0.072 ±0.003 ppm (Armstrong, 1965). This content increases proportionally with depth up to 1000 m (Gulbrandsen, 1969 and Roberson, 1966 cited in El Haddi, 2014). This mechanism was first proposed by Kazakov (1937); its role is played essentially by ascending currents or "upwelling," the latter bringing up cold waters from the depths rich in dissolved phosphate towards the platforms (Mouflih, 2015). Several genetic models have been developed to explain the genesis of phosphates; the best known is the Kazakov (1937) model, which is a model of sedimentary environments in direct contact with the open sea and allows the spreading of ascending currents "upwellings". The scientific community adopted this model, but there was discussion and criticism regarding the mechanism of direct precipitation from seawater (El Bamiki, 2020a).

Upwellings ensure the redistribution of phosphorus from deep waters to surface waters in the phosphogenic zone (Pufahl & Groat, 2017). Biological productivity is manifested by phytoplankton and zooplankton, which can reduce the concentration of phosphorus and trigger the massive death of organisms and the settling of organic matter to which phosphorus is coupled (El Bamiki, 2020a).

2.3 Phosphate deposits in North Africa

2.3.1 Overview of Maghreb phosphate deposits

The Maghreb phosphate deposits (Northern Africa) were deposited during the Upper Cretaceous and the Eocene. They are natural deposits of sedimentary type linked to mountain ranges in Tunisia, Algeria, Sub-Saharan Africa, and Morocco (Zargouni, 1985). The Maghreb phosphate series is part of the South Tethyan phosphogenic province which ranges from the Middle East to northwest Africa (Notholt, 1985). The main Maghreb phosphate basins are in Tunisia, Algeria, and Morocco.

Tunisian phosphate deposits occupy the tenth position globally for phosphate production, with a capacity of 4.1 million tons in 2019 (USGS, 2021). The phosphate deposits in Tunisia are located in three Eocene basins: the Sra Ouertane Basin in the North, the Maknassy Basin in the East, and the Gafsa Basin in the South (Ettoumi, 2020). Currently, more than 90% of the phosphate rock produced in Tunisia is extracted from the Gafsa basin in the South (Abbes et al., 2020). In this basin, five production centers are active (Internal CPG report, cited in Ettoumi, 2020): Métlaoui Kef Schfaier, Métlaoui Kef Eddour, Moularès, Redeyef and M'Dhilla. The phosphates of the Gafsa

basin are essentially composed of cryptocrystalline phosphate minerals the most frequently encountered mineral is fluorapatite carbonate, also called francolite (Ettoumi, 2020).

Algeria's phosphate deposits are concentrated in the Djebel Onk district, part of the Tebessa region in northeastern Algeria on the border with Tunisia (Merchichi et al., 2021). It's has significant phosphate reserves estimated at 2.2 billion tons, ranked third in the world (USGS, 2018). The Djebel Onk district includes several deposits: Kef Es-Sennoun, Djemi Djema, North of Djbel Onk, Oued Betita, and Bled El Hadba (Merchichi et al., 2021). This district appears as a series of highly asymmetrical anticlines and synclines (Dassamiour, 2012) plunging 10° to 15° towards the south (Merchichi et al., 2021). The lithological composition of the Djebel Onk region comprises a succession of sedimentary layers around 500 m in thickness, deposited during the Upper Cretaceous (Maestrichtian) to Middle Eocene (Lutetian) (Kechiched et al., 2018). The phosphate series is covered by a continental sandy-clay series dating from the Miocene and Quaternary (Dassamiour, 2012). The average P_2O_5 content ranges from 25 to 27.9% (53.8 to 65.4% BPL (Bone Phosphate Lime)) (Bezzi et al., 2012; Merchichi et al., 2021).

2.3.2 Moroccan phosphate deposits

Morocco is renowned for its vast sedimentary phosphate deposits, making it the global leader in this valuable resource. With approximately 37 billion tons produced in 2020, Morocco is the second-largest phosphate producer worldwide (USGS, 2021). The phosphate found in Moroccan basins is primarily of the sedimentary type, formed during a geological period spanning from the terminal Cretaceous (Maastrichtian) to the middle Eocene (Lutetian) (Boujo, 1976). These basins are home to the most prominent phosphate deposits in the country, including the Ouled Abdoun, Gantour, Meskala, and Oued Eddahab basins (Figure 2-2). Each basin holds its unique characteristics in terms of surface area and phosphate content, contributing to the diversity of phosphate resources in Morocco. The abundance of sedimentary phosphate in Morocco has not only positioned the country as a global leader in production, but it has also made phosphate mining a significant sector in its economy, driving growth and development.

The Ouled Abdoun basin is the most important in Morocco in terms of phosphate reserves and content (Salvan, 1986 cited by El Bamiki, 2020a). The basin occupies an area of around 10,000 km^2. It is located 120 km southeast of the city of Casablanca, bordered to the north by the Massif Central and to the west by the Paleozoic Rehamna massif. The Ouled Abdoun basin corresponds

to a stable platform (El Haddi, 2014), and is recognized by the Khouribga site, which includes four extraction sites (Sidi Daoui, Merah Lahrach, Sidi Chennane and Beni Amir). Phosphates from Ouled Abdoun present various qualities, with high P_2O_5 contents of up to 80% in BPL.

The Meskala basin is located approximately 150 km south of Youssoufia, at the foot of the Atlas and 70 km southwest of the Western Jebilet. It includes 3 zones: Meskala, Chichaoua and Imi-n'Tanout zones. The phosphate series of the Meskala basin is very similar to the Gantour basin (El Haddi, 2014), the whole phosphate series is 110 to 140 m in thickness (Mouflih, 2015) and occurs in the form of synclinal troughs (El Bamiki, 2020a).

The Oued Eddahab basin is located in the Saharan provinces of Morocco, 100 km southeast of the city of Laâyoune. It is part of the Meso-Cenozoic basins which constitute the Atlantic edge of North Africa (El Bamiki, 2020a). It is between the Precambrian and the Paleozoic of the Rguibat ridge and the Atlantic Ocean (Mouflih, 2015). The phosphate series of the basin contains two layers rich in friable phosphate, often coprolitic, these layers are intercalated with non-phosphate layers of variable lithologies (El Bamiki, 2020a).

The Gantour basin extends over an area of around 1000 km², between the Rehamna massif to the north and the Jbilet massif to the south. The basin contains two mining sites: Youssoufia and Benguérir. The Gantour basin is part of the Western Meseta (Michard, 1976), essentially formed by phosphate layers of Meso-Cenozoic age. The stratigraphic series begins in the Maastrichtian and ends in the Lutetian (Boujo, 1976; Wadjinny, 1979).

The study area of this research project is part of the Gantour Basin (Benguerir mine), and the following section presents in detail the location, geology, stratigraphy, and mining framework of this mine, in addition to the composition and management of PWR.

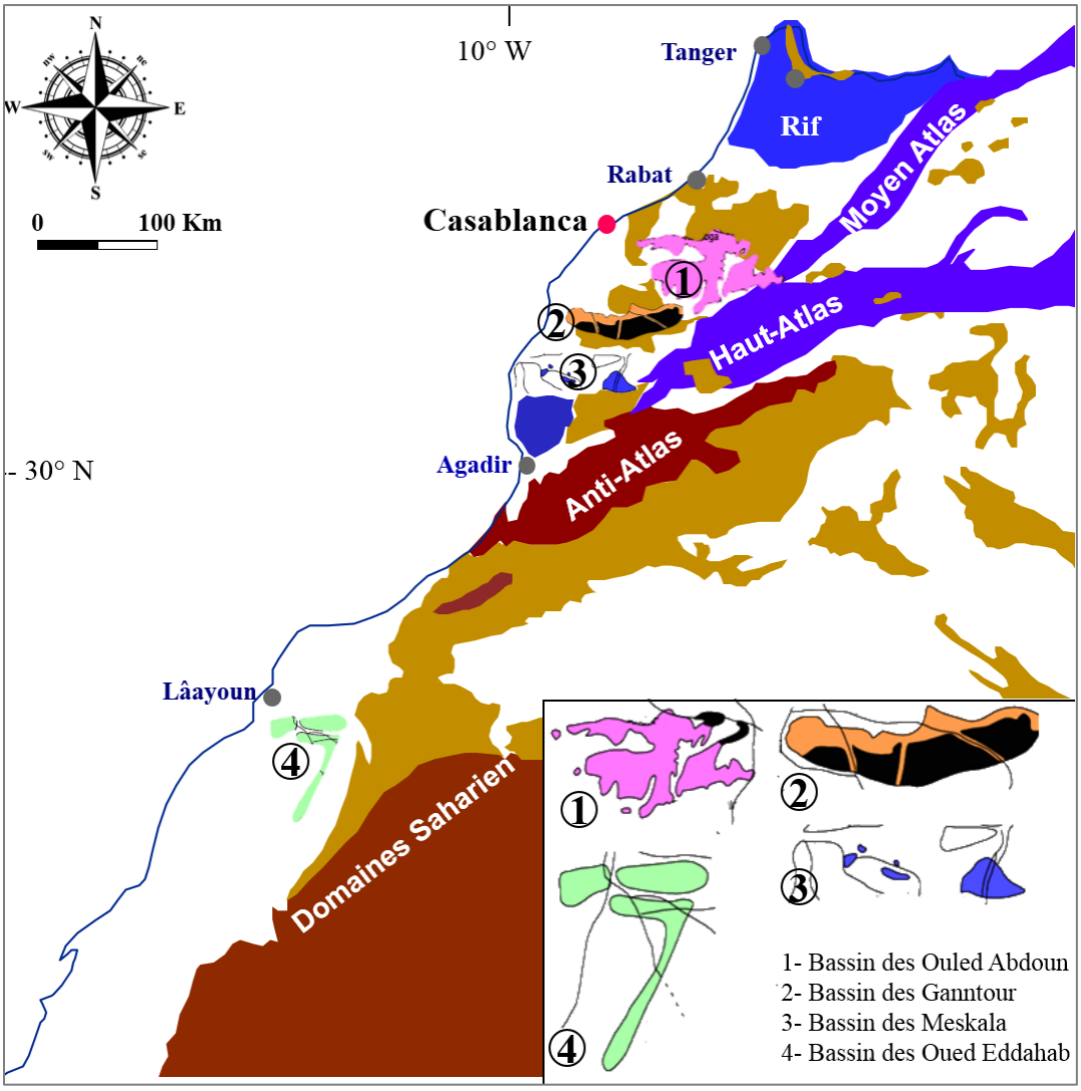

Figure 2-2: Phosphate basins of Morocco (El Haddi, 2014; Moody, 2002)

2.4 Benguerir mining site

2.4.1 Geographic and geological context

The Benguerir mining site is one of the parcels of the Gantour Basin, located 70 km north of Marrakech and 17 km east of Benguerir, at altitudes ranging from 396 to 596 m. It lies in the Western Meseta and is bounded by two well-defined Paleozoic massifs: the Rehamna massif to the north and the Jbilet massif to the south (Figure 2-3A-B).

The Benguerir deposit is sedimentary and contains several phosphate layers. In this deposit, the phosphate series are composed of phosphate and waste layers (overburden and interburdens). This

deposit is characterized by weak structures in the form of flexures and low-rejection faults affecting the phosphate series (Boujo, 1976).

Stratigraphically, the phosphate series extends from the Maastrichtian to the Lutetian (Boujo, 1976), resting in angular discordance on Paleozoic rocks (mica schists and granites) (Mouflih, 2015). The phosphate series is made up of alternating layers of soft to indurated phosphate and waste layers called interburdens, which are of varied lithological nature (e.g., clay minerals, marl, limestone, and flint). The whole is covered by a carbonate slab known as the "Thersites slab", topped by Quaternary alluvium (Boujo, 1976). The litho-stratigraphic section of the Benguerir mine and its characteristics are presented in Figure 2-3C and Table 2-1.

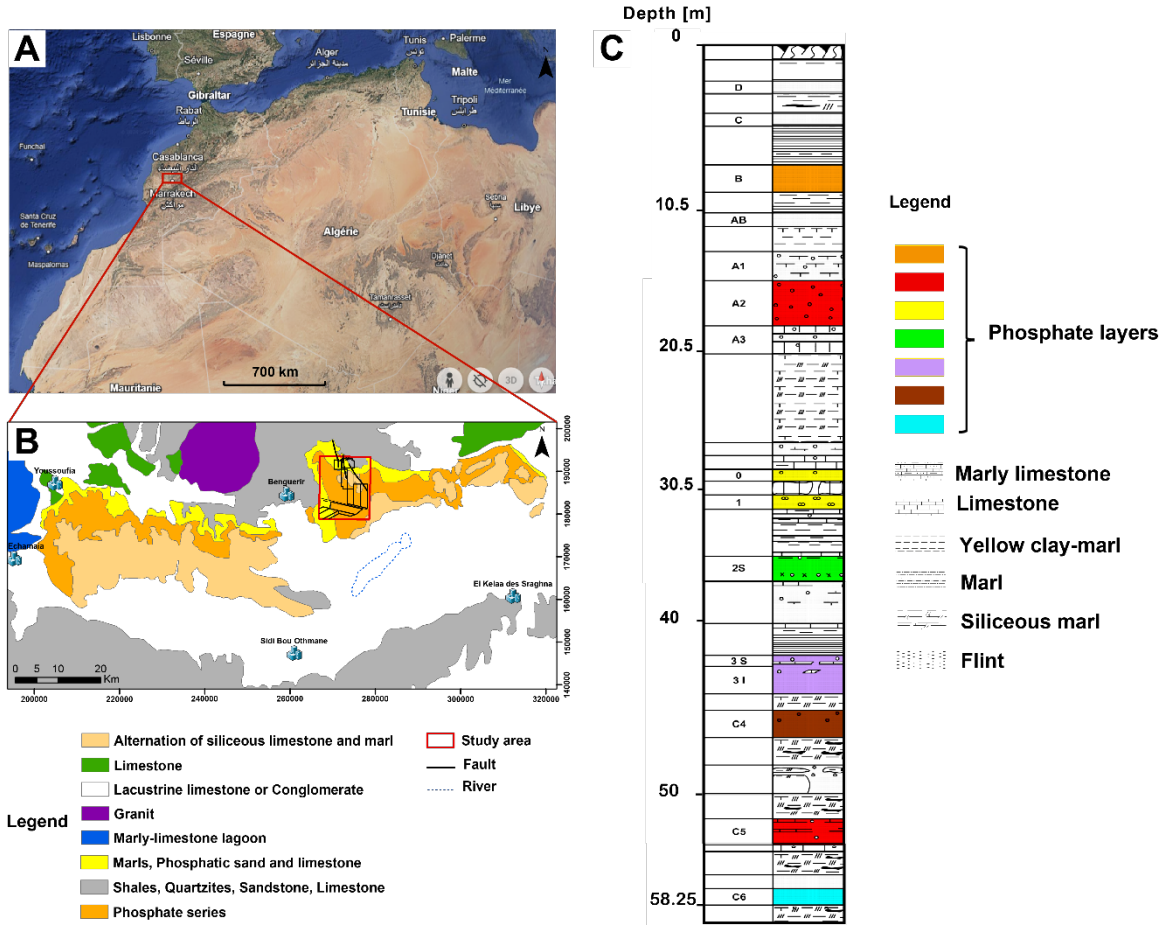

Figure 2-3: Location and stratigraphy of the study area: (A) General location of the Gantour basin study area in North Africa (Google Earth), (B) Simplified geological map of the Gantour basin (based on the 1:1,000,000 geological map of Morocco), (C) litho-stratigraphic section of the Benguerir mine (OCP Group).

Table 2-1: Characteristics of the Benguerir phosphate series (OCP)

Stage	Layers		Thickness (m)	BPL (%)	State
Lutetian	Overburden	Topsoil	0.4		Not extracted
		Thersites slab	1.8		
Ypresian		SD	0.6		
		Interburden	1.5		
		SC	0.8		
		Interburden	2.9		
	SB		0.9	66.4	Extracted
	Interburden AB/SB		1.6		Not extracted
	AB		0.8		
	Interburden SA/AB		1.9		
Thanetian	SA	A1	2.1		
		A2	3.4	57.8	Extracted
		A3	1.7		Not extracted
	Interburden C0/SA		10		
Danien	C0		0.8	61.2	Extracted
	C1/C0		0.3		
	C1		1.5	65.9	
Maastrichtian	Interburden C2/C1		3		Not extracted
	C2	$C2_{sup}$	1.7	64.8	Extracted
		$C2_{inf}$	2.2		Not extracted
	Interburden C3/C2		2.5		Not extracted
	C3	C3 sup	0.9	50.0	Extracted
		Couche 3 inf	0.7	67.8	
	Interburden C4/C3		1.2		Not extracted
	C4		1.44	63.8	Extracted
	Interburden C5/C4		4.6		Not extracted
	C5		2.7	59.6	Extracted
	Interburden C6/C5		3.4		Not extracted
	C6		0.6	66.3	Extracted

2.4.2 Benguerir mining context

The Benguerir mine started phosphate production in 1980, with a capacity of 3.7 million dry and commercial tons (MDCT) and reserves of 440 MDCT. Phosphates are produced in various grades: very low content (VLC) at 55% in BPL, low content (LC) at 58-60% in BPL, and medium content (MC) at 65% in BPL. The deposit comprises two zones: Benguerir Nord and Benguerir Sud, separated by regional road 206 linking the cities of Benguérir and Elkalaa des Sraghnas. The Benguerir mine is divided into panels: a piece of land or a portion of the deposit, limited according to factors such as the number of existing phosphate layers, recovery, and phosphate quality. Each panel is cut into trenches with an average width of 40 m. The trenches are subdivided into 100 m long blocks.

The Benguerir mine is an open pit mining operation, involving a series of mining operations to extract the phosphate rock. Operations are carried out using the strip-mining method, with trenches 40 m wide, and then cutting the trenches into 40 m × 100 m blocks (Idrissi et al., 2021). There are two mining techniques: the selective technique, which consists of extracting the phosphate layers and interlayers separately, and the overall technique, which consists in extracting the phosphate layers and interlayers as a group. In this method, drilling and blasting involve the entire phosphate layer. Both techniques have their advantages and disadvantages, as shown in Table 2-2.

Table 2-2: Selective and global techniques advantages and disadvantages

Technique	Advantages	Disadvantages
Selective	Preserving the grades of rich layers	Increasing the number of operations Difficulties of organization Low rate of equipment utilization Low equipment efficiency Increased costs
Overall	Improving the productivity Improving equipment efficiency Reducing the operation number	Mixing waste rock with phosphate during blasting

The mining operations of the Benguerir mine include drilling, blasting, stripping, loading and transport. Figure 2-4 summarizes the extraction stages at the Benguerir mine.

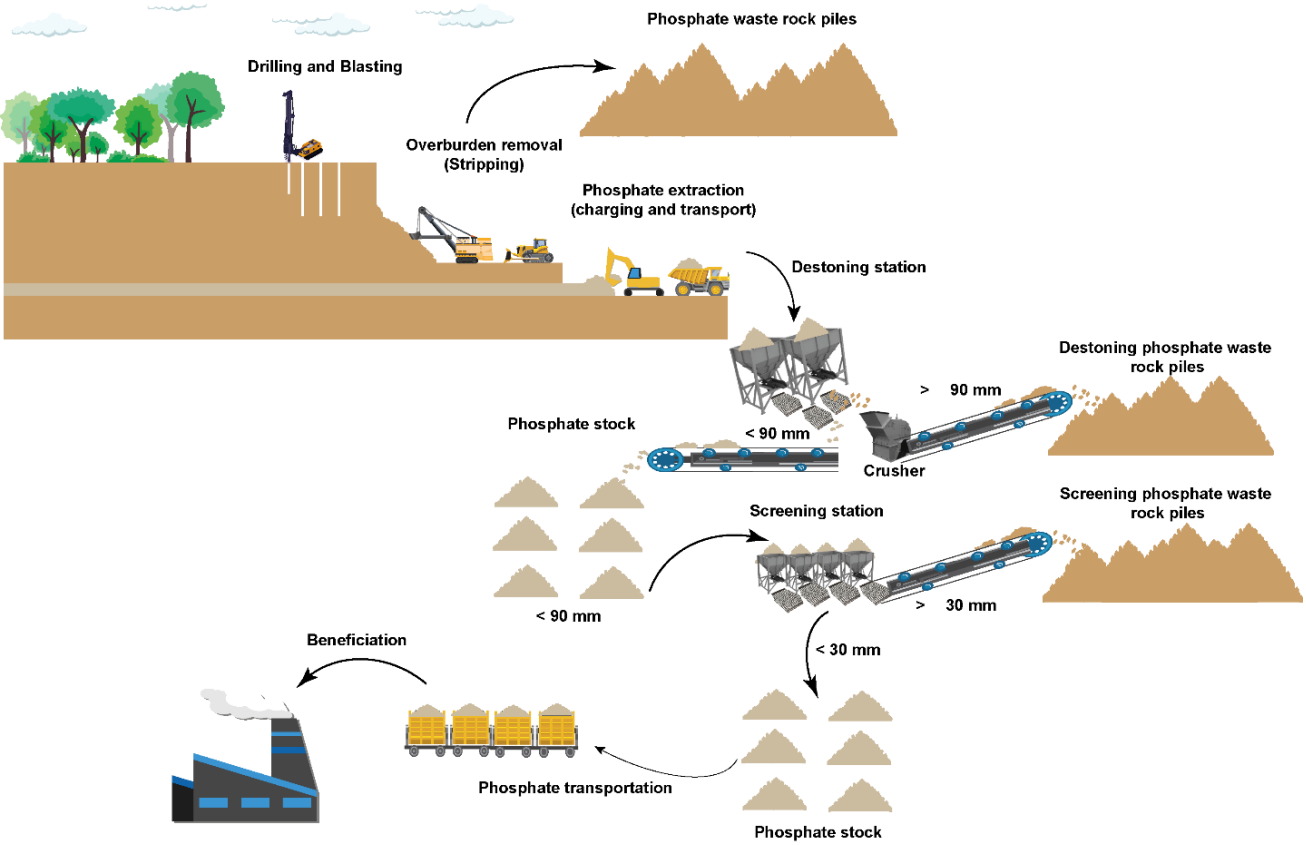

Figure 2-4: The mining operations at the Benguerir mine

Drilling involves the creation of vertical or inclined holes that span from the earth's surface to the valuable layers deep within. The drilling technique used is roto-percussion. The key factors that define drilling are the diameter and mesh of the holes. The mesh plays a crucial role in designing a drilling plan by considering the explosive charges for each hole. However, due to the diverse nature of the land, determining the optimal (load; mesh) combination required for effective fragmentation becomes challenging. This determination is achieved through a series of rigorous tests that account for factors such as rock hardness, explosive power, and the desired particle size.

Blasting is the operation aimed at fragmenting the ground, filling the holes drilled by the explosive (fuel nitrate), considering a firing pattern and a suitable loading mode. It essentially produces a particle size adapted to both the stripping machine, the loading machine, and the destoning station. After blasting comes the stripping step, which is the operation that consists of removing the waste

rock (overburden or interburden) to extract the phosphate layer. The main methods of stripping are pushing by Bulls D11, casement by dragline, and transport. This waste rock can be discharged into the previous trench already exploited or transported to a stock area. The selection of stripping techniques and machinery is contingent upon the geomorphological characteristics of the deposit. Once the waste rock is removed, the next step is to load and transport the phosphate from the construction site to the destoning and screening stations. This can be considered the final phase of operation.

Phosphate trucks discharge into two hoppers supplying two 90 x 90 mm stone crushers. Waste rock over 90 mm in size is evacuated to the destoning PWR after being crushed. The de-stoned phosphate is conveyed to a stockpile. It is then transported via conveyor links to the screening station (equipped with five 30 x 30 mm mesh screens). The waste rock is conveyed to the screening PWR piles, where it is re-screened. The screened product is conveyed to stockpiles for homogenization and the manufacture of phosphate qualities. Four qualities of phosphate are produced by the Benguerir mine: medium grade for the calcination plant, very low grade for the washing plant, standard low grade, and special low grade.

2.4.3 Phosphate waste rock composition and management

The estimated mass of waste rock stored in piles is 12.3 Mt (OCP Group, 2022). The origins and composition of this waste rock have been studied extensively in recent years to better understand its potential environmental impact and its potential applications. According to previous work (Idrissi et al. (2021); Safhi et al. (2022) and field missions carried out, the waste rock layers at the Benguerir mine are mainly composed of carbonate (limestone, dolomite), flint, clays, marl. Figure 2-5 shows pictures of some waste rock levels.

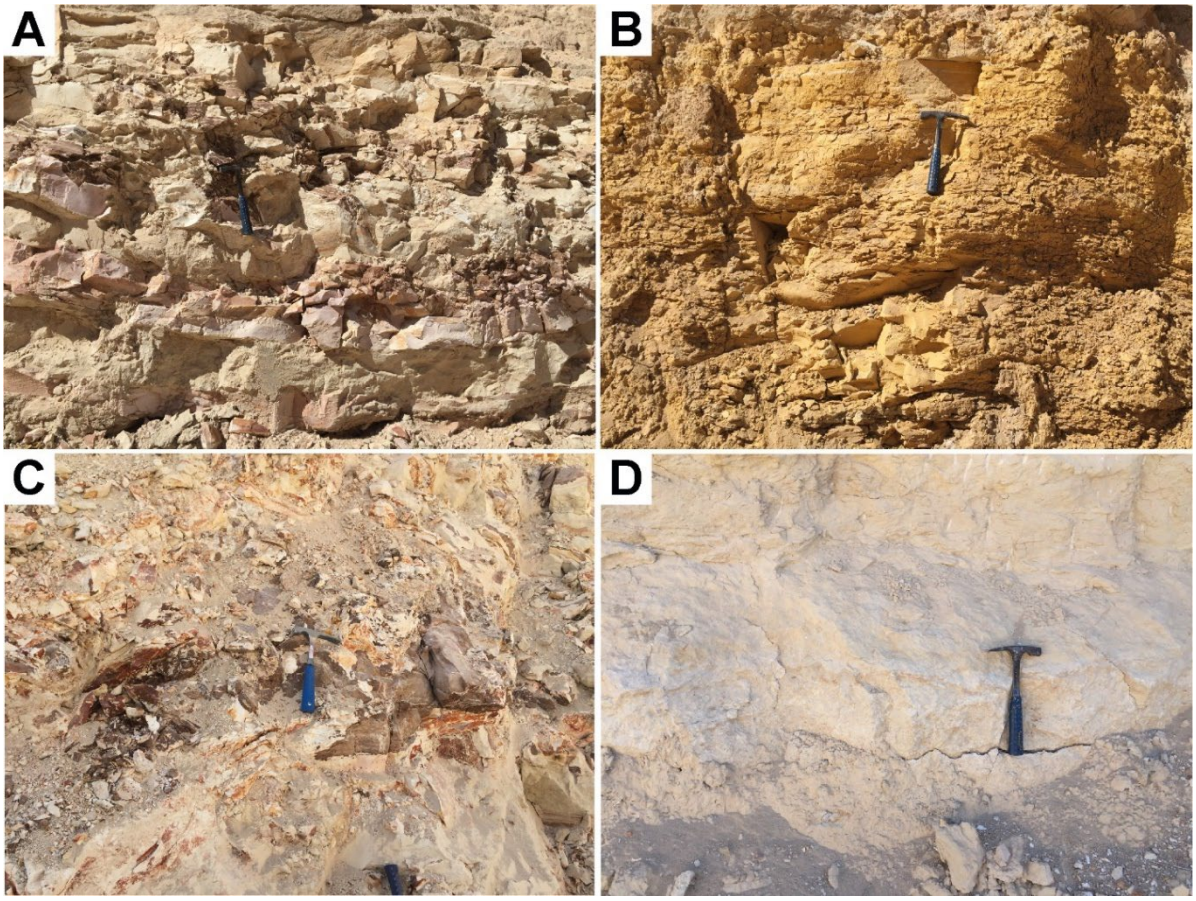

Figure 2-5: Some waste rock interburdens: A) Siliceous marl, B) Yellow marl-clay, C) Alternating flint and siliceous marl, D) Limestone

Carbonate rocks are the most abundant rocks in Benguerir mine. They are divided into limestones and dolomites, with the presence of other lithologies depending on the percentage of calcite and dolomite (Figure 2-6) (Prothero & Schwab, 2013). The origin of constituents of carbonate rocks are mostly marine, and mainly from biological and biochemical processes (Deconinck et al., 2016).

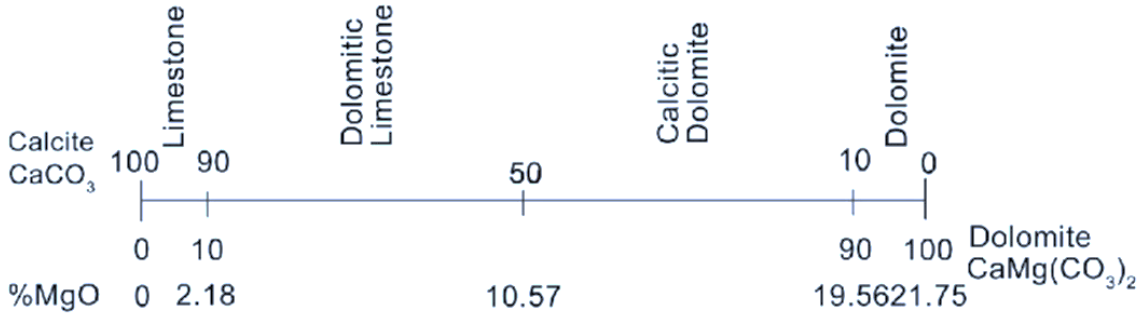

Figure 2-6: Chemical classification of carbonate rocks based on percentages of calcite and dolomite (Carozzi, 1953).

Carbonate rocks have a bimodal particle size distribution: on the one hand they contain allochemical grains (allochems) of relatively large size such as fossils, intraclasts, oolites and peloids, on the other hand a binder (micrite), which corresponds either to a matrix of primary origin or a cement of secondary origin (Deconinck et al., 2016) and sparite (well crystallized calcite or dolomite). Carbonate rocks can be classified based on their texture and composition (Deconinck et al., 2016). Two descriptive classifications, the most used, were proposed by i) Folk (1959; 1962) based on the presence of grains (allochems) and the presence of micritic matrix or sparite-type calcitic cement (Deconinck et al., 2016), and ii) Dunham (1962) based essentially on the texture of the rock and the type of connection between the grains, completed by Embry and Klovan (1971).

Clay rocks include all siliciclastic sedimentary rocks whose grains are essentially clayey size (< 1/256 mm) or silty size (between 1/16 mm and 1/256 mm) (Prothero & Schwab, 2013). Siliciclastic sediments designate the mineralogical nature of the sediments, which are dominated by silicates for the coarse fractions of the sediments and clay minerals (phyllosilicates) for the fine fractions. Among the best-known clay minerals found in phosphate mining waste, we distinguish kaolinite ($Al_2Si_2O_5(OH)_4$), illite ($(K,H_3O)(Al,Mg,Fe)_2(Si,Al)_4O_{10}[(OH)_2,(H_2O)]$), and smectite ($X_{0.3}Y_{2-3}Z_4O_{10}(OH)_2\ nH_2O$, where X represents an interfoliar cation (alkali or alkaline earth element), Y an octahedral cationa, Z a tetrahedral cationa). The marl rocks found in large quantities in PWR are clayey rocks which contain limestone (Tucker, 2001). They are soft, finely porous, friable when dry and plastic when wet. But they are different from clays because they effervesce with acids because of the presence of limestone.

Siliceous rocks are sedimentary rocks consisting mainly of silicon dioxide SiO_2 (silica). It appears in an amorphous form or in different crystalline forms. The characteristics of detrital siliceous rocks are the same as biochemical and chemical siliceous rocks, they have a hardness of order 7, with conchoidal breakage in the shape of a shell, unattackable by acids except hydrofluoric acid (El Haddi, 2014). According to previous geological and petrographic studies carried out on the Benguérir phosphate basin, the siliceous rocks present are of the flint family (Boujo, 1976; El Haddi, 2014; Mouflih, 2015); they included:

- *Flint*: siliceous rocks, formed of silica (chalcedony, quartz, some opal) of biochemical origin, precipitating at the beginning of diagenesis in the sediment, which is still soft (El

Haddi, 2014). They come in various colors: light yellow, brown to black. They can be found in continuous beds or in the form of disseminated flint knobs in the chalk.

- *Phosphate flint*: siliceous rocks characterized by the presence of coprolites, these phosphate flints have various names such as coprolite pudding or phosphate gravel (El Haddi, 2014).
- *Silexite*: siliceous sedimentary rock with very fine grains, it is generally siliceous marl. These flints are the result of the phenomenon of silicification which affects carbonates and phosphates in general (El Haddi, 2014).

Phosphate mining is carried out using the open-pit method. This method generates large quantities of waste rock, which is deposited in rock piles in the proximity of the mines. To manage the waste rock, heavy machinery such as bulldozers or draglines are employed to push the rock towards previously mined trenches, denoted as (n-1). By doing so, the waste rock is stacked on top of each other, forming large piles that can extend for hundreds of meters. However, these waste rock piles exhibit certain characteristics that pose challenges. Firstly, their grading is heterogeneous, meaning that the size and composition of the waste rock particles can vary significantly. Additionally, the high void index of the piles implies that there are numerous empty spaces or gaps within the rock pile. The accumulation of waste rocks in these piles can lead to various issues. Firstly, from an aesthetic perspective, the waste rock piles can be a source of landscape nuisance. The sight of these vast piles of discarded material can disrupt the visual appeal of the surrounding environment. Moreover, the accumulation of by-products in these rock piles can exacerbate the problem. These by-products, which may include hazardous materials, can potentially cause storage problems. The presence of such substances may require proper management and disposal to prevent any negative impacts on the environment.

The way in which waste rock is deposited in piles generates segregation of fine and coarse materials. This process presents significant challenges due to the heterogeneity of the waste rock, with geotechnical and chemical instability, depending on the mineralogy and chemistry of the materials, being the primary concerns (Aubertin et al., 2002). Various factors contribute to the physical instability of these piles, including geometric configuration, material properties, site topography, construction method, and climatic and hydrological conditions. When analyzing the geotechnical stability of such structures, it is essential to consider all these factors to select an appropriate design and assess the potential risks associated with the liquefaction of materials

caused by pore pressures (Aubertin et al., 2002). On the other hand, when it comes to chemical stability, the risk of surface and groundwater contamination in phosphate mining is generally low due to the high carbonate content found in waste rock (Bossé et al., 2013; Hakkou et al., 2009).

2.5 Review of valorization pathways for phosphate waste rock

The valorization of mine waste is an international challenge with economic and environmental benefits. It preserves natural resources and releases areas dedicated to waste rock storage. Today, the management of industrial waste is an environmental, social, and economic emergency for companies. Phosphate mine waste rock is a by-product of the phosphate mining industry. Indeed, the potential reuse of phosphate mining by-products has been studied over the last 10 years (Hakkou et al., 2016), to minimize the intense generation of waste rock from phosphate extraction and improve environmental management practices. In this state-of-the-art review, we will address this issue by providing an overview of existing pathways for the valorization of mine waste rock, examining how it can be reused and utilized in various applications. In addition, we explore the Moroccan legislative framework. By examining these supporting points, we aim to highlight potential solutions and advances in this field, thereby contributing to a more sustainable and efficient approach to waste rock management in the phosphate mining industry.

2.5.1 Moroccan legislation on mine waste valorization

In 2015, Morocco adopted a new mining code (Law: 33-13) that repeals the old mining code dating from 1951. According to the former Minister of Energy and Mines, Mr. Abdelkader Amara, this is a change that "was necessary both to meet national and international needs and also out of the need to rehabilitate the mining sector in order to allow it to amply enjoy its place in the national economy and contribute to its development" (Amara, 2014). The new Moroccan mining code (Law 33-13) presents changes in different provisions. In our case, we are interested in authorizing the exploitation of waste dumps (piles). This title promulgates the institution of the authorization for the exploitation of waste dumps to enrich or benefit from the rejected materials from mining operations (MEMEE, 2015). This authorization is granted after agreement from the owner of the land concerned and serves to establish the following: i) the perimeter of the land; ii) Its surface area, which must not exceed 1 km^2; and iii) its duration of validity, which must be at most five years. However, the authorization is renewable only once for the same duration. The waste dumps are authorized only to a legal entity under Moroccan law or to a mining cooperative (MEMEE,

2015). Only holders of an exploitation license who exploit the waste piles resulting from their mining activity are exempt from obtaining authorization for waste piles. To date, no regulations or laws exist in Morocco regarding the use of mining by-products in other sectors.

However, in Canada (Quebec), the Quebec Ministry of the Environment has authorized specific uses of mine by-products, relying in particular on the guide for the reclamation of non-hazardous materials to classify the materials (Ministère de l'Environnement, 2002). This guide is an initial version of the guidelines for evaluating projects for reclamation of non-hazardous inorganic waste from industrial sources as a construction material (Ministère de l'Environnement, 2002).

2.5.2 Valorization pathways for PWR

This section aims to examine PWR, its possible pathways of valorization, and its uses in civil applications. Phosphate mining is a significant industry worldwide, but it generates a considerable amount of waste rock that can have detrimental environmental impacts. Morocco is one of the world's largest producers of phosphate rock, which is a crucial component in the production of fertilizers. However, this has led to a significant amount of PWR being generated in the process. The origins and composition of this waste rock have been studied extensively in recent years to better understand its potential environmental impact and its potential applications Table 2-3. According to Idrissi et al. (2021), the PWR in Morocco is primarily composed of fluorapatite, which is the same mineral that is mined for phosphate. This means that the waste rock contains a significant amount of phosphate, which can potentially be valorized or recovered (Amar et al., 2022; Safhi et al., 2022). Additionally, the waste rock contains various other minerals, including quartz, dolomite, calcite, and mineral clays (Idrissi et al., 2021). It is important to understand the composition of the waste rock in order to develop effective strategies for managing and mitigating its environmental impact.

Table 2-3: The aspect and texture, mineralogical and chemical composition of PWR

Lithology	Aspect and texture	Modal mineralogy (w.t %)					Chemical composition (w.t %)					References
		Apatite	Calcite	Dolomite	Quartz	Clay minerals	P_2O_5	CaO	MgO	SiO_2	Al_2O_3	
Indurated Phosphate	Consolidated grains with greyish color	48-67	16-13	3-30	7-9	-	18.2-23	42-45.3	1.3-5	14.8-16	0.33-0.66	(Amar et al., 2023; Safhi et al., 2022)
Phosphate flint	Sharp angle, cutting ribs, massive, and dense with light black color	39-58	6-10	2-4	21-48	-	18.5-25	33-35	0.4-0.63	33.9-35	0.44	(Amar et al., 2023; Safhi et al., 2022)
Flintstone	Sharp angle and dense with brown to light black color	1.2	1.8	2	95	-	1.85	1.55	0.43	93.6	0.28	(Amar et al., 2023; El Machi et al., 2021a; Safhi et al., 2022)
Silexite	Light material and massive with move purplish color	-	-	38	62	-	0.7	4.54	3.70	80.1	1.03	(Amar et al., 2023; Safhi et al., 2022)
Limestone	Massive and dense with a whitish-beige color	-	-	-	-	-	12-0.98	42-28.4	4.32-23	7.84-12	0.37-0.93	(Amar et al., 2023; Ouakibi et al., 2013; Safhi et al., 2022)
Dolomitic limestone	Massive and very dense with a whitish-beige color	-	35	52	8	-	0.9-1.4	28-36	11-23	4.6-7.8	0.37	(Idrissi et al., 2021)
Marls / Clays	Compact, light, and sticky on the tongue with a whitish-beige color	1.13	-	52.5	12	36.4	0.42-1.88	7.23-17	4.52-12	30-74	1.49-7	(Mabroum et al., 2020)

According to the literature, the PWR can be used in a variety of applications in different sectors (Figure 2-7) (Chlahbi et al., 2023; Hakkou et al., 2016; Safhi et al., 2022; Taha et al., 2021). The valorization of PWR can provide economic and environmental benefits by reducing waste disposal costs, creating new revenue streams, and improving land restoration efforts. Hakkou et al. (2016) and Safhi et al. (2022) suggested that the valorization of PWR can be achieved through various approaches, such as the use of waste rock in civil engineering applications, ceramics, cement industries, soil amendment, and fertilizer. The use of PWR as a construction material has been demonstrated in many studies and can be used in road construction, embankment, and other civil engineering applications (Amrani et al., 2019; Taha et al., 2021). Additionally, the use of PWR as fertilizer can reduce the reliance on chemical fertilizers (EFMA, 2000), thereby reducing the environmental impacts of agriculture. Moreover, the use of PWR as soil amendment can improve soil properties and increase crop productivity (Hakkou et al., 2016; Vassilev & Vassileva, 2003). However, careful consideration must be given to the potential environmental impact of these uses.

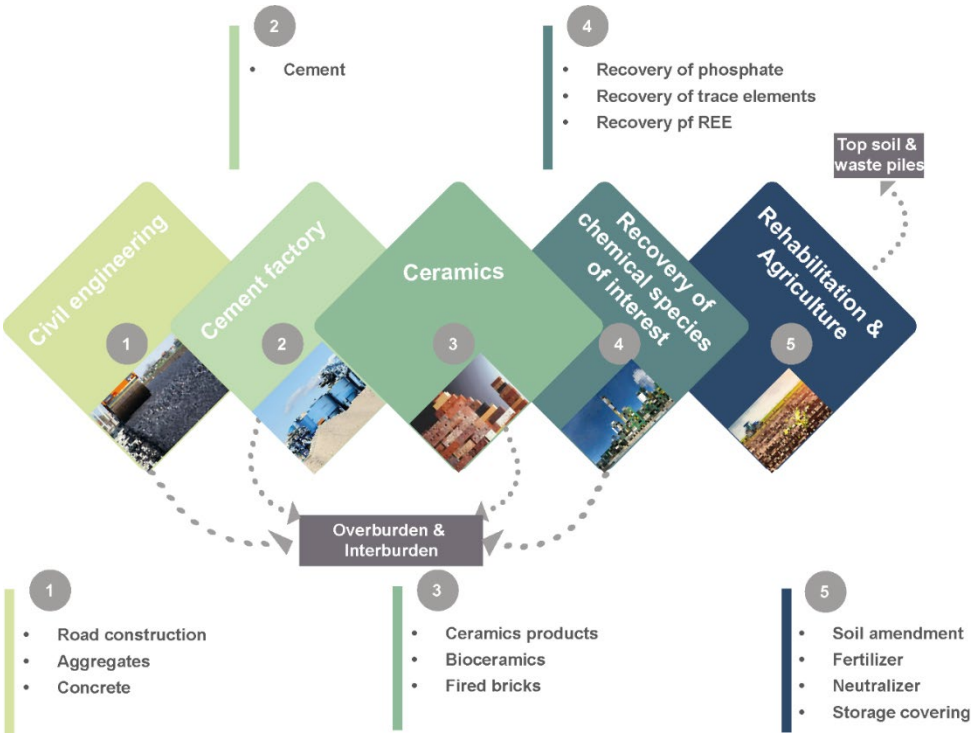

Figure 2-7 : Valorization pathways for PWR (REE: rare earth elements).

2.5.3 Valorization of PWR in civil engineering

Civil engineering includes all civil construction techniques (road construction, concrete, aggregates, etc.). The field of road construction is a large consumer of raw materials (aggregates), and various actors in this sector must face the increasing demand for the raw materials used in road infrastructures. Civil engineering has played a vital role in developing safe and efficient waste rock disposal methods. One common technique is to use waste rock as construction material in civil engineering projects such as road embankments, retaining walls, and dams (Ahmed & Abouzeid, 2009; Amrani et al., 2020; Amrani et al., 2019; Segui et al., 2023). The use of waste rock as a construction material not only helps in managing waste rock but also reduces the cost of construction materials. Hakkou et al. (2016) suggested that the use of waste rock as a construction material is sustainable and can contribute to reducing the environmental impact of mining activities. However, the use of waste rock in civil engineering projects requires proper characterization to ensure that the material is suitable for construction purposes. The characterization includes evaluating the physical, mechanical, and chemical properties of the waste rock. In addition, the potential environmental impacts of using mine waste rock as construction material must be assessed to ensure that the material does not pose any risks to human health and the environment. Overall, the use of waste rock as a construction material in civil engineering projects can provide an effective waste management solution and contribute to sustainable development. The pavement structure consists of a series of materials of varying thickness, organized into one or more distinct layers, each fulfilling a specific function. Its function is to i) resist the mechanical actions of vehicles for as long as possible, ii) attenuate the loads reaching the adjacent layers, and iii) protect the subgrade soil with a low bearing capacity which is sometimes very sensitive to water. Using unusual industrial by-products in civil engineering can contribute to conserving non-renewable natural resources and reducing the waste produced by specific industries. Phosphate rock is a potential secondary raw material for road construction and foundations. Table 2-4 presents a synthesis of the main works on the valorization of PWR in civil engineering.

Table 2-4: Summary of the main works on the valorization of PWR in civil engineering. CBR: California Bearing Ratio

Mine	Main use	Results	Properties	References
Phosphate mine, Benguerir, Morocco	Use of PWR as alternative raw materials in road construction	The study found that PWR possesses satisfactory physical, geotechnical, chemical, mineralogical, and environmental properties. They meet the required geotechnical standards for embankments and do not release any contaminants in leaching tests. In addition, these rocks have been successfully used in experimental pilot testing.	Specific density > 26 kN/m^3, 45% < LA < 58%, MBV < 1 g/100 g, PI < 20%. Leaching tests = none released any contaminants.	(Amrani et al., 2019)
	Use of PWR as an alternative material for constructing dry compacted embankments	The results showed that the applied stress level, dry density, and clay minerals influenced the structural deformation of PWR on wetting. PWR can be used as embankment materials at dry moisture content under certain conditions.	Dry moisture content under total overburden stress < 200 kPa ensuring a dry density of at least 95%	(Amrani et al., 2021)
	Use of PWR (flint) as aggregates for concrete	Flint from PWR can be successfully used as a substitute for ordinary concrete, promoting the circular economy and greener mining practices.	Lower strength (29 MPa) at 28 days. Higher flexural strengths (4.90 MPa) and a stronger interfacial transition zone	(El Machi et al., 2021a)
El-Nassar Mining Company at Sebaeya, Egypt	Use of phosphate coarse solid wastes (PCSW) as aggregates in road paving	The research findings can be summarized as follows: i) The properties of PCSW aggregates are similar to conventional mineral aggregates used in road construction. ii) Deviations in size grading can be corrected by crushing a specific fraction of the sample. iii) The produced aggregates are suitable for constructing local low-volume roads.	Dry density of 1.95 g/cm³ was achieved. crushing part of the -3/4 inch + 4 mesh size fraction.	(Ahmed & Abouzeid, 2009; Negm & Abouzeid, 2008)
	Use of PCSW as aggregates in concrete mix	The results indicate that the waste can be used in concrete mix for civil constructions, with a mean uniaxial compressive strength within the acceptable range.	Bulk density (g/cm³): 1.4, water absorption (wt.%)6, crushing strength: 29%, UCS_{28}: 240 kg/cm²	(Ahmed & Abouzeid, 2011)
Phosphate mine and quarrying of granit and marbre, Egypt	Use of PCSW and solid waste of quarrying in road construction (subbase and base)	Experimental tests conducted on these wastes demonstrated their favorable physical, mechanical, and chemical properties, meeting Egyptian standards. The results confirmed that these waste materials can be effectively utilized in base and sub-base layers for road construction and as replacement soil in foundations.	The CBR values: 88% for phosphate waste, 41 to 95% for crushed solid waste of quarrying, 2.02 g/cm³ dry density with an optimum moisture content of 12% was achieved.	(Ahmed et al., 2014)

2.5.4 Valorization of PWR in the cement industry

The valorization of PWR in cement production has gained significant attention in recent years (Bahhou et al., 2021b). This is primarily due to the abundance of PWR and its potential to serve as a valuable alternative raw material in cement manufacturing. PWR plays a significant role in cement production due to its potential for use as raw material or alternative fuel in the manufacturing process. According to Bahhou et al. (2021a) and Idrissi et al. (2021), the utilization of waste materials in cement production has gained attention as a sustainable solution to reduce both environmental impacts and the consumption of natural resources. Phosphate waste rock, a byproduct of the phosphate mining industry, contains high levels of carbonate minerals and other minerals that are essential for cement production. The incorporation of this waste material in cement manufacturing can help to reduce the reliance on traditional raw materials such as limestone and clay minerals, which are finite resources. Therefore, the importance of PWR in cement production lies in its potential to enhance the sustainability and efficiency of the cement manufacturing process, as well as to reduce environmental impacts.

The study of Bahhou et al. (2021b) evaluated the potential use of clay minerals produced during phosphate mining as supplementary cementitious materials. Clay minerals were thermally activated, and their physical, chemical, and mineralogical characteristics were determined. The results showed that the optimal activation temperature was 800°C for 3 h. Substituting 20% of clinker with calcined clay resulted in a compressive strength higher than 22 MPa at 28 days. The consistency and initial setting time values were in accordance with the required cement standard. This research highlights the potential of utilizing thermally activated clay minerals from phosphate mining as a sustainable alternative in cement production. Another study by Slimane et al. (2017) investigated the use of rejection of black phosphate screening from Djebel Onk in the production of mortars and concrete. They conducted a study where they replaced a certain percentage of clinker with phosphate reject. The mortar with 10% phosphate rejects showed the best flexural resistance compared to the reference mortar and other mortars.

2.5.5 Valorization of PWR in the ceramic industry

The valorization of PWR in the ceramic industry holds significant importance for both environmental sustainability and economic viability. Firstly, the incorporation of this waste material into ceramic production processes offers a solution to the growing problem of waste disposal. Additionally, it provides an opportunity to reduce the reliance on traditional raw materials, such as clay minerals and feldspars, which are depleting resources. Techniques for incorporating PWR into ceramics have been developed, ensuring compatibility with existing manufacturing processes. However, recent research has shown that this waste material can be utilized as a valuable resource in the ceramic industry. According to Hakkou et al. (2016), the incorporation of PWR in ceramic production can enhance the physical and mechanical properties of ceramic products. This is attributed to the high content of phosphorus and other minerals (clay minerals) in the waste rock, which act as fluxing agents and contribute to improved sintering and densification processes. According to Idrissi et al. (2021), PWR contains high levels of mineral phases such as quartz, apatite, and mica, which can act as reinforcing agents, improving the strength and toughness of ceramics.

Among the unexploited phosphate interlayers in Benguerir mine, there lies a valuable resource that is often overlooked - clay layers. These clay layers, which are commonly considered waste rock, have the potential to be reused in an environmentally friendly manner. What makes these layers intriguing is the fact that they vary in terms of clay mineralogy. The predominant clay minerals found are smectite ($X_{0.3}Y_{2-3}Z_4O_{10}(OH)_2$ nH_2O), sepiolite ($Mg_4Si_6O_{15}(OH)_2$-$6(H_2O)$), and palygorskite ($(Mg,Al)_2Si_4O_{10}(OH)$-$4(H_2O)$), as identified by Loutou et al. (2019).

In the Gantour phosphate basin, Chahi et al. (1993) conducted research that shed light on the genesis of palygorskite. Through the examination of ratios such as Al_2O_3/rare earth elements and the analysis of infrared characteristics, Chahi et al. (1993) argue in favor of the mechanism of crystallization by dissolution. This suggests that palygorskite is formed through a process of dissolution and subsequent crystallization. The formation and stability of fibrous clay minerals, such as palygorskite, within the sedimentary series necessitate an alkaline environment characterized by a high concentration of silica and magnesium, a low

concentration of aluminum, and elevated temperatures. These findings were supported by Bouza et al. (2007); Singer et al. (1995). Considering the mineralogical composition of these PWR, it becomes evident that they hold potential for the manufacturing of ceramics. Hakkou et al. (2016) found that these waste rocks possess a mineralogical composition suitable for ceramic production. This discovery opens new possibilities for the utilization of these waste rocks, transforming them from unwanted by-products into valuable resources. Table 2-5 summarizes the main attempts to valorize PWR in the ceramic field.

Table 2-5: Summary of the main works on the valorization of PWR in the ceramic field

Mine	Main use	Results	Properties	References
Benguerir Phosphate mine, Morocco	Use of PWR (clay) in ceramics, specifically fired clay bricks	The results show that increasing the sintering temperature leads to changes in clay minerals, vitrification of the bricks, and the formation of micro-porosity. The bricks exhibit acceptable water absorption capacity, firing shrinkage rate, and good flexural strength, indicating their potential use in brick manufacturing.	Pressure of 5 MPa, temperature of 1050°C, and time of 2.5 hours	(Loutou et al., 2019)
Phosphate mine	Use of PWR in the manufacture of potentially useful ceramic products	The results showed that slip-resistant road aggregates can be manufactured using Na_2CO_3 to produce a water-insoluble glass bond and controlled porosity in an unpressed mixture of silicate particles.	-	(Ramsey & Davis, 1975)
Gantour, El Youssoufia region, Morocco	Use of PWR to produce compressed stabilized earth bricks using cement stabilizer	The laboratory results showed that this mixture had satisfactory mechanical and durability properties. The bricks also had low water absorption coefficients and met the requested limits of the standard for compressive strength. The addition of cement improved the cohesiveness, rigidity, and mechanical properties of the bricks.	Bulk density (g/cm^3):2.18, UCS: 2.56-5.7 MPa, Water absorption: 13.89 %.	(Mouih et al., 2023b; Mouih et al., 2023a)
Maroc Phosphore, Jorf Lasfar. Recette VI (Bouchan), Morocco	Use of PWR, phosphogypsium (PG) and cement to manufacture the compressed bricks	The most optimized mixture consists of 40% PG and 8% ordinary Portland cement, achieving compressive strength of 8.1 MPa at the laboratory scale and 7.7 MPa at the pilot scale after 28 days, and interesting thermal conductivity. The bulk density and water absorption coefficient meet standards.	Bulk density (g/cm^3):1.75-7.8, UCS: 3.17-8.11 MPa, Water absorption: 14.48-14.61 %. Thermal conductivity (W/m/K): 0.45-0.51	(Oubaha et al., 2022)
Djebel Onk phosphate mine, Tebéssa-Algeria	Use of screen rejects >15 mm black phosphate for bioceramics production	The results of ceramics obtained from zirconia fired at 1200°C and 1300°C, lead to a bioceramic material with satisfactory chemical (durability against acids and bases) and mechanical (Young's modulus) properties.	-	(Djellal et al., 2015)

2.5.6 Valorization of PWR in other sectors

In addition to the civil engineering, ceramics, and cement sectors, waste rock from phosphate extraction holds tremendous potential for various other industries. This versatile resource can be effectively utilized in mine restoration and rehabilitation, contributing to the sustainable development of ecosystems. Furthermore, waste rock offers exciting prospects in agriculture and soil improvement, where its application can enhance soil fertility and crop productivity. Additionally, waste rock contains valuable elements that can be extracted, presenting both opportunities and challenges in the quest for resource recovery. Table 2-6 presents the main valorization of PWR in other sectors.

The valorization and reuse of PWR present a promising opportunity to address both resource conservation and environmental impact in civil engineering. Traditional methods involve utilizing mixed PWR, but this thesis project takes an approach by examining each lithology of PWR separately. This distinction is essential because different lithologies may possess varying physical and chemical properties, influencing their suitability as secondary raw materials. Addressing each lithological type could yield insights into adapting valorization processes more efficiently, potentially enhancing the quality of the derived materials while optimizing their performance in construction applications. Therefore, valorizing PWR not only aligns with sustainable development goals by reducing the depletion of primary raw materials but also offers a strategic response to environmental management challenges posed by traditional mining activities.

Table 2-6: Summary of the main work to valorize PWR in other sectors. DE-XRT: dual-energy X-ray transmission.

Mine	Main use	Results	Properties	References
Phosphate mine, Morocco	Use of PWR as a component of a Store-and-Release Cover	The results confirmed the ability of PWR to prevent water infiltration and oxidation of mining waste in Kettara, Morocco. Based on these results, they designed a storage and release cover that uses capillary barrier effects and prevents water percolation by storing and evaporating water during wet and dry climatic periods.	The thickness of the store-and-release layer is between 50 and 100 cm	(Bossé et al., 2013)
	Use of alkaline PWR for the control of acidic mine drainage (AMD)	Laboratory tests showed that adding 15 wt% alkaline PWR to the Kettara tailings resulted in leachates with lower acidity and metal concentrations compared to untreated samples. The neutralization was attributed to calcite, while dolomite dissolution was minimal and fluorapatite remained stable. However, when the treated solution encountered unweathered Kettara tailings, the pH became acidic, although metal concentrations remained low.	The neutralizing potential is between 500 and 680 kg $CaCO_3$/t	(Hakkou et al., 2009)
	Use of PWR (limestone) in the passive treatment of AMD	The phosphate limestone waste effectively increased alkalinity and pH, leading to the precipitation of most metals. Batch tests showed a significant decrease in concentrations of Fe, Al, and Cu under both anoxic and oxic conditions. Column tests also demonstrated a decrease in Al and Cu concentrations, although Fe decreased less significantly.	The initial AMD value increased from 3 to 6.5 during the batch tests and 8 in the columns. Significant decrease in concentrations (Fe, Al, Cu)	(Ouakibi et al., 2013)
	Use of phosphate waste as a phosphorus source for alfalfa growth	The researchers found that the main minerals in the phosphate waste rocks, namely carbonates and fluorapatite, were respectively involved in the formation of labradorite/anorthite and they also found that due to the release of phosphorus from the granules embedded in the soil, the growth of alfalfa plants improved.	Absorbed quantity of phosphorus (0.12%)	(Loutou et al., 2016)
	Mine waste rock reprocessing using sensor-based sorting	The study discusses the potential of PWR as a resource for phosphorous beneficiation. found that the PWR contained up to 17.5 wt % P_2O_5, with various minerals present. Hand sorting revealed that over 50% of the PWR in the coarse fraction (>30 mm) was indurated phosphate. The tests showed that DE-XRT sorting technology had the highest efficiency.	P_2O_5 recovery of 70 wt% and an increase in P_2O_5 content from 13.5 wt% to 18.5 wt%.	(Amar et al., 2023)

CHAPTER 3 MATERIALS AND METHODS

In this chapter, we delve into the materials and methods employed in this thesis, providing a comprehensive overview of the research process. Our primary aim is to shed light on the objectives of the present study.

3.1 Methodology

The methodology adopted in this project is illustrated in Figure 3-1. The initial step involves conducting a comprehensive bibliographic and benchmarking study to gather all the relevant data about the thesis project. Following this, field missions were conducted to carry out core drilling, sample collection, and the creation of lithological sections. These field missions were crucial in establishing litho-stratigraphic correlations, which helped in understanding the geological formation and structure of the area under investigation.

The sampling strategy for this project was carefully designed to ensure a comprehensive and representative data collection process. It involved a combination of two methods, namely the random method and the targeted method, to account for varied factors influencing the selection of samples. The first criterion we considered was the facies, which refer to the different rock types or sedimentary structures present in the study area. The second criterion was the availability of the quantities required for analysis. We considered the practicality of obtaining enough samples that could be processed and analyzed within the project's time and resource constraints. This approach ensured that the collected samples were not only representative but also feasible to handle in terms of laboratory analysis. By combining these two methods and considering these criteria, our sampling strategy aimed to provide a robust dataset that would support accurate and meaningful analysis for the project. The sampling strategy for each study is detailed in Chapters 4, 5, and 6.

Once the samples from the drill cores and trenches were obtained, a series of characterization tests and analyses were performed. These tests/ analyses encompassed geological, geomechanical, petrographic, mineralogical, chemical, and environmental analyses. The geomechanical characterization involved evaluating the physical and mechanical properties of the samples, such as grain size distribution, Atterberg limits, strength, degradability, and fragmentability. The petrographic and mineralogical analysis focused on identifying the mineral composition of the samples, which provides insights into the geological history and the potential presence of valuable

minerals. Chemical analysis is carried out to determine the elemental composition of the samples, aiding in understanding any potential environmental implications or chemical reactions. Lastly, the environmental characterization was done by using leaching tests (semi-dynamic and static tests), this characterization has been used to assess the environmental behavior. The description detail of each characterization and analysis used is presented in Chapters 4, 5, and 6.

After the various characterizations have been carried out, the geomodelling step began. The parameters used for geomodelling are derived from the geological description and the thickness of interburdens. By incorporating these parameters into the model, it becomes possible to obtain a comprehensive understanding of the deposit being studied. The model output, on the other hand, represents essential information that can be useful in decision-making processes. The primary outputs include volume estimations. Additionally, the model output provides insights into the spatial continuity of the deposit, allowing for a better understanding of its distribution and potential variations throughout the area of interest. Furthermore, the model output can shed light on the properties of waste rock levels, aiding in the development of efficient waste management strategies.

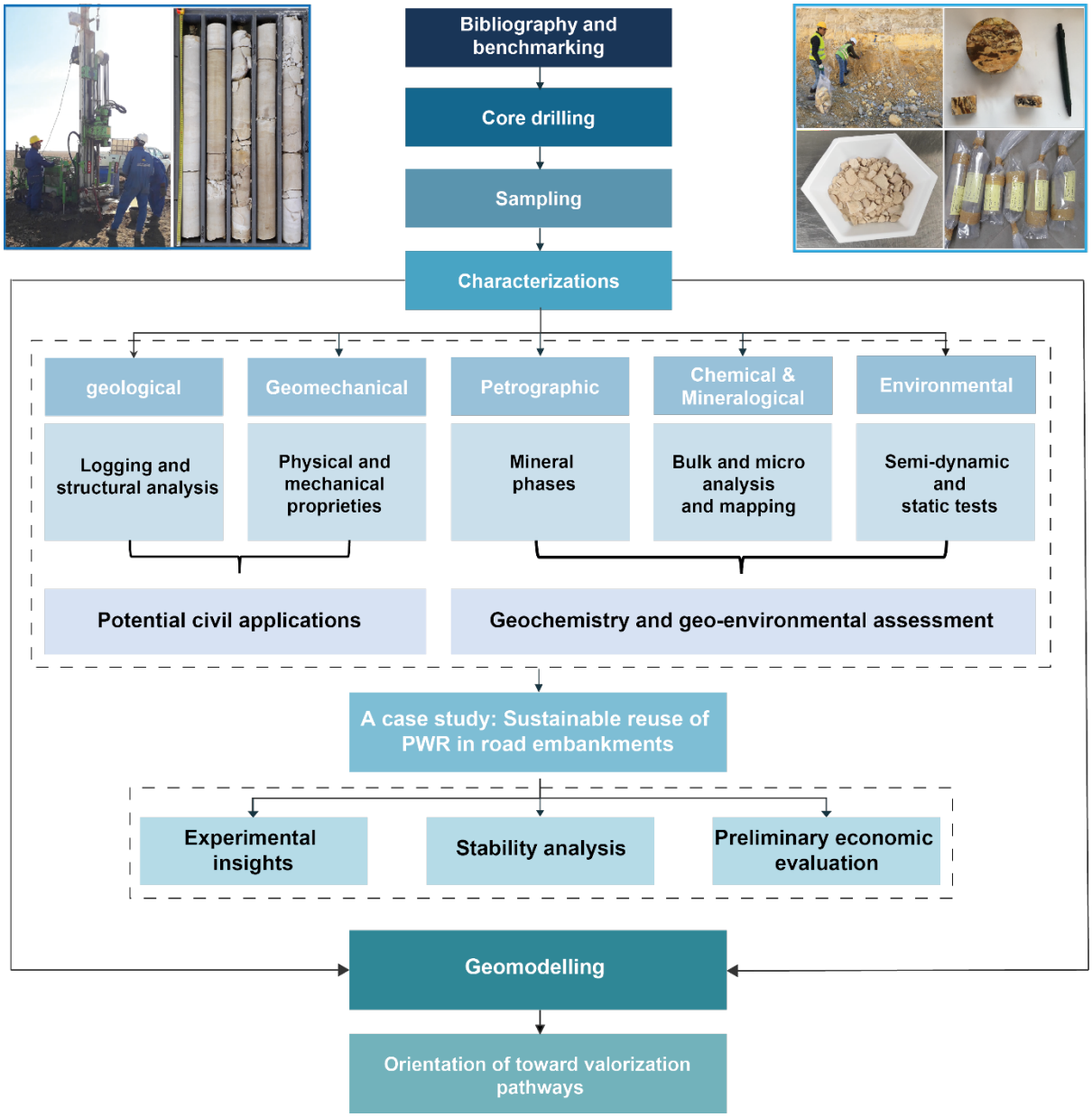

Figure 3-1: General methodology of the thesis project.

3.2 Materials and analytical methods

Preliminary soil/rock investigation plays a crucial role in gathering essential information, providing valuable insights into its characteristics and potential risks. By conducting this initial assessment, we can understand the sample's composition comprehensively, including the nature of the layers present, their position, thickness, and direction. Furthermore, it allows us to determine the presence or absence of the water table, including its depth and mobility.

Various techniques were employed during soil/rock investigation, with core drilling and core logging commonly used. Core drilling involved extracting cylindrical samples, which were then analyzed to determine their properties. This technique provides valuable data on the sample's composition. However, core logging is an essential step that follows core drilling. It involves showing the succession of different geological layers on a borehole, by analyzing the samples, noting their color, texture, grain size, moisture content, and any other relevant characteristics.

3.2.1 Core drilling and samples collection

To investigate the structure and composition of the phosphate series in the Benguerir mine, we carried out six vertical core drillings (non-destructive) of varying depths ranging from 60 to 95.50 m, with a total length of 425 m. The drillings were carried out by *Laboratoire Public d'Essais et d'Etudes* (LPEE) in accordance with XP P94-202 standard (XPP94-202, 1995). The location of the boreholes was chosen to ensure that the entire mine was covered while targeting the future mining trenches. Table 3-1 shows the lamber coordinates for the six boreholes. Some photographs of core boxes (SC06) are shown in Appendix A.

Table 3-1: Lambert coordinates and depths for drill cores

	X (m)	Y (m)	Z (m)	P (m)
SC02	273973.00	187767.00	545.82	95.5
SC03	276526.00	184054.00	474.57	60.0
SC04	275527.00	186026.00	495.66	61.0
SC05	277050.00	181498.00	461.81	73.9
SC06	275494.00	179792.00	453.44	70.0
SC07	271812.00	179718.00	464.27	64.3

For each borehole, a well-prepared platform must be established to ensure the installation of drilling equipment aligns with the best practices. Additionally, the environmental impact of drilling activities should be minimized by implementing sustainable practices. This includes properly managing waste materials, minimizing water usage, and preventing any potential contamination of soil or nearby water sources. The equipment required for core drilling is:

- Drilling rigs: in our case, we used two drilling rigs (Silea "SL 700/22" and "S700/13" from FORDIA Europe) (Figure 3-2A).
- Borehole parameter recorder to measure and record, during drilling, physical quantities called borehole parameters (pressure, speed, and depth), whose variations correlate with

the geomechanical properties of the ground traversed, in our case, we installed the recording equipment (BAP 160) (Figure 3-2B).

- Settling basin to create a reservoir for drilling in a closed circuit, and to increase the useful life of drilling fluids by promoting the settling of sediments generated during drilling.
- A water barrel and tank are installed to mix water with additives and as a reservoir.

The rock is cut by a diamond-impregnated tubular tool (crown) (Figure 3-2C). The cylinder cut of rock is progressively inserted into the 1.5 m long, 116 mm inner diameter tube of the corer. The coring technique uses an injection of water mixed with additives such as bentonite and polymer (Figure 3-2D-E) to facilitate drilling, improve rod lubrication, cool the crown, and control any fluid ingress or loss (by stabilizing the borehole walls). This technique makes it possible to recover a continuous, intact sample cylinder (core) from the traversed terrain and preserve geological structures (faults, joints, diaclases) as well as rock textures (Urien et al., 2017).

To mitigate the risk of contamination between core samples during the core drilling, a series of precautions are employed to preserve sample integrity. One fundamental measure involves using sampling bags, thus preventing contamination that could arise from direct contact with other samples or external elements. Additionally, control over the sampling environment plays an important role; it must be meticulously clean and organized to prevent dust, dirt, or strange particles to avoid the risk of contamination. This controlled environment safeguards against environmental factors that might otherwise introduce contaminant variables into the studied core samples. Furthermore, when transitioning from one facies to another, there is an imperative change in handling equipment such as gans, another critical procedural step.

Once the drilling had been completed, all the equipment was moved to the next drilling site, and the surface borehole was plugged with rocks. Any residual cuttings and sludge from the settling tanks are collected and disposed of in a designated area. The ground is re-spread to restore the original model of the drilling site.

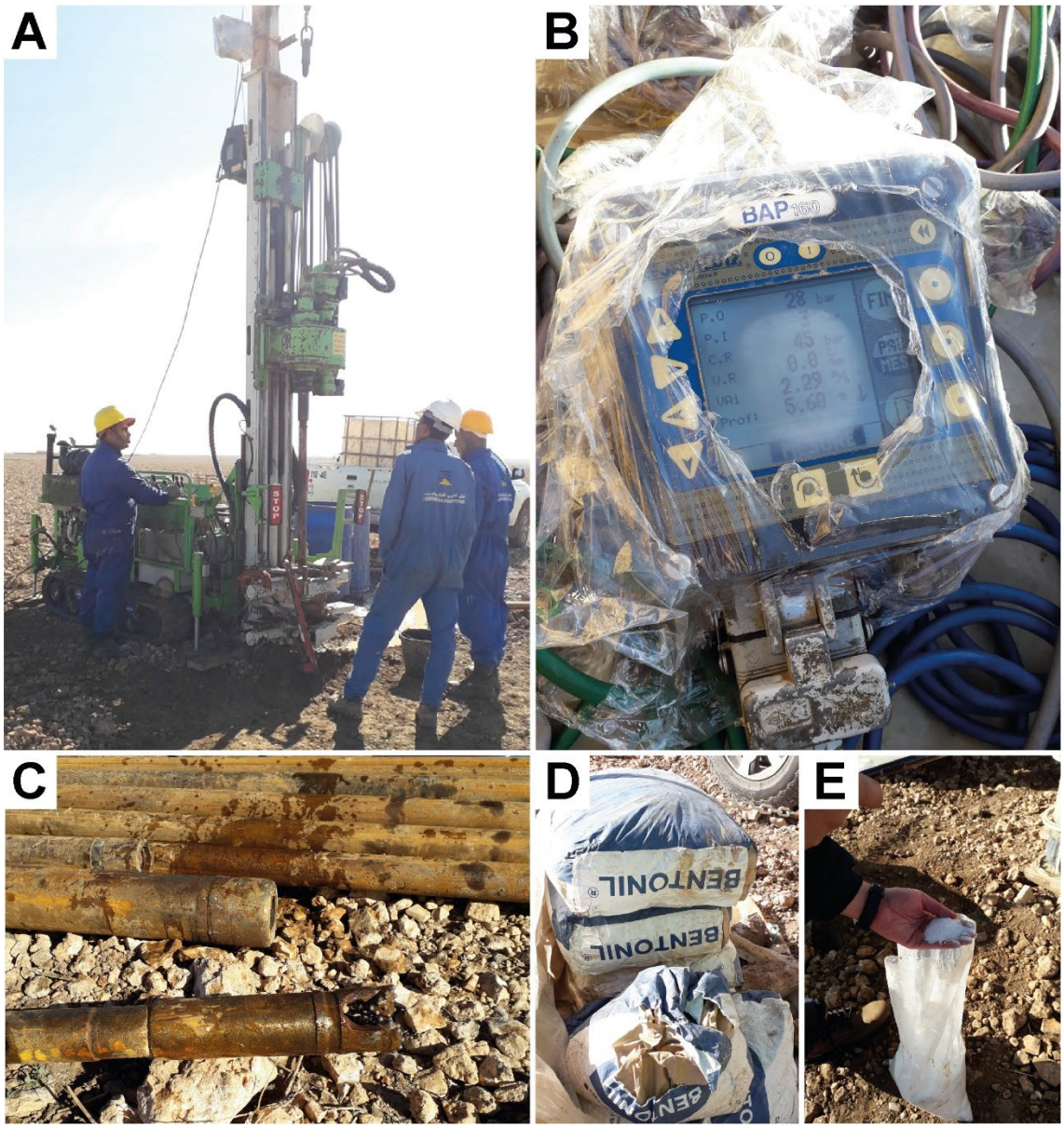

Figure 3-2: A) Photograph of the drilling rig used. B) Photograph of the device used to record borehole parameters. C) Diamond-impregnated tubular tool (crown). Additives added during core drill excavation, D): Bentonite; E): Polymer

3.2.2 Analysis of the core drilled samples

Drilled cores are the real image of the terrain crossed. The cores were deposited, according to the natural order, by the sounder in boxes (crates) which are designed for this purpose. Typically, each box contains five rows (5 m). Once the cores were placed in the boxes, we began the geological and structural description stage in order to draw up the stratigraphic log. A stratigraphic log is a

column that presents the succession of different geological layers on a survey. In the description of the core or logging, we wet the cores to bring out the contrasts. Then, we described and studied the geological characteristics of the cores. In the log, we described and explained the following elements: the thickness of each crossed layer, the chronological succession of geological layers (from the youngest to the oldest), the presence of figured elements, choice scale, etc.

The drill hole analysis was based on two parameters: facies identification, total core recovery (TCR), and rock quality designation (RQD). The facies identification involves lithology identification (limestone, marl, clay, phosphate, etc.). The TCR consists of measuring the total quantity of core recovered over the length of each drilled pass. In other words, it's the ratio: recovered length / drilled length, while the RQD is a rock quality assessment parameter developed in 1967 by Deere et al. (1967), in response to the need for a rapid, objective technique for estimating rock quality. As a result of the in-situ investigation, we identified the lithological formations, the TCR, and RQD surveys for each core drill, they are presented in detail in Appendix A and the following Chapter (4).

The sampling strategy used in this study combined two methods: the random and the targeted methods. The sampling strategy adopted for each study is described in the following sections, providing a clear understanding of how samples were selected and how the data collection process unfolded. Some photographs of the sampling (core drilling and mining trenches) are presented in Appendix A.

In this chapter, we limit ourselves here to avoid redundancy since chapter 4, which follows, presents the results of the geological characterization of the core holes.

3.2.3 Geomodelling data

Like any modeling process, geomodelling starts with the collection of data. This data is gathered through core drilling and historical boreholes, allowing for a comprehensive database. Each core drill is installed alongside a historical borehole to ensure accurate comparisons of results, enabling the construction of a uniform database in terms of lithological description. The data used in this study come from ninety boreholes (six of which correspond to core drilling) with a grid spacing of 500 m.

The geomodelling software used in this project is Datamine. This software is highly regarded for its wide range of integrated mining solutions covering all mine development processes. According to Desharnais (2019), Datamine software offers a comprehensive suite of tools, including resource modeling, mine planning, strategic optimization, detailed design, and short-term decision-making capabilities. The software integrates Studio RM, Studio OP, Studio EM modules, Minescape, etc. However, this project focuses on the Studio RM software, which is considered Datamine's flagship product. Studio RM is designed to facilitate the modeling and evaluation of mineral resources and reserves.

The geomodelling process using Datamine software (Studio RM) comprises the following steps: i) creation and import of the survey database, ii) creation of the wireframe, and iii) creation of the block model. The first step involves creating and importing the survey database in a file compatible with Datamine software (i.e., MS Excel). This step is crucial as it lays the foundation for the modeling process. By importing the survey data, which includes information such as the location of the various boreholes (X, Y, and Z coordinates), depth, deviation, lithology, results of the various characterizations and analyses (geomechanical, geochemical, environmental, etc.). The data in each sheet is arranged according to precise organization (Figure 3-3):

- *Collars sheet*: contains all information concerning borehole identification, location (X, Y, Z coordinates), depth, etc.
- *Surveys sheet*: contains information on azimuth and inclination deviations and all deviation measurements, if available.
- *Lithology sheet*: contains the lithological description of the facies crossed by the boreholes.
- *Assays sheets*: contain all the results of characterizations and analyses carried out (RQD, geomechanics, geochemistry, etc.).

	A	B	C	D	E	F	G	H	I
1	BHID	XCOLLAR	YCOLLAR	ZCOLLAR	BRG	DIP	DEPTH	Zone	Type_Sd
2	SC02	273973,00	187767,00	545,82	0,00	90,00	95,50	Mine Nord Panneau 7	Carotté
3	SC03	276526,00	184054,00	474,57	0,00	90,00	60,00	Mine Nord Panneau 8	Carotté
4	SC04	275527,00	186026,00	495,66	0,00	90,00	61,00	Mine Nord Panneau 8 & 5	Carotté
5	SC05	277050,00	181498,00	461,81	0,00	90,00	73,90	Mine Nord Panneau 8	Carotté
6	SC06	275494,00	179792,00	453,44	0,00	90,00	70,00	Mine Sud Panneau 1	Carotté
7	SC07	271812,00	179718,00	464,27	0,00	90,00	64,30	Mine Sud Panneau 1	Carotté
8	P750	268994,16	178508,93	451,38	0,00	90,00	50,00	Mine Sud Panneau 1	Puit
9	P387	271501,44	179498,26	460,49	0,00	90,00	53,70	Mine Sud Panneau 1	Puit
10	P189	275000,00	179500,00	452,72	0,00	90,00	52,50	Mine Sud Panneau 1	Puit
11	P210	277009,10	181508,80	459,32	0,00	90,00	66,50	Mine Nord Panneau 8	Puit
12	P245	276506,30	184013,00	473,45	0,00	90,00	59,80	Mine Nord Panneau 8	Puit
13	P269	275503,88	186011,61	495,98	0,00	90,00	62,30	Mine Nord Panneau 7	Puit
14	P1411	273999,99	187747,63	546,50	0,00	90,00	93,55	Mine Nord Panneau 7	Puit
15	P190	275502,50	179500,00	455,23	0,00	90,00	56,90	Mine Sud Panneau 1	Puit
16	P192	275499,90	180001,69	459,54	0,00	90,00	60,60	Mine Sud Panneau 1	Puit
17	P268	274500,00	185997,00	506,97	0,00	90,00	65,10	Mine Nord Panneau 7	Puit
18	P286	275000,80	186500,01	504,92	0,00	90,00	65,10	Mine Nord Panneau 7	Puit
19	P17	276052,85	184490,64	477,30	0,00	90,00	57,65	Mine Nord Panneau 8	Puit
20	P253	277010,70	184518,40	480,76	0,00	90,00	67,90	Mine Nord Panneau 8	Puit
21	P257	275495,80	185009,00	482,45	0,00	90,00	54,30	Mine Nord Panneau 8	Puit
22	P258	276503,00	185016,00	482,23	0,00	90,00	57,90	Mine Nord Panneau 8	Puit
23	P263	276004,00	185509,70	486,50	0,00	90,00	55,80	Mine Nord Panneau 8	Puit

Collars Surveys Litho RQD geomechanical geochemistry Environmental

Ready

Figure 3-3: Example of the “COLLARS” sheet.

Once the database is complete and ready, it can be imported into the software via the ODBC (Open Data Base Connectivity) link to filter multi-source data, correct it, and eliminate errors. ODBC establishes a connection between the database and the software. The software also offers the capability of graphic visualization of the different boreholes (Figure 3-4). This feature provides a visual representation of the data, making it easier to identify patterns, trends, and anomalies.

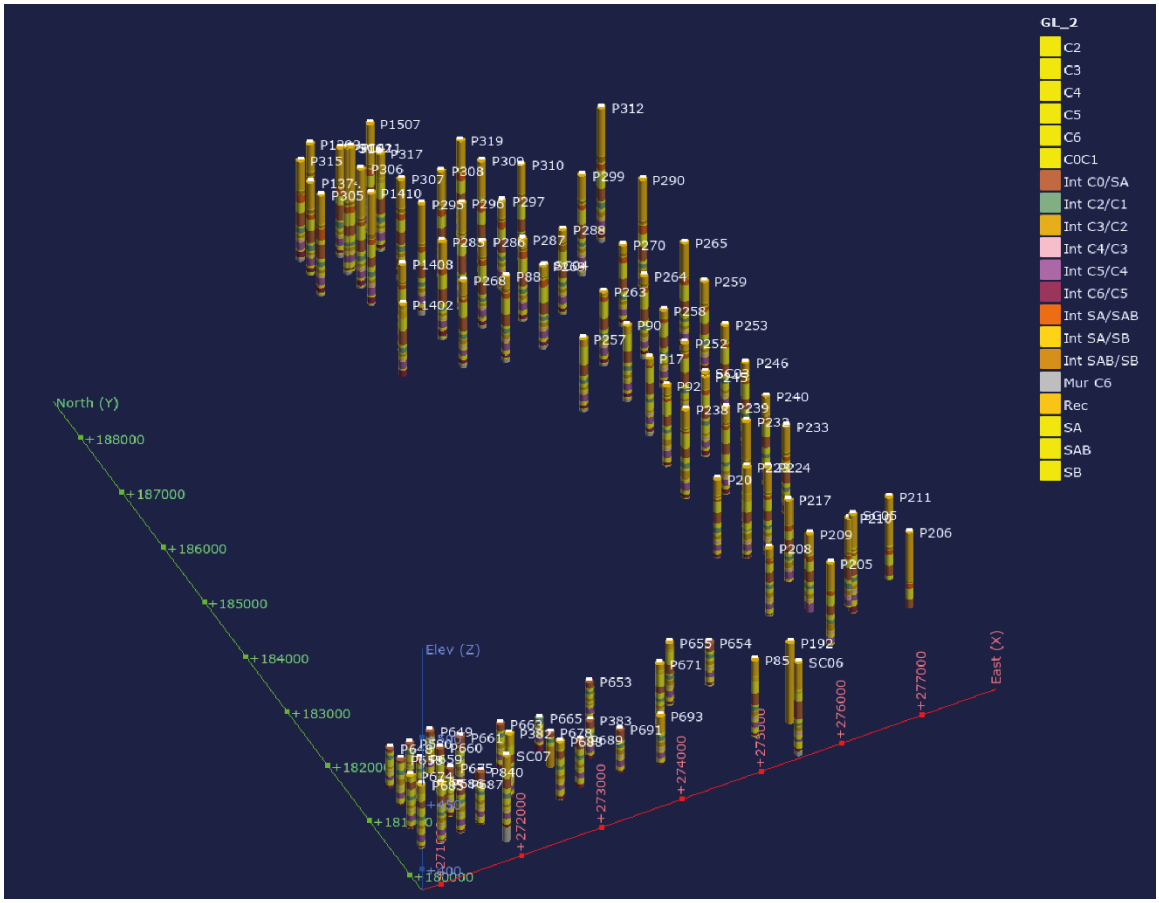

Figure 3-4: Graphic visualization of different boreholes.

The second step in the geomodelling process is the creation of the wireframe. Wireframing involves constructing a three-dimensional representation of the geological features based on the collected data in the database. Creating wireframes involves creating the topographic model and waste interburdens, including phosphate layers. To create a wireframe, a series of strings must be created, which must then be linked to form the outline of the 3D surface (Datamine, 2004). The digital terrain model (DTM) tool can generate the topographic wireframe. The concept of wireframe creation is based on triangulation. Each point is linked to form a series of triangles (Figure 3-5).

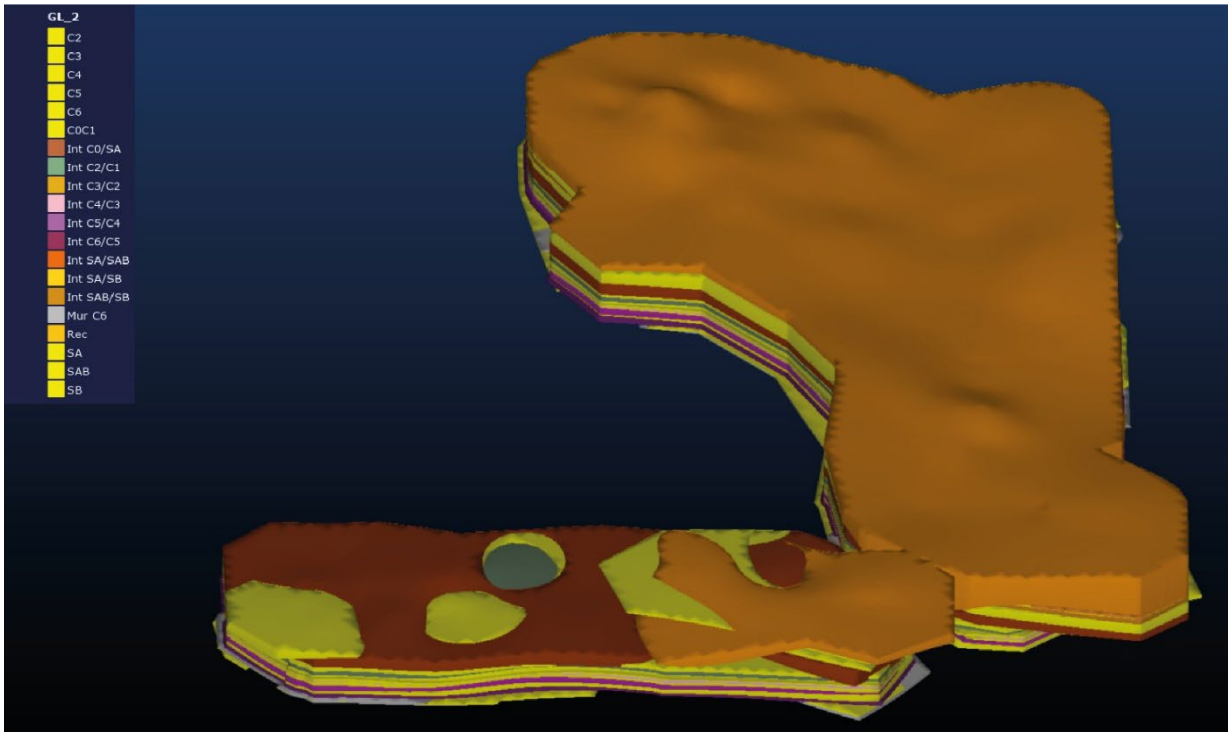

Figure 3-5: Creation of the wireframe of the study area.

Once the wireframe has been created, it must be checked for errors. This process includes checking the edges of the solids as well as the separate surfaces. After this, the volumes can be calculated (Figure 3-6).

The overburden has the highest estimated volume, standing at approximately 580 Mm^3. This is followed by the interburden Int C0/SA with 312 Mm^3, Int C5/C4 with 185 Mm^3, and Int C2/C1 with 120 Mm^3. The Other interburden: Int AB/SB, Int SA/AB, Int SA/SB, and Int C6/C5, have significantly lower volumes of less than 100 Mm^3 each. On the other hand, the phosphate layers in these areas present a different distribution of volumes. The SA layer, which is the thickest and most extensive, has an estimated volume of 302 Mm^3, making it the largest among all the phosphate layers. It is followed by the C5 layer with 114 Mm^3, C0C1 with 107 Mm^3, and C2 with 100 Mm^3. The remaining layers, including SB, AB, C3, and C4, have volumes of less than 100 Mm^3 each.

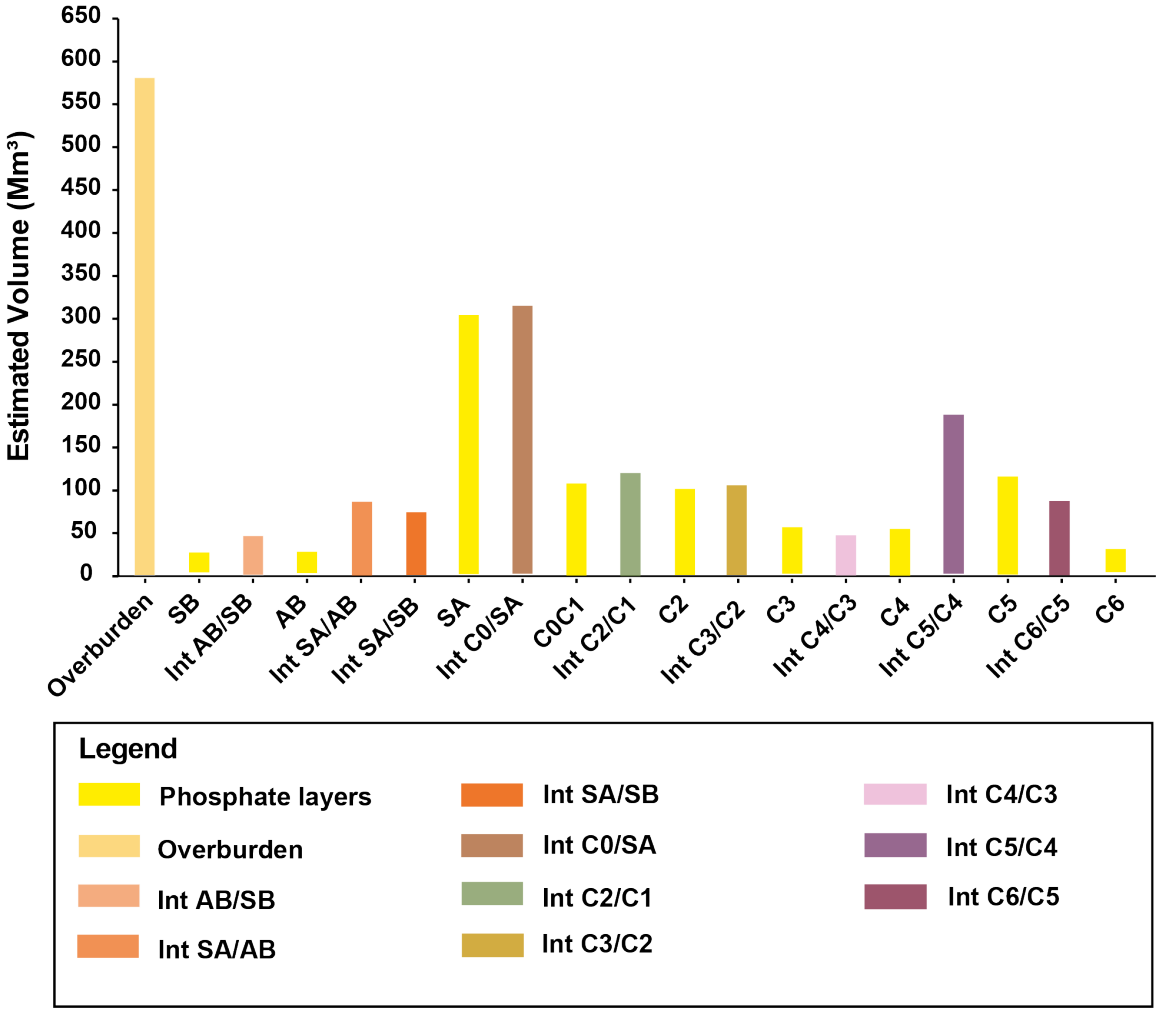

Figure 3-6: Estimated volume in Mm³ of phosphate layers and interburdens.

Once the wireframe is established, the next step is creating the block model. The block model is a discretized representation of the geological deposit, where the deposit is divided into smaller blocks or cells. Each block is assigned properties such as grade and other geological attributes. This step involves interpolating and estimating the values for each block based on the data available in the survey database and the wireframe. The final element of the 3D modeling process is to combine the waste rock and phosphate layer model blocks into a single model for presentation, economic optimization, or evaluation purposes (Desharnais, 2019).

3.3 Impact and anticipated outcomes of the project

Morocco's phosphate mines, which the OCP Group operates, play a crucial role in the country's economy. As one of the key players among public enterprises and establishments, the OCP Group contributes significantly to mitigating Morocco's internal and external macroeconomic imbalances (Labaronne, 2015). The phosphate mines hold immense importance due to their large reserves and production capacity. However, one of the significant challenges associated with these open-pit mines is the production of substantial quantities of PWR. Previous studies related to the issue of PWR have provided valuable insights into its characteristics and behavior. PWR refers to the mixture of materials deposited in stockpiles after various mining operations. The waste rock undergoes changes that alter its initial properties throughout the fragmentation, stripping, crating, and transport. These PWR are stored on the surface near the mines and become a source of landscape nuisance. The presence of these PWR piles requires extensive rehabilitation and restoration efforts. The costs involved in addressing this issue are substantial, highlighting the need for sustainable practices to minimize the impact of PWR.

This research project aims to study PWR upstream of the mining chain by adopting the geometallurgical approach. By conducting a detailed characterization, we can comprehensively understand the PWR's composition, structure, and properties. This information is crucial to predict valorization pathways and management challenges and, in turn, can help the proposition of valorization pathways. The long-term success of this endeavor will have multiple benefits, including reducing the costs associated with mine site rehabilitation and restoration. Instead of treating waste rock as a liability, the project recognizes its potential as a valuable resource that can be utilized in various industries such as civil engineering, and cement. By considering PWR as a raw material for these industries, there is an opportunity to reduce waste and contribute to the sustainable production of essential materials. By exploring these possibilities, the project seeks to promote a circular economy approach in the mining sector, where waste is transformed into valuable resources, benefiting both the environment and the economy.

Overall, this research project contributes to understanding waste rock behavior and properties and offers practical solutions for its valorization and utilization.

CHAPTER 4 ARTICLE 1: GEOLOGICAL AND GEOMECHANICAL CHARACTERIZATION OF PHOSPHATE MINE WASTE ROCK IN VIEW OF THEIR POTENTIAL CIVIL APPLICATIONS: A CASE STUDY OF THE BENGUERIR MINE SITE, MOROCCO

Preamble: This article was published in MDPI's journal *Minerals on 03 October 2023*

Minerals 2023 Vol. 13 Issue 10 Pages 1291

Accession Number: doi:10.3390/min13101291

https://www.mdpi.com/2075-163X/13/10/1291

Safa Chlahbi[1,2,*], Tikou Belem[2], Abdellatif Elghali[1], Samia Rochdane[1], Essaid Zerouali[3], Omar Inabi[1] and Mostafa Benzaazoua[1]

[1]Geology and Sustainable Mining Institute (GSMI), Mohammed VI Polytechnic University (UM6P), Benguerir 43150, Morocco.

[2]Research Institute of Mines and Environment (RIME), Université du Québec en Abitibi-Témiscamingue (UQAT), 445 Boul. de l'Université, Rouyn-Noranda, QC J9X 5E4, Canada.

[3]OCP Group, Department of Method, Planning, and Performance Benguerir, 2 Street Al Abtal Hay, B.P. Maârif, Casablanca 5196, Morocco.

4.1 Abstract

Sedimentary phosphate extraction in open-pit operations generates large volumes of waste rock (WR), which are mainly overburdens and interburdens. Traditionally, the WR is mixed and stored on the surface in waste rock piles (WRPs). This paper presents a case study of the Benguerir mine site in Morocco. It investigates the potential valorization of each WR lithology based on the geological and geomechanical properties to reduce their environmental footprint and create added value to "waste." The WR samples (soils and rocks) were collected from drill cores and mining trenches in the Benguerir mine. The geological characterization results using petrographic descriptions indicate the presence of nine phosphate layers and, in addition to the overburdens, eight interburdens. Four types of WR are identified: carbonate, siliceous, marly clay, and phosphate. The geomechanical characterization of soil-like samples showed an average plasticity index (PI) of 50% according to the methylene blue value (MBV) of 7.1, classifying them in the

A3–A4 categories as plastic and clayey marl soils. The hard rock samples have excellent mechanical properties in terms of their uniaxial compressive strength (UCS), Los Angeles abrasion value (LA), and micro-Deval value (MD). The average compressive strength is 104 MPa for the flint, 35 MPa for the phosphate flint, 32 MPa for the silexite, 26 MPa for the limestone, 11 MPa for the indurated phosphate, and 8 MPa for the marly limestone. Based on the results obtained, these WRs can be considered as an excellent alternative secondary raw material for use in civil engineering applications, ceramics, and cement industries**.**

Keywords: phosphate waste rock; valorization pathways; geological characterization; geomechanical properties.

4.2 Introduction

Mining operations throughout the world generate large amounts of mining waste (e.g., waste rock, tailings, and sludge), most of which is stored in surface stockpiles, such as waste rock piles or tailings storage facilities (TSFs) for tailings or sludges (Amos et al., 2015). Mining, minerals, and sustainable development (MMSD) assesses around 3500 active mining waste sites all around the globe, including TSFs and WRPs (Krishna et al., 2020). Mining operations generate approximately 100 billion tons of solid waste annually (Tayebi-Khorami et al., 2019). This mining waste may create major environmental hazards if not properly managed and can significantly contribute to environmental pollution through air pathways and water leaching (Adiansyah et al., 2015; Krishna et al., 2020; Lèbre & Corder, 2015). Mine waste management activities contribute to removing or minimizing environmental issues. During the last decade, several strategies emerged to provide a framework for sustainable mining development. With this initiative in mind, the mining industry must find ways to reuse or valorize waste to mitigate the environmental impact of its mining operations.

In the context of mining in Morocco, the exploitation of immense phosphate deposits presents the approaches in a favorable geological context, thus guaranteeing the diversity and abundance of mineral resources. Thus, the mining industry occupies an important place in the development of the national economy. Phosphate ore in Morocco is extracted by open-pit mining method. The extraction is performed through the strip-mining method. This method involves cutting the deposits into a group of panels and dividing the panels into 40 m-large trenches. This method includes a set of mining operations: the drilling, blasting, stripping, loading, and transportation of phosphate. The

stripping ratio represents the amount of waste (overburden) that must be removed to extract a given amount of ore. A strip ratio of 3:1 means that 3 tons of waste rock are produced to extract 1 ton of phosphate rock. For 4.2 million tons (Mt) of phosphate rock annually extracted in 2020, the estimated mass of waste rock stored in piles was 12.3 Mt (OCP Group Benguerir Mine, Benguerir, Morocco). Indeed, this extraction method generates large volumes of waste (~3.8 million m^3) composed mainly of carbonates, clays, marls, and flints, which correspond to overburdens and interburdens. Preliminary studies showed that this waste may present properties similar to many raw materials used in the civil engineering sector (Hakkou et al., 2016). The extracted phosphate waste is pushed by D11 bulldozers or moved by dragline into the previous trench already exploited (n − 1) to form piles or is transported to a storage area. This waste is a source of landscape nuisance due to the accumulation of by-products in large areas, which are rehabilitated with difficulty.

The deposition of WR in piles generates the segregation of fine and coarse materials (Amos et al., 2015). The waste rock is considered as a heterogeneous material in terms of its physical, chemical, mineralogical, and geomechanical properties (Elghali et al., 2018; Lahmira et al., 2016). This heterogeneity is the main challenge in WR piling (Aubertin et al., 2002). For instance, the main factors influencing the piles' physical (geotechnical) instability are the geometric configuration, the properties of the materials, the topography of the site, the construction method, and the climatic and hydrological conditions (Aubertin, 2013; Aubertin et al., 2002; Maknoon & Aubertin, 2021). The stability analysis of WRPs must consider all these factors for the optimal design selection and determination of the probable risks (Aubertin, 2013). In terms of chemical stability, the risk of surface and groundwater pollution due to phosphate mining operations is generally low because of the high carbonate content in waste rocks (Bossé et al., 2013).

The valorization or reuse of mining waste is challenging for the global mining industry because of economic reasons and the climate emergency (Nwaila et al., 2021; Tayebi-Khorami et al., 2019). This can alleviate the growing demand for construction materials or civil engineering works by preserving the natural resources in materials and can reduce land use. Indeed, the potential reuse of mining by-products has been studied in the last decade to reduce or minimize the intense generation of mining waste and improve environmental management (Hakkou et al., 2016; Krishna et al., 2020). In general mining industry practice, waste rock is reused on the surface for road construction and reclamation purposes (Bossé et al., 2013; Hakkou et al., 2009; Hakkou et al., 2016) and underground as cemented or uncemented rock fill (Lee & Gu, 2017; Liu et al., 2017;

Pagé et al., 2019). However, outside of mining sites, the reuse of WR still needs to be improved (Aubertin et al., 2002; Taha et al., 2017b; Zhang, 2013). Indeed, several studies have evaluated the technical potential of the valorization and reuse of mining waste as secondary or alternative raw materials to supply other industries, such as civil engineering, ceramic industries, cement, and geopolymers manufacturing.

Some authors (Amrani et al., 2019; Hakkou et al., 2016) suggest that PWR presents promising geotechnical properties and can be reused as materials for road construction. In addition, mining waste can be used as an alternative material to produce aggregates (El Machi et al., 2021a; Loutou et al., 2013), fired bricks (Loutou et al., 2019; Taha et al., 2017b; Zhang, 2013), ceramic materials (Taha et al.,Abbas et al., 2017; Ahmari & Zhang, 2012; Eliche-Quesada et al., 2015; Guo et al., 2014; 2016a; Yang et al., 2013), and cement (Peyronnard & Benzaazoua, 2011); they can also be used for the restoration of mining sites (Bossé et al., 2013; Hakkou et al., 2009). The valorization or reuse of PWR as a secondary raw material might allow the conservation of natural resources and the reduction in the environmental footprint (Loutou et al., 2019). The reuse of mine WR in any valorization pathway depends on its basic chemical, mineralogical, and geotechnical properties.

This paper focuses on the lithology of phosphate extraction waste from the Benguerir mine in Morocco. The novelty of this paper lies in the fact that it deals with the problem of managing natural materials (which, at present, have the status of waste) upstream of the mining chain. Most papers deal with the problem downstream, i.e., after the ore is recovered and everything else is mixed and deposited. This approach is crucial because it allows for a more comprehensive understanding of the entire process, from extraction to disposal, and identifies opportunities for improvement at every stage. For this purpose, the main objective of this study is to describe the different lithologies of the interburdens and to evaluate their geomechanical proprieties in view of their potential applications. The specific objectives of this paper are: i) the detailed geological and geomechanical characterizations of WR found in the interburdens, and ii) the proposition of valorization scenarios for the studied WR based on their characteristics.

4.3 Materials and methods

4.3.1 Mine site and drill core locations

The study area is one of the parcels of the Gantour basin, "Benguerir mine," located 70 km north of Marrakech and 17 km east of Benguerir city. The Benguerir deposit is located in Western Meseta. Two well-individualized Paleozoic massifs are bound it: the Rehamna massif to the north (metamorphic and crystalline rocks) and the Jbilet massif (schists) to the south. The Benguerir deposit is a sedimentary type (El Bamiki et al., 2021; Mouflih, 2015). The phosphate series extends from Maastrichtian to Lutetian and is presented as phosphate layers and waste interburdens (Boujo, 1976). This deposit is an extended east–west plateau, with altitudes ranging between 396 and 596 m (Figure 4-1).

Six vertical drill cores (non-destructive technique) of varying depths between 60 and 95.5 m were created to understand the structure and composition of the Benguerir phosphate series (Figure 4-1). The core drillings were labeled as SC02, SC03, SC04, SC05, SC06, and SC07. Core drillings were conducted by the PTSL (Public Testing and Studies Laboratory), according to the XP P94-202 standard (XPP94-202, 1995). The cut rock cylinder was progressively placed in the inner tube of the core, which was 1.5 m long and 116 mm in diameter.

The coring technique used an injection of water mixed with additives (bentonite and polymer) to facilitate drilling, improve the lubrication of the rod, cool the crown, and control any possible influx or loss of fluids by stabilizing the borehole walls.

The location of the drill holes was chosen so that the entire mine was covered while targeting future mining trenches. The non-destructive technique made it possible to recover a continuous and intact sample cylinder (core) from the existing lithologies and to preserve the geological structures (faults, joints) as well as the textures of the rocks. For the characterization tests, some core samples were wrapped in paraffin films to preserve their natural moisture levels.

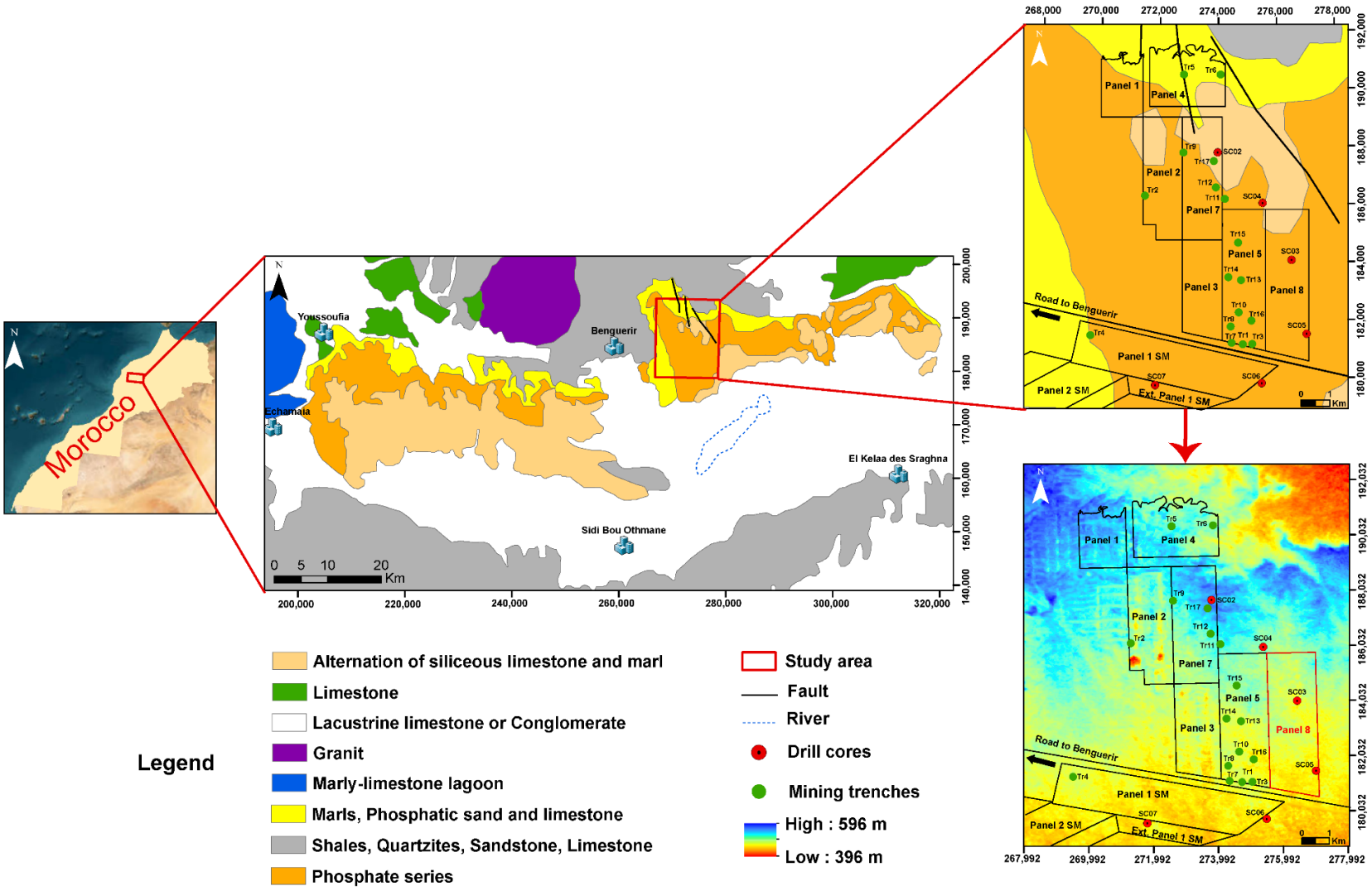

Figure 4-1: Schematic description of the Gantour basin geology (based on the 1:1000000 geological map of Morocco)

4.3.2 Sampling strategy and methodology

The sampling strategy for this study was performed by combining random and targeted methods. Two criteria were used: the facies and the availability of the quantities needed for the analysis. The random method was used to collect samples from the mining trenches (Tr1, Tr2, Tr3, Tr4, Tr5, Tr6, Tr7, Tr8, Tr9, Tr10, Tr11, Tr12, Tr13, Tr14, Tr15, Tr16, and Tr17), depending on the availability and accessibility of the layers to be sampled. The targeted method was used to obtain samples from the drill cores (SC02, SC03, SC04, SC05, SC06, and SC07). To ensure a representative sample, attention was paid to the lithological and structural descriptions to identify the parameters likely to impact the geomechanical characterization. These sampling approaches enabled us to collect representative intact samples. The methodology adopted for this study is shown in Figure 4-2.

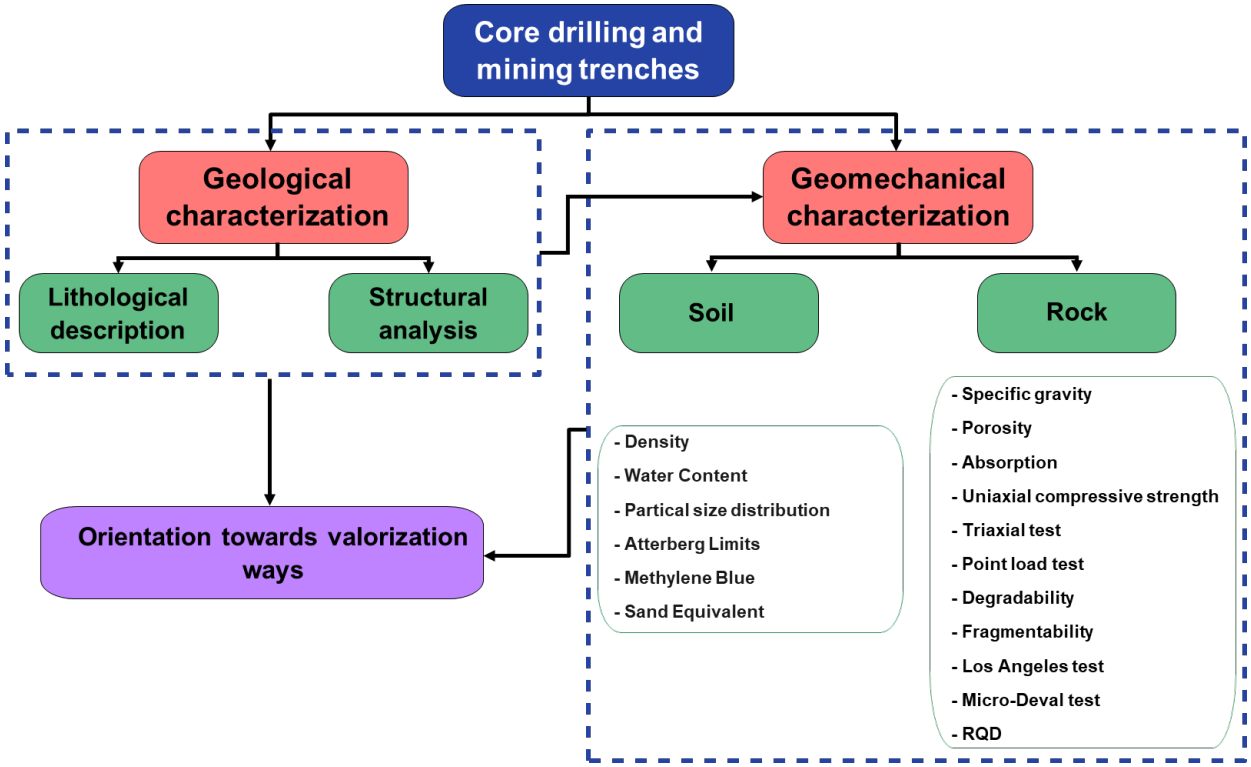

Figure 4-2: Schematic view of the methodological approach used

Seven soil samples were collected from the C2/C3 interburdens of the Benguerir mine (see Figure 4-3), which was a thick interburden and remarkable for its yellow color. Three samples (A, B, and C) were taken from boreholes (SC02, SC04, and SC06), and four samples (Tr1, Tr2, Tr3, and Tr4)

from mining trenches. The samples collected from the mining trenches involved using a hammer and hand shovel. The samples collected were placed in plastic bags, while the samples collected from the core were wrapped in paraffin film to keep their initial properties.

4.3.3 Structural characterization

The structural characterization allowed us to obtain general information about the layers' nature, position, thickness, dip, etc. The techniques used in the structural characterization included core logging and structural analysis using the rock quality designation (RQD). The cores were deposited in a natural order. Geological and structural descriptions were created to establish the lithological log. Drill core logging was performed as follows:

- Wetting the core to reveal the contrasts;
- Using hydrochloric acid (HCl) to test the presence or absence of carbonate;
- Identifying the hardness of the samples using basic techniques (glass, finger, or steel scraping);
- Petrographic descriptions.

In the logging, the following parameters were described: the thickness of each lithology, the chronological succession of the geological layers, and the presence of allochemes.

The structural descriptions of the drill cores were created using the rock quality designation, which was a crude indicator of rock quality(Deere, 1964). RQD is defined as the percentage of intact drill core pieces longer than 100 mm over the total drilling length (Farid, 2013), and it is calculated as illustrated in Equation (4.1):

$$RQD = \frac{\sum Length\ of\ core\ pieces > 100\ mm\ length}{Total\ length\ of\ core\ run} \times 100 \qquad (4.1)$$

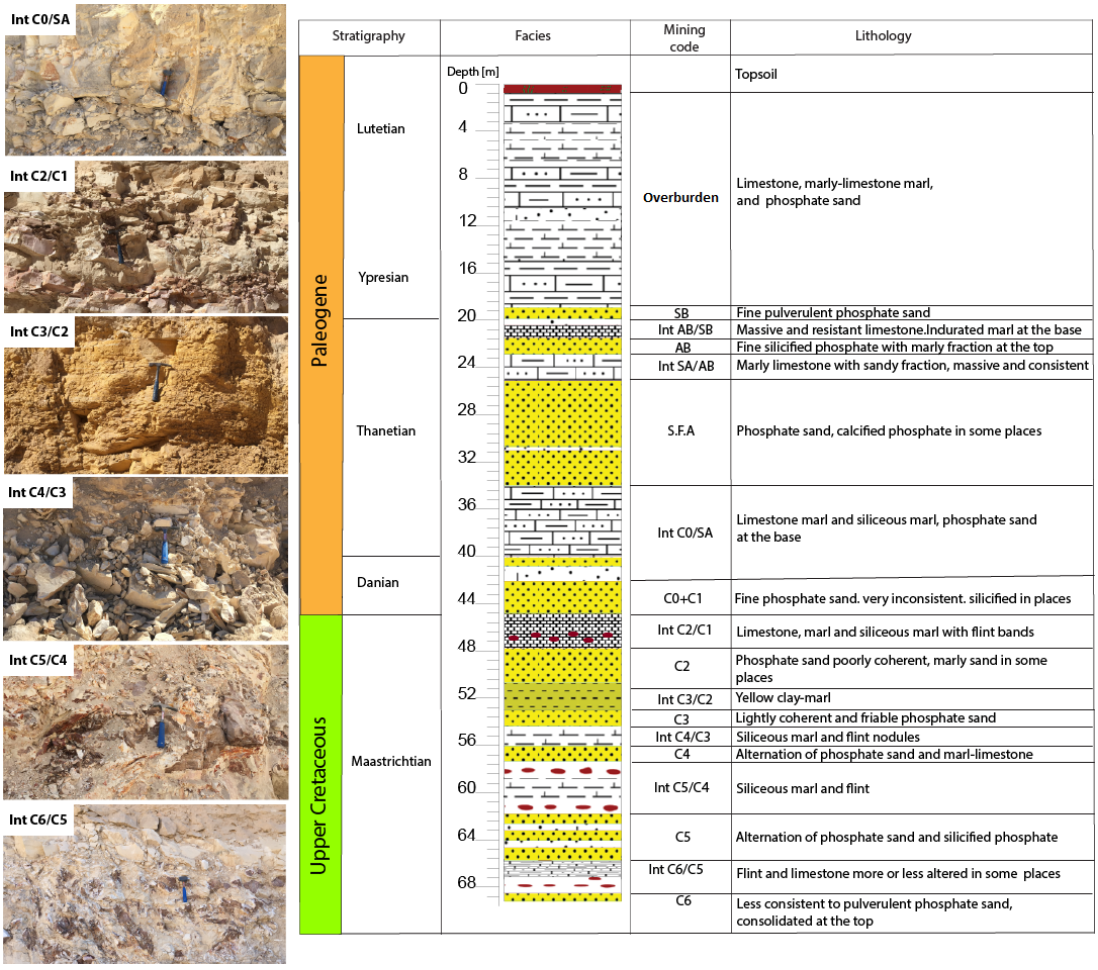

Figure 4-3: Synthetic litho-stratigraphic section of the Benguerir mine

4.3.4 Geomechanical characterization

The geomechanical characterization presented in this paper involves rocks and soil-like samples taken from different lithologies and depths. The geomechanical characterization was performed for each core drilling, and some samples were taken from the mining trenches. Laboratory tests were conducted to determine the mechanical and physical properties.

The gravimetric water content of the samples was measured using the oven-drying method (NM13.1.152) (NM13.1.152, 2011), while the bulk density was measured using the water-immersion method (NM13.1.119) (NM13.1.119, 2009). The particle size distribution was determined using two techniques: dry sieving after washing to remove particles more than 80 µm in size and sedimentation with deflocculant for fine particles (NM00.8.083 and NM13.1.008 standards) (NM00.8.083, 2015; NM13.1.008, 1998). The Atterberg limit test was performed on the

0/400 µm fraction to determine the liquid limit (LL), plastic limit (PL), and plasticity index (PI) according to the NF-P94-052-1 and NF-P94-051 standards (NF-P94-051, 1993; NF-P94-052-1, 1995). The methylene blue value (MBV), which measured the adsorption capacity of soil material, was determined on a fraction < 5 mm, according to the NM00.8.095 standard (NM00.8.095, 2015). The sand equivalent (SE) was measured on the 0/2 mm fraction in fine aggregates according to the NF EN 933-8+A1 standard (NF EN 933–8+A1, 2015). This test aimed to rapidly evaluate the relative portion of clay in the sand.

The characterization of hard rock samples was evaluated for the various rock units within the interburdens. Six lithological facies (limestone, marly limestone, flint, phosphate flint, silexite, and indurated phosphate) were studied. The tests on the hard rock samples allowed us to determine the physical and mechanical properties, the uniaxial compressive strength (UCS or σ_c), and the resistance to fragmentation and wear by mutual friction of the elements of an aggregate. Specific gravity, porosity, and absorption are the primary physical properties of rocks. These properties were measured in accordance with NF P94-410-1, NF P94-410-2, and NF P94-410-3 standards (NF P94-410-1, 2001; NF P94-410-2, 2001; NF P94-410-3, 2001). These physical properties were widely used to evaluate and compare different correlations between the samples and lithologies. The UCS should be determined from uniaxial compression tests. However, in this study, the UCS values were indirectly derived from other tests, such as point load and triaxial tests, using empirical equations in order to obtain more compressive strength data. The UCS test was performed in accordance with the NF P94-420 standard (NF P94-420, 2000) on core samples (cylindrical specimens with a circular cross-section). The triaxial tests were performed under consolidated-drained (CD) conditions in accordance with the NF P94-074 standard (P94-074, 1994). This test involved shearing at least three specimens from the same sample. The intrinsic parameters obtained from this test were cohesion (c') and friction angle (ϕ). These parameters were used to calculate the uniaxial compressive strength. The PLT is an alternative method to obtain the UCS indirectly and can be performed on rock samples without using special preparation techniques. The rock samples were compressed between two conical steel plates until failure occurred, in accordance with the XP P 94-429 standard (XP P 94-429, 2002).

In order to measure the sensitivity of these materials to fragmentation and degradability under the effect of mechanical stress and climatic cycles, several geomechanical characterization tests were performed to evaluate the materials' resistance regarding fragmentation and wear under the effect

of mechanical solicitations. The fraction of +10/-14 mm was chosen for the determination of the Los Angeles abrasion and micro-Deval values in accordance with the NF EN 1097-1 and NM.10.1.138 standards (NF EN 1097-1, 2011; NM.10.1.138, 1995). The resistance to the fragmentation and degradability coefficients of the samples were measured on the 40/80 mm fraction in accordance with the NF P94-066 and NF P94-067 standards (NF P94-066, 1992; NF P94-067, 1992), respectively.

4.4 Results and discussion

4.4.1 Geological characterization: Lithological description and rock quality by RQD

- **Lithological description and rock quality by RQD**

A significant variety of lithological formations characterized the phosphate series of the Benguerir mine. This series comprised nine phosphate and eight waste layers (interburdens) (Figure 4-3). In addition to the interburdens, other layers were called “phosphate Slabs” with carbonate or siliceous matrices. They were generally found at the wall or between the phosphate layers, and their numbers differed from one area to another. Four types of waste rock were identified: carbonate (limestone and marly limestone), siliceous (flint and silexite), marly clay, and phosphate (phosphate flint and indurated phosphate). The nine interburdens were left in place in piles. From top to bottom, the following interburdens (Int) were identified:

- Int AB/SB: composed of massive and competent limestones, topped by a phosphate limestone/ phosphate flint with coprolites. Indurated marl at the base.
- Int SA/AB: composed of marly limestone with a sandy fraction. It is large and consistent.
- Int C0/SA: this interburden has a thickness that exceeds 8 m and is composed of limestone and whitish siliceous marl mottled with iron and manganese oxides. Phosphate sand at the base.
- Int C2/C1: composed of an alternation in grayish limestone, whitish siliceous marl, and compact beige marl with flint bands at the base.
- Int C3/C2: composed of yellow clay marl. At the top, there is a calcified sandy marl.
- Int C4/ C3: composed of siliceous marl and brown flint nodules.
- Int C5/C4: composed of an alternation in whitish siliceous marl with brown flint. Passage of phosphate marly sand in the middle.
- Int C6/C5: composed of an alternation of limestone and brown flint.

The phosphate rock series of the Benguerir mine is affected by silicification and dolomitization. Due to the circulation of groundwater rich in silica or magnesium in the existing veins and fractures, the silica is deposited, and depending on the degree of silicification, nodules of quartz or flint are formed. However, in the case of dolomitization, the magnesium ions replace the calcium ions present in the carbonate rocks; therefore, the limestone rocks are transformed into dolomites.

According to the litho-stratigraphic correlation presented in Figure 4, the study area constitutes a non-horizontal litho-stratigraphic series (folded series) with quasi-variable thicknesses. This deformation can be justified by the presence of faults to the north of the series and by being adjacent to the Paleozoic basement of Rehamna. The average thickness of each unit can be seen in Figure 4-3. The sequence of units appears to be relatively stable in space but with quasi-variable thicknesses and sometimes interrupted units (i.e., no thickness in some drill holes, the case of AB interburdens).

The total RQD of the study area was calculated by averaging the RQD values of each borehole (Figure 4-4). The effect of the difference in run lengths could be eliminated by weighing this average by the length of each run for each drill hole (geometric average). The total RQD was 23%; therefore, according to Deere's classification in 1968, the rock mass quality of the studied area could be qualified as very poor (fractured rock mass).

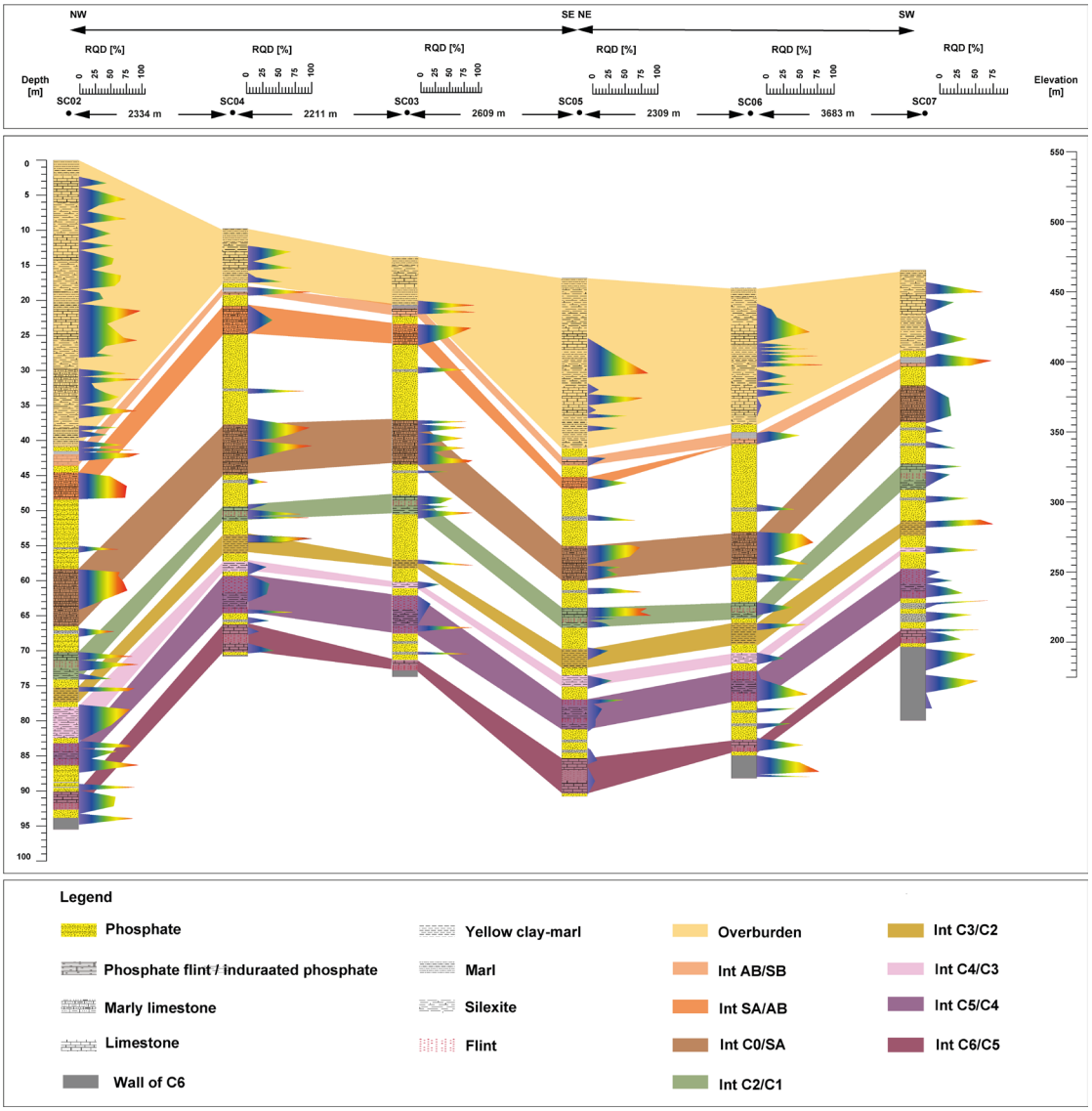

Figure 4-4: Cross section NW-SE and NE SW and the variation of RQD of the Benguerir mine

4.4.2 Geomechanical characterization

a. Soil-like samples

Table 4-1 presents the results of the physical and geomechanical characterizations of the soil-like samples. The studied soil-like samples, located in the C3/C2 interburdens, were characterized by a thickness exceeding 3 m, and the mustard yellow color was remarkable in the phosphate series. The C3/C2-level soils had relatively low natural water contents that varied between 4.5% and 7.5%, with an average of 5.9%. These variations in the natural water content could be related to the quantity of fine or clayey elements in the analyzed samples. The bulk density varied between 1824

and 1917 kg/m^3 with an average of 1886 kg/m^3. The sand equivalent test result shows the presence of a fine material. The results of the methylene blue values obtained vary between 6 and 10, which indicates the presence of clayey soil. Indeed, the soil-like samples were composed of particles sized $d < 80$ µm (or $P_{80\mu m}$) to at least 91%, except for sample (C) where $P_{80\mu m} = 64\%$. Particles smaller than 2 µm (clay size) were present in more than 38%. The Atterberg limits showed that these soils were plastic to very plastic. Figure 4-5A shows the plasticity chart; most of the samples are located above the "A Line", which means that they are clays with high plasticity, except for sample "Tr4", which is located below this line and corresponds either to inorganic silts of variable compressibility or to elastic silts or organic clay.

Table 4-1: Physical and geotechnical properties of soil-like samples.

		Samples C3/C2							Standard deviation
Variables	Units	A	B	C	Tr1	Tr2	Tr3	Tr4	
w	[%]	-	-	-	4.5	7.5	5.1	6.5	1
ρ	[kg/m^3]	-	-	-	1892	1917	1824	1912	31
P_{max}	mm	0.1	10	25	0.3	1	0.3	0.1	7
$P_{80\mu m}$	[%]	100	91	64	98	97	98	100	8.6
$P_{2\mu m}$	[%]	74	70	52	38	41	38	45	12
MBV	-	9.2	10	6	6.13	6.22	6.07	6.32	1.4
SE	[-]	-	-	-	*FS*	*FS*	*FS*	*FS*	-
LL	[%]	106	109	95	75	83	65	60	16
PL	[%]	37	39	35	32	38	27	35	3
PI	[%]	69	70	60	43	45	38	25	14

w: water content; ρ: bulk density; P: particle size; *MBV*: methylene blue value; *SE*: sand equivalent; *LL*: liquid limit; *PL*: plastic limit; *IP*: plasticity index; *FS*: fine sand.

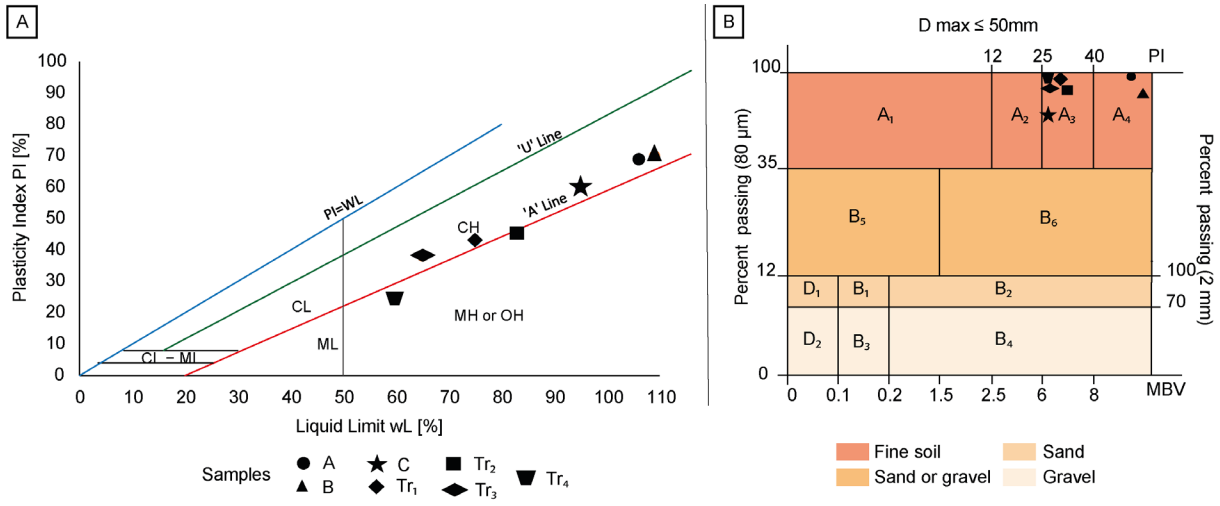

Figure 4-5: A) Plasticity chart, and B) Classification of studied soil-like based on soil classification (NF-P11-300, 1992).

According to the results of the physical characterization and the road earthwork guide (REG) classification NF-P11-300 (NF-P11-300, 1992), the C3/C2 interburden soil can be classified in the A3–A4 category (fine soil); plastic to very plastic; and the category of clayey marl (Figure 4-5B). This soil was significantly cohesive with medium and low water contents and was sticky or slippery when wet.

b. Hard rock samples

Figure 4-6 shows the variation in the UCS with the depth and rock unit for each borehole. The overall results show that the variation in the UCS does not depend on the depth, but rather on the facies encountered and on the quality of the terrain, i.e., the presence of micro-faults and faults that affect the geomechanical properties of the rock unit. Flint has the highest average UCS value of 104 MPa, followed by phosphate flint (35 MPa), silexite (32 MPa), limestone (26 MPa), indurated phosphate (11 MPa), and marly limestone (8 MPa) (Appendix B). Specific gravity, porosity, and absorption are shown in Appendix B. The specific gravity values vary in the range 1.4–2.5. Flint and phosphate flint have high specific gravity values and low porosity and absorption values. For the limestone, three categories can be distinguished: i) porous limestone with more than 30% porosity, with a specific gravity in the 1.5–1.8 range; ii) medium-porosity limestone (the most abundant type) with a porosity value between 10% and 30% and an average specific gravity value in the 1.7–2.3 range; and iii) compact limestone with a porosity lower than 10% and a specific gravity value in the 2.3–2.5 range. Silexite has a medium specific gravity value (1.6) and low

porosity and absorption values (< 16%). Marly limestone and indurated phosphate present higher porosity and absorption values (44.5% and 31% for Marly limestone and 38% and 23% for indurated phosphate) and low specific gravity values (< 2).

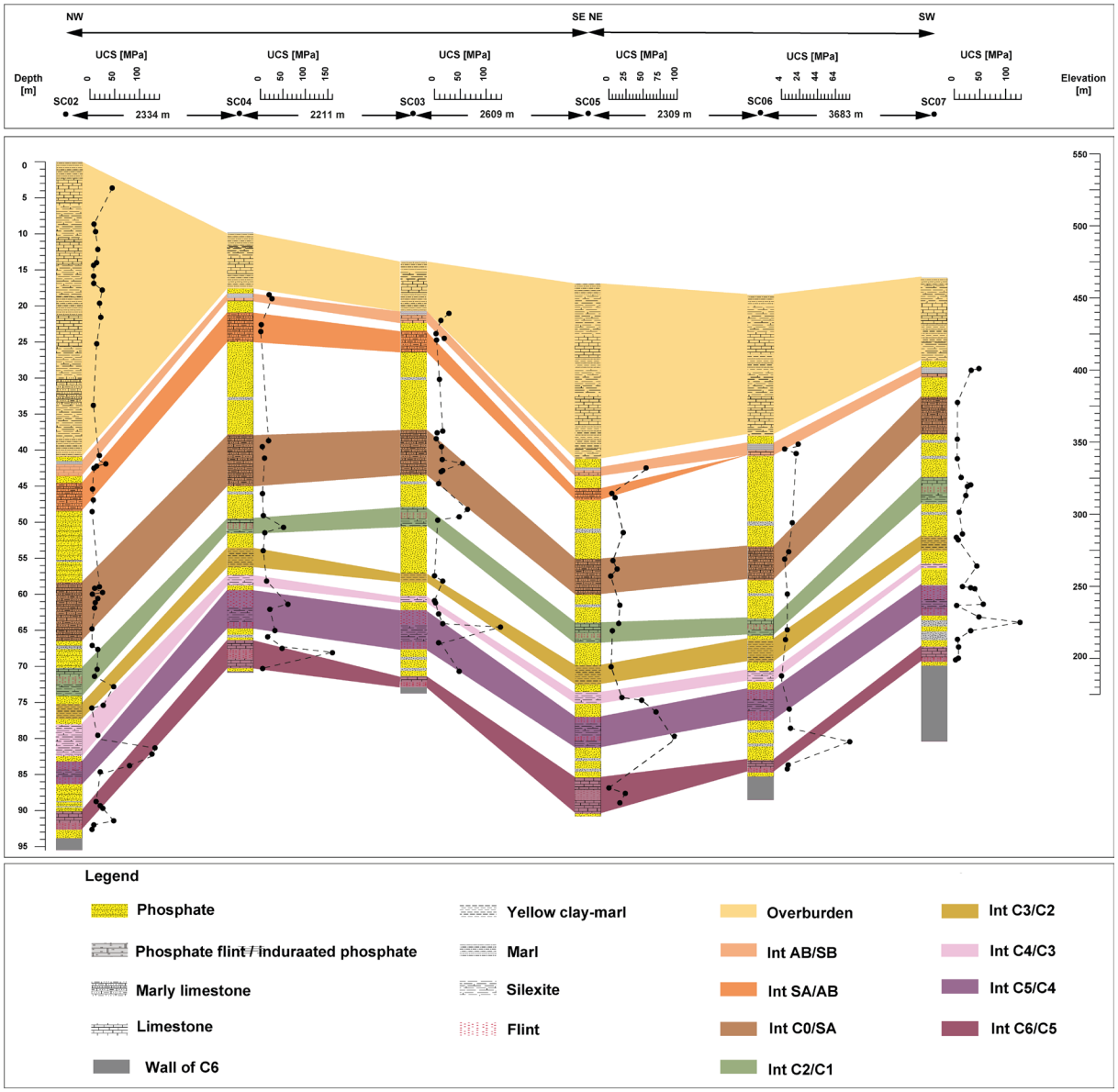

Figure 4-6: Variation of the UCS with the depth and the rock unit for each borehole.

The results of the mechanical characterization tests are summarized in Table 4-2. The fragmentability and degradability indices are, respectively, lower than thresholds 7 and 5 of the earthwork's material classification NF-P11-300 standard (NF-P11-300, 1992), except for a few samples of indurated phosphate, phosphate flint, and limestone. The tested materials can be considered poorly to moderately fragmentable and degradable under hydric solicitations. For the Los Angeles test, the flint, phosphate flint, and a few samples of limestone and silexite have LA (%) values below the 50% threshold. These results mean that these samples have good fragmentation resistance and good hardness properties according to the ACI 211.1 and NF EN 12620 standards (Dixon et al., 1991; NF EN 12620, 2008). Thus, these waste rocks can be used as aggregate and support the various stresses associated with pavement foundation constructions (El Machi et al., 2021a; Safhi et al., 2022). The micro-Deval coefficient values show that flint and some phosphate flint samples have values lower than 35%; they are the most suitable for use as aggregates.

Table 4-2: Physical properties of the hard rock samples.

Tests	**Los Angeles (%)**	**Micro-Deval (%)**	**Fragmentability**	**Degradability**
Flint	22–39 (6)	9–48 (12)	1–2 (0.5)	1 (0)
Phosphate flint	29–33 (2)	28–40 (6)	2 (0)	1 (0)
Silexite	35–75 (13)	39–88 (15)	2–6 (1.5)	1–1.4 (0.2)
Limestone	24–77 (15)	37–98 (18)	1–6 (1.1)	1–12 (4.3)
Indurated phosphate	76–93 (4.5)	94–100 (2)	6–11 (2.3)	1–5 (2)
Marly limestone	86–99 (2)	96–100 (6)	6–9 (0)	1–5 (0)

Values in parenthesis refer to the standard deviation.

4.4.3 Implication results and discussion

The phosphate waste rock from the Benguerir mine presented a wide range of properties (lithological, mineralogical, and physical–mechanical), promoting their use in several applications. The geomechanical properties and potential ways of valorizing PWRs are summarized in Table 4-3. The results of the characterization of the hard rock samples show that the C5/C4 and Int C6/C5 interburden flints have good physical and mechanical properties in terms of UCS (up to 64 MPa), LA (lower than 40%), and MD (lower than 48%). The flint is a siliceous, cryptocrystalline, and extremely hard siliceous rock with an average UCS of about 600 MPa (Aliyu et al., 2019). In a study performed by (Safhi et al., 2022), the flint from Benguerir mine revealed the presence of SiO_2 (93.6%), CaO (1.6%), P_2O_5 (1.9%), and 1.8% loss on ignition (LOI), with a corresponding mineralogical composition of quartz (95%), calcite (1.8%), and apatite (1.2%). This flint can be used in the civil engineering sector. Flint lithology requires simple crushing to be used as an aggregate in the ballasts of railroads, embankments, layers forming road structures, or other advanced uses, such as an aggregate of high-performance concrete. (El Machi et al., 2021a; Safhi et al., 2022; Sidibé, 1995).

Table 4-3: The geomechanical properties and potential valorization methods.

			Lithology						
		Units	Flint	Phosphate Flint	Silexite	Limestone	Indurated Phosphate	Marly Limestone	Clayey Marl
Geomechanical proprieties	*UCS*	[MPa]	104	35	32	26	11	8	
	LA	[%]	33	31	50	62	88	95	
	MD	[%]	33	34	65	81	98	98	
	Fragmentability	-	2	2	3	4	9	7	
	Degradability	-	1	1	1	4	2	3	
	Specific gravity	-	2.5	2.2	1.6	1.9	1.9	1.7	
	Porosity	[%]	3	19	12	25	28	33	
	Absorption	[%]	1	9	6	14	15	20	
	w	[%]							6
	ρ	[kg/m^3]							1886
	D_{max}	mm							5
	< 80 µm	[%]							93
	< 2 µm	[%]							51
	MBV	-							7
	SE	[%]							Fine sand
	LL	[%]							85
	PL	[%]							35
Valorization methods	Aggregate		X	X	X	X			
	Lightweight aggregate				X				
	Concrete		X		X	X			
	Asphalt		X			X			
	Road construction		X	X		X			
	Embankment							X	X
	Brick manufacturing								X
	Cement				X	X		X	X
	Field ceramics								X
	Neutralization					X		X	
	Recovery of phosphate			X			X		

Silexite is generally located at Int C4/C3 and Int C5/C4. It is a siliceous marl with a purplish-pink color. The silexite mainly comprises 80% SiO_2, 4.5% of CaO, and 3.7% of MgO, with a corresponding mineralogical composition of quartz and dolomite (Safhi et al., 2022; Sidibé, 1995). Using silexite in civil engineering projects can provide a range of economic benefits. Its importance in civil engineering is due to its ability to provide ideal material for construction purposes (aggregate), particularly in the form of crushed stone, sand, and gravel. This rock is also used in various forms as a lightweight aggregate due to its low density, which is used in the production of concrete and other building materials. Furthermore, due to its high strength and low cost, silexite can be used as an aggregate for construction projects, such as bridges, dams, and other structures. Additionally, silexite can be used as a natural filler in the production of concrete in order to reduce the cost of the material without compromising its strength and durability (Safhi et al., 2022).

Phosphate flint and indurated phosphate are generally located at Int AB/SB, A3/A2, C5M/C5S, and C5I/C5M. These two facies (phosphate flint and indurated phosphate) are grouped in the phosphate waste category. In a previous study by Safhi et al. (2022), the mineralogical characterization of phosphate flint revealed the presence of phosphate grains as apatite (38.3%) and quartz (47.5%), which were the major minerals that cemented the phosphate grains. Indurated phosphate constitutes the phosphate grain as fluorapatite (48%), bioclasts, and coprolites; these elements are cemented by micrite dominated by carbonates (Redclift, 2005). The geomechanical characterization of phosphate flint presents good mechanical properties (UCS = 35 MPa, LA = 31%, and MD = 34%), which means that it can be valorized as an aggregate and for road construction due to its high resistance to weathering, and its ability to provide a durable and cost-effective pavement material. While indurated phosphate presents weak properties (UCS = 11 MPa, LA = 84%, and MD = 97%) and it is not recommended to use or valorize it in the field of civil engineering, on the other hand, approaches to exploit it have been introduced in the studies, such as screening, sorting, and further processing methods (Amar et al., 2022; Safhi et al., 2022).

The carbonate category (limestone and marly limestone) is the most abundant in the phosphate series, almost occurring in all the interburdens. This category presents a variation in mechanical properties ranging from low to high values. They can be valorized as raw materials in civil engineering (El Machi et al., 2021b; Safhi et al., 2022), ceramic applications, and the cement industry (Bahhou et al., 2021a). Additionally, they can be used to control acid mine drainage, due

to their high carbonate content (43%) (Amar et al., 2022; Bossé et al., 2013), and as a stabilizing agent for acidic tailings (Hakkou et al., 2009; Knidiri et al., 2015).

The soil-like samples analyzed in this study were located at the Int C3/C2 interburden. It corresponded to clayey marl with high plasticity. These samples were materials with good geotechnical behavior, which could be used as raw materials, especially in embankment brick manufacturing, cement, and field ceramics (Bahhou et al., 2021b; Bayoussef et al., 2021a; Hanein et al., 2021; Safhi et al., 2022; Safhi, 2022).

The valorization of PWR is an important step in overcoming the challenge of waste management and reducing the environmental impacts of phosphate mining. It can produce valuable waste products, supporting green production and recycling in the phosphate industry. Moreover, it can create economic and environmental benefits for local communities by providing additional resources that can be sold for profits. Furthermore, the technologies used in the valorization of phosphate waste rock can be applied in other industries to create sustainable solutions. It is evident that the valorization of PWR can effectively address the problem of phosphate waste disposal and should be considered when implementing clean and efficient solutions in the phosphate industry.

The integration of the mining circular economy in the mining industry relies on the creation of a sustainable model that satisfies a three-facet equilibrium: economic, environmental, and social (Amar et al., 2022; Redclift, 2005) (Figure 4-7). The valorization of PWR is a major concern regarding their environmental footprint and the development of the mine. The phosphate industry can ensure the valorization of waste rock to preserve natural resources and reduce land-use impacts.

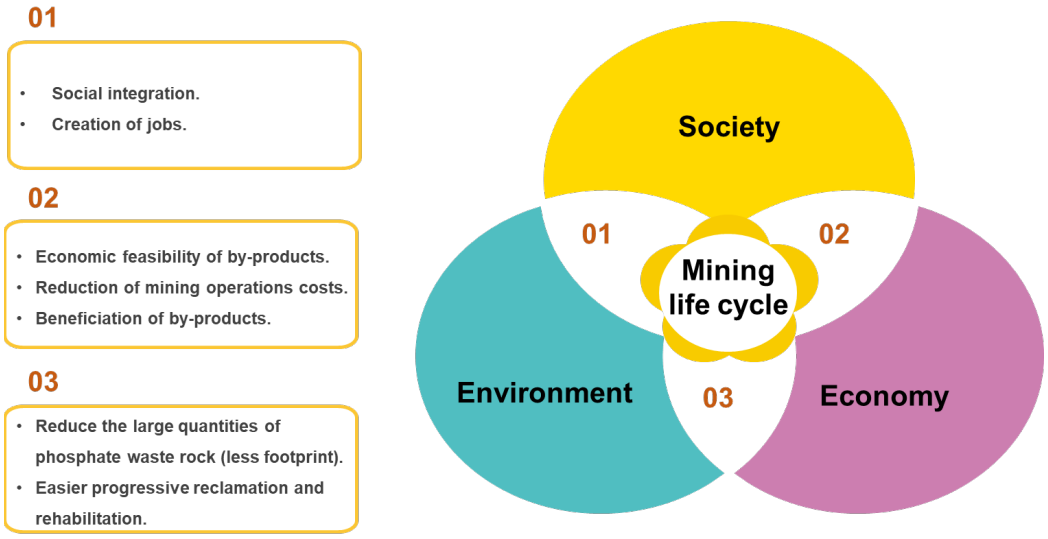

Figure 4-7: Sustainable mining practices

4.5 Conclusions

The present study investigated the potential application of each PWR lithology sample based on geological and geomechanical properties. The experimental work on the soil-like and hard rock samples collected from the six drill cores and mining trenches at the Benguerir mine site in Morocco presented the following conclusions:

- The Benguerir phosphate series was composed, in addition to overburden, of nine phosphate and eight waste layers (interburdens). The existence of other levels called "phosphate slabs" with carbonate or siliceous matrix was present.
- Four types of waste rock were identified: carbonate (limestone and marly limestone), siliceous (flint), marl clay, and phosphate (phosphate flint and indurated phosphate).
- The unit sequences of the Benguerir deposit appeared to be relatively stable in space but with variable thicknesses and sometimes interrupted units.
- The soil-like samples were classified in the category A3–A4 (fine soil), plastic to very plastic, and the category of clayey marl. They could be used as raw materials, especially for brick manufacturing, cement, and field ceramics.
- The hard rock samples presented promising geomechanical properties and could be considered an excellent alternative secondary raw material for civil engineering, the cement industry, and phosphate recovery.

It is recommended to complete this study by other types of characterizations (chemical, mineralogical, and environmental) to evaluate all the properties.

Supplementary Materials: The following supporting information can be downloaded at: https://www.mdpi.com/article/10.3390/min13101291/s1, Figure S1: UCS intervals for the six facies.; Figure S2: variations in specific gravity values with porosity for the six facies; Figure S3: variations in porosity values with absorption for the five facies.

Author Contributions: S.C. conceptualization, formal analysis, writing—original draft, writing—review and editing. T.B. conceptualization, writing—review and editing, supervision. A.E. conceptualization, writing—review and editing, co-supervision. S.R. writing—review and editing. E.Z. writing—review and editing. O.I. writing—review and editing. M.B. conceptualization, writing—review and editing, supervision. All authors have read and agreed to the published version of the manuscript.

Funding: This project received funding from the OCP Group (grant number RE04).

Data Availability Statement: Data is available upon request from the authors.

Acknowledgments: The authors would like to thank the OCP Group (Benguerir mine) and the experimental mine in Morocco for their support in the framework of the project (RE04). The authors would also like to thank OCP collaborators (Nor eddine El Allam, Saloua Belhabchia, Elhoussine El Mahfoudi, Abdelmajid El Alami, and Hicham Aggadi), the public laboratory for the tests and studies (LPEE), and the staff of the Geo-analytical Lab in the Mohammed VI Polytechnic University for the help with the sampling and characterization tests.

Conflicts of Interest: The authors declare no conflicts of interest.

References

Abbas, S., Saleem, M. A., Kazmi, S. M. S., & Munir, M. J. (2017). Production of sustainable clay bricks using waste fly ash: Mechanical and durability properties. *Journal of Building Engineering*, *14*, 7-14. https://doi.org/https://doi.org/10.1016/j.jobe.2017.09.008

Adiansyah, J. S., Rosano, M., Vink, S., & Keir, G. (2015). A framework for a sustainable approach to mine tailings management: disposal strategies. *Journal of Cleaner Production*, *108*, 1050-1062. https://doi.org/https://doi.org/10.1016/j.jclepro.2015.07.139

Ahmari, S. A. L., & Zhang, L. (2012). Production of eco-friendly bricks from copper mine tailings through geopolymerization. *Construction and Building Materials*, *29*, 323-331.

Aliyu, M. M., Shang, J., Murphy, W., Lawrence, J. A., Collier, R., Kong, F., & Zhao, Z. (2019). Assessing the uniaxial compressive strength of extremely hard cryptocrystalline flint. *International Journal of Rock Mechanics and Mining Sciences*, *113*, 310-321. https://doi.org/https://doi.org/10.1016/j.ijrmms.2018.12.002

Amar, H., Benzaazoua, M., Elghali, A., Hakkou, R., & Taha, Y. (2022). Waste rock reprocessing to enhance the sustainability of phosphate reserves: A critical review. *Journal of Cleaner Production*, *381*, 135151. https://doi.org/https://doi.org/10.1016/j.jclepro.2022.135151

Amos, R. T., Blowes, D. W., Bailey, B. L., Sego, D. C., Smith, L., & Ritchie, A. I. M. (2015). Waste-rock hydrogeology and geochemistry. *Applied Geochemistry*, *57*, 140-156. https://doi.org/https://doi.org/10.1016/j.apgeochem.2014.06.020

Amrani, M., Taha, Y., Kchikach, A., Benzaazoua, M., & Hakkou, R. (2019). Valorization of Phosphate Mine Waste Rocks as Materials for Road Construction. *Minerals*, *9*(4). https://doi.org/10.3390/min9040237

Aubertin, M. (2013). Waste rock disposal to improve the geotechnical and geochemical stability of piles. World Mining Congress, Montreal, QC, Canada,

Aubertin, M., Bussière, B., Bernier, L., Chapuis, R., Julien, M., Belem, T., Simon, R., Mbonimpa, M., Benzaazoua, M., & Li, L. (2002, 5-8 June). *La gestion des rejets miniers dans un contexte de développement durable et de protection de l'environnement* Congrès annuel de la société canadienne de génie civil, Montréal, Québec, Canada,.

Bahhou, A., Taha, Y., El Khessaimi, Y., Idrissi, H., Hakkou, R., Amalik, J., & Benzaazoua, M. (2021a). Use of phosphate mine by-products as supplementary cementitious materials. *Materials Today: Proceedings*, *37*, 3781-3788. https://doi.org/https://doi.org/10.1016/j.matpr.2020.07.619

Bayoussef, A., Oubani, M., Loutou, M., Taha, Y., Benzaazoua, M., Manoun, B., & Hakkou, R. (2021a). Manufacturing of high-performance ceramics using clays by-product from phosphate mines. *Materials Today: Proceedings*, *37*, 3994-4000. https://doi.org/https://doi.org/10.1016/j.matpr.2020.10.800

Bossé, B., Bussière, B., Hakkou, R., Maqsoud, A., & Benzaazoua, M. (2013). Assessment of Phosphate Limestone Wastes as a Component of a Store-and-Release Cover in a Semiarid Climate. *Mine Water and the Environment*, *32*(2), 152-167. https://doi.org/10.1007/s10230-013-0225-9

Boujo, A. (1976). *Contribution à l'étude géologique du gisement de phosphate crétacé-éocène des Ganntour (Maroc occidental)* (Publication Number 43) Université Louis-Pasteur]. www.persee.fr. Strasbourg : Institut de Géologie https://www.persee.fr/doc/sgeol_0302-2684_1976_mon_43_1

Deere, D. U. (1964). Technical description of rock cores for engineering purpose. *Rock Mechanics and Engineering Geology*, *1*(1), 17-22.

Dixon, D. E., Prestrera, J. R., Burg, G., Chairman, S. A., Abdun-Nur, E. A., Barton, S. G., Bell, L. W., Blas Jr, S. J., Carrasquillo, R. L., & Carrasquillo, P. M. (1991). Standard practice for selecting proportions for normal, heavyweight, and mass concrete (ACI 211.1-91). *Farmington Hills: ACI.*

El Bamiki, R., Raji, O., Ouabid, M., Elghali, A., Khadiri Yazami, O., & Bodinier, J.-L. (2021). Phosphate Rocks: A Review of Sedimentary and Igneous Occurrences in Morocco. *Minerals*, *11*(10). https://doi.org/10.3390/min11101137

El Machi, A., Mabroum, S., Taha, Y., Tagnit-Hamou, A., Benzaazoua, M., & Hakkou, R. (2021a). Use of flint from phosphate mine waste rocks as an alternative aggregates for concrete. *Construction and Building Materials*, *271*. https://doi.org/10.1016/j.conbuildmat.2020.121886

El Machi, A., Mabroum, S., Taha, Y., Tagnit-Hamou, A., Benzaazoua, M., & Hakkou, R. (2021b). Valorization of phosphate mine waste rocks as aggregates for concrete. *Materials Today: Proceedings*, *37*, 3840-3846. https://doi.org/10.1016/j.matpr.2020.08.404

Elghali, A., Benzaazoua, M., Bouzahzah, H., Bussière, B., & Villarraga-Gómez, H. (2018). Determination of the available acid-generating potential of waste rock, part I: Mineralogical approach. *Applied Geochemistry*, *99*, 31-41. https://doi.org/https://doi.org/10.1016/j.apgeochem.2018.10.021

Eliche-Quesada, D., Azevedo-Da Cunha, R., & Corpas-Iglesias, F. A. (2015). Effect of sludge from oil refining industry or sludge from pomace oil extraction industry addition to clay ceramics. *Applied Clay Science*, *114*, 202-211. https://doi.org/https://doi.org/10.1016/j.clay.2015.06.009

Farid, A. T. M. (2013). Modified Value of Rock Quality Designation Index RQD in Rock Formation. International Conference on Case Histories in Geotechnical Engineering. 1, Chicago, Illinois.

Guo, Y., Zhang, Y., Huang, H., Meng, K., Hu, K., Hu, P., Wang, X., Zhang, Z., & Meng, X. (2014). Novel glass ceramic foams materials based on red mud. *Ceramics International*, *40*(5), 6677-6683. https://doi.org/https://doi.org/10.1016/j.ceramint.2013.11.128

Hakkou, R., Benzaazoua, M., & Bussière, B. (2009). Laboratory Evaluation of the Use of Alkaline Phosphate Wastes for the Control of Acidic Mine Drainage. *Mine Water and the Environment*, *28*(3). https://doi.org/10.1007/s10230-009-0081-9

Hakkou, R., Benzaazoua, M., & Bussière, B. (2016). Valorization of Phosphate Waste Rocks and Sludge from the Moroccan Phosphate Mines: Challenges and Perspectives. *Procedia Engineering*, *138*, 110-118. https://doi.org/10.1016/j.proeng.2016.02.068

Hanein, T., Thienel, K.-C., Zunino, F., Marsh, A. T. M., Maier, M., Wang, B., Canut, M., Juenger, M. C. G., Ben Haha, M., Avet, F., Parashar, A., Al-Jaberi, L. A., Almenares-Reyes, R. S., Alujas-Diaz, A., Scrivener, K. L., Bernal, S. A., Provis, J. L., Sui, T., Bishnoi, S., & Martirena-Hernández, F. (2021). Clay calcination technology: state-of-the-art review by the RILEM TC 282-CCL. *Materials and Structures*, *55*(1), 3. https://doi.org/10.1617/s11527-021-01807-6

Knidiri, J., Bussière, B., Hakkou, R., Benzaazoua, M., Parent, E., & Maqsoud, A. (2015). Design, construction and preliminary results for an inclined store-and-release cover experimental cell built on an abandoned mine site in Morocco. Proceeding for the 10th ICARD, International Conference on Acid Rock Drainage, and IMWA, International Mine Water Association,

Krishna, R. S., Mishra, J., Meher, S., Das, S. K., Mustakim, S. M., & Singh, S. K. (2020). Industrial solid waste management through sustainable green technology: Case study insights from steel and mining industry in Keonjhar, India. *Materials Today: Proceedings*, *33*, 5243-5249. https://doi.org/10.1016/j.matpr.2020.02.949

Lahmira, B., Lefebvre, R., Aubertin, M., & Bussière, B. (2016). Effect of heterogeneity and anisotropy related to the construction method on transfer processes in waste rock piles. *Journal of Contaminant Hydrology*, *184*, 35-49. https://doi.org/https://doi.org/10.1016/j.jconhyd.2015.12.002

Lèbre, É., & Corder, G. (2015). Integrating Industrial Ecology Thinking into the Management of Mining Waste. *Resources*, *4*(4), 765-786. https://www.mdpi.com/2079-9276/4/4/765

Lee, C., & Gu, F. (2017, 11-13 October). *Co-disposal of waste rock with backfill* UMT 2017: Proceedings of the First International Conference on Underground Mining Technology, Sudbury. https://papers.acg.uwa.edu.au/p/1710_27_Lee/

Liu, G., Li, L., Yao, M., Landry, D., Malek, F., Yang, X., & Guo, L. (2017). An Investigation of the Uniaxial Compressive Strength of a Cemented Hydraulic Backfill Made of Alluvial Sand. *Minerals*, *7*(1), 4. https://www.mdpi.com/2075-163X/7/1/4

Loutou, M., Hajjaji, M., Mansori, M., Favotto, C., & Hakkou, R. (2013). Phosphate sludge: thermal transformation and use as lightweight aggregate material. *J Environ Manage*, *130*, 354-360. https://doi.org/10.1016/j.jenvman.2013.09.004

Loutou, M., Taha, Y., Benzaazoua, M., Daafi, Y., & Hakkou, R. (2019). Valorization of clay by-product from moroccan phosphate mines for the production of fired bricks. *Journal of Cleaner Production*, *229*, 169-179. https://doi.org/10.1016/j.jclepro.2019.05.003

Maknoon, M., & Aubertin, M. (2021). On the Use of Bench Construction to Improve the Stability of Unsaturated Waste Rock Piles. *Geotechnical and Geological Engineering*, *39*, 1-25. https://doi.org/10.1007/s10706-020-01567-0

Mouflih, M. (2015). *Les phosphates du maroc central et du moyen atlas (maastrichtien-lutetien, maroc) : Sedimentologie, stratigraphie sequentielle, contexte genetique et valorisation* Universite Cadi Ayyad.

NF-P11-300. (1992). Exécution des Terrassements—Classification des Matériaux Utilisables dans la Construction des Remblais et des Couches de Forme d'infrastructures Routières. In *Association Française de Normalisation: Paris, France.*

NF-P94-051. (1993). Soil: Investigation and Testing. Determination of Atterberg's Limits. Liquid Limit Test Using Cassagrande Apparatus. Plastic Limit Test on Rolled Thread—Sols: Reconnaissance et Essais; Association Française de Normalisation: Paris, France. In.

NF-P94-052-1. (1995). Soil: Investigation and Testing. Atterberg Limit Determination. Part 1: Liquid Limit. Cone Penetrometer Method—Sols: Reconnaissance et essais. In: Association Française de Normalisation Paris, France.

NF EN 933–8+A1. (2015). Tests for geometrical properties of aggregates - Part 8 : assessment of fines - Sand equivalent test. In.

NF EN 1097-1. (2011). Tests for mechanical and physical properties of aggregates - Part 1 : determination of the resistance to wear (micro-Deval). In.

NF EN 12620. (2008). Aggregates for concrete. In.

NF P94-066. (1992). Soils: Investigation and Tests. Fragmentability Coefficient of Rocky Material—Sols: Reconnaissance et essais; Association Française de Normalisation: Paris, France. In.

NF P94-067. (1992). Soils: Investigation and Tests. Degradability Coefficient of ROCKY material—Sols: Reconnaissance et essais; Association Française de Normalisation: Paris, France. In.

NF P94-410-1. (2001). Rock - Test for physical properties of rock - Part 1 : determination of water content of rock - Oven-drying method. In.

NF P94-410-2. (2001). Rock - Tests for physical properties of rock - Part 2 : determination of density - Cutting curb - Water immersion methods. In.

NF P94-410-3. (2001). Rock - Tests for physical properties of rock - Part 3 : determination of porosity. In.

NF P94-420. (2000). Rock - Determination of the uniaxial compressive strength. In.

NM00.8.083. (2015). Soils: recognition and test of granulometric analysis of soils sedimentation method. In: IMANOR.

NM00.8.095. (2015). Soils: Investigation and Testing. Measuring of the Methylene Blue Adsorption Capacity of à Rocky Soil. Determination of the Methylene Blue of à Soil by Means of the Stain test. In.

NM13.1.008. (1998). Granulometric Analysis. Dry Sieving Method after Washing. In.

NM13.1.119. (2009). Soils - Recognition and Testing - Laboratory Density Determination of Fine Soils - Cutting Kit, Mold and Water Immersion Methods. In: IMANOR.

NM13.1.152. (2011). Soils: Investigation and testing - Determination of the water content by weight of materials - Oven Drying Method. In.

NM.10.1.138. (1995). Aggregates: Los Angeles Test. In.

Nwaila, G. T., Ghorbani, Y., Zhang, S. E., Frimmel, H. E., Tolmay, L. C. K., Rose, D. H., Nwaila, P. C., & Bourdeau, J. E. (2021). Valorisation of mine waste - Part I: Characteristics of, and sampling methodology for, consolidated mineralised tailings by

using Witwatersrand gold mines (South Africa) as an example. *Journal of Environmental Management*, *295*, 113013. https://doi.org/https://doi.org/10.1016/j.jenvman.2021.113013

P94-074, N. (1994). Sols : reconnaissance et essais - Essais à l'appareil triaxial de révolution - Appareillage - Préparation des éprouvettes - Essai (UU) non consolidé non drainé - Essai (Cu+U) consolidé non drainé avec mesure de pression interstitielle - Essai (CD) consolidé drainé. MO. In.

Pagé, P., Li, L., Yang, P., & Simon, R. (2019). Numerical investigation of the stability of a base-exposed sill mat made of cemented backfill. *International Journal of Rock Mechanics and Mining Sciences*, *114*, 195-207. https://doi.org/https://doi.org/10.1016/j.ijrmms.2018.10.008

Peyronnard, O., & Benzaazoua, M. (2011). Estimation of the cementitious properties of various industrial by-products for applications requiring low mechanical strength. *Resources, Conservation and Recycling*, *56*(1), 22-33. https://doi.org/https://doi.org/10.1016/j.resconrec.2011.08.008

Redclift, M. (2005). Sustainable development (1987–2005): an oxymoron comes of age. *Sustainable Development*, *13*(4), 212-227. https://doi.org/https://doi.org/10.1002/sd.281

Safhi, A. e. M., Amar, H., El Berdai, Y., El Ghorfi, M., Taha, Y., Hakkou, R., Al-Dahhan, M., & Benzaazoua, M. (2022). Characterizations and potential recovery pathways of phosphate mines waste rocks. *Journal of Cleaner Production*, *374*, 134034. https://doi.org/https://doi.org/10.1016/j.jclepro.2022.134034

Safhi, A. E. M. E., (1st ed.). CRC Press. . (2022). *Valorization of Dredged Sediments as Sustainable Construction Resources* ((1st ed.) ed.). CRC Press. https://doi.org/https://doi.org/10.1201/9781003315551

Sidibé, M. (1995). *Etude de l'utilisation des granulats de type silexlte en géotechnique routière (notamment en couches de base et revêtement des couches de chaussées).* Ecole Polytechnique de Thiès.].

Taha, Y., Benzaazoua, M., Hakkou, R., & Mansori, M. (2017). Coal mine wastes recycling for coal recovery and eco-friendly bricks production. *Minerals Engineering*, *107*, 123-138. https://doi.org/https://doi.org/10.1016/j.mineng.2016.09.001

Taha, Y., Benzaazoua, M., Mansori, M., Yvon, J., Kanari, N., & Hakkou, R. (2016). Manufacturing of ceramic products using calamine hydrometallurgical processing wastes. *Journal of Cleaner Production*, *127*, 500-510. https://doi.org/https://doi.org/10.1016/j.jclepro.2016.04.056

Tayebi-Khorami, M., Edraki, M., Corder, G., & Golev, A. (2019). Re-Thinking Mining Waste through an Integrative Approach Led by Circular Economy Aspirations. *Minerals*, *9*(5). https://doi.org/10.3390/min9050286

XP P 94-429. (2002). Rock - Point load strength test - Franklin test. In.

XPP94-202. (1995). Soil : investigation and testing. Soil sampling. Methodology and procedures. In.

Yang, Z., lin, Q., Xia, J., He, Y., Liao, G., & Ke, Y. (2013). Preparation and crystallization of glass–ceramics derived from iron-rich copper slag. *Journal of Alloys and Compounds*, *574*, 354-360. https://doi.org/https://doi.org/10.1016/j.jallcom.2013.05.091

Zhang, L. (2013). Production of bricks from waste materials – A review. *Construction and Building Materials*, *47*, 643-655. https://doi.org/https://doi.org/10.1016/j.conbuildmat.2013.05.043

CHAPTER 5 ARTICLE 2: AN UPSTREAM GEO-ENVIRONMENTAL ASSESSMENT OF SEDIMENTARY PHOSPHATE WASTE ROCK

Preamble: this article was submitted for publication in the "*Journal of Environmental Management*" on 20 May 2024

Safa Chlahbi[1,2,*], Mostafa Benzaazoua[1], Abdellatif Elghali[1], Samia Rochdane[1], Essaid Zerouali[3], Tikou Belem[2]

[1]Mohammed VI Polytechnic University (UM6P), Geology and Sustainable Mining Institute (GSMI), 43150 Benguerir, Morocco

[2]Université du Québec en Abitibi-Témiscamingue (UQAT), Research Institute of Mines and Environment (RIME), 445 Boul. de l'Université, QC J9X 5E4 Rouyn-Noranda, Canada

[3]OCP group, Department of Method, Planning, and Performance Benguerir, 2 Street Al Abtal Hay, Casablanca B.P. Maârif 5196, Morocco

5.1 Abstract

Phosphate mines produce large quantities of waste rock. These waste rocks are mixed and managed on the surface as large unsaturated piles, which makes them difficult to rehabilitate. They are primarily composed of carbonates, clays, marls, and flints. In many cases, the unrestored mine sites, when exposed to normal climatic conditions, could frequently produce toxicity, environmental pollution, and significant ecological disruptions. This research aims to assess the phosphate waste rock's (PWR) geochemistry and environmental behavior upstream of the extraction process. For this purpose, different core drilling specimens and data were collected from different lithologies and depths in the interburdens of the Benguerir mine to forecast the environmental profile and determine the mobility of the analyzed chemical species. These samples were analyzed for their petrographical, chemical, and mineralogical compositions, static leaching tests, and semi-dynamic tests. The results showed that the PWR mainly consists of calcite, dolomite, apatite, and quartz, with minor phases such as clay minerals. Chemically, the PWRs are dominated by the following major oxides: CaO (1.2-53.5 %) and MgO (0.2-19.5 %), followed by SiO_2 (2.4-94 %) and P_2O_5 (0.2-25 %). Trace elements can be classified into three groups based on their concentrations: group of Ba, Zn and Cr (> 150 ppm), group of Ba, V, Ni, Zr, Y, U, Cu, Cd, Co (10 to 150 ppm), and group of trace elements with relatively low concentrations (< 10 ppm): Rb, Pb, As, Mo, Se, Sc, Ga, Nb, Th, Hf, Sb and Cs. Environmentally, the pH of the leachates was neutral to alkaline (6 ± 0.6 to 9.3) for all the

samples, which have a high neutralizing potential (38 to 991 kg $CaCO_3$/t). The release of major and trace elements in the leaching test remains below international standard limits. Consequently, the leaching test results confirm the non-hazardous nature of the PWR. Therefore, the studied PWR could be considered a natural raw material for civil applications.

Keywords: phosphate waste rock, upstream geo-environmental, geochemistry and mineralogy characterization, environmental behavior.

5.2 Introduction

In past decades, mining activities have generated huge quantities of mine waste, most often dumped in surface sites in the form of waste rock piles (coarse fraction) and large tailings ponds (fine fraction). In many cases, the unrestored mine sites can be the source of toxicity and environmental pollution (soil and groundwater contamination) and significant ecological disruptions after exposure to natural climatic conditions (Benarchid et al., 2019; Boumaza et al., 2021a; da Silva et al., 2010; Hakkou et al., 2008; Khalil et al., 2013; Khelifi et al., 2021; Krishna et al., 2020).

In Morocco, the mining sector contributes 10% of the gross domestic product (GDP), with 90% coming from the phosphate industry in 2014 (Mehahad & Bounar, 2020). In 2019, total production reached 54.81 million tons (Mt), including 35.20 Mt of raw phosphate, 16.70 Mt of processed products (P_2O_5 and fertilizers), and 2.90 Mt for other mining products, with a turnover of 61.30 billion dirhams (MMDH) (Ministre de la Transition Energétique et du Développement Durable, 2021). The Moroccan sedimentary phosphate deposits have the world's largest phosphate rock reserves, with more than 70% of the world's phosphate reserves; it is the second-largest producer of phosphate rock after China (Jasinski, 2022). Phosphate mines occupy an important place in national economic development. The Benguerir mine, exploited by the OCP Group, is in the western Meseta, approximately 17 km east of Benguerir and 70 km north of Marrakech (Figure 5-1). Strip mining is the preferred surface mining used to retrieve phosphate. This extraction method generates large quantities of phosphate waste rock (PWR), approximately 12.3 Mt annually, which is typically dumped on the surface as waste rock piles within phosphate mining areas. PWR mainly comprises carbonates, marl/clay, flintstone, etc. (Safhi et al., 2022). However, waste rocks exhibit physical, chemical, and hydrogeological heterogeneity (Amos et al., 2015; Aubertin et al., 2002; Elghali et al., 2019). These heterogeneities represent a significant challenge for waste rock disposal and management (Aubertin et al., 2002). During mining operations and/or before, waste rock's environmental

behavior is typically evaluated using static and kinetic testing (Elghali et al., 2018; Plante et al., 2011; Sapsford et al., 2009). These tests are used to predict and determine the contaminant-leaching potential of mine waste from the perspective of designing suitable waste control plans as early as possible during the mine life cycle.

Numerous studies conducted in Northern Africa have placed significant emphasis on investigating the environmental impact of phosphate mining waste (Boumaza et al., 2023; Boumaza et al., 2021b; Khelifi et al., 2019; Khelifi et al., 2021; Khelifi et al., 2020). Some studies Boumaza et al. (2023) and Boumaza et al. (2021b) have examined the potential risks associated with phosphate mine wastes in Algeria, including their impact on soil quality, water contamination, and overall ecosystem health. The results of their study showed that both raw phosphorites and their wastes contain hazardous trace metal elements (e,g., U, Cd, Cr, Mo, V, and Tl) that exceed soil standards (Boumaza et al., 2023; Boumaza et al., 2021b), posing potential harm to the environment and human health due to waste exposure and mobilization by wind and rainfall. Their results also indicate that water sources are contaminated with trace metal elements, specifically Pb, U, Fe, Li, Se, and Mn. The observed levels suggest poor water quality, with the groundwater showing a higher hazard quotient of 1. It was concluded that consuming these waters without treatment could adversely affect human health, especially in children. Khelifi et al. (2021) examined the risk assessment of phosphate mining and processing activities on the environment and human health. Their study focuses on investigating the inhalation and dermal bioaccessibility of potentially toxic elements (PTEs) in the sediments of an industrial site in the Gafsa-Metlaoui mining basin of phosphate in Tunisia. The results showed that the concentrations of PTE were found to be higher than background levels, with a tendency to accumulate in fine particles. The bioaccessibility of PTE varies depending on the medium used for testing. Overall, the exposure to bioaccessible fractions or pseudo-total concentrations of PTE was not found to pose serious non-carcinogenic and carcinogenic risks to human health according to the USEPA risk assessment.

Sabiha et al. (2009) investigated the metal contamination from phosphate rock; their study aimed to determine the concentration of Co, K, Mg, Mn, and Na (common elements) and Cd, Cu, Cr, Ni, Pb, Zn (environmental pollutants, i.e., toxic elements) in phosphate rocks used for fertilizer production in Pakistan. The results of this study showed that Pakistani phosphate's metal concentration was lower and below safe levels except for lead. On the other hand, this phosphate rock is a cause of metal contamination of the air, land, water, food chain, etc. Jiang et al. (2016) have investigated the phosphorus leaching from PWR in China under different

percolating conditions. The results indicate that the mechanism of phosphorus release is controlled by solubility when the pH decreases the release of phosphorus from waste rock increases. Therefore, PWR deposited in this study area is considered a phosphorus point pollution source (Mar & Okazaki, 2012; Sabiha et al., 2009).

Previous studies have investigated the chemical and mineralogical composition as well as the environmental behavior of Benguerir PWR (Amrani et al., 2019; Hakkou et al., 2008; Hakkou et al., 2009; Idrissi et al., 2021; Mabroum et al., 2020). However, it is important to note that these studies primarily focused on either the mixed waste rock deposited on the surface or specific layers within the waste rock, such as the yellow marl/clays layer. As a result, the available geochemical data and knowledge regarding the environmental behavior of the interburdens remain relatively limited. Consequently, there is a gap in understanding the comprehensive geochemical characteristics and environmental implications associated with the interburdens of Benguerir PWR. Further research in this area could provide valuable insights into the overall composition and potential environmental impacts of these interburden layers, contributing to a more comprehensive understanding of the waste rock as a whole.

In this study, our main focus revolves around the geochemical and environmental characterization of the PWR (interburdens) upstream of the exploitation sequence. Our primary objectives encompass two key aspects. Firstly, we aim to provide comprehensive information concerning the abundance of major and trace elements in the interburdens and their distribution patterns. Secondly, assess their environmental behavior, which involves evaluating their potential interactions with the surrounding ecosystem. By conducting this study, we hope to contribute to the existing body of knowledge and provide valuable insights that can assist in the development of sustainable management strategies for PWR.

5.3 Materials and methods

Six vertical drill cores (SC02, SC03, SC04, SC05, SC06, and SC07) were carried out in the different panels of the Benguerir phosphate series. Additional details about core drilling can be found in (Chlahbi et al., 2023). The samples analyzed in this study were collected from the borehole SC02 located in panel 7 at the Benguerir mine Figure 5-1. The choice of the borehole SC02 is motivated by the presence of all the phosphate layers and the interburdens: “complete phosphate series”, which means the representative character of the different components of the stratigraphic column of the study area. A total of thirty samples (S2-I1 to S2-I30) from different depths and lithologies were studied. According to Chlahbi et al. (2023), these samples can be

classified in 4 classes: i) carbonates, including dolomite and limestone (S2-I3, S2-I4, S2-I7, S2-I8, S2-I9, S2-I11, S2-I12, S2-I13,, S2-I15, S2-I18, S2-I25, S2-I29, and S2-I30), ii) phosphates (S2-I1, S2-I2, S2-I5, S2-I6, S2-I14, S2-I16, S2-I23, S2-I26, and S2-I27), iii) siliceous (S2-I10, S2-I17, S2-I22, S2-I24, and S2-I28) and iv) marly-clay (S2-I19, S2-I20, and S2-I21). This sampling choice was made to characterize the geochemistry of all the lithologies present in the interburdens and to assess their environmental behavior.

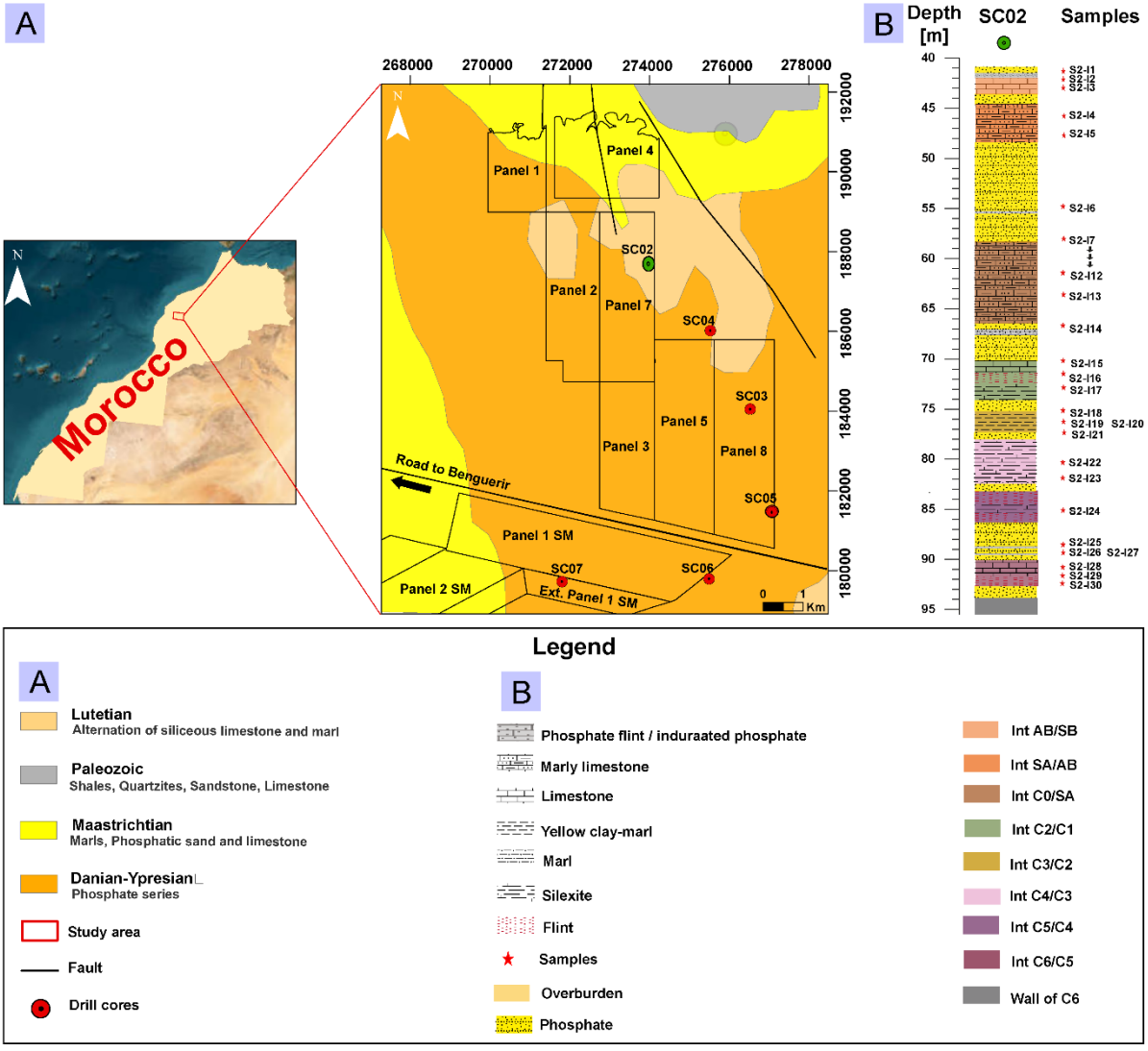

Figure 5-1: Simplified geological map of the study area and lithological section of the borehole SC02 with sample positions.

The collected PWR samples were dried, homogenized, crushed, ground, and used for chemical and mineralogical analyses and static leaching, while the petrography analyses and the monolith leaching test (MLT) were performed on monolithic blocks. The methodology approach used in this study is summarized in Figure 5-2.

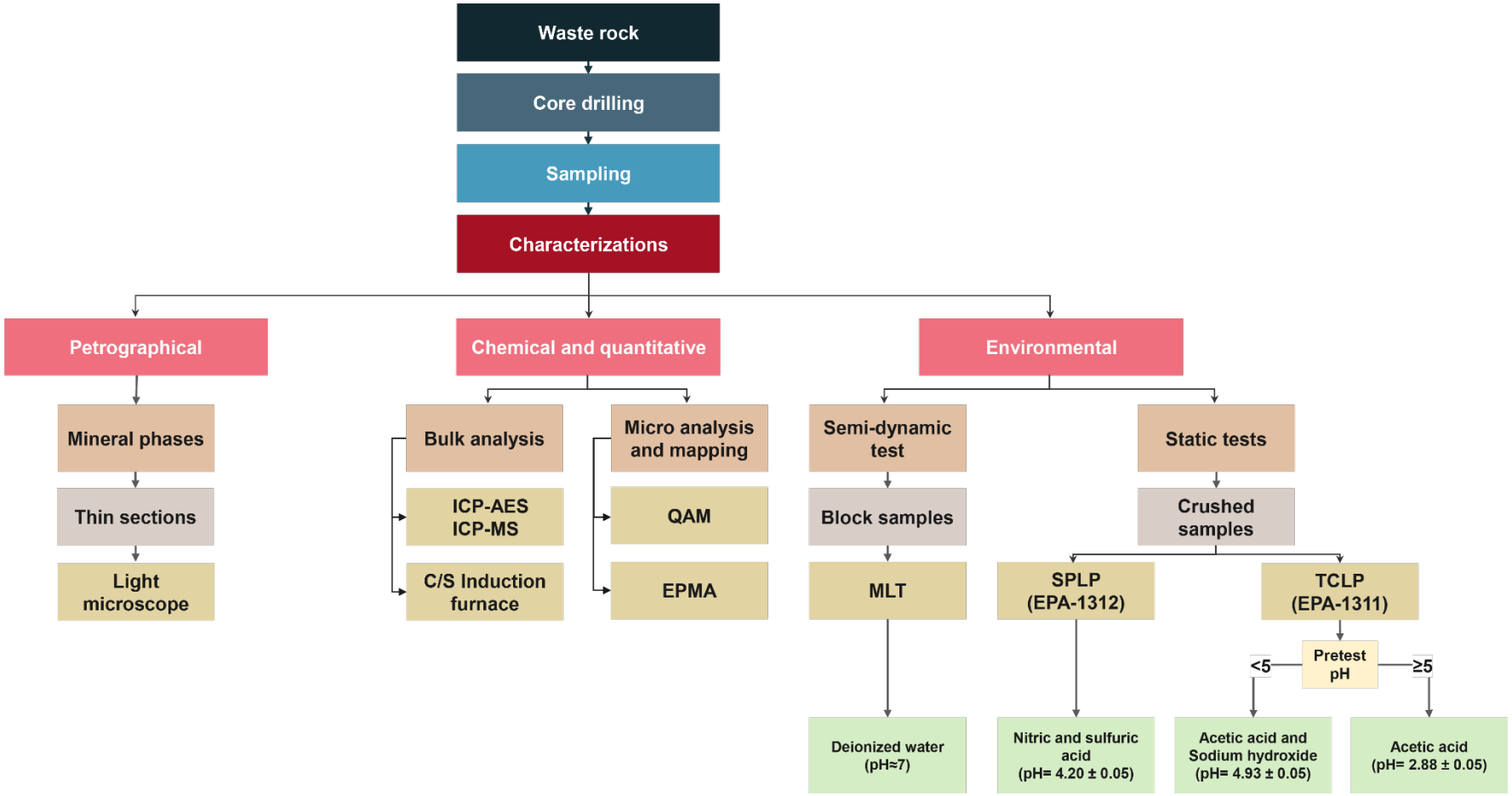

Figure 5-2: Summary of the methodological approach used. ICP: inductively coupled plasma. AES: atomic emission spectrometry. MS: mass spectrometry. QAM: quantitative automated mineralogy. EPMA: Electron probe microanalysis. MLT: monolithic leaching test. SPLP: synthetic precipitation leaching procedure. TCLP: toxicity characteristic leaching procedure. EPA: Environmental Protection Agency

5.3.1 Petrography, chemical, and mineralogical characterization

The petrography characterization was examined using thin polished sections under a light microscope using transmitted light (Carl Zeiss® Axio Imager A2) at RIME-UQAT. The bulk chemical composition of the different samples was performed at Actlabs (Ontario, Canada). Major elements (SiO_2, Al_2O_3, Fe_2O_3, Na_2O, K_2O, CaO, MgO, P_2O_5, and TiO_2) were obtained by fusion decomposition followed by inductively coupled plasma - atomic emission spectrometry (ICP-AES) analysis, (ME_ICP06). Selected trace elements (TEs) (Ba, Cr, Cs, Ga, Hf, Nb, Rb, Sr, Th, V, Y, Zr), and rare-earth elements (La, Ce, Pr, Nd, Sm, Eu, Gd, Tb, Dy, Ho, Er, Tm, Yb, Lu) were obtained by lithium borate fusion followed by acid dissolution and ICP-AES measurement (ME-MS81™). Other TEs (As, Bi, Sb, Se) (ME-MS42) were measured with aqua regia digestion followed by mass spectrometry ICP-MS measurement, while base metal (Ag, Cd, Co, Cu, Li, Mo, Ni, Pb, Sc, Zn) were obtained by four acid digestion followed ICP-AES measurement (ME-4ACD81). Total sulfur (TS) and total carbon (TC) contents were analyzed by induction furnace (ELTRA CS-2000; detection limit of 0.09%), where the total sulfur was equal to sulfur sulfide.

The mineralogical characterization was determined by Quantitative Evaluation of Materials by Scanning Electron Microscopy (QEMSCAN®, FEI, Quanta 650 platform with Field Emission Gun) at Expert Process Solutions (XPS) in Sudbury, Ontario, Canada. It's an automated method that uses a collection of rapidly captured X-rays to produce particle maps (color-coded by mineral). This equipment is equipped with Bruker SDD energy dispersive spectrometers (EDS). Electron probe microanalysis (EPMA) was also carried out to verify the mineral identification and chemical composition. EPMA was also performed at the XPS laboratory using a Cameca SX-100 electron microprobe with at least ten particles of each mineral. Four high-resolution wavelength-dispersive X-ray spectrometers (WDS) were coupled to the instrument. The quantitative analyses (EPMA) were performed using a focused beam at 20 kV accelerating voltage and 20 nA constant beam current. A series of calibration standards (apatite, orthoclase, hematite, periclase, and wollastonite) were used to conduct a quantitative analysis of the materials and enable precise measurements.

5.3.2 Statistical analysis

In order to investigate the processes governing the geochemistry of PWR interburdens, a series of analytical techniques were employed. Initially, descriptive statistics were utilized to provide a summary and description of the fundamental characteristics of the dataset. The Shapiro-Wilk

test, introduced by Shapiro and Wilk (1965), and the QQ plot (Hazen, 1914), were employed to determine the distribution of the data. Furthermore, the suitability of the data for factor analysis was assessed using the Kaiser-Meyer-Olkin (KMO) test, which measures the adequacy of sampling. Subsequently, to understand the relationship between the analyzed elements and to identify the associations between variables and individuals, Principal Component Analysis (PCA) was applied. PCA is a statistical technique commonly used for dimensionality reduction and data visualization (Hasan & Abdulazeez, 2021). The present study applied PCA to geochemical analyses from PWR in interburdens. Given the geochemical data's compositional nature, the raw data were transformed into centered-log ratios (CLR) before applying PCA. This transformation is often recommended for analyzing compositional data (CoDa) (Barcelo-Vidal & Martín-Fernández, 2016; Boumaza et al., 2024; Egozcue et al., 2024; Reimann & Filzmoser, 2000). The CLR transformation involves taking the logarithm of the ratio of each element to the geometric mean of all elements in a sample and then centering (Aitchison, 1982). Statistical treatments (PCA and statistical tests) were conducted using XLSTAT software, and the CoDaPack software was used for the CLR transformation of raw data.

5.3.3 Environmental characterization

The acid generation potential (AP) was calculated using sulfur sulfide (AP (kg $CaCO_3$/t) = 31.25 × $S_{sulphides}$) and carbonate neutralization potential (NP) using total carbon (NP = 83.3 × TC wt% (kg $CaCO_3$/t)) (Miller et al., 1991; Sobek, 1978). The Net neutralization potential (NNP) was calculated by subtracting the AP from the NP (Miller et al., 1991; Weber et al., 2004). Based on NNP, three zones were recognized: i) NNP value higher than 20 kg $CaCO_3$/t classifies the sample as non-acid-generating, ii) NNP lower than -20 kg $CaCO_3$/t indicates an acid-generating material, and iii) NNP values between -20 and 20 kg $CaCO_3$/t is uncertainty zone (Bouzahzah et al., 2015; Sobek, 1978). The neutralization potential ratio (NPR = NP/AP) is a further indicator used to assess the potential of acid generation. A sample is often classified acid-generating if the NPR value is less than 1, uncertain if it is between 1 and 2.5, and non-acid generating if it is greater than 2.5 (Benzaazoua et al., 2004; Elghali et al., 2018; Elghali et al., 2023).

The environmental behavior of the samples from the study area was assessed using static leaching tests and semi-dynamic tests:

i) Toxicity characteristic leaching procedure (TCLP) was performed to assess the inorganic species mobility for evaluating whether a residue is considered a leachable material or not

(USEPA, 1992). A pretest was essential to determine the leaching solution by adding 96.5 ml of Hi-Pure water to 5 g of the solid phase into a borosilicate glass beaker. The beaker was covered with a watch glass and stirred vigorously for 5 min using a magnetic stirrer. After that, 3.5 ml of hydrochloric acid (HCl) was added, the beaker was covered, and it was heated at 50°C ± 5°C for 10 minutes with stirring. After one hour, the solution was homogenized, and the pH was measured. If the pH was less than 5.0, leach solution number 1 (acetic acid and sodium hydroxide (pH = 4.93 ± 0.05)) was used, and if the pH was higher than or equal to 5.0, leaching solution number 2 (acetic acid with a pH = 2.88 ± 0.05) was used (Jong & Parry, 2005; USEPA, 1992).

ii) Synthetic precipitation leaching procedure (SPLP) was used to determine the concentration of inorganic species potentially leached by acid rain contact (USEPA, 1994), prepared with a nitric and sulfuric acid mixed with deionized water (pH = 4.2 ± 0.05, L/S ratio of 20/1)

iii) Semi-dynamic monolithic leaching test (MLT) was used to evaluate the leaching potential of contaminants during the life of a monolith (Nen, 2004; USEPA, 2017). The MLT is based on the mass transfer of contaminants from the block to the leaching solution (deionized water) (Jouini et al., 2020; Nen, 2004; USEPA, 2017). The solid/liquid ratio was 1:10. The deionized water was renewed for each sample after 0.25, 1, 2.25, 4, 9, 16, 36 and 64 days. This test measures the degree to which the waste releases various metals and other contaminants into the solution and provides valuable information about the potential risks associated with the waste.

For each static and semi-dynamic test, leachate samples were filtered using a 0.45 μm nylon mesh filter and acidified using 2% v/v HNO_3 for preservation immediately after collection. The chemical composition was then analyzed using ICP-AES at H2Lab in Rouyn-Noranda, Canada. The leachate's pH, redox potential (Eh), and electrical conductivity (EC) were measured using a pH electrode Orion Pt Electrode, and a conductometer, respectively, at RIME-UQAT. The results of the chemical concentration during these tests were compared with different standards and regulations such as United States Environmental Protection Agency (USEPA) regulations (USEPA., 2009) and the worldwide or universal treatment standard (UTS) (UTS, 2017).

Static tests (TCLP and SPLP) involve exposing the samples under constant conditions without any flow or movement of the solution. It provided information on the initial release or leaching of contaminants and the equilibrium concentrations that may be reached over time. However, they may not accurately represent real-world scenarios where dynamic flow and transport processes occur. Semi-dynamic test (MLT) involves the periodic renewal or replenishment of

the solution in contact with the material. It's used to understand the time-dependent behavior of contaminants, including their release and attenuation in a dynamic environment. In semi-dynamic tests, the solution is periodically renewed to simulate the movement of contaminants through the material or system. The flow rate, duration, and frequency of renewal can be adjusted to mimic specific environmental conditions. Overall, while static tests provide information on initial release or equilibrium conditions, semi-dynamic tests offer a more realistic representation of contaminant behavior by considering dynamic processes (Kosson et al., 2002).

5.4 Results and discussions

5.4.1 Petrography results

The phosphate series presents a complex sedimentological aspect due to their facies variations (vertical and lateral) (El Bamiki, 2020b; Prévôt, 1988). The petrography of PWR is an essential factor to consider when assessing the environmental impact. The mineralogical observation on the thin section shows that the PWR from the interburdens of the Benguerir mine is dominated by four facies: i) carbonates (Cab), ii) siliceous, iii) marly-clay, and iv) phosphate minerals as shown in Figure 5-3.

Carbonates are a significant constituent of the Benguerir phosphate series, in massive layers or alternating with phosphates. Carbonate rocks are made up of dolomite (Dol), and calcite (Cal). These two minerals are often associated in the analyzed facies, but also alternately with phosphates (El Bamiki, 2020b; Prévôt, 1988). Dolomite occurs as rhombohedral crystals in a micritic texture. This texture can be classified as a mudstone according to Dunham (1962). Calcite has an abundant microcrystalline texture.

Siliceous (silica) minerals are generally represented by quartz (Qtz). The siliceous phases are usually presented in the form of flint, but also in more or less advanced silicifications of the different sedimentary layers such as phosphate flint and silexite.

As shown in Figure 5-3, the phosphate constituents are peloids (P), coprolites (Cop), coated grain (CG), and bioclasts including bone fragments (BF). These constituents are cemented by variable non-phosphatic constituents such as dolomite, calcite, and siliceous. Phosphate grains are presented by an ovoid/elliptical morphology of a size of 100–600 μm (Mouflih, 2015).

The marl and clay facies are characterized by the dominance of clay minerals (silicates) and calcite. Clays are generally present but not abundant, except in a few reference layer (C3/C2) (Boujo, 1976).

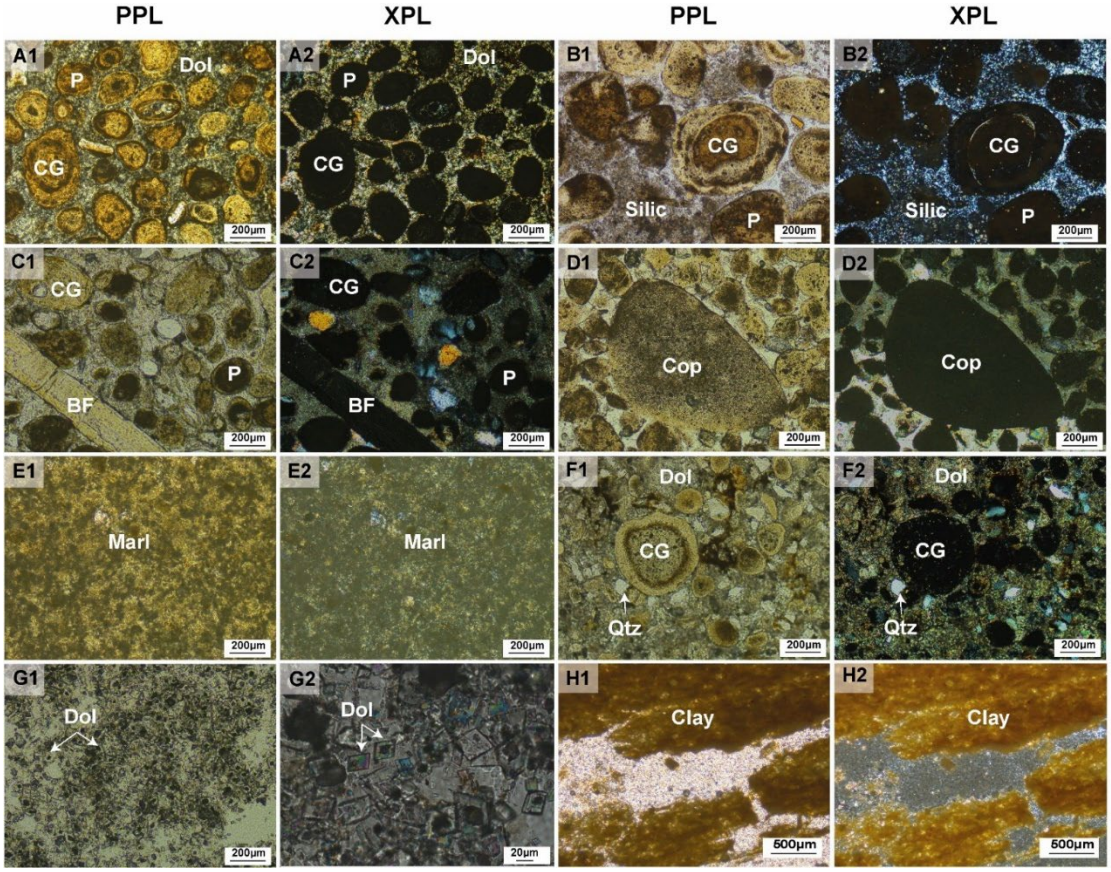

Figure 5-3: Petrographic characterization of phosphate waste rocks based on optical observations. (A1, A2 and B1, B2) PPL (Plane Polarized Light) and XPL (Cross Polarized Light) photomicrographs showing phosphatic peloids and coated grain surrounded by dolomitic and siliceous matrix, respectively. (C1, C2) Photomicrograph in PPL and XPL showing bioclasts including bone fragment associated with phosphatic peloids and coated grain. (D1, D2) Photomicrograph in PPL and XPL showing a phosphatic coprolite associated with phosphatic peloids. (E1, E2 and H1, H2) Photomicrograph in PPL and XPL showing marl and clay facies characterized by a detrital of clay mineral. (F1, F2) Photomicrograph in PPL and XPL showing a coated grain observed in a carbonate matrix associated with phosphate particles with an important quartz fraction. (G1, G2) Photomicrograph in PPL and XPL showing dolomite minerals. PPL: plane polarized light. XPL: crossed polarized light. P: peloids; CG: coated grain; Dol: dolomite; Silic: siliceous; BF: bone fragment; Cop: coprolite; Qtz: quartz.

5.4.2 Mineralogy and geochemistry results

Sedimentary phosphate deposits are identified as being enriched in many trace elements (TEs) and rare-earth elements (REEs) compared to other sedimentary rocks (Garnit et al., 2017;

Prévôt, 1990). The results of major elements, TEs, and rare-REE obtained in the present study are presented in Appendix C

5.4.2.1 Modal mineralogy and major elements

Figure 5-4 shows the variation of modal mineralogy and major elements in SC02 interburdens of the Benguerir mine. Major oxides in the interburdens samples are dominated by CaO (1.2-53.5 %) and MgO (0.2-19.5 %), followed by SiO_2 (2.4-94 %) and P_2O_5 (0.2-25 %). The content of other elements (e.g., Al_2O_3, Fe_2O_3, Na_2O, K_2O, TiO_2) is less than 11 wt.%.

The results of the automated mineralogy analyses by the QEMSCAN® method allowed the identification of the modal phases, the liberation degree of the phases of interest, and the nature of the existing mineralogical associations. The modal mineralogy results show the presence of five main phases: calcite, dolomite, apatite, quartz, and clay mineral. The QEMSCAN® images (Figure 5-5) show the existence of seven lithologies in the Benguerir interburdens:

i) Limestone: shows high concentration of CaO ranging from 32 to 54 wt.%, existence of few concentrations of P_2O_5 (ranging from 3 to 10 wt.%).

ii) Dolomite: characterized by high concentration of CaO ranging from 22 to 36 wt.% and concentration of MgO ranging from 13 to 20 wt.%.

iii) Phosphates lithology in the interburdens: presented a high proportion of P_2O_5 ranging from 14 to 25 wt.%) corresponding to Carbonate fluor apatite.

iv) In this facie we find two lithologies: indurated phosphate and phosphate flint. The first is generally characterized by its soft appearance and light colors while the second is characterized by its strong hardness and its generally brown color. Indurated phosphate has two textures, the first with a calcitic matrix (~50 wt. of CaO) and the second with a dolomitic matrix (up to 5 wt.% of MgO). whereas the phosphate flint is characterized by a siliceous matrix (~ 52 wt.% of SiO_2).

v) Flint: presented highest proportion of SiO_2 (up to 94 wt.%), it reflects to the quartz. These concentrations are recorded in samples S2-I22 and S2-I28.

vi) Silexite: this lithology is characterized by high concentration of SiO_2 (65-85 wt.%) and carbonate: Calcite ~ 20 wt.% or Dolomite ~ 5 wt.%.

vii) Marly clay: in this lithology, SiO_2 presented high concentration (ranging from 24 to 48 wt.%) and Al_2O_3 and Fe_2O_3 concentrations show significant value (5-11 wt.% and 2-5 wt.% respectively) in samples S2-I19, S2-I20, and S2-I21 which corresponds to a marly clay.

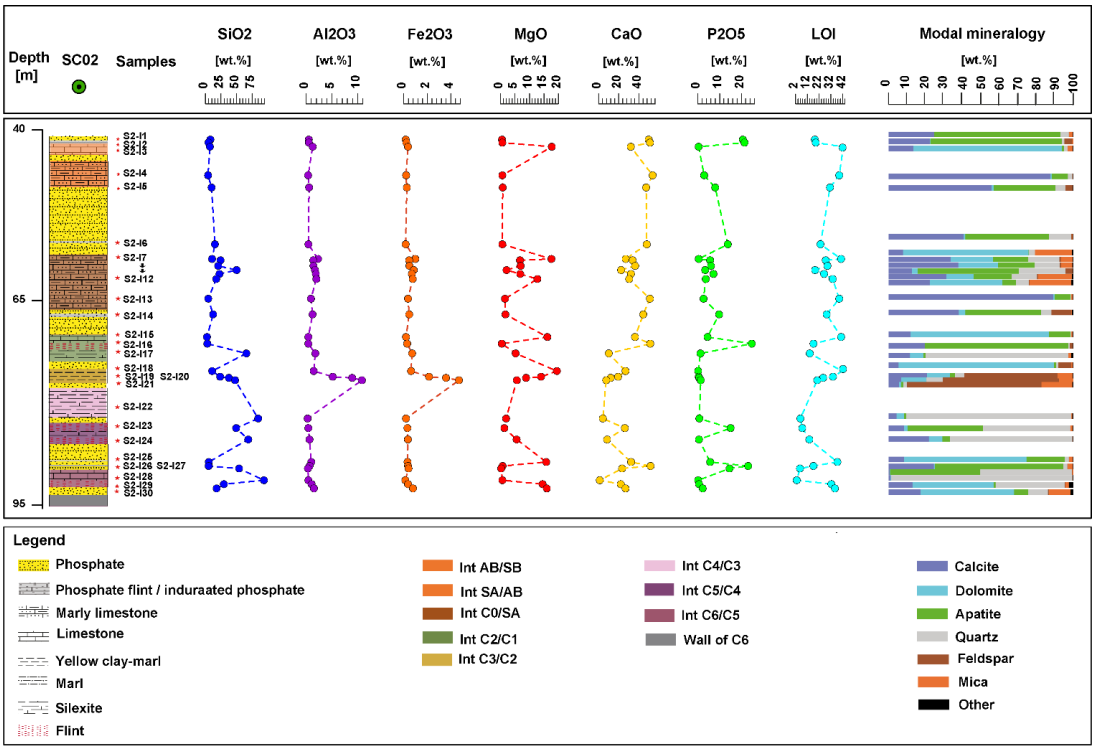

Figure 5-4: Major element and modal mineralogy variation diagrams for SC02 interburdens of Benguerir mine

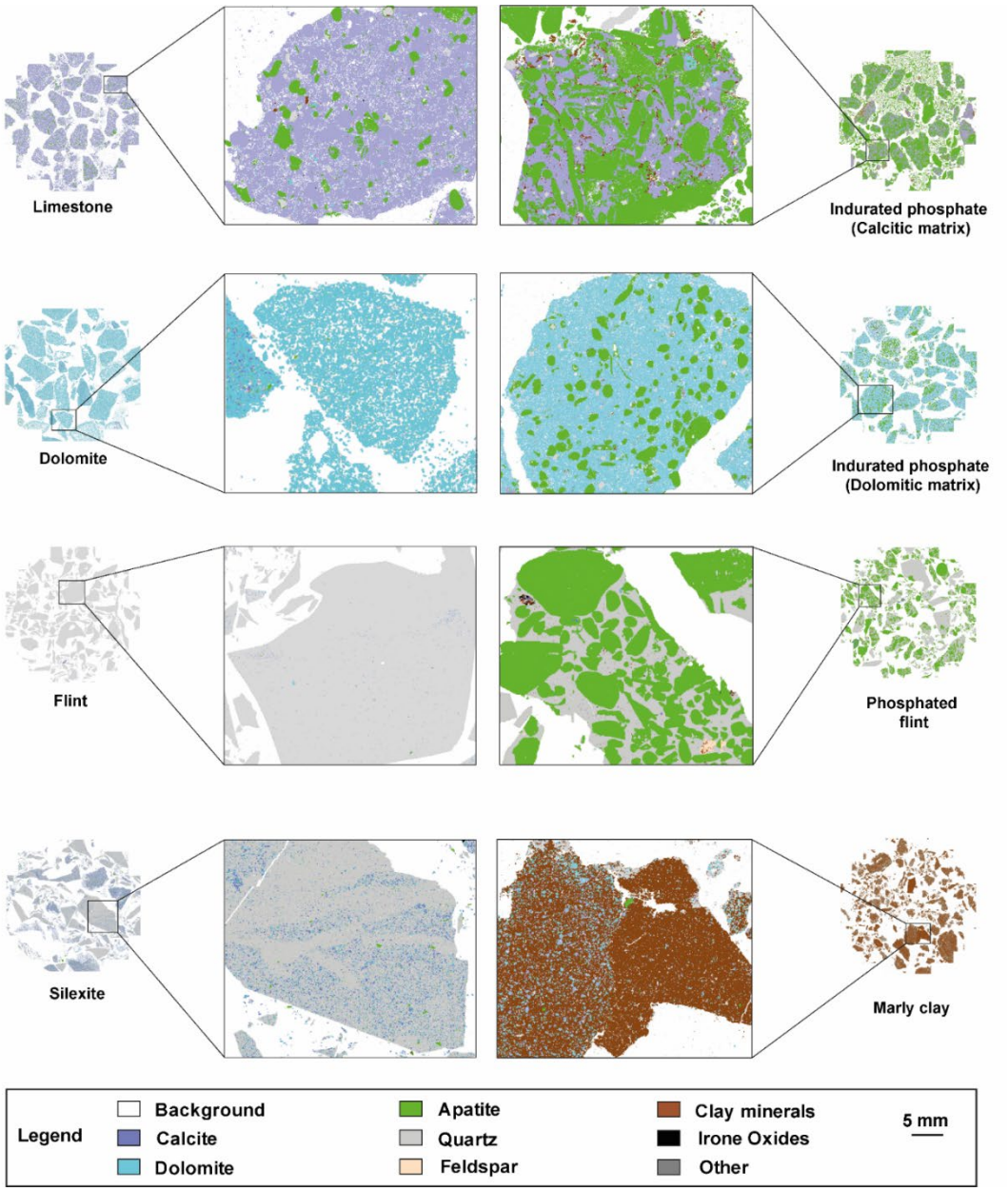

Figure 5-5: QEMSCAN® images of existing lithologies

5.4.2.2 Trace elements

As shown in Figure 5-6 and Appendix C, the chemical composition varies with lithology and depth. Across all samples, the mean abundance (ppm) of TE, in decreasing order is Sr (410), Zn (235), Cr (150), V (115), Ba (113), Ni (65), Zr (48), Y (41), U (27), Cu (19), Cd (18), Rb (9), Pb (5), As (3), Mo (3), Sc (4), Ga (3), Se (3), Nb (2), Th (2), Hf (1.24), Sb (0.63) and Cs (1). The high concentration of Sr (~1120 ppm), an element that can easily substitute for Ca in francolite (Garnit et al., 2017; Jarvis, 1994), is recorded in phosphate samples. Based on statistical analysis (collecting all concentration data and identifying minimum, maximum, and distribution values) and visualization of the data with a histogram, three categories of elements

were identified as "high," "moderate," and "low" based on their concentrations are next shown. The first group consists of Sr, Zn and Cr with relatively high concentrations (> 150 ppm). The second group contains TRs with moderate concentrations (10 to 150 ppm): V, Ba, Ni, Zr, Y, U, Cu, and Cd. The third group consists of TRs with relatively low concentrations (< 10 ppm): Rb, Pb, As, Mo, Sc, Se, Ga, Nb, Th, Hf, Sb, and Cs.

In the phosphate category, the Cd concentration varies between 7 and 58, U varies between 41 and 120 ppm, and Y is between 35 and 184 ppm, while the Th concentrations are lower than 2 ppm. Siliceous samples show high concentrations of Ba (61 – 1150 ppm) and Sr (44 – 278 ppm). In the category of carbonate, the Sr (86 – 976 ppm), Zn, Cr, V, Ni, Zr, Cd, and Ba present high concentrations (140-380 ppm). The marly clay shows high concentration compared to other lithologies in terms of Zn (308-618 ppm), V (180-283 ppm), Cr (131-282 ppm), Sr (103-136 ppm).

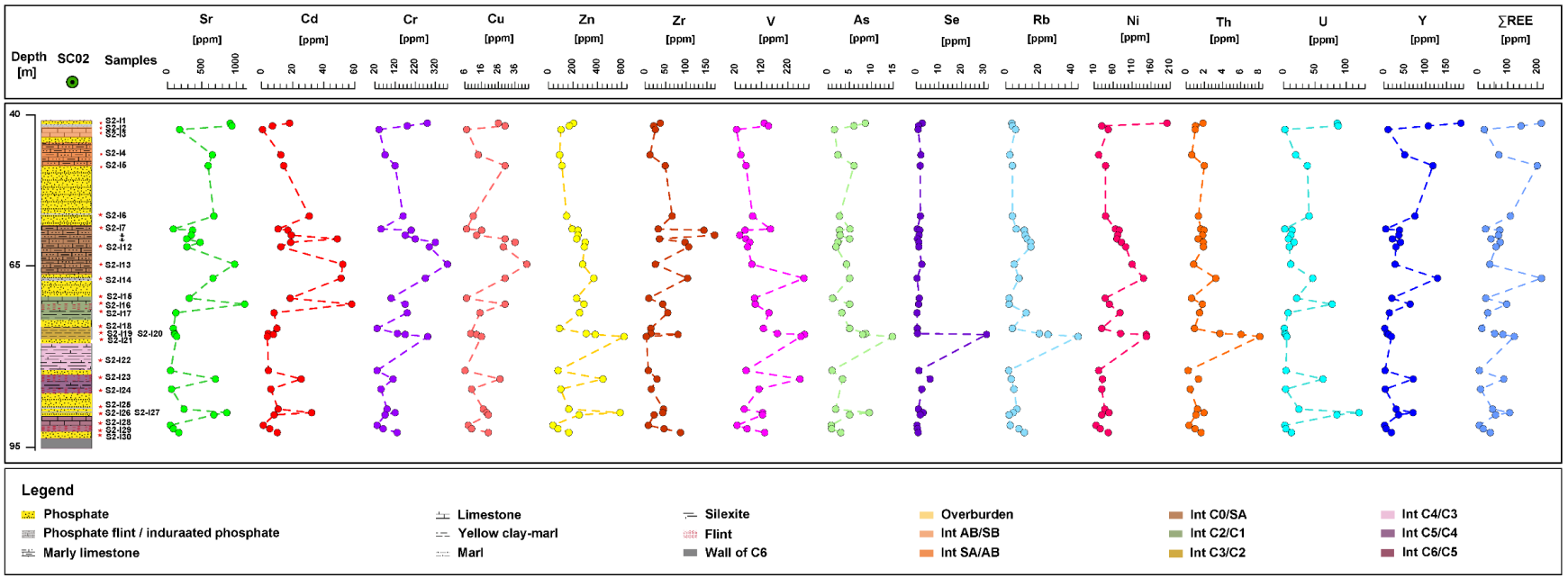

Figure 5-6: Trace element variation diagrams for SC02 interburdens of Benguerir mine

5.4.2.3 Rare earth elements (REE)

Total REE (∑REE) concentrations show considerable variation, ranging from 4 to 214 ppm (Figure 5-6). The phosphate category has higher REE contents than the other samples (∑REE ranging between 60 and 213 ppm). The Moroccan phosphates deposit have lower REE values than other samples from around the world (∑REE exhibit a median varying between 314.5 and 289.21 ppm) (Buccione et al., 2021; El Bamiki et al., 2021). The most abundant REEs in the samples from the Benguerir's interburdens are: La (< 70 ppm), Ce (< 52 ppm), and Nd (< 50 ppm), which correspond to light rare earth elements (LREE), while heavy rare earth elements (HREE) present lower concentration. The lowest ∑REE concentration was recorded in siliceous samples (~ 4 ppm). The ∑REE show a positive correlation with P_2O_5 (El Bamiki et al., 2023), but no correlation was observed for SiO_2 and MgO. According to Alharshan et al. (2021) and Garnit et al. (2017), the correlation between ∑REE and P_2O_5 is higher in sedimentary phosphate deposits compared to igneous deposits. This is because sedimentary deposits are formed through precipitation and accumulation of phosphate minerals in a reduced environment. The study of REE distribution in Moroccan deposits (in fossil bioapatite, along with other geochemical proxies), revealed that phosphogenesis took place in environments with early diagenetic fluids dominated by seawater (Kocsis et al., 2016). These environments were characterized by oxic to sub-oxic conditions and experienced minimal diagenetic alteration (Aubineau et al., 2022; El Bamiki et al., 2023; Kocsis et al., 2016; Kocsis et al., 2021).

5.4.2.4 Statistical analysis of data

The results of the statistical analysis (descriptive statistics, normality testing, and factor analysis) are presented in Appendix C. The distribution of raw data using the Shapiro-Wilk test (Shapiro & Wilk, 1965) and the QQ plot (Hazen, 1914) indicates that nearly all of the measured elements do not exhibit a normal distribution Appendix C. The Pearson's correlations are the most basic form of statistical data analysis technique. It was used to investigate the affinities between the different chemical compositions. The chemical elements show positive and other negative correlations, among these correlations appear (Appendix C):

- P_2O_5 shows a positive correlation (> 0.5) with: CaO, MgO, Na_2O, Sr, U, Cd, Y and REE.
- CaO is positively correlated with Na_2O, P_2O_5, Sr, U, Cd, Cu, Mo, Y and REE

- MgO shows negative correlation with: P_2O_5, Sr, U, Y, and REE.
- SiO_2 is negatively correlated with CaO, Sr, Cd, Y and REE and positively with Ba.

However, issues arise when applying Pearson's correlations to compositional data, as discussed by various authors (Filzmoser et al., 2010; Reimann et al., 2016; Reimann et al., 2015). They proposed solutions for bivariate analysis, emphasizing that classical correlations on log-transformed data might not accurately represent relationships due to neglecting the effect of all variables. Symmetrical coordinates were suggested for better interpreting geochemical processes (Kynčlová et al., 2017). Principal Component Analysis (PCA) reduces dimensionality and explains correlations between variables in large datasets. A centered log ratio (CLR) transformation is recommended to address the closure effect on correlations before applying PCA (Aitchison, 1982; Pesenson et al., 2015).

Figure 5-7 and Appendix C illustrate the results of PCA analysis using XLSTAT software. The current research shows that the data transformed using CLR method have a Kaiser-Meyer-Olkin (KMO) test result of 0.619, which is above the acceptable threshold of 0.5, indicating their appropriateness for factor analysis (See Appendix C). Principal components were derived from a correlation matrix of the CLR-transformed data and subjected to Varimax rotation. The analysis revealed that the two primary components, PC1 and PC2, account for 68.15% of the total variance (PC1 = 37.09%, PC2 = 31.05%). Given that other components contribute less variance, above 9%, only PC1 and PC2 were retained for generating a biplot illustrating the relationships between variables and individuals (See Appendix C).

Figure 5-7A shows the position of the loadings in the plane defined by the axes of principal components 1 and 2. PC1 is characterized by high positive loadings on REEs, Y, and P_2O_5, U, Sr, CaO, Na_2O, Cd, and high negative loadings towards Al_2O_3, Fe_2O_3, TiO_2, and K_2O, together with a range of TRs (e.g., Th, Sc, Ni, Pb, and Ce). The elements of the negative loading of PC1 are regarded as a detrital mineral factor since they are connected to clays and heavy elements. The extremely high positive loading values on Sr, U, P_2O_5, Y, and REEs show how these elements play a significant role in determining the geochemical variety in phosphate rock, which occur as REE-Y substitute for calcium (Ca) in apatite values (Garnit et al., 2017). The moderate positive loadings for Na_2O, and CaO, and trace elements Cd, Se, Cu, and Mo, this loading can be explained by the

depositional environment and diagenesis and the seawater source. This component divides major elements and TEs into two major clusters. One group includes phosphate rock and related elements with positive loadings on PC1, while the other consists of silicates and heavy elements with negative loadings on PC1. Principal component 2 is characterized by high to moderate positive loading in REEs, Y, and Ce. On the other hand, PC2 displays high to moderate negative loading of SiO_2, MgO, LOI, and TRs (e.g., Nb, Cr, Cu, Ba, Pb, V, and Z). This can be interpreted by the presence of organic matter and siliceous matrix.

Figure 5-7B shows the plotting of individual samples within variable space. Four groups are identified from the samples. Most samples (carbonates: calcite and dolomite) form a group with low negative values of PC1 and positive values of PC2. The phosphorite samples form a group with positive values of PC1 and PC2, while siliceous samples with negative values of PC1 and PC2. A small cluster of samples S2-I19, S2-I20, and S2-I21 is localized in the negative sector of PC1 and positive of PC2.

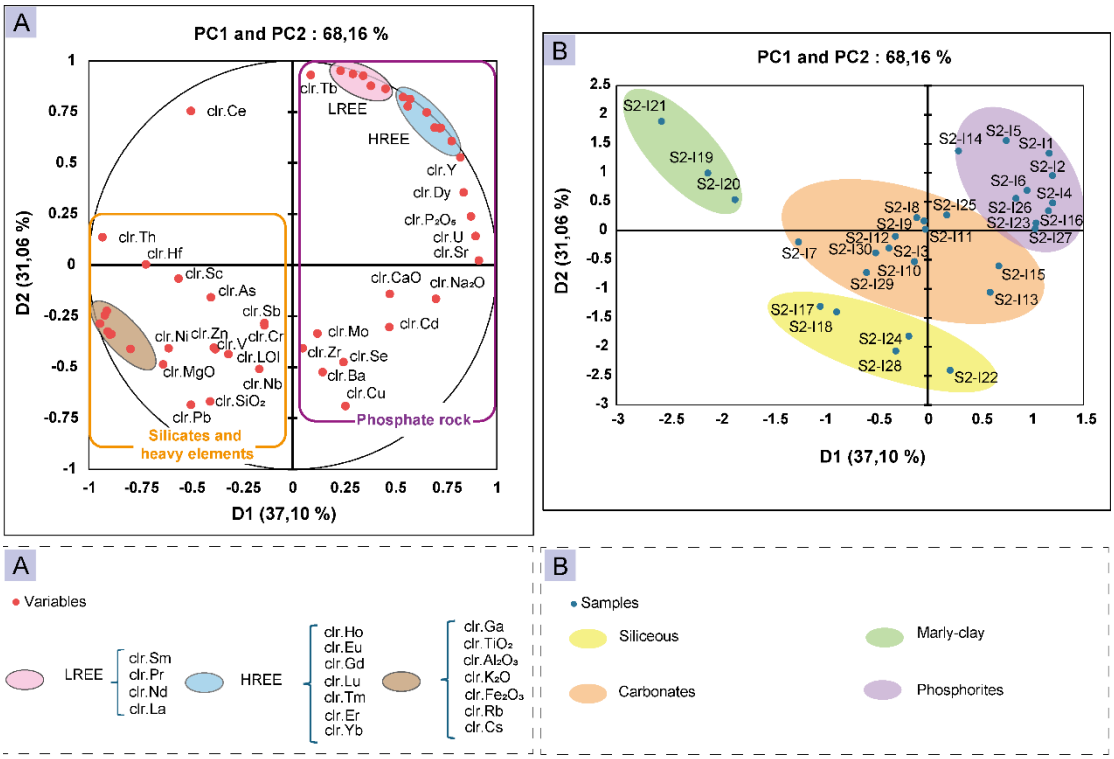

Figure 5-7: Loading plots for the first two factors from the principal components analysis (PCA) of SC02 interburdens geochemical data: (A) geochemical constituent plot, (B) sample plot.

5.4.3 Environmental characterization

Phosphate mining is a significant source of economic development in many parts of the world, with the production of fertilizers and other products being a significant driver of economic growth. However, the mining process produces a significant amount of waste rock which can have detrimental effects on the environment. This section focuses on the environmental characterization of PWR, exploring the methods (acid-generating potential and leachate tests) to assess its behavior. Environmental characterization in PWR typically involves assessing various parameters (pH, CE, Acid-Base Accounting (ABA), and leaching tests) to evaluate the potential impact of waste rock on the surrounding environment.

a. Acid-generating potential assessment

The results of acid generating potential assessment are shown in Table 5-1 and Figure 5-8. The samples studied showed high NP (38 to 991 kg $CaCO_3$/t) and low AP (0.31 to 16 kg $CaCO_3$/t) (Figure 5-8). The carbonates (dolomite and calcite) showed a high value of NP (500 to 991 kg $CaCO_3$/t), while siliceous samples showed lower NP values (38 to 360 kg $CaCO_3$/t). The Net Neutralization Potential (NNP) shows positive values for all samples ranging from (36 to 990 kg $CaCO_3$/t). According to the classification criteria proposed by Miller et al. (1991), all samples are non-acid generating (NNP > 20 kg $CaCO_3$/t). The NP/AP ratio shows values higher than 2.5 which means that PWR are non-acid generating.

Table 5-1: The results of C/S analysis and acid-generating potential assessment. AP: acid generation potential, NP: carbonate neutralization potential; NNP: net neutralization potential; NPR: Neutralization potential ratio.

	Carbon	**Sulfur**	**AP**	**NP**	**NNP**	**NPR**
	%			**KgCaCO$_3$/t**		
S2-I1	4.72	0.39	12.19	393.18	380.99	32.26
S2-I2	4.59	0.27	8.44	382.35	373.91	45.32
S2-I3	11.90	0.03	0.94	991.27	990.33	1057.35
S2-I4	10.75	0.07	2.19	895.48	893.29	409.36
S2-I5	8.50	0.12	3.75	708.05	704.30	188.81
S2-I6	6.45	0.23	7.19	537.29	530.10	74.75
S2-I7	10.65	0.01	0.31	887.15	886.83	2838.86
S2-I8	7.45	0.11	3.44	620.59	617.15	180.53
S2-I9	7.98	0.11	3.44	664.73	661.30	193.38
S2-I10	4.33	0.28	8.75	360.69	351.94	41.22
S2-I11	6.75	0.12	3.75	562.28	558.53	149.94
S2-I12	9.07	0.09	2.81	755.53	752.72	268.63
S2-I13	10.95	0.08	2.50	912.14	909.64	364.85
S2-I14	7.43	0.11	3.44	618.92	615.48	180.05
S2-I15	11.60	0.08	2.50	966.28	963.78	386.51
S2-I16	4.44	0.25	7.81	369.85	362.04	47.34
S2-I17	3.44	0.05	1.56	286.55	284.99	183.39
S2-I18	9.93	0.10	3.13	827.17	824.04	264.69
S2-I19	3.80	0.02	0.63	316.54	315.92	506.46
S2-I20	4.41	0.03	0.94	367.35	366.42	391.84
S2-I21	4.20	0.03	0.94	349.86	348.92	373.18
S2-I22	1.49	0.04	1.25	124.12	122.87	99.29
S2-I23	1.68	0.40	12.50	139.94	127.44	11.20
S2-I24	3.36	0.05	1.56	279.89	278.33	179.13
S2-I25	10.15	0.11	3.44	845.50	842.06	245.96
S2-I26	4.63	0.49	15.31	385.68	370.37	25.19
S2-I27	0.94	0.50	15.63	78.30	62.68	5.01
S2-I28	0.45	0.04	1.25	37.49	36.24	29.99
S2-I29	9.01	0.03	0.94	750.53	749.60	800.57
S2-I30	9.73	0.07	2.19	810.51	808.32	370.52

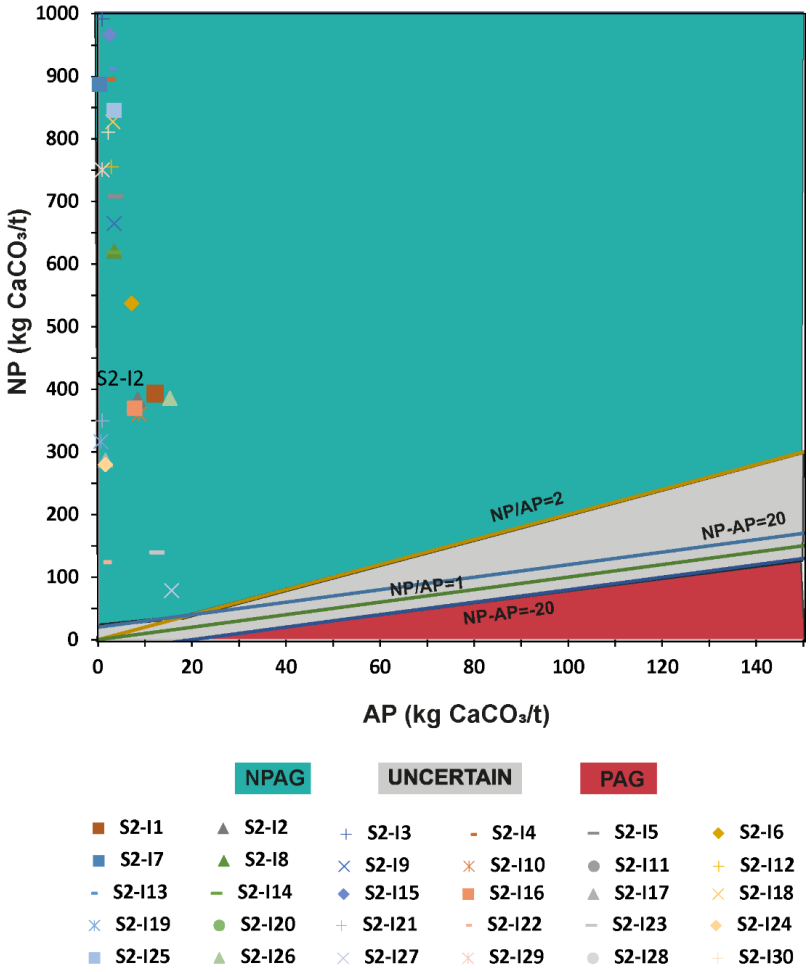

Figure 5-8: Graph presenting the acid generation potential results

b. Semi-dynamic test: monolith leaching test

The Monolith Leaching Test (MLT) is an essential method for evaluating the potential environmental impact of PWR. This test provides a comprehensive understanding of the leaching behavior of contaminants present in waste rock for 64 days, helping to identify potential environmental risks.

- **Electrochemical analysis: pH, EC, and Eh**

The results of pH, EC, and Eh are presented in Figure 5-9A. Regardless of the type of samples, the evolution of pH, EC, and Eh in leachates showed a similar trend. The pH values remained alkaline for the whole duration of the test ranging from 8.3 to 10. At the end of the test, the pH stabilized at

9 ±0.4. The EC values were low in the first days (ranging from 18 to 39 µS/cm) and increased after the first week to attain values around 56 µS/cm, while the Eh was around 600 mV. The increase in electrical conductivity at the end of the test is explained by the presence of salinity due to ions such as sodium (Na^+). Calcite and dolomite are the main phases of PWR, their pH of solution is above 9, while the pH of apatite and silicon solution is near 7 (Somasundaran & Wang, 2006). Therefore, this is why the pH of PWR should behave as alkaline.

- **Release of major (Ca, Mg, K, Si, Sr, and P) and trace elements (As, Ba, Cd, Cr, Se, U) in MLT**

Based on the results of mineralogical and chemical analysis, the major elements analyzed are Ca, Mg, K, Si, Sr, and P. The concentration (µg/L) of major elements are presented in Figure 5-9B. The main abundant concentrations (µg/L) are Si >1550, Mg >265, P >60, K >50, Ca >30, and Sr > 5. In general, all these major elements had high mobility at the beginning of the test and after a month they attained the stable state. High release of soluble major elements (Ca, Mg, K and Sr) was identified in all samples. Most of these elements are contained in carbonates and phosphate minerals. The pH of the leachate remained high due to the high neutralization potential of the samples. The mobility of Si and P was higher in all samples than the other elements. Silicon is provided by mainly silicate dissolution, while phosphor is provided by apatite dissolution.

Concentration of contaminants (As, Ba, Cd, Cr, Se, U) during the MLT are presented in Figure 5-9B. Low concentrations were measured during the first month, which then stabilized after this period over time. The main abundant concentrations (µg/l) are ranging from: 0.5-1.2 for As, 0.5-12 for Ba, 0.02-0.1 for Cd, 0.6-7.8 for Cr, 0.5-24 for Se, and 1-3 for U. The contaminants concentrations were insignificant or below detection limits for the ICP-AES analysis. Comparing these results with the USEPA and UTS standards (Table 5-2), we find that they are below the regulatory limits, which could be considered as non-hazardous waste.

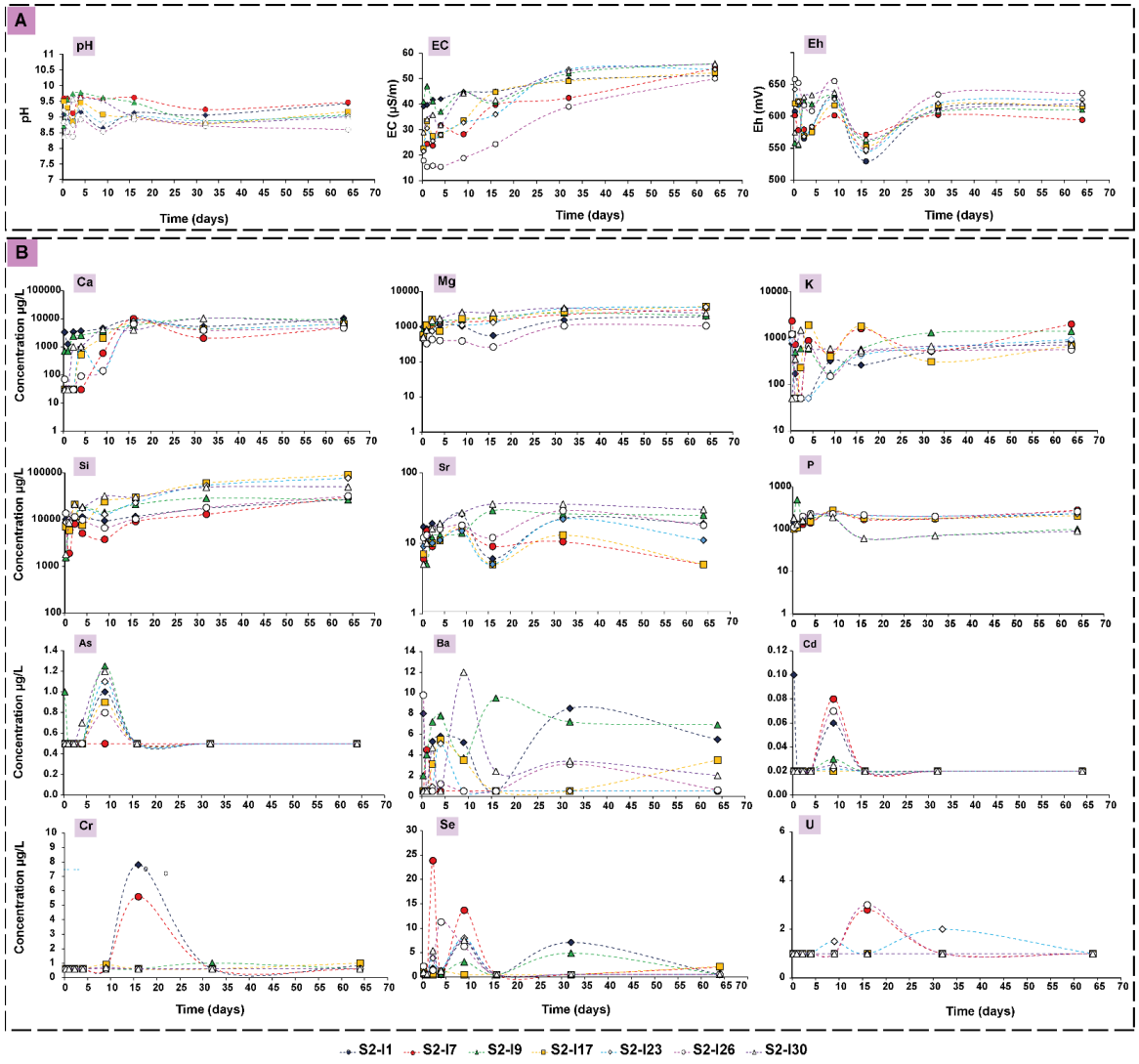

Figure 5-9: A) Evolution of pH, EC, and Eh and B) Release of major elements (Ca, Mg, K, Si, Sr, and P) and trace elements (As, Ba, Cd, Cr, Se, and U) during MLT.

c. Static tests: TCLP and SPLP

Results of the toxicity characteristic leaching procedure (TCLP) tests and Synthetic Precipitation Leaching Procedure (SPLP) are presented in Figure 5-10 and Figure 5-11.

- **Electrochemical analysis: pH**

Figure 5-10 shows the behavior of initial and final pH for TCLP and SPLP tests for each sample. The initial pH of the leachates in the TCLP test showed acidic values ranging from 3.47 to 5.52,

At the end of the test the pH increased to attain circumneutral values. The TCLP test was performed under acidic pH conditions (2.88 to 4.93 ± 0.05) while the final pH attained circumneutral values (pH = 6 ± 0.6), which can be explained by the dissolution of neutralizing minerals (carbonates). The initial and final pH of the SPLP test remains neutral to alkaline, ranging from 7 to 10 and 7.19 to 9.3 for initial pH and final pH, respectively. The initial SPLP pH values are all above 4.20, whereas the SPLP solution has a starting pH of 4.20, mainly due to the high reactivity and neutralization capacity present in the PWR samples.

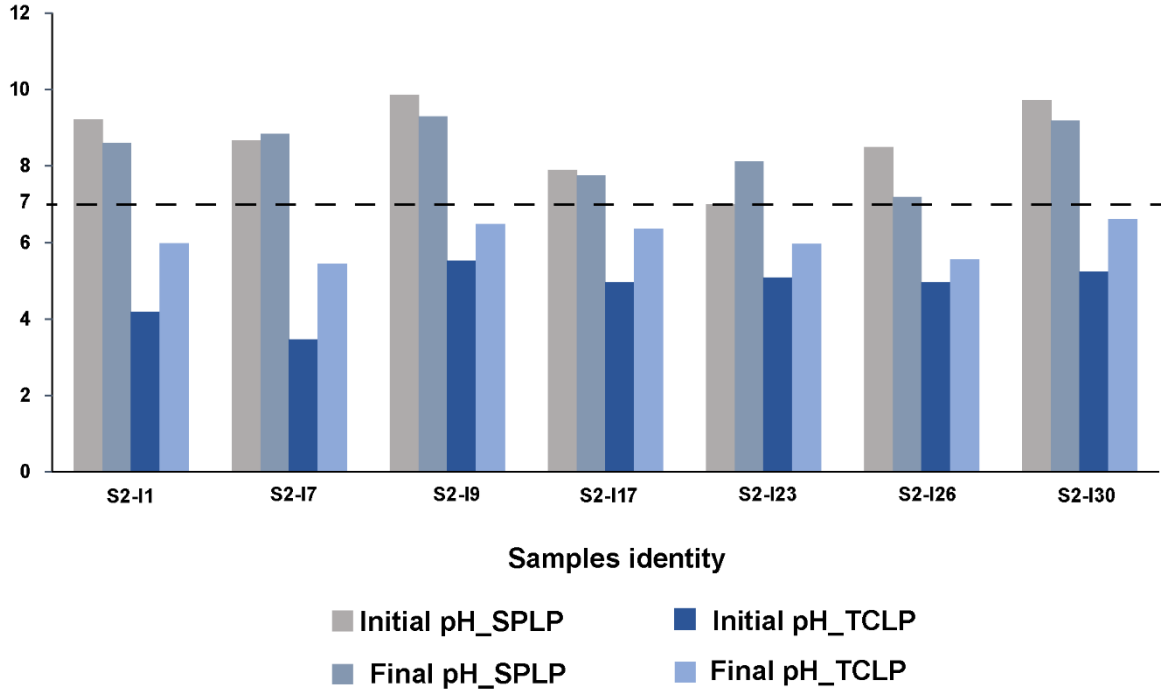

Figure 5-10: Behavior of initial and final pH for TCLP and SPLP tests

- **Release of major (Ca, Mg, K, Si, Sr, and P) and trace (As, Ba, Cd, Cr, Se, U) elements in TCLP and SPLP tests**

The results of major elements (Ca, Mg, K, Si, Sr, and P) in both tests are presented in Figure 5-11. The concentration (mg/L) in TCLP and SPLP tests, respectively, is Ca < 2560 and < 18, Mg < 712 and < 4.7, K < 10 and < 4.18, Si < 47 and < 74, Sr < 1.23 and < 0.11, P < 1.25 and 5.15. The release of these major elements from PWR is influenced by several factors, including mineralogy and the chemical of the rock and pH of the environment. The presence of apatite, calcite and dolomite contribute to the release of P, Ca, Mg and Sr. Alkhraisat et al. (2010) investigated the effect of

different pH levels on strontium release from strontium-containing hydroxyapatite (Sr-HA) particles. The study found that acidic conditions led to increased strontium release, with pH levels of 4 and 5 resulting in the highest amount of strontium release compared to neutral pH levels. While the release of Si depends on the presence of siliceous minerals like quartz. The release of potassium depends on the mineralogy of PWR, specifically the presence of potassium-bearing minerals such as K-feldspar.

Figure 5-11 shows the release of As, Ba, Cd, Cr, Se, and U in both tests. The concentration of each element is not similar; it depends on each sample. The mobility of As, Ba, Cd, and U is higher in TCLP than in SPLP, of Cr and U is almost the same in most samples in both tests. On the contrary, the release of Se is higher in SPLP than in TCLP. Qualitatively, for TCLP and SPLP tests the order of trace elements release was Ba > Cd > As > U > Se > Cr, and Ba > Se > U > Cr > As > Cd, respectively. Quantitatively, the chemical species release rates (µg/L) in each test TCLP and SPLP, respectively were 0.5 – 14 and 0.5 for As, 103 – 793 and 2 – 47 for Ba, 3 – 95 and 0.02 – 0.52 for Cd, 0.6 – 5.4 and 0.6 – 4.6 for Cr, 0.5 – 5.3 and 4 – 13 for Se, 1 – 13 and 1 – 4.5 for U. This results indicate that the release of trace elements in TCLP and SPLP (Table 5-2) is below the regulatory limits (MDDELCC, 2013; USEPA., 2009; UTS, 2017).

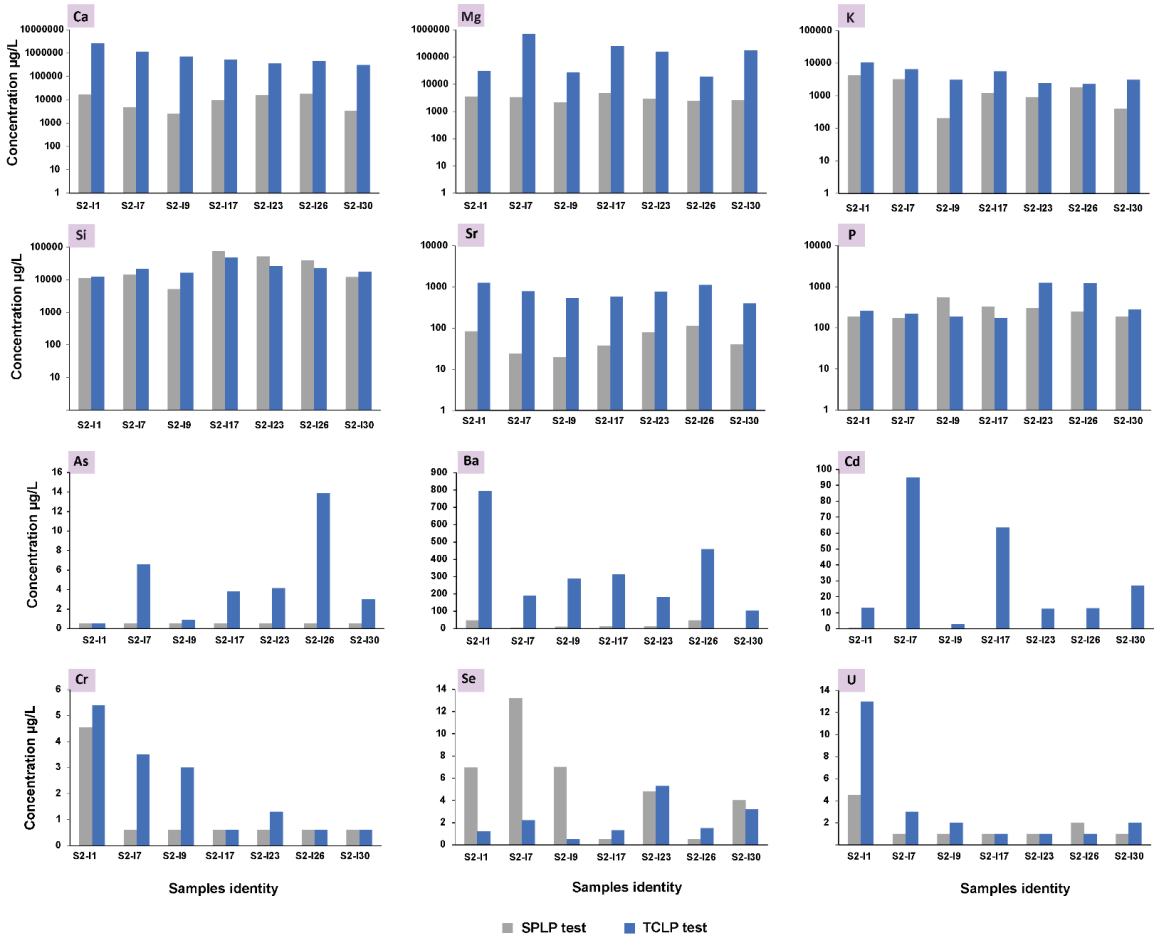

Figure 5-11: Release of major elements (Ca, Mg, K, Sr, and P) and trace elements (As, Ba, Cd, Cr, Se, and U) during TCLP and SPLP tests

5.4.4 Comparison between static and semi-dynamic behavior of contaminants and classification of residues

Static and semi-dynamic tests are commonly used in environmental assessments to evaluate the behavior of contaminants in various materials or systems.

Generally, pH, leaching solution, particle size, reaction time, and agitation are all crucial factors that play a significant role in determining the outcome of leaching (Elghali et al., 2022; Li et al., 2006; Liu et al., 2022). The pH values at the end of the SPLP and MLT tests were alkaline (~10). However, the pH values in the TCLP leachates were below neutral pH (< 7). It is important to note that leaching capacity is highly related to the pH of the leaching environment (Król et al., 2020),

the more acidic the pH results, the higher the leaching of elements. Some metals (e.g., Cr, and Cd) were not mobilized during the SPLP and MLT tests, whereas, compared to the results of TCLP tests, they showed high concentrations, which means the important role of the leaching solution (deionized water in MLT, nitric and sulfuric acid in SPLP, and acetic acid in TCLP), because acetic acid could complex metal, and therefore, increase its mobility (Jouini et al., 2019). Se concentration was significant in the leachates of the MLT and SPLP tests. However, the Se concentration during the TCLP test was much lower than that measured in the MLT leachates. This could be explained by the difference in pH values during leaching (Torres et al., 2011). The solubility of the elements increases with increasing pH.

The particle size of the samples can greatly affect the reaction kinetics and the release of elements (Elghali et al., 2019). Smaller particle sizes (i.e., TCLP and SPLP < 9.5 mm) provide a larger surface area, facilitating the contact between the leaching solution and the solid material, and allowing for more efficient reactions and increased reaction rates (Liu et al., 2022; Stöber et al., 1968). Conversely, larger particle sizes (i.e., MLT > 3 cm) exhibited lower extraction efficiency due to reduced surface area and slower leaching rates. Additionally, the presence of agitation and the duration of the reaction time can significantly impact reaction rates and yields. Agitation promotes mixing and enhances mass transfer, improving the contact between reactants and facilitating faster reactions. These findings highlight the crucial role of particle size, agitation, and duration of the reaction in leaching tests (TCLP and SPLP for 18 h, while MLT is designed to simulate the long-term leaching for 64 days) and emphasize the need to carefully consider and control them when designing and conducting such experiments.

The major elements Ca, Mg, K, and Sr were much more leached during the static TCLP and SPLP tests. Indeed, as expected, the leaching depends on the type of sample (crushed or monolith). For all the crushed samples (TCLP and SPLP tests), the elements' leaching was higher than that observed for the samples of whole blocks (MLT). This is attributed to the increased surface area of the ground sample with the leaching solution. This finding suggests that using crushed samples for leaching tests may provide a more realistic representation of the potential release of contaminants from the materials in question. Concerning Si and P, their concentrations were very similar in the leachates of the static tests, which is near to that obtained from the MLT test.

The study of PWR upstream of the operating sequence - trough leaching tests - shows that all the samples had concentrations below the limits for non-hazardous waste (Table 5-2) fixed by the United States Environmental Protection Agency (USEPA) regulations and the worldwide or universal treatment standard (UTS) (USEPA, 1992; USEPA., 2009). According to these standards, the PWR of the Benguerir mine in Morocco could be considered as non-hazardous waste.

Table 5-2: Average TEs concentrations of the trace elements in the leachates collected after TCLP, SPLP, and MLT tests relative to standard regulations.

		As	**Ba**	**Cd**	**Cr**	**Se**	**U**
Standards (µg/L)	USEPA	5000	100 x10³	1000	5000	1000	2000
	UTS	5000	21000	110	600	5700	-
Tests (µg/L)	TCLP	7.2 ± 6.7	448 ±345	49 ±46	3.0 ±2.4	3.0 ± 2.4	7 ±6
	SPLP	0.5	24.65 ±22	0.27 ± 0.25	2.575 ±1.9	6.85 ±6.35	2.75 ± 1.75
	MLT	1.15 ± 0.65	20.15 ± 19	0.775 ± 7.55	4.2 ± 3.6	12.2 ± 11.7	2.5 ± 1.5

5.5 Conclusions

The present study evaluated the geochemical and environmental behavior of PWR by carrying out chemical and mineralogical characterizations and leaching tests. This study aims to provide a full characterization of PWR samples. The results obtained lead to the following conclusions:

- The mineralogical characterization revealed that the PWR is mostly composed of calcite, dolomite, apatite (carbonate fluor apatite), and quartz with the presence of minor phases such as clay minerals (feldspar and mica) and Fe oxides as identified by QEMSCAN.
- Chemically, major oxides in the interburdens samples are dominated by CaO and MgO, followed by SiO_2 and P_2O_5. Seven lithologies are identified in the Benguerir mine: limestone, dolomite, phosphated flint, indurated phosphate, flint, silexite, and marly clay. Trace elements can be classified into three groups: i) group of Zn and Cr (>150 ppm) ii) group of Ba, V, Ni, Zr, Y, U, Cu, Cd, Co (10 to 150 ppm), and iii) group of TEs with relatively low concentrations (<10 ppm): Rb, Pb, As, Mo, Se, Sc, Ga, Nb, Th, Hf, Sb and Cs.
- Environmentally the PWR samples are:

i) exhibit high neutralizing potential,

ii) The pHs of the leachates are neutral to alkaline for all the samples,

iii) The results of the static and semi-dynamic tests have confirmed the non-hazardousness of the waste.

Therefore, the studied PWR cannot be classified as hazardous waste and could be considered natural raw materials for use in different sectors.

Acknowledgments

The authors thank OCP Group (Benguerir mine) and the experimental mine Morocco for their support in the framework of the project RE04. The authors would like also to thank RIME staff for their support with materials testing and analyses, and the Expert Process Solutions (XPS) staff for their help with data analysis. The authors would like also to thank OCP collaborators and the staff of the Geo-analytical Lab of Mohammed VI Polytechnic University for the great help concerning the sampling, and the preparation.

Author contribution

Safa Chlahbi: conceptualization, methodology, validation, formal analysis, Investigation, writing—original draft, writing, review and editing, visualization. Mostafa Benzaazoua: conceptualization, writing review and editing, supervision, funding acquisition. Abdellatif Elghali: conceptualization, validation, writing, review and editing, supervision. Samia Rochdane: review and editing. Essaid Zarouali: review and editing. Tikou Belem: conceptualization, writing, review and editing, supervision.

Funding

This work was supported by OCP Group (Grant number RE04).

Declarations

Ethical approval: Not applicable.

Consent to participate: All authors consent to participate.

Consent for publication: All authors consent to publish.

Competing interests: The authors declare no competing interests.

References

Aitchison, J. (1982). The statistical analysis of compositional data. *Journal of the Royal Statistical Society: Series B (Methodological)*, *44*(2), 139-160.

Alharshan, G., Eke, C., & Al-Buriahi, M. (2021). Radiation-transmission and self-absorption factors of P2O5 – SrO – Sb2O3 glass system. *Radiation Physics and Chemistry*, *193*, 109938. https://doi.org/10.1016/j.radphyschem.2021.109938

Alkhraisat, M. H., Rueda, C., Cabrejos-Azama, J., Lucas-Aparicio, J., Mariño, F. T., Torres García-Denche, J., Jerez, L. B., Gbureck, U., & Cabarcos, E. L. (2010). Loading and release of doxycycline hyclate from strontium-substituted calcium phosphate cement. *Acta Biomaterialia*, *6*(4), 1522-1528. https://doi.org/https://doi.org/10.1016/j.actbio.2009.10.043

Amos, R. T., Blowes, D. W., Bailey, B. L., Sego, D. C., Smith, L., & Ritchie, A. I. M. (2015). Waste-rock hydrogeology and geochemistry. *Applied Geochemistry*, *57*, 140-156. https://doi.org/https://doi.org/10.1016/j.apgeochem.2014.06.020

Amrani, M., Taha, Y., Kchikach, A., Benzaazoua, M., & Hakkou, R. (2019). Valorization of Phosphate Mine Waste Rocks as Materials for Road Construction. *Minerals*, *9*(4). https://doi.org/10.3390/min9040237

Aubertin, M., Bussière, B., Bernier, L., Chapuis, R., Julien, M., Belem, T., Simon, R., Mbonimpa, M., Benzaazoua, M., & Li, L. (2002, 5-8 June). *La gestion des rejets miniers dans un contexte de développement durable et de protection de l'environnement* Congrès annuel de la société canadienne de génie civil, Montréal, Québec, Canada.

Aubineau, J., Parat, F., Elghali, A., Raji, O., Addou, A., Bonnet, C., Muñoz, M., Mauguin, O., Baron, F., Jouti, M. B., Yazami, O. K., & Bodinier, J.-L. (2022). Highly variable content of fluorapatite-hosted CO32−in the Upper Cretaceous/Paleogene phosphorites (Morocco) and implications for paleodepositional conditions. *Chemical Geology*, *597*, 120818. https://doi.org/https://doi.org/10.1016/j.chemgeo.2022.120818

Barcelo-Vidal, C., & Martín-Fernández, J.-A. (2016). The Mathematics of Compositional Analysis. *Austrian Journal of Statistics*, *45*(4), 57-71. https://doi.org/10.17713/ajs.v45i4.142

Benarchid, Y., Taha, Y., Argane, R., Tagnit-Hamou, A., & Benzaazoua, M. (2019). Concrete containing low-sulphide waste rocks as fine and coarse aggregates: Preliminary assessment of materials. *Journal of Cleaner Production*, *221*, 419-429. https://doi.org/https://doi.org/10.1016/j.jclepro.2019.02.227

Benzaazoua, M., Bussière, B., Dagenais, A. M., & Archambault, M. (2004). Kinetic tests comparison and interpretation for prediction of the Joutel tailings acid generation potential. Environmental Geology,

Boujo, A. (1976). *Contribution à l'étude géologique du gisement de phosphate crétacé-éocène des Ganntour (Maroc occidental)* (Publication Number 43) Université Louis-Pasteur]. www.persee.fr. Strasbourg : Institut de Géologie https://www.persee.fr/doc/sgeol_0302-2684_1976_mon_43_1

Boumaza, B., Chekushina, T. V., Kechiched, R., Benabdeslam, N., Brahmi, L., Kucher, D. E., & Rebouh, N. Y. (2023). Environmental Geochemistry of Potentially Toxic Metals in Phosphate Rocks, Products, and Their Wastes in the Algerian Phosphate Mining Area (Tébessa, NE Algeria). *Minerals*, *13*(7), 853. https://www.mdpi.com/2075-163X/13/7/853

Boumaza, B., Chekushina, T. V., Vorobyev, K. A., & Schesnyak, L. E. (2021b). The heavy metal pollution in groundwater, surface and spring water in phosphorite mining area of Tebessa (Algeria). *Environmental Nanotechnology, Monitoring & Management*, *16*, 100591. https://doi.org/https://doi.org/10.1016/j.enmm.2021.100591

Boumaza, B., Kechiched, R., & Chekushina, T. V. (2021a). Trace metal elements in phosphate rock wastes from the Djebel Onk mining area (Tébessa, eastern Algeria): A geochemical study and environmental implications. *Applied Geochemistry*, *127*. https://doi.org/10.1016/j.apgeochem.2021.104910

Boumaza, B., Kechiched, R., Chekushina, T. V., Benabdeslam, N., Senouci, K., Hamitouche, A. y.-e., Merzeg, F. A., Rezgui, W., Rebouh, N. Y., & Harizi, K. (2024). Geochemical distribution and environmental assessment of potentially toxic elements in farmland soils, sediments, and tailings from phosphate industrial area (NE Algeria). *Journal of Hazardous Materials*, *465*, 133110. https://doi.org/https://doi.org/10.1016/j.jhazmat.2023.133110

Bouzahzah, H., Benzaazoua, M., Plante, B., & Bussiere, B. (2015). A quantitative approach for the estimation of the "fizz rating" parameter in the acid-base accounting tests: A new adaptations of the Sobek test. *Journal of Geochemical Exploration*, *153*, 53-65. https://doi.org/https://doi.org/10.1016/j.gexplo.2015.03.003

Buccione, R., Kechiched, R., Mongelli, G., & Sinisi, R. (2021). REEs in the North Africa P-Bearing Deposits, Paleoenvironments, and Economic Perspectives: A Review. *Minerals*, *11*(2), 214. https://www.mdpi.com/2075-163X/11/2/214

Chlahbi, S., Belem, T., Elghali, A., Rochdane, S., Zerouali, E., Inabi, O., & Benzaazoua, M. (2023). Geological and Geomechanical Characterization of Phosphate Mine Waste Rock in View of Their Potential Civil Applications: A Case Study of the Benguerir Mine Site, Morocco. *Minerals*, *13*(10), 1291. https://www.mdpi.com/2075-163X/13/10/1291

da Silva, E. F., Mlayah, A., Gomes, C., Noronha, F., Charef, A., Sequeira, C., Esteves, V., & Marques, A. R. (2010). Heavy elements in the phosphorite from Kalaat Khasba mine (North-western Tunisia): potential implications on the environment and human health. *J Hazard Mater*, *182*(1-3), 232-245. https://doi.org/10.1016/j.jhazmat.2010.06.020

Dunham, R. J. (1962). Classification of Carbonate Rocks According to Depositional Texture in Classification of Carbonate Rockes. . *Sympo AAPG.*

Egozcue, J. J., Gozzi, C., Buccianti, A., & Pawlowsky-Glahn, V. (2024). Exploring geochemical data using compositional techniques: A practical guide. *Journal of Geochemical Exploration*, *258*, 107385. https://doi.org/https://doi.org/10.1016/j.gexplo.2024.107385

El Bamiki, R. (2020). *Étude géologique des occurrences phosphatées du Haut-Atlas Marocain: Compréhension des contrôles géologiques sur l'accumulation du phosphate* Université Montpellier; Université Cadi Ayyad (Marrakech, Maroc)].

El Bamiki, R., Raji, O., Ouabid, M., Elghali, A., Khadiri Yazami, O., & Bodinier, J.-L. (2021). Phosphate Rocks: A Review of Sedimentary and Igneous Occurrences in Morocco. *Minerals*, *11*(10). https://doi.org/10.3390/min11101137

El Bamiki, R., Séranne, M., Parat, F., Aubineau, J., Chellaï, E. H., Marzoqi, M., & Bodinier, J.-L. (2023). Post-phosphogenesis processes and the natural beneficiation of phosphates: Geochemical evidence from the Moroccan High Atlas phosphate-rich sediments. *Chemical Geology*, *631*, 121523. https://doi.org/https://doi.org/10.1016/j.chemgeo.2023.121523

Elghali, A., Benzaazoua, M., Bouzahzah, H., Bussière, B., & Villarraga-Gómez, H. (2018). Determination of the available acid-generating potential of waste rock, part I: Mineralogical approach. *Applied Geochemistry*, *99*, 31-41. https://doi.org/https://doi.org/10.1016/j.apgeochem.2018.10.021

Elghali, A., Benzaazoua, M., Bussière, B., & Bouzahzah, H. (2019). Determination of the available acid-generating potential of waste rock, part II: Waste management involvement. *Applied Geochemistry*, *100*, 316-325. https://doi.org/https://doi.org/10.1016/j.apgeochem.2018.12.010

Elghali, A., Benzaazoua, M., Couvidat, J., Taha, Y., Darricau, L., Neculita, C. M., & Chatain, V. (2022). Chapter 7 - Stabilization/solidification of sediments: challenges and novelties. In D. C. W. Tsang & L. Wang (Eds.), *Low Carbon Stabilization and Solidification of Hazardous Wastes* (pp. 93-112). Elsevier. https://doi.org/https://doi.org/10.1016/B978-0-12-824004-5.00023-2

Elghali, A., Benzaazoua, M., Taha, Y., Amar, H., Ait-khouia, Y., Bouzahzah, H., & Hakkou, R. (2023). Prediction of acid mine drainage: Where we are. *Earth-Science Reviews*, *241*, 104421. https://doi.org/https://doi.org/10.1016/j.earscirev.2023.104421

Filzmoser, P., Hron, K., & Reimann, C. (2010). The bivariate statistical analysis of environmental (compositional) data. *Science of The Total Environment*, *408*(19), 4230-4238. https://doi.org/https://doi.org/10.1016/j.scitotenv.2010.05.011

Garnit, H., Bouhlel, S., & Jarvis, I. (2017). Geochemistry and depositional environments of Paleocene–Eocene phosphorites: Metlaoui Group, Tunisia. *Journal of African Earth Sciences*, *134*, 704-736. https://doi.org/https://doi.org/10.1016/j.jafrearsci.2017.07.021

Hakkou, R., Benzaazoua, M., & Bussière, B. (2008). Acid Mine Drainage at the Abandoned Kettara Mine (Morocco): 1. Environmental Characterization. *Mine Water and the Environment*, *27*(3), 145-159. https://doi.org/10.1007/s10230-008-0036-6

Hakkou, R., Benzaazoua, M., & Bussière, B. (2009). Laboratory Evaluation of the Use of Alkaline Phosphate Wastes for the Control of Acidic Mine Drainage. *Mine Water and the Environment*, *28*(3). https://doi.org/10.1007/s10230-009-0081-9

Hazen, A. (1914). Storage to be provided in impounding municipal water supply. *Transactions of the American society of civil engineers*, *77*(1), 1539-1640.

Idrissi, H., Taha, Y., Elghali, A., El Khessaimi, Y., Aboulayt, A., Amalik, J., Hakkou, R., & Benzaazoua, M. (2021). Sustainable use of phosphate waste rocks: From characterization

to potential applications. *Materials Chemistry and Physics*, *260*. https://doi.org/10.1016/j.matchemphys.2020.124119

Jarvis, I. (1994). Phosphorite geochemistry: state-of-the-art and environmental concerns. *Eclogae Geologicae Helvetiae*, *87*, 643-700.

Jasinski, S. M. (2022). Mineral commodity summaries: Phosphate Rock. *U.S. Geological Survey*.

Jiang, L.-g., Liang, B., Xue, Q., & Yin, C.-w. (2016). Characterization of phosphorus leaching from phosphate waste rock in the Xiangxi River watershed, Three Gorges Reservoir, China. *Chemosphere*, *150*, 130-138. https://doi.org/https://doi.org/10.1016/j.chemosphere.2016.02.008

Jong, T., & Parry, D. L. (2005). Evaluation of the stability of arsenic immobilized by microbial sulfate reduction using TCLP extractions and long-term leaching techniques. *Chemosphere*, *60*(2), 254-265. https://doi.org/https://doi.org/10.1016/j.chemosphere.2004.12.046

Jouini, M., Benzaazoua, M., Neculita, C. M., & Genty, T. (2020). Performances of stabilization/solidification process of acid mine drainage passive treatment residues: Assessment of the environmental and mechanical behaviors. *Journal of Environmental Management*, *269*, 110764. https://doi.org/https://doi.org/10.1016/j.jenvman.2020.110764

Jouini, M., Rakotonimaro, T. V., Neculita, C. M., Genty, T., & Benzaazoua, M. (2019). Prediction of the environmental behavior of residues from the passive treatment of acid mine drainage. *Applied Geochemistry*, *110*, 104421. https://doi.org/https://doi.org/10.1016/j.apgeochem.2019.104421

Khalil, A., Hanich, L., Bannari, A., Zouhri, L., Pourret, O., & Hakkou, R. (2013). Assessment of soil contamination around an abandoned mine in a semi-arid environment using geochemistry and geostatistics: Pre-work of geochemical process modeling with numerical models. *Journal of Geochemical Exploration*, *125*, 117-129. https://doi.org/10.1016/j.gexplo.2012.11.018

Khelifi, F., Besser, H., Ayadi, Y., Liu, G., Yousaf, B., Harabi, S., Bedoui, S., Zighmi, K., & Hamed, Y. (2019). Evaluation of potentially toxic elements' (PTEs) vertical distribution in sediments of Gafsa–Metlaoui mining basin (Southwestern Tunisia) using geochemical and multivariate statistical analysis approaches. *Environmental Earth Sciences*, *78*(2), 53. https://doi.org/10.1007/s12665-019-8048-z

Khelifi, F., Caporale, A. G., Hamed, Y., & Adamo, P. (2021). Bioaccessibility of potentially toxic metals in soil, sediments and tailings from a north Africa phosphate-mining area: Insight into human health risk assessment. *Journal of Environmental Management*, *279*, 111634. https://doi.org/https://doi.org/10.1016/j.jenvman.2020.111634

Khelifi, F., Melki, A., Hamed, Y., Adamo, P., & Caporale, A. G. (2020). Environmental and human health risk assessment of potentially toxic elements in soil, sediments, and ore-processing wastes from a mining area of southwestern Tunisia. *Environmental Geochemistry and Health*, *42*(12), 4125-4139. https://doi.org/10.1007/s10653-019-00434-z

Kocsis, L., Gheerbrant, E., Mouflih, M., Cappetta, H., Ulianov, A., Chiaradia, M., & Bardet, N. (2016). Gradual changes in upwelled seawater conditions (redox, pH) from the late Cretaceous through early Paleogene at the northwest coast of Africa: Negative Ce anomaly trend recorded in fossil bio-apatite. *Chemical Geology*, *421*, 44-54. https://doi.org/https://doi.org/10.1016/j.chemgeo.2015.12.001

Kocsis, L., Ulianov, A., Mouflih, M., Khaldoune, F., & Gheerbrant, E. (2021). Geochemical investigation of the taphonomy, stratigraphy, and palaeoecology of the mammals from the Ouled Abdoun Basin (Paleocene-Eocene of Morocco). *Palaeogeography, Palaeoclimatology, Palaeoecology*, *577*, 110523. https://doi.org/https://doi.org/10.1016/j.palaeo.2021.110523

Krishna, R. S., Mishra, J., Meher, S., Das, S. K., Mustakim, S. M., & Singh, S. K. (2020). Industrial solid waste management through sustainable green technology: Case study insights from steel and mining industry in Keonjhar, India. *Materials Today: Proceedings*, *33*, 5243-5249. https://doi.org/10.1016/j.matpr.2020.02.949

Król, A., Mizerna, K., & Bożym, M. (2020). An assessment of pH-dependent release and mobility of heavy metals from metallurgical slag. *Journal of Hazardous Materials*, *384*, 121502. https://doi.org/https://doi.org/10.1016/j.jhazmat.2019.121502

Kynčlová, P., Hron, K., & Filzmoser, P. (2017). Correlation Between Compositional Parts Based on Symmetric Balances. *Mathematical Geosciences*, *49*(6), 777-796. https://doi.org/10.1007/s11004-016-9669-3

Li, Y., Richardson, J. B., Walker, A. K., & Yuan, P.-C. (2006). TCLP Heavy Metal Leaching of Personal Computer Components. *Journal of Environmental Engineering*, *132*(4), 497-504. https://doi.org/doi:10.1061/(ASCE)0733-9372(2006)132:4(497)

Liu, Q., Wang, X., Gao, M., Guan, Y., Wu, C., Wang, Q., Rao, Y., & Liu, S. (2022). Heavy metal leaching behaviour and long-term environmental risk assessment of cement-solidified municipal solid waste incineration fly ash in sanitary landfill. *Chemosphere*, *300*, 134571. https://doi.org/https://doi.org/10.1016/j.chemosphere.2022.134571

Mabroum, S., Aboulayt, A., Taha, Y., Benzaazoua, M., Semlal, N., & Hakkou, R. (2020). Elaboration of geopolymers based on clays by-products from phosphate mines for construction applications. *Journal of Cleaner Production*, *261*. https://doi.org/10.1016/j.jclepro.2020.121317

Mar, S. S., & Okazaki, M. (2012). Investigation of Cd contents in several phosphate rocks used for the production of fertilizer. *Microchemical Journal*, *104*, 17-21. https://doi.org/https://doi.org/10.1016/j.microc.2012.03.020

MDDELCC, M. d. D. D., de l'Environnement et Lutte Contre les Changements Climatiques. (2013). *Ministère du Développement Durable, de l'Environnement et Lutte Contre les Changements*

Climatiques. Critère de qualité de l'eau de surface. Direction de suivi de l'état de l'environnement. Bibliothèque et Archives Nationales du Québec, QC, Canada, 510p.

Mehahad, M. S., & Bounar, A. (2020). Phosphate mining, corporate social responsibility and community development in the Gantour Basin, Morocco. *The Extractive Industries and Society*, *7*(1), 170-180. https://doi.org/10.1016/j.exis.2019.11.016

Miller, S., Jeffery, J., & Wong, J. (1991). Use and misuse of the acid base account for "AMD" prediction. Proceedings of the 2nd International Conference on the Abatement of Acidic Drainage, Montréal, Que,

Ministre de la Transition Energétique et du Développement Durable. (2021). *Mines*. https://www.mem.gov.ma/Pages/secteur.aspx?e=7

Mouflih, M. (2015). *Les phosphates du maroc central et du moyen atlas (maastrichtien-lutetien, maroc) : Sedimentologie, stratigraphie sequentielle, contexte genetique et valorisation* Universite Cadi Ayyad.

Nen, E., . 7375:2004 (2004). Leaching characteristics of moulded or monolithic building and waste materials. Determination of leaching of inorganic components with the diffusion test, NNIS (Netherlands Normalisation Institute Standard). In.

Pesenson, M. Z., Suram, S. K., & Gregoire, J. M. (2015). Statistical analysis and interpolation of compositional data in materials science. *ACS combinatorial science*, *17*(2), 130-136.

Plante, B., Benzaazoua, M., & Bussière, B. (2011). Predicting Geochemical Behaviour of Waste Rock with Low Acid Generating Potential Using Laboratory Kinetic Tests. *Mine Water and the Environment*, *30*, 2-21. https://doi.org/10.1007/s10230-010-0127-z

Prévôt, L. (1988). *Geochimie et petrographie de la formation a phosphate des ganntour (maroc) : utilisation pour une explication de la genese des phosphorites cretace-eocenes*

Prévôt, L. (1990). Geochemistry, petrography, genesis of Cretaceous-Eocene phosphorites: the Ganntour deposit (Morocco)-A type example. *Soc. Geol. France, Memoire*, *158*, 232.

Reimann, C., Fabian, K., Flem, B., Schilling, J., Roberts, D., & Englmaier, P. (2016). Pb concentrations and isotope ratios of soil O and C horizons in Nord-Trøndelag, central Norway: Anthropogenic or natural sources? *Applied Geochemistry*, *74*, 56-66. https://doi.org/https://doi.org/10.1016/j.apgeochem.2016.09.002

Reimann, C., & Filzmoser, P. (2000). Normal and lognormal data distribution in geochemistry: death of a myth. Consequences for the statistical treatment of geochemical and environmental data. *Environmental Geology*, *39*(9), 1001-1014. https://doi.org/10.1007/s002549900081

Reimann, C., Schilling, J., Roberts, D., & Fabian, K. (2015). A regional-scale geochemical survey of soil O and C horizon samples in Nord-Trøndelag, Central Norway: Geology and mineral potential. *Applied Geochemistry*, *61*, 192-205. https://doi.org/https://doi.org/10.1016/j.apgeochem.2015.05.019

Sabiha, J., Mehmood, T., Chaudhry, M. M., Tufail, M., & Irfan, N. (2009). Heavy metal pollution from phosphate rock used for the production of fertilizer in Pakistan. *Microchemical Journal*, *91*(1), 94-99. https://doi.org/https://doi.org/10.1016/j.microc.2008.08.009

Safhi, A. e. M., Amar, H., El Berdai, Y., El Ghorfi, M., Taha, Y., Hakkou, R., Al-Dahhan, M., & Benzaazoua, M. (2022). Characterizations and potential recovery pathways of phosphate mines waste rocks. *Journal of Cleaner Production*, *374*, 134034. https://doi.org/https://doi.org/10.1016/j.jclepro.2022.134034

Sapsford, D. J., Bowell, R. J., Dey, M., & Williams, K. P. (2009). Humidity cell tests for the prediction of acid rock drainage. *Minerals Engineering*, *22*(1), 25-36. https://doi.org/https://doi.org/10.1016/j.mineng.2008.03.008

Shapiro, S. S., & Wilk, M. B. (1965). An Analysis of Variance Test for Normality (Complete Samples). *Biometrika*, *52*(3/4), 591-611. https://doi.org/10.2307/2333709

Sobek, A. A. (1978). *Field and laboratory methods applicable to overburdens and minesoils*. Industrial Environmental Research Laboratory, Office of Research and ….

Somasundaran, P., & Wang, D. (2006). Chapter 3 Mineral–solution equilibria. In D. Wang (Ed.), *Developments in Mineral Processing* (Vol. 17, pp. 45-72). Elsevier. https://doi.org/https://doi.org/10.1016/S0167-4528(06)17003-9

Stöber, W., Fink, A., & Bohn, E. (1968). Controlled growth of monodisperse silica spheres in the micron size range. *Journal of Colloid and Interface Science*, *26*(1), 62-69. https://doi.org/https://doi.org/10.1016/0021-9797(68)90272-5

USEPA. (1992). Method 1311: toxicity characteristic leaching procedure, SW-846: Test methods for evaluating solid waste - Physical/Chemical Methods. Washington, D.C. In.

USEPA. (1994). Method 1312: synthetic precipitation leaching procedure, SW-846: part of test methods for evaluating solid waste, physical/chemical methods. In.

USEPA. (2017). Method 1315 : mass transfer rates of constituents in monolithic or compacted granular materials using a semi-dynamic tank leaching procedure. In.

USEPA. (2009). HazardousWaste Characteristics. In *AUser-Friendly Reference Document; EPA:Washington, DC, USA*.

UTS, U. (2017). Land disposal restrictions, rules and regulations. In *https://www.epa.gov/hw/land-disposal-restrictions-hazardous-waste*.

Weber, P. A., Thomas, J. E., Skinner, W. M., & Smart, R. S. C. (2004). Improved acid neutralisation capacity assessment of iron carbonates by titration and theoretical calculation. *Applied Geochemistry*, *19*(5), 687-694. https://doi.org/https://doi.org/10.1016/j.apgeochem.2003.09.002

CHAPTER 6 ARTICLE 3: INTEGRATED APPROACH TO SUSTAINABLE UTILIZATION OF PHOSPHATE WASTE ROCK IN ROAD EMBANKMENTS: EXPERIMENTAL INSIGHTS, STABILITY ANALYSIS, AND PRELIMINARY ECONOMIC EVALUATION

Preamble: This article was published in the "Case Studies in Construction Materials" journal on 27 April 2024.

Case Studies in Construction Materials 20 (2024) e03222

https://doi.org/10.1016/j.cscm.2024.e03222

Safa Chlahbi[1,2], Abdellatif Elghali[1], Omar Inabi[1], Tikou Belem[2], Essaid Zerouali[3], Mostafa Benzaazoua[1]

[1]Mohammed VI Polytechnic University (UM6P), Geology and Sustainable Mining Institute (GSMI), 43150 Benguerir, Morocco

[2]Université du Québec en Abitibi-Témiscamingue (UQAT), Research Institute of Mines and Environment (RIME), 445 Boul. de l'Université, QC J9X 5E4 Rouyn-Noranda, Canada

[3]OCP group, Department of Method, Planning, and Performance Benguerir, 2 Street Al Abtal Hay, Casablanca B.P. Maârif 5196, Morocco

6.1 Abstract

This paper highlights an issue that has not received much attention, which is the use of phosphate waste rock (PWR) in road embankments. This study focuses on the valorization of marly clay and marly limestone lithologies, which are abundant but often unused or undervalued, being simply deposited around mine sites. Investigating the potential use of these materials in road embankments requires a combination of experimentation, stability analysis, and economic evaluation. The materials were collected from mining trenches in the Benguerir mine (Morocco). The samples were subjected to i) chemical and mineralogical characterization; ii) environmental characterization; and iii) geotechnical characterization. The results of the characterization show that the samples are chemically dominated by CaO (12–33 wt%), SiO_2 (23–38 wt%), and MgO (7–9 wt%); mineralogically, the main phases are quartz, calcite, dolomite, apatite, and clay minerals. The environmental characterization classified the studied materials as non-hazardous waste. In terms

of geotechnical characterization, the marly limestone and marly clay belong to the A3 and R33 categories, which means that they can be successfully used as a sustainable alternative material for the embankment. This finding supports their safe utilization. The stability analysis reveals that embankments up to 10 m in height can be constructed with marly clay without significant physical instability risks. Satisfactory safety factors (SF) were found (SF = 1.97 for H = 5 m and SF = 1.54 for H = 10 m). For marly limestone, the height limit is less than 10 m (SF = 1.74 for H = 5 m and SF = 1.33 for H = 10 m), but it can be increased to 10 m by adding a bench of rock fill with a safety factor of 1.64. Finally, an economic evaluation demonstrates that PWR can be used as embankment materials within a radius of 28 km around the mine site. It appears to be a cost-effective alternative compared to conventional materials.

Keywords: phosphate waste rock, sustainability, road embankments, stability analysis.

Nomenclature

Gt	Gigatonne
PWR	Phosphate waste rocks
LA	Los Angeles Abrasion value
MD	Micro-Deval value
CBR	California bearing ratio
C0/SA	Interburden codes
C3/C2	Interburden codes
ICP-AES	Inductively coupled plasma - atomic emission spectrometry
QAM	Quantitative automated mineralogical
TCLP	Toxicity characteristic leaching procedure
PSD	Particle size distribution
MBV	Methylene blue test value
UCS	Uniaxial compressive strength
TS	Total sulfur
TC	Total carbon
XPS	Expert process solutions
EDS	Energy dispersive spectrometers
AP	Acid generation potential
NP	Neutralization potential
NNP	Net neutralization potential
USEPA	United states environmental protection agency
GRE	Guide for road earthworks
LL	Liquid limit
PL	Plastic limit
PI	Plasticity index

UCS	Uniaxial compressive strength
SF	Safety factor
H	Height embankment
α	Embankment slope
L	Width of surface layer
LOI	Loss on ignition
D.L	Detection limit
D max	Maximal particle size. In mm
D 85%	The size for which the passing distribution is equal to 85 %, in mm
w_{opn}	Optimum Moisture content
$\gamma_{d\ max}$	Maximum dry density
C’	Effective cohesion
φ'	Effective friction angle
R33	Subclass code of R3 “Marly rock: low fragmentability and low degradable “
A3	Class code “Clays and marly clays, very plastic silts”
A_3m	Subclass code of A3 “3 < IPI ≤ 10 “
1V:2H 1V:3H	Embankment slope
CAPEX	Capital expenditure
P	Purchase of materials
R	Radius of profitability
T	Cost of transport
CE	Expansion coefficient
OP	Other prices (implementation, extraction, loading…)
PM	Profit margin
SP:	Sale price
MAD	Moroccan dirhams

6.2 Introduction

Construction materials are expected to increase significantly from 35 Gt in 2011 to 82 Gt in 2060 (Oberle et al., 2019). Given their close ties to investment and construction requirements, as well as the lack of high-value recycling, their use will increase particularly quickly shortly. Construction materials requirements play a crucial role in the field of civil engineering, as they directly impact the quality and durability of construction projects. Factors such as project specifications, budget constraints, and environmental considerations significantly influence the raw material requirements in civil engineering (Allen & Iano, 2019). Additionally, sustainable approaches to raw material management have gained traction in recent years, aiming to minimize waste, reduce

environmental impact, and promote long-term sustainability (Derakhshanalavijeh & Teixeira, 2017).

At the same time, large amounts of mining waste rocks are produced annually by phosphate mines (Chlahbi et al., 2023; El Ghorfi et al., 2024; Yang et al., 2014). Due to the production of enormous open voids, surface mining typically results in greater land use and degradation than underground mining (Morin & Hutt, 2001). This issue poses significant environmental challenges. Within the context of the circular economy and the goals of sustainable development, phosphate waste rocks (PWR) could be an alternative resource in the construction industry (Taha et al., 2021). This solution will preserve natural resources and reduce the environmental impact of this waste. To minimize the footprint of PWR management, sustainable practices, and technological advancements are crucial. Sustainable practices such as waste rock reclamation, valorization, or reuse and reprocessing can help in mitigating these impacts. By reclaiming waste rock through techniques such as contouring and regrading, the land can be restored to its pre-mining condition, reducing the ecological footprint of waste rock management.

Many examples have been examined in the literature to valorize and reuse mining waste as alternative raw materials. The aim is to produce construction and building materials from mining waste, such as road construction, fired bricks, ceramics, lightweight aggregates, concrete, mortar. For example, Amrani et al. (2019) focused on the use of PWR in the construction of a mine haul road in the Gantour mine area in Morocco. The researchers reported that the waste rock was able to meet the required specifications for road construction, including stability, durability, and resistance to deformation. This successful application demonstrated the potential of utilizing PWR as a viable alternative to traditional road construction materials. Mining waste can also be utilized as an alternative raw material in the production of aggregates for concrete and fine sands for mortar (Argane et al., 2015, 2016; El Machi et al., 2021a; Loutou et al., 2013). In addition, mining waste can be used as alternative materials to produce fired bricks (Loutou et al., 2019; Mouih et al., 2023a; Oubaha et al., 2022; Taha et al., 2016b, 2017b), cementitious materials (Bahhou et al., 2021a; Peyronnard et al., 2011), and high performance ceramics and lightweight aggregates by using phosphate sludge and clay byproduct from phosphate mines (Bayoussef et al., 2021b; Bayoussef et al., 2021a; Loutou et al., 2013). It may be possible to preserve natural resources and

lessen the environmental impact by valuing or reusing the PWR as alternative raw materials (Loutou et al., 2019; Safhi et al., 2022).

The reuse of mining waste rock as road embankment material was investigated recently and has shown that their repurposing can offer several benefits (Ahmed et al., 2014; Amrani et al., 2020; Amrani et al., 2019; Durante Ingunza et al., 2020; Malaoui et al., 2023; Segui et al., 2023). Amrani et al. (2020), examined the potential of using coal mine waste rocks as an alternative material for road construction (embankments and pavement layers), while also promoting sustainable waste management and conserving natural resources. Their experiment's findings proved that weathered coal mine waste rocks could potentially be utilized successfully as a sustainable alternative material for the embankment. Additionally, using coal mine waste rocks in road sub-base layers for high-trac pavements is permitted by applying stabilizing agents (fly ash and hydraulic road binder) (Amrani et al., 2020). Malaoui et al. (2023) tested PWR (phosphatic limestone and limestone) from Kef-Essenoun mine in Algeria to be used in road pavement and foundations built. The geotechnical findings show that Los Angeles Abrasion (LA) and Micro-Deval (MD) values ranged from 59.9 to 90.4 % and 42.0 to 86.3 % for phosphatic limestone and from 43.6 to 95.8 % and 38.2to 75 % for limestone, while the CBR values of phosphatic limestone and limestone were found to be 10.5 % and 18.7 %, respectively. These results showed that these materials could be used in capping layers and pavement backfilling but must be treated with a hydraulic binder to improve their properties.

Failures of road embankments are a major infrastructure and transportation concern. It is essential to recognize the main factors contributing to instability in road embankments in order to implement effective mitigation strategies (Johnston et al., 2021; Xie et al., 2023). Failures can result from inadequate compaction during construction, the presence of weak soils like clay or peat, and poor drainage leading to excess pore pressure (Estabragh et al., 2004; Mori et al., 2012; Rapti et al., 2018; Xie et al., 2023; Yamaguchi et al., 2012). Identifying these factors is essential for devising effective solutions that mitigate road embankment failures. Generally, road embankment's major failure modes are: circular arc failure, sliding block failure, infinite slope failure and lateral squeeze of foundation soil (Azarafza et al., 2021; Collin et al., 2005). These failure modes can be classified as internal or external (Kiser & Kolay, 2013). Internal stability problems (i.e., infinite slope failure) within embankments can be caused by poor-quality embankment materials or adequation compaction of embankment; While external stability problems (i.e., circular arc failure, sliding

block failure, and lateral squeeze of foundation soil) can be caused by the overstressing of the foundation sol, vibration and drawdown (Collin et al., 2005; Kiser & Kolay, 2013).

The current paper presents the importance of mine waste utilization and drives the objectives of a circular economy by transforming what is conventionally considered 'waste' into valuable construction materials. The objective of this study is to evaluate the potential reuse of specific lithologies (marly limestone and marly clay) collected upstream of the mining chain in the Benguerir mine as an alternative material for road embankment. However, the availability of suitable materials for constructing embankments is becoming a growing concern due to the depletion of natural resources and environmental considerations. These lithologies are abundantly available and can potentially serve as sustainable substitutes for traditional embankment materials (Chlahbi et al., 2023). Utilizing these materials in road embankments can reduce the need for traditional construction materials. It can help to conserve natural resources and reduce the environmental impact of sourcing and transporting these materials. Additionally, utilizing these materials can also have economic benefits, such as reducing the cost of road construction because the mining companies can sell their waste material to construction companies at a lower cost than traditional materials. The evaluation will involve assessing their experimental insights, stability analysis, and initial economic evaluation to determine their suitability for embankment construction. Experimentation aims to understand the behavior of these materials and determine their suitability for embankment construction. This involves conducting various laboratory tests to analyze the physical and geotechnical properties of marly limestone and marly clay. Stability analysis is another important aspect to consider when using these materials in embankment construction. This involves assessing the stability of the embankment under different conditions by considering slope stability. The preliminary economic evaluation was also considered in this study to determine the profitability radius. Additionally, the paper will investigate the chemical and mineralogical analysis and environmental impact of using these materials. Additionally, the paper will investigate the chemical and mineralogical analysis and environmental impact of using these materials.

6.3 Materials and methodsMine site location and sampling strategy

The PWR samples were collected from the interburden presenting an important thickness; located in the Benguerir mine, Morocco (Figure 6-1A). The study area constitutes one of the parcels of the Gantour basin; it's a sedimentary phosphate deposit (El Bamiki et al., 2021), extracted by an open-pit mining method. Based on the thickness of the waste interburden (Chlahbi et al., 2023) and for an area of 9 Mm², which corresponds to an area of panel 8, the volume of the main facies is presented in Figure 6-1B. The marly limestone and marly clay facies present a significant potential of 27 Mm³ and 22 Mm³, respectively. These two lithologies are mixed with the other facies and deposited in surface waste rock piles.

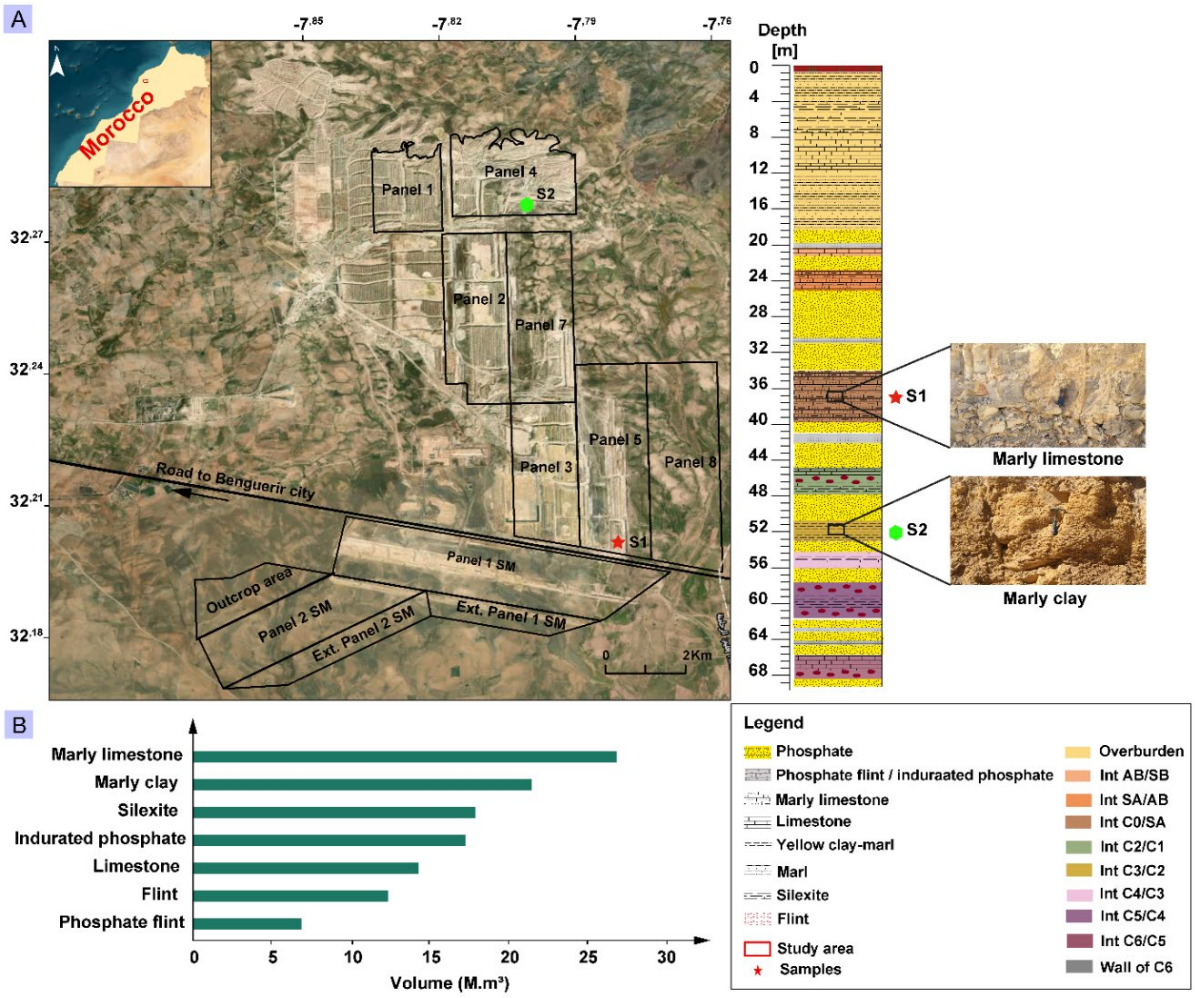

Figure 6-1: Schematic description of the study area. A) Mine site location and lithological section. B) Estimated the volume of the main facies.

6.3.2 Methodology

In this study, the embankment was examined according to an experimental protocol (field tests are not presented in this study) involving the examination of these two lithologies (marly limestone and marly clay) as raw material. According to Chlahbi et al. (2023), the litho-stratigraphic correlation in the Benguerir deposit appears to be relatively stable in space, it has more or less the same facies and the same interburdens. For this purpose, the sampling approach consisted of collecting samples from two locations (panel 4 and panel 5 of Benguerir mine) upstream of the mining chain. The marly limestone and the marly clay were, respectively, collected from C0/SA and C3/C2 interburdens. For each facies, one tone of the sample was collected from the top, middle, and bottom along the interburden. These samples were then homogenized in situ by loader truck and transported to the laboratory for further analysis. In the laboratory, the collected samples were crushed, homogenized by using quartering, and analyzed for their chemical properties, mineralogical composition, environmental behavior, and physical and geotechnical characteristics. The methodology used in this study is summarized in Figure 6-2. The main goal of this methodology is to provide a comprehensive approach for the efficient and effective valorization of PWR, with the ultimate goal of promoting sustainability. By following this approach, future researchers can easily adapt and implement this methodology anywhere, regardless of their location or resources. This not only encourages the reuse of mining waste but also contributes to the circular economy by creating a closed-loop system where materials can be continuously repurposed.

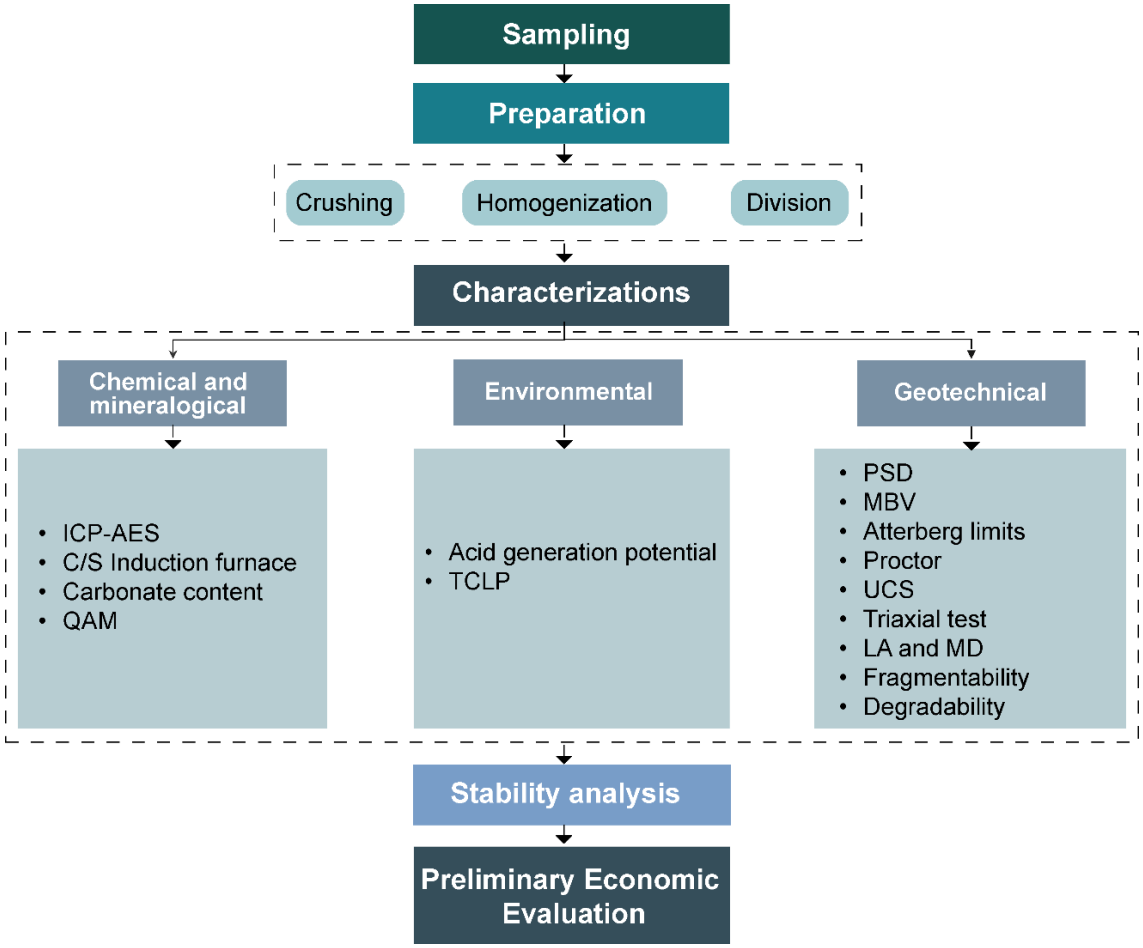

Figure 6-2: Summary of the methodology used. ICP-AES: inductively coupled plasma-atomic emission spectrometry. QAM: quantitative automated mineralogy. TCLP: toxicity characteristic leaching procedure. PSD: particle size distribution. MBV: methylene blue test value. UCS: uniaxial compressive strength. LA: Los Angeles abrasion value. MD: Micro Deval value.

a. Chemical and mineralogical characterization

The bulk chemical composition analysis of the different samples was conducted at Actlabs (Ontario, Canada). In order to determine the major elements (SiO_2, Al_2O_3, Fe_2O_3, CaO, MgO, and P_2O_5), a fusion decomposition technique followed by inductively coupled plasma-atomic emission spectrometry (ICP-AES) analysis was employed. By using an induction furnace (ELTRA CS-2000; detection limit of 0.09%), the total sulfur (TS) and total carbon (TC) contents were determined. Due to the presence of carbonate rocks, the carbonate content was determined on milled samples (~ 50 µm) by using a calcination technique at the furnace (950°).

The mineralogical characterization of a sample was conducted using the quantitative automated mineralogical (QAM) technique at Expert Process Solutions (XPS) in Sudbury, Ontario, Canada. This method is known as Quantitative Evaluation of Materials by Scanning Electron Microscopy (QEMSCAN®, FEI, Quanta 650 platform with Field Emission Gun). The QEMSCAN technique utilizes a collection of rapidly captured X-rays to generate particle maps that are color-coded by minerals. This allows for a detailed analysis of the mineral composition of the sample. The equipment used in this process is equipped with 30 mm² Bruker SDD energy dispersive spectrometers (EDS).

b. Environmental characterization

The environmental behavior of the samples from the study area was assessed using acid generation potential (AP) and static leaching test: toxicity characteristic leaching procedure (TCLP). The AP was calculated using sulfur sulfide content according to equation (6.1) and carbonate neutralization potential (NP) using total carbon content according to equation (6.2) (Miller et al., 1991; Sobek, 1978). By subtracting the AP from the NP, the Net neutralization potential (NNP) was determined (Weber et al., 2004). The sample is considered non-acidogenic if its NNP is higher than 20 kg $CaCO_3$/t, uncertain its NNP value is in the interval −20 and 20 kg $CaCO_3$/t, and acid generating if its NNP is lower than −20 kg $CaCO_3$/t (Bouzahzah et al., 2015; Elghali et al., 2018; Elghali et al., 2023; Sobek, 1978).

$$AP = 31.25 \times S_{Sulfide} \quad (kg\ CaCO_3/t);\ (6.1)$$

$$NP = 83.3 \times C_{Total} \quad (kg\ CaCO_3/t);\ (6.2)$$

The TCLP was performed to assess the inorganic species mobility (USEPA, 1992) by using leach solution (acetic acid and sodium hydroxide (pH= 4.93 ± 0.05)) (Jong & Parry, 2005; USEPA, 1992). Leachate samples were filtered through a 0.45 m nylon mesh filter and immediately acidified with 2% v/v HNO_3 for preservation. ICP-AES was then used to evaluate the chemical composition. The results of the chemical concentrations of the standardized chemical species were compared with the United States Environmental Protection Agency (USEPA) regulation (USEPA., 2009).

c. Geotechnical characterization

To determine the physical and geotechnical proprieties, laboratory tests have been carried out. The two facies were classified according to Guide for Road Earthworks (GRE) NF P11-300. The main aims of this guide are to classify materials and present the conditions for using them in embankments. The identification tests of the material samples consist of analyzing particle size distribution (PSD), Atterberg limit, and methylene blue value. The PSD was determined using dry sieving for coarse particles according to the standard NF-P94-056. The Atterberg limit test was carried out to determine the liquid limit (LL), plastic limit (PL), and plasticity index (PI) according to NF-P94-051 and NF-P94-052-1 standards, and the methylene blue value (MBV) was measured on the 0/5-mm fraction to determine the adsorption capacity of material according to the standard NF-P94-068. Several tests were carried out to evaluate the mechanical behavior and the resistance of the material regarding the fragmentation, the wear, and the PSD evolution under the effect of mechanical solicitations. The uniaxial compressive strength (UCS) test was carried out in accordance with the NF P94-420 standard. In accordance with NF EN 1097-1 and NM.10.0.138, the fraction +10/-14 mm was selected for the determination of the Los Angeles abrasion value (LA) and Micro Deval value (MD). According to NF P94-066 and NF P94-067, the samples' resistance to fragmentation coefficient and degradability coefficient were assessed on the 40/80 mm fraction.

The compaction characteristics were determined by the Proctor test in accordance with the standard NF P94-093. These characteristics are optimum moisture content (w_{opn}) and maximum dry density ($\gamma_{d\ max}$). For studying the behavior of these materials after compaction, triaxial tests were carried out on reconstituted materials under consolidated-undrained conditions, including the measurement of interstitial pressure. The triaxial test enables us to determine the intrinsic parameters (effective cohesion (c') and effective angle of friction (φ')). The intrinsic parameters are used as input in the stability analysis. The reconstituted material specimens were prepared by ramming/kneading/vibrating the material in several layers inside a split mold, with the membrane placed inside. It is advisable to wait sufficiently (16 h) before compaction so that the water mixed with the material is distributed evenly throughout the soil mass (NF EN ISO 17892-9, 2018).

d. Modeling stability analysis

Stability analysis is a key factor in the design of road embankments, as it ensures the safety and durability of these structures. This analysis involves understanding the importance and purpose of stability analysis in road embankment design. It allows us to assess the stability of the embankment and identify potential failure modes, such as slope instability. By understanding these risks, we can make informed decisions during the design process to mitigate them and ensure the long-term stability of the road embankment.

The stability of the embankment and the safety factor (SF) can be evaluated after determining the properties of the soil (i.e., physical and mechanical properties) through laboratory testing (Ahangari Nanehkaran et al., 2022). The safety factor is defined in equation (6.3). The safety factor used for stability calculations is SF > 1.5 (Day, 2010).

$$SF = \frac{Resisting\ strength}{Forces\ causing\ failure} \tag{6.3}$$

Modeling of embankment behavior was studied to understand the failure mode of embankments. Several techniques are available such as limit equilibrium methods, limit analysis, and finite element methods (Bishop, 1955; NAVFAC, 1982). Many studies comparing finite element approaches and classical limit equilibrium have demonstrated that the obtained results stay relatively similar (Cai & Ugai, 2001; Göktepe & Keskin, 2018; Memon, 2018; Wubalem, 2022). To carry out our study on slope stability, we chose to use the limit equilibrium method, which is considered as the most used to analyze the stability of slope (Azadi et al., 2022; Inabi et al., 2023; Mamat et al., 2019).

The bishop slice method (Bishop, 1955) has emerged as a reliable tool for analyzing stability and predicting potential failure mechanisms. The bishop slice method allows us to understand the factors contributing to slope failure, such as soil properties, water content, and overall slope geometry. By dividing the slope into multiple slices, each representing a small section of the embankment, the method calculates the SF for each slice based on the forces acting on it. This analysis provides valuable insights into the stability of the embankment and helps identify potential failure modes.

The geometry of the embankment, including its height (H), Embankment slope (α), and width (L), must be defined (Figure 6-3). This information determines the overall shape and dimensions of the embankment, which directly impacts its stability. For our study, these parameters represent the input parameters. An embankment slope of 1V:2H was chosen with a width of 12 m, which corresponds to the width of two-way national Moroccan roads (GMTR, 2002). Additionally, a load of 20 KN/m² distributed over the road was considered (GMTR, 2002).

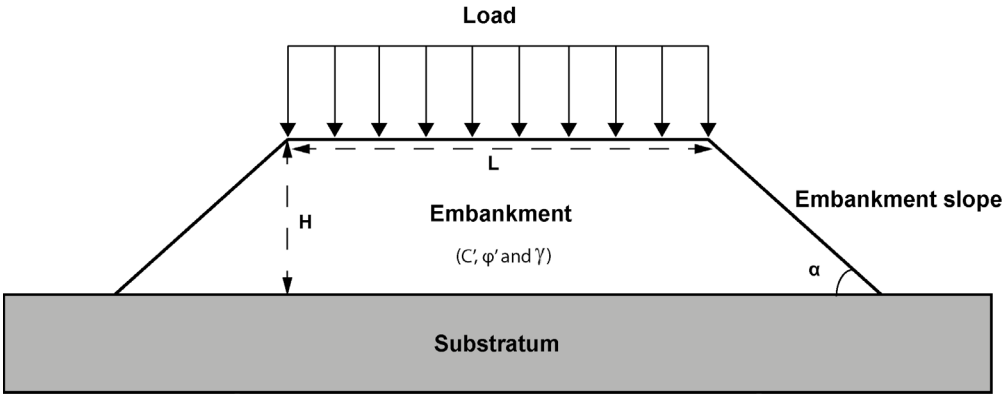

Figure 6-3:The geometry of the embankment model used.

6.4 Results and discussion

6.4.1 Experimental insights

a. Chemical and mineralogical composition

The chemical and mineralogical composition of marly limestone and marly clay are presented in Table 6-1. Major elements in marly limestone and marly clay samples are dominated by CaO (12 - 33 wt.%) and SiO_2 (23 - 38 wt.%), followed by MgO and P_2O_5 (0.6 - 6.4 wt.%). The other elements are less than 1.5 wt.%, except for C_{Total}. The loss on ignition (LOI) shows a high value for both samples (> 25 %), which means that when these samples are heated to high temperatures, they lose > 25 % of their original weight. This weight loss is primarily due to the evaporation and combustion of volatile compounds, such as water, carbonates, and organic matter, present in these samples. For this purpose, the carbonate content was determined. The results indicate that carbonate content was 29 wt.% and 21 wt.% for marly limestone and marly clay, respectively.

The results of the automated mineralogy analyses show the presence of five main phases including quartz, calcite, dolomite, apatite, and clay minerals. The other phases are less than 4 wt.%. Marly clay shows a high concentration of clay minerals phase (67 wt.%) and dolomite (13.5 wt.%). The Marly limestone sample presented high concentration of carbonate minerals: calcite (33 wt.%) and dolomite (18.7 wt.%), while this sample exhibited the low content of clay minerals (11 wt.%), which could provide good mechanical features.

Table 6-1: Chemical and mineralogical composition.

Samples	**Marly limestone**	**Marly clay**
	S1	S2
Major element (wt. %)		
	D.L (%)	
SiO_2	0.01	23	38
Al_2O_3	0.01	2	10
Fe_2O_3	0.01	0.6	4.5
CaO	0.01	33	12
MgO	0.01	7	9
P_2O_5	0.01	6.4	0.6
Others	-	0.8	1
LOI	-	27	25
C_{Total}	0.09	6.1	4.5
S_{Total}	0.09	0.2	0.01
Carbonate content	-	29	21
Mineralogical composition (wt. %)		
Calcite		33	7
Dolomite		18.7	13.5
Apatite		19	0.2
Quartz		15	9
Clay minerals		11	67
Others		3	4

b. Environmental Behavior of Materials

Figure 6-4 shows the results of the acid-generating potential assessment. The marly limestone and marly clay samples showed high neutralization potential (507 – 376 kg $CaCO_3$/t, respectively) and low acid potential (7.5 and 0.6 kg $CaCO_3$/t, respectively). This indicates that they can neutralize acidity and maintain a balanced pH level. The net neutralization potential (NNP = NP - AP) shows

positive values for all samples ranging from 500 to 375 kg $CaCO_3$/t. According to the classification criteria proposed by Miller et al. (1991), all samples are non-acid generating (NNP > 20 kg $CaCO_3$/t). This is a significant finding, as it suggests that these samples are not likely to harm the surrounding environment.

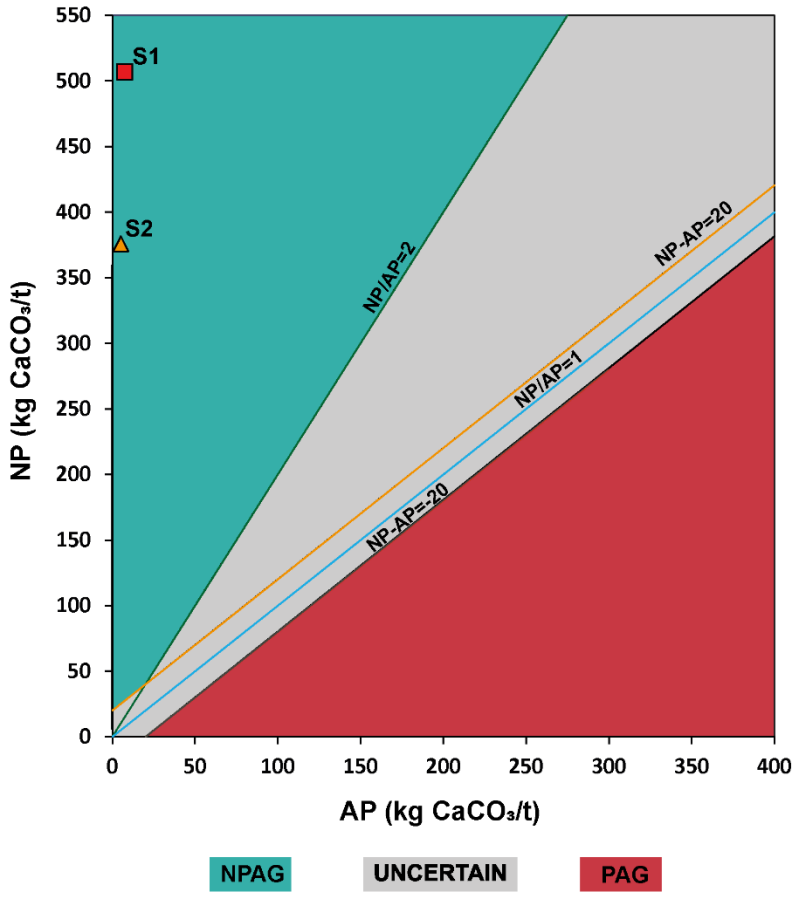

Figure 6-4: Graph representing results of acid generation potential by ABA tests. AP: acidification potential. NP: neutralization potential. NPAG: non-potentially acid-generating. PAG: potentially acid-generating.

The Toxicity characteristics leaching procedure (TCLP) was carried out to determine the release of contaminants (As, Ba, Cd, Cu, Cr, Se, and U). The results of leaching for marly clay and marly limestone using the TCLP are summarized in Table 6-2. The environmental behavior of marly clay and marly limestone trough leaching tests shows that all concentrations are below the limits recommended by the United States Environmental Protection Agency (USEPA) standard. According to this standard, marly clay and marly limestone of the Benguerir mine could be

considered non-hazardous waste. The use of these non-hazardous waste in road embankments has several implications. It provides a cost-effective and sustainable solution for the disposal of this waste material (Amrani et al., 2020). Using it in road construction avoids the need for additional landfills and reduces the environmental impact of storing it in large piles. Additionally, it is an alternative to traditional materials, such as natural aggregates, which are becoming increasingly scarce (Hakkou et al., 2016; Taha et al., 2021).

Table 6-2: Results of environmental characterization.

Test	Sample	Trace element (µg/L)						
		As	Ba	Cd	Cu	Cr	Se	U
TCLP	Marly limestone (S1)	400	3085	108	2	7	<100	<100
	Marly clay (S2)	600	3060	151	3	6	<100	<100
Standard (USEPA)		5000	100x10³	1000	-	5000	1000	2000

c. Physical and geotechnical properties

The results of the physical and geotechnical identification tests are summarized in Table 6-3. The PSD of both samples: marly limestone and marly clay (Figure 6-5) shows a maximum diameter of 20 mm and a D 85 of 12 and 2.5 mm, respectively. The results of the methylene blue values obtained from both samples vary between 5 and 7, which indicates the presence of a clayey fraction. The results of Atterberg limits tests showed that marly limestone and marly clay exhibited a plasticity index higher than 23, which means that they are plastic.

The uniaxial compressive strength (UCS) of both samples was less than 9 MPa. Additionally, the values of Los Angeles and micro-Deval tests were, then 50% and 35 %, respectively, for the marly limestone. Marly limestone has been found to be low resistant to attrition, contain moderately high percentages of carbonate, low amounts of clay minerals, and have high to low mechanical proprieties. Adequately high strength properties and high resistance to attrition are essential for acceptable construction performance (Mohamed Ali & Yang, 2014). It's therefore not appropriate for use as materials for road construction (NF EN 12620). The fragmentability and degradability tests were conducted in order to simulate the particle degradation that occurs in the field. These experiments evaluated the resistance to breakage and the susceptibility to the effects of wetting-

drying cycles. The fragmentability and degradability for marly limestone are less than 7 and 5, respectively (NF-P11-300, 1992), which means that marly limestone is poorly fragmentable and degradable. Compared to the findings of the mechanical proprieties (UCS, LA, and MD), fragmentability and degradability tests show that the marly limestone has properties that make it resistant to breaking apart or decomposing easily. This characterization shows their suitability to be used as construction materials in road embankments. However, for marly clay, we were not able to measure LA, MD, fragmentability, and degradability, due to the high clay mineral content.

Table 6-3: Physical and geotechnical properties of marly limestone and marly clay (NM: non-measured)

Samples		**Marly limestone**	**Marly clay**
		S1	S2
Physical proprieties			
D max	mm	20	20
D 85	mm	12	2.5
Methylene blue value (MVB)	-	5	7
Liquid limit (LL)	%	53	55
Plastic limit (PL)	%	29	28
Plasticity index (PI)	%	24	27
Geotechnical properties			
Uniaxial compressive strength (UCS)	MPa	8	0.1
Los Angeles (LA)	%	95	NM
Micro Deval (MD)	%	98	NM
Degradability	-	3	NM
Fragmentability	-	7	NM
Optimum Moisture content (w_{opn})	%	22.2	23.1
Maximum dry density ($\gamma_{d\ max}$)	t/m³	1.352	1.518
Friction angle	Degrees	18	16
Cohesion	kPa	11	17
Material classification (Setra & LCPC, 1992)	-	R33	A3

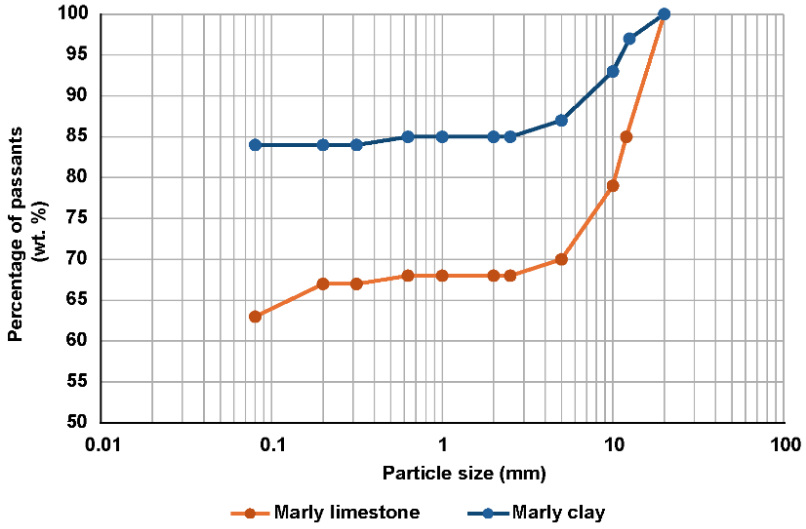

Figure 6-5: Particle size distribution of marly limestone and marly clay samples.

The results of the triaxial tests, as displayed in Table 6-3 Figure 6-6, provide valuable insights into the behavior of marly limestone and marly clay under different rupture states. Mohr circles (Figure 6-6A2 and B2) illustrate the effective cohesion (c') and effective friction angle (ϕ') of these two materials. It is observed that the effective cohesion of marly limestone is 11 kPa and 17 kPa for marly clay. Similarly, the effective friction angle of the marly limestone is recorded at 18°, while that of marly clay is slightly lower at 16°. Figure 6-6A1 and B1 show the evolution of the deviator stress ($q = \sigma_1 - \sigma_3$) according to the axial strain for the three applied confining pressures (σ_c) (140 kPa, 300 kPa and 500 kPa for marly limestone and 160 kPa, 300 kPa, and 500 kPa for marly clay). The non-linearity of the deformation curves is visible, almost at all levels of deformation. Furthermore, this deformation curve closely matched the usual behavior of conventional materials (Amrani et al., 2021). The peak of deviator stress obtained at low strain increases at high confining pressure. Moreover, the responses to deformation show a significant contraction phase followed by a slight expansion phase for large deformations. The strain curves show that the mechanical behavior of the marly limestone and marly clay samples match that of granular material that contains cohesive elements.

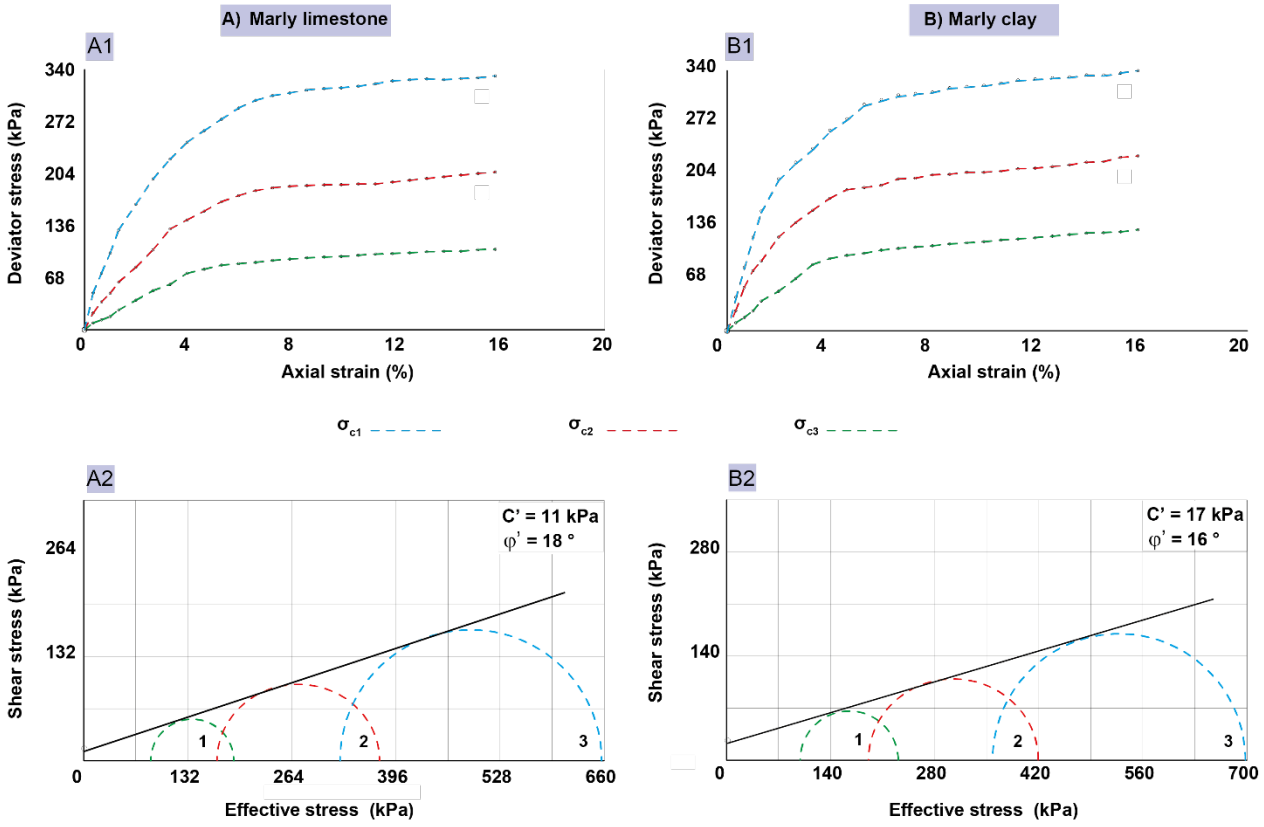

Figure 6-6: Triaxial test results: A) Marly limestone and B) Marly clay. A1 and B1: Variation of deviatoric stress according to axial strain. A2 and B2: Mohr cycles. σ_c: confining pressure.

The Proctor tests conducted for the two samples, marly limestone, and marly clay, have yielded considerable results. In the case of marly limestone, which represents marly limestone, the maximum dry density obtained was 1.35 t/m³. This indicates the maximum mass of the material per unit volume that can be achieved when it is compacted to its highest extent without the presence of moisture. It is interesting to note that this density was achieved at the optimum moisture content (w_{opn}) of 22.2%. Similarly, for sample marly clay, which represents marly clay, the Proctor tests revealed a maximum dry density of 1.52 t/m³. This density was achieved at the optimum moisture content (w_{opn}) of 23.1%. The variations in maximum dry density and optimum moisture content between marly limestone and marly clay suggest that each material has unique characteristics that influence their compaction behaviors.

According to the results of the physical and geotechnical characterization, the studied samples marly limestone and marly clay, respectively, belong to the R33 and A3 categories (Setra & LCPC,

1992). This means that the marly limestone corresponds to marly rock, characterized by the fact that it has a structure (usually carbonate) that is more or less resistant, poorly fragmentable, and degradable, releasing fine, plastic particles (Setra & LCPC, 1992). Marly clay corresponds to marly clay soil, very cohesive with medium to low water content, and sticky or slippery when wet (Chlahbi et al., 2023; Setra & LCPC, 1992). Thus, these materials can be utilized in the construction of road embankments according to the compaction table as proposed by the guide to earthworks, embankments, and subgrade construction (Setra & LCPC, 1992).

6.4.2 Stability analysis

In this work, the software Terrasol/Talren (v.6.1.9) was used to investigate the embankment slope stability. The application generates an embankment SF after defining all material proprieties, dimensions, the presumed failure surface (circle radius and position), and the failure analysis method (Bishop). The failure surface was first assumed, and the failure surface with the lowest safety factor was then found. The software was designed to model several scenarios for each lithology: marly clay (γ = 18 kN/m³, c'= 17 kPa and φ'= 16°) and marly limestone (γ = 18 kN/m³, c' = 11 kPa and φ' = 18°). For this purpose, seven scenarios were considered (Table 6-4). Scenarios 1, 2, and 3 correspond to the use of marly clay under normal rainfall conditions and without significant evaporation, with an embankment height of 5, 10, and 12 m. Scenarios 4 and 5 correspond to using marly limestone under normal rainfall conditions, with or without significant evaporation, with an embankment height of 5 and 10 m. Scenario 6 uses marly limestone at $H \geq 10$ m with specific studies (adding a bench). Scenario 7 uses marly limestone at $H \geq 10$ m with specific studies (changing the Embankment slope).

The results of slope stability analysis of the marly clay and marly limestone are plotted in Figure 6-7, and Figure 6-8. Table 6-4 presents each scenario's description and corresponding SF.

Table 6-4: Description of each scenario along with a corresponding. (SF: safety factor).

Scenario Number	Description of the case	Embankment slope	Embankment height (m)	SF
1	Use of **marly clay** under normal rainfall conditions and without significant evaporation	1V:2H	5	1.97
2			10	1.54
3			12	1.48
4	Use of **marly limestone** under normal rainfall conditions, with or without significant evaporation		5	1.74
5			10	1.33
6	Use of **marly limestone** at H ≥ 10 m with specific disposition (adding a bench)		10	1.64
7	Use of **marly limestone** at H ≥ 10 m with specific studies (changing the Embankment slope)	1V:3H	10	1.80

The use of class A3 materials (A_3m) in low rainfall conditions and without significant evaporation, particularly at an average embankment height of less than 10 m, is strongly recommended by guide to earthworks, embankments, and subgrade construction (Setra & LCPC, 1992). This recommendation has been validated through the different simulations performed (Figure 6-7, Figure 6-8, and Figure 6-9). When examining the stability of embankments, for scenario 1 (H = 5 m) the SF was found to be 1.97 (Figure 6-7A). This high SF (1.97) was expected due to the low design height (H = 5 m). While it was found that even at a height of 10 m, the SF remained at a satisfactory level of 1.54 (Figure 6-7B). However, when the height was increased to 12 m, the SF decreased to 1.48 (Figure 6-7C). This indicates that there is a decrease in stability when the embankment height exceeds 10 m. The embankment, which is built below the critical height, serves as a vital control mechanism for managing the deformation and ensuring the stability of the foundation (Mamat et al., 2019). It is important to note that the choice of materials becomes crucial in ensuring the stability and safety of embankments.

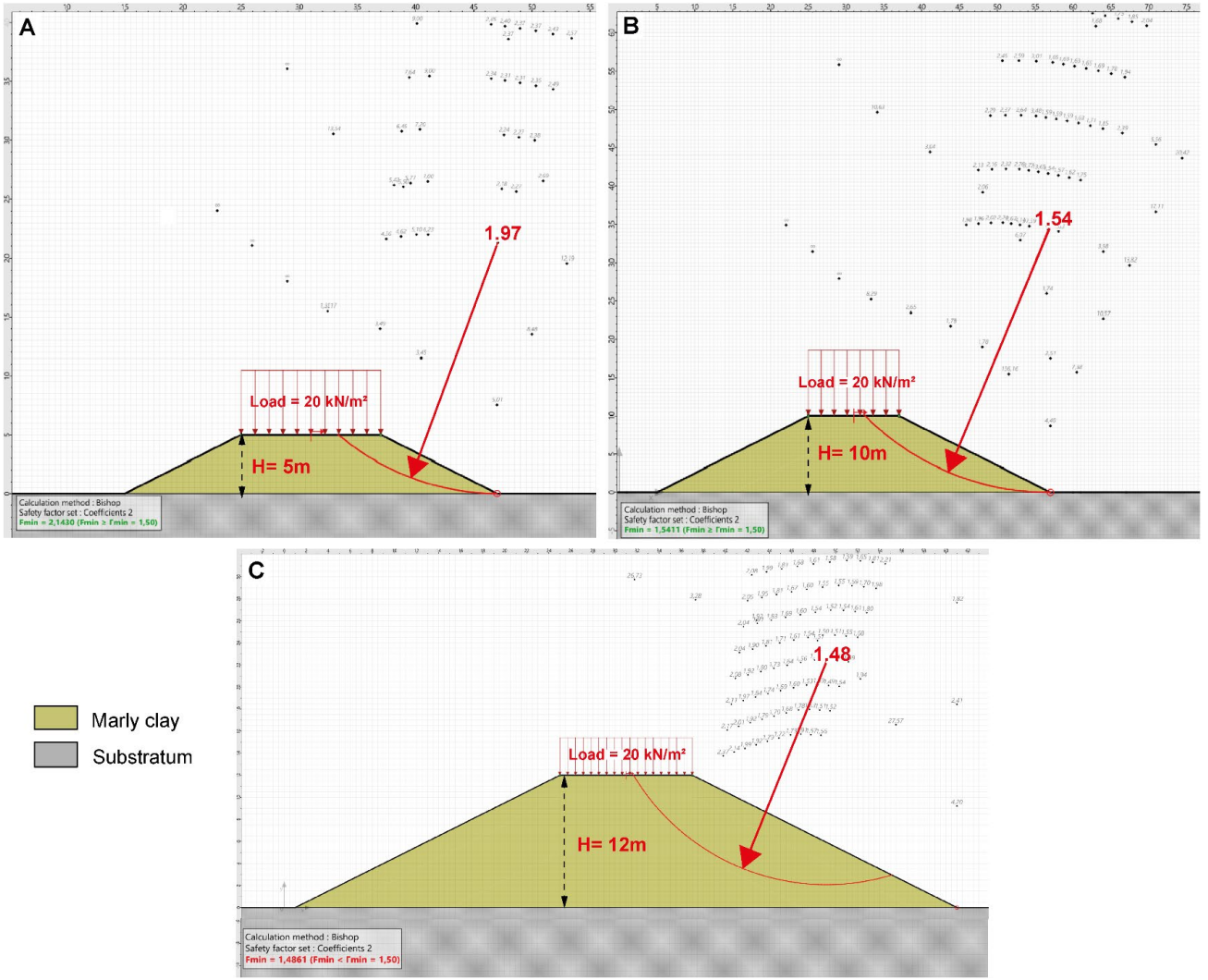

Figure 6-7: Slope stability using Bishop's method for marly clay with heights of A) 5 m, B) 10 m, and C) 12 m.

When comparing scenario 1 with scenario 4, slope geometry remained constant between the two scenarios, while the change from marly clay to marly limestone has a notable impact on the SF. The SF decreased from 1.97 to 1.74 in scenario 4 (Figure 6-8A). This change can be attributed to variations in material properties affecting shear strength, such as effective cohesion and effective angle of friction (Kiser & Kolay, 2013). This comparison highlights the significance of considering material properties when assessing slope stability and underscores the importance of accurate characterizations of soil or rock types to ensure reliable analysis and design in geotechnical engineering projects. As seen in Figure 6-B, the SF decreased to 1.33. This reduction in the SF at a height of 10 m further emphasizes the impact of the change in material properties. It raises concerns about the stability of the slope, especially at greater heights. To enhance SF in scenario 5, extensive research and simulations were conducted to explore potential solutions. One of the approaches considered was the addition of a bench seat, which could serve as a safety feature (Figure 6-9A). This bench was carefully designed and composed of rock fill, with specific dimensions. It was decided that the length of the bench would be equal to 1/3 of the platform width and 1/2 the height of the embankment. The rock fill is characterized by $\gamma = 25$ kN/m³, $c' = 1$ kPa and $\phi' = 43°$. By incorporating a bench into scenario 5, the SF has increased from 1.33 to 1.64. Another approach to improve the stability and SF of an embankment is to modify its angle. By adjusting the slope to 1V:3H instead of 1V:2H, the SF has increased to 1.80 (Figure 6-9B). The angle of an embankment plays a crucial role in determining its stability, as steeper slopes are more prone to erosion, landslides, and instability.

When comparing scenario 6 with scenario 7, it becomes evident that both scenarios exhibit a satisfactory SF, which is greater than 1.5 (SF (scenario 6) = 1.64 and SF (scenario 7) = 1.80). This is a significant observation as it implies that both scenarios offer a level of safety that surpasses the minimum (minimal SF = 1.5 (Day, 2010)). In this case, we have thoroughly evaluated the various scenarios that contribute to the consumption of most materials. Through meticulous calculations of the surface area of the material involved, our analysis has revealed that scenario 7 emerges as the frontrunner, demanding the highest amount of material. Scenario 7, characterized by the utilization of a steep slope angle of 1H:3V, not only necessitates an important quantity of material but also prompts the need for additional measures to accommodate this requirement. Specifically, the selection of this scenario mandates the inclusion of an extra surface area of 1.2 Ha/km to facilitate the successful execution of the project.

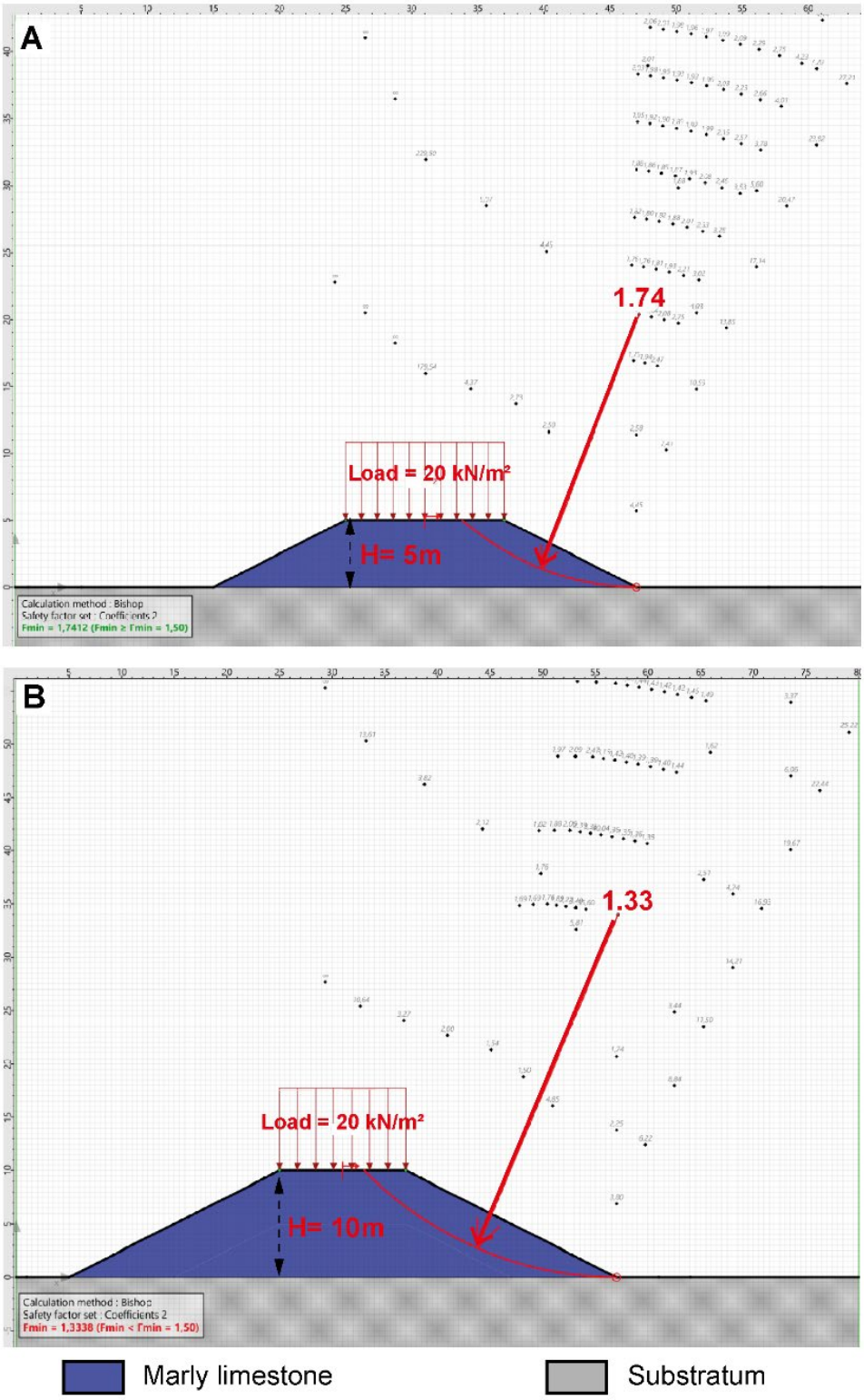

Figure 6-8: Slope stability using Bishop's method for marly limestone. A) At a height of 5 m. B) At a height of 10 m.

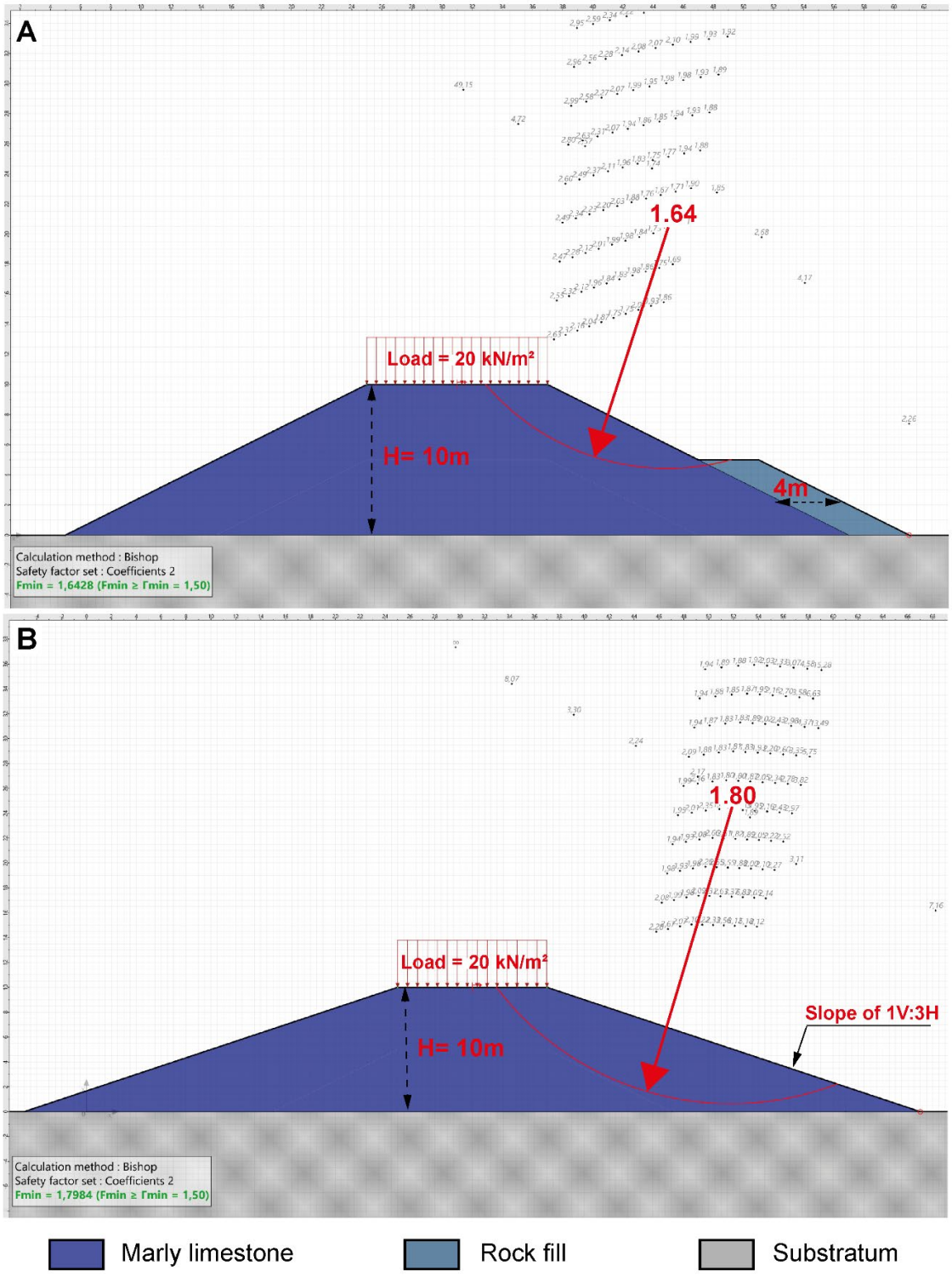

Figure 6-9: Slope stability using Bishop's method for marly limestone at a height of 10 m. A) with a bench seat. B) with a slope embankment of 1V:3H.

6.4.3 Preliminary economic evaluation

The purpose of this initial economic investigation is to determine the profitability radius beyond which local materials in Benguerir City will no longer be cost-effective compared to conventional materials for constructing road embankments. The evaluation focuses on comparing the main costs associated with using local materials versus conventional materials, with a specific emphasis on the construction costs life cycle (CAPEX), assuming similar maintenance and operating costs.

The construction process of a road embankment involves several steps, including material extraction, loading, transportation, unloading, and implementation. However, the key factor influencing overall costs is transportation, particularly the distance between the supply resources and the construction site. To calculate the total transportation cost, a 15 m³ truck capacity was considered under normal conditions, considering both variable and fixed costs (Amrani et al., 2020). Figure 6-10A provides a breakdown of these transportation costs and presents the underlying assumptions used to calculate the profitability radius.

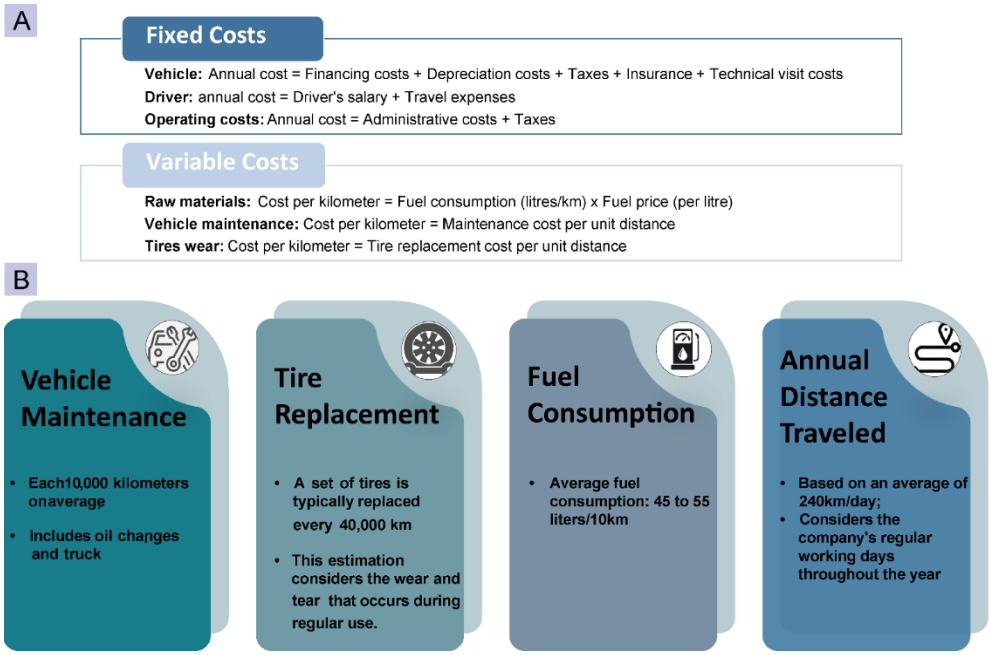

Figure 6-10: A) Variable and fixed costs for transporting road materials, B) Operating costs description (Amrani et al., 2020).

When dealing with a construction company involved in road construction, several operating expenses must be considered. These expenses encompass vehicle maintenance, tire replacements,

and fuel consumption (Figure 6-10 B). The following assumptions have been made regarding these factors. However, it is important to note that these costs can vary based on various factors such as specific circumstances, truck, and road conditions. Therefore, it is necessary to adjust for accurate and precise cost calculations. Table 6-5 presents the annual expenses associated with road embankment construction services. The different costs and prices were obtained from construction contracts in Benguerir City.

Table 6-5: Annual expenses associated with the different services rendered for road embankment construction.

Designation Costs (MAD**)**	**Costs (MAD)**
Depreciation expense	35 000
Expenses driving staff	96 000
Insurance fees	15 000
Dues and taxes	14 600
Total Fixed Fees (MAD)	**160 600**
Fuel and lubricant	344 760
Pneumatic	22 000
Maintenance and repair	25 000
Total Variables Fees (MAD)	**391 760**
Operating costs	28 750
Other costs	11 500
Total structure fees (MAD)	40 250
Total return price (MAD)	**592 610**
Average distance travelled per year (km)	74 880
Cost price per kilometer rolled (MAD)	7,91
Cost price in m^3/km (MAD)	**0,53**

The radius of profitability (R) is calculated using the following equation (6.4) (Amrani et al., 2020):

$$\left(\left((Pu + R \times T) \times CE\right) + \sum(OP)\right) \times PM = SP \quad (6.4)$$

Where:

Pu: Purchase of materials; **R:** Radius of profitability; **T:** Cost of transport; **CE:** Expansion coefficient; **OP:** Other prices (implementation, extraction, loading…); **PM:** Profit margin, **SP:** Sale price.

Table 6-6 gives the calculation of radius of profitability, based on Equation (6.4). The calculation was performed with the assumption that the city has access to nearby conventional resources.

Table 6-6: Calculation of profitability radius.

Average costs (excluding taxes)	**Mining waste materials**	**Conventional embankment materials**
Purchase of materials (MAD/m^3)	2	12
Expansion and losses (%)	15	15
Loading costs (MAD/m^3)	5	5
Water supply (MAD/m^3)	3	3
Implementation fees (MAD/m^3)	12	12
Transportation fees (MAD.m^3/km)	0,53	0,53
Profit margin (%)	15	15
Average selling price (MAD/m^3)	45	45
Radius of profitability (km)	28	9

According to this preliminary calculation, it was demonstrated that mining waste materials can be utilized as embankment materials within a 28 km radius around the Benguerir mine. In contrast, conventional materials become economically unviable beyond a distance of 9 km. This finding highlights the potential of PWR as a sustainable solution for environmental protection.

The integration of PWR in road embankments not only reduces material costs but also has the potential to revolutionize the construction industry by promoting a more ecologically sound

approach. Traditionally, road embankments have been constructed using materials such as gravel, sand, and crushed stone, which can be expensive and have a negative impact on the environment. However, by using PWR, a byproduct of the mining industry, as a substitute for these traditional materials, both cost and environmental concerns can be addressed. The research of Ahmed and Abouzeid (2009); Amrani et al. (2021); Amrani et al. (2019) reveal that integrating PWR not only reduces material expenses but also proves to be more environmentally friendly compared to conventional construction practices. Their research, as determined in this study, reveal how utilizing PWR significantly curtails expenses tied to raw materials while avoiding the extensive environmental degradation characteristic of conventional mining. The decision to use PWR for road construction is a strategic blend of economic efficiency and stability. This choice stands out not just for its cost-effectiveness and environmental benefits, but also for signaling a forward-looking transformation in industry norms by giving value to materials previously seen as waste. By considering economic assessments, we move toward a conclusion where cost-effectiveness aligns with an impactful approach of utilizing PWR in road construction projects.

In light of these findings, there is a need for further research and development in this area in order to fully explore the potential applications of PWR in road construction. However, to fully understand its suitability for long-term use, it is crucial to examine both its environmental and mechanical performance. This is an important aspect of any comprehensive study on the subject. In the current study, we have focused on laboratory tests and stability analysis to evaluate the properties of PWR as an embankment material. These tests have provided valuable insights into the material's behavior. Therefore, it is recommended that field tests be conducted to further investigate the long-term environmental and mechanical performance of PWR as embankment material. Furthermore, it is important to consider the potential economic benefits of using PWR, as well as any potential challenges or limitations that may arise.

In order to fully realize the potential of using PWR in road construction, the Moroccan government must update the current guidelines and regulations for road construction. The Moroccan Guide for Road should be revised to allow PWR to be classified as natural aggregates, thus encouraging its use in road construction projects. This would require collaboration between government agencies,

mining companies, and road construction firms to establish standards and specifications for the use of this material, ensuring its safe and effective integration into road-building practices.

6.5 Conclusions

This paper aimed to assess the feasibility of utilizing PWR, specifically focusing on the lithology of marly clay and marly limestone, in the construction of road embankments. These two lithologies exhibit substantial potential volume (27 Mm^3), making them attractive materials for such applications. Through extensive experimentation, including stability analysis, and preliminary economic evaluation of the raw material, an integrated approach towards the utilization of PWR is provided. The main conclusions to assess the potential use of these materials for road embankment are the following:

i) Chemically, the materials studied are dominated by CaO (12 - 33 wt.%), SiO_2 (23 - 38 wt.%), and MgO (7 – 9 wt.%); mineralogically, the main phases are quartz, calcite, dolomite, apatite, and clay minerals. The environmental characterization classified the studied materials as non-hazardous waste.

ii) Based on the results of the physical (MBV: 5-7 and PI: > 23%) and geotechnical (UCS: < 9 MPa, LA: > 50%, MD: > 35 %, γ_{dmax}: 1.352-1.518 t/m^3, c': 18-16 kPa, and ϕ': 11-17°) characterizations the studied materials marly limestone and marly clay belong to the R33 and A3 categories respectively, which means that these materials can be utilized in the construction of road embankments.

iii) The results of stability analysis showed that embankments up to 10 m in height can be constructed with marly clay without any significant physical instability risks. Satisfactory SF was found (SF = 1.97 for H = 5 m and SF = 1.54 for H = 10 m). Whereas the use of marly limestone is limited to a height of less than 10 m (SF = 1.74 for H = 5 m and SF = 1.33 for H = 10 m), this height can be increased by adding a bench of rock fill (SF = 1.64) or by adjusting the slope to 1V:3H (SF = 1.80).

iv) The economic evaluation indicates that PWR can be utilized as embankment materials in a radius of 28 km around the Benguerir mine, keeping a lower cost compared to conventional materials.

The utilization of PWR not only can address the issue of combatting land degradation, but we can also contribute to the preservation of the surrounding ecosystem and environmental protection. By utilizing this waste as embankment material, it can be effectively repurposed and contribute to the construction of environmentally friendly structures. Moreover, this material can reduce the demand for traditional construction materials, which are often extracted from natural resources. This approach aligns with the principles of circular economy, where waste materials are recycled and used as valuable resources.

Ethical approval

Not applicable.

Funding

This work was supported by OCP Group (Grant number RE04).

Credit authorship contribution statement

Safa Chlahbi: Conceptualization, Methodology, Data curation, Software, Formal analysis, Writing – original draft, Writing – review & editing, Visualization. **Abdellatif Elghali:** Conceptualization, Validation, Writing – review & editing, Supervision. **Omar Inabi:** Conceptualization, Methodology, Validation, Data curation, Writing – review & editing. **Tikou Belem:** Conceptualization, Writing – review & editing, Supervision. **Essaid Zerouali:** Writing – review & editing. **Mostafa Benzaazoua:** Conceptualization, Writing – review & editing, Supervision.

Declaration of Competing Interest

The authors declare the following financial interests/personal relationships which may be considered as potential competing interests: Mostafa Benzaazoua reports financial support was provided by OCP Group. If there are other authors, they declare that they have no known competing financial interests or personal relationships that could have appeared to influence the work reported in this paper.

Data availability

Data will be made available on request.

Acknowledgments

The authors thank OCP Group (Benguerir mine) and the experimental mine Morocco for their support in the framework of the project RE04. The authors would like also to thank the staff of Public Testing and Research Laboratory (LPEE) for their support with materials testing. The authors would like also to thank OCP collaborators and the staff of the Geo-analytical Lab and the Green Geomaterials Lab of Mohammed VI Polytechnic University for the great help concerning the sampling, and the preparation.

Consent to participate

All authors consent to participate.

Consent for publication

All authors consent to publish.

References

Ahangari Nanehkaran, Y., Pusatli, T., Chengyong, J., Chen, J., Cemiloglu, A., Azarafza, M., & Derakhshani, R. (2022). Application of Machine Learning Techniques for the Estimation of the Safety Factor in Slope Stability Analysis. *Water*, *14*(22), 3743. https://www.mdpi.com/2073-4441/14/22/3743

Ahmed, A. A., & Abouzeid, A. Z. M. (2009). Potential use of phosphate wastes as aggregates in road construction. *Journal of Engineering Sciences*, *37*, 413-422.

Ahmed, A. A. M., Abdel Kareem, K. H., Altohamy, A. M., & Rizk, S. A. M. (2014). Potential use of mines and quarries solid waste in road construction and as replacement soil under foundations. *JES. Journal of Engineering Sciences*, *42*(No 4), 1094-1105. https://doi.org/10.21608/jesaun.2014.115043

Allen, E., & Iano, J. (2019). *Fundamentals of Building Construction: Materials and Methods*. John Wiley & Sons. https://books.google.co.ma/books?id=2HGqDwAAQBAJ&printsec=frontcover&hl=fr#v=onepage&q&f=false

Amrani, M., Taha, Y., El Haloui, Y., Benzaazoua, M., & Hakkou, R. (2020). Sustainable Reuse of Coal Mine Waste: Experimental and Economic Assessments for Embankments and Pavement Layer Applications in Morocco. *Minerals*, *10*(10). https://doi.org/10.3390/min10100851

Amrani, M., Taha, Y., Elghali, A., Benzaazoua, M., Kchikach, A., & Hakkou, R. (2021). An experimental investigation on collapsible behavior of dry compacted phosphate mine

waste rock in road embankment. *Transportation Geotechnics*, *26*. https://doi.org/10.1016/j.trgeo.2020.100439

Amrani, M., Taha, Y., Kchikach, A., Benzaazoua, M., & Hakkou, R. (2019). Valorization of Phosphate Mine Waste Rocks as Materials for Road Construction. *Minerals*, *9*(4). https://doi.org/10.3390/min9040237

Argane, R., Benzaazoua, M., Hakkou, R., & Bouamrane, A. (2015). Reuse of base-metal tailings as aggregates for rendering mortars: Assessment of immobilization performances and environmental behavior. *Construction and Building Materials*, *96*, 296-306. https://doi.org/https://doi.org/10.1016/j.conbuildmat.2015.08.029

Argane, R., Benzaazoua, M., Hakkou, R., & Bouamrane, A. (2016). A comparative study on the practical use of low sulfide base-metal tailings as aggregates for rendering and masonry mortars. *Journal of Cleaner Production*, *112*, 914-925. https://doi.org/https://doi.org/10.1016/j.jclepro.2015.06.004

Azadi, A., Esmatkhah Irani, A., Azarafza, M., Hajialilue Bonab, M., Sarand, F. B., & Derakhshani, R. (2022). Coupled Numerical and Analytical Stability Analysis Charts for an Earth-Fill Dam under Rapid Drawdown Conditions. *Applied Sciences*, *12*(9), 4550. https://www.mdpi.com/2076-3417/12/9/4550

Azarafza, M., Hajialilue Bonab, M., & Akgun, H. (2021). Numerical analysis and stability assessment of complex secondary toppling failures: A case study for the south pars special zone. *Geomechanics and Engineering*, *27*, 481-495. https://doi.org/10.12989/gae.2021.27.5.481

Bahhou, A., Taha, Y., El Khessaimi, Y., Idrissi, H., Hakkou, R., Amalik, J., & Benzaazoua, M. (2021b). Use of phosphate mine by-products as supplementary cementitious materials. *Materials Today: Proceedings*, *37*, 3781-3788. https://doi.org/https://doi.org/10.1016/j.matpr.2020.07.619

Bayoussef, A., Loutou, M., Taha, Y., Mansori, M., Benzaazoua, M., Manoun, B., & Hakkou, R. (2021b). Use of clays by-products from phosphate mines for the manufacture of sustainable lightweight aggregates. *Journal of Cleaner Production*, *280*, 124361. https://doi.org/https://doi.org/10.1016/j.jclepro.2020.124361

Bayoussef, A., Oubani, M., Loutou, M., Taha, Y., Benzaazoua, M., Manoun, B., & Hakkou, R. (2021a). Manufacturing of high-performance ceramics using clays by-product from phosphate mines. *Materials Today: Proceedings*, *37*, 3994-4000. https://doi.org/https://doi.org/10.1016/j.matpr.2020.10.800

Bishop, A. W. (1955). The use of the Slip Circle in the Stability Analysis of Slopes. *Geotechnique*, *5*(1), 7-17. https://doi.org/10.1680/geot.1955.5.1.7

Bouzahzah, H., Benzaazoua, M., Plante, B., & Bussiere, B. (2015). A quantitative approach for the estimation of the "fizz rating" parameter in the acid-base accounting tests: A new adaptations of the Sobek test. *Journal of Geochemical Exploration*, *153*, 53-65. https://doi.org/https://doi.org/10.1016/j.gexplo.2015.03.003

Cai, F., & Ugai, K. (2001). Discussion: Slope stability analysis by finite elements. *Geotechnique*, *51*(7), 653-654. https://doi.org/10.1680/geot.2001.51.7.653

Chlahbi, S., Belem, T., Elghali, A., Rochdane, S., Zerouali, E., Inabi, O., & Benzaazoua, M. (2023). Geological and Geomechanical Characterization of Phosphate Mine Waste Rock in View of Their Potential Civil Applications: A Case Study of the Benguerir Mine Site, Morocco. *Minerals*, *13*(10), 1291. https://www.mdpi.com/2075-163X/13/10/1291

Collin, J. G., Leshchinsky, D., Hung, C. J. J., Parsons, B., Quade, Douglas, Institute, N. H., & Administration, U. S. F. H. (2005). *Soil Slope and Embankment Design: Reference Manual*. United States Department of Transportation, Federal Highway Administration, National Highway Institute. https://books.google.co.ma/books?id=ZfD1jgEACAAJ

Day, R. W. (2010). *Foundation engineering handbook: design and construction with the 2009 international building code*. McGraw-Hill Education.

Derakhshanalavijeh, R., & Teixeira, J. M. C. (2017). Cost overrun in construction projects in developing countries, gas-oil industry of Iran as a case study. *Journal of Civil Engineering and Management*, *23*(1), 125-136.

Durante Ingunza, M. d. P., dos Santos Júnior, O. F., & Gerab, A. T. F. d. S. C. (2020). Potential Use of Sandy Mining Wastes as Raw Material in Road Construction. *Geotechnical and Geological Engineering*, *38*(5), 5681-5691. https://doi.org/10.1007/s10706-020-01382-7

El Bamiki, R., Raji, O., Ouabid, M., Elghali, A., Khadiri Yazami, O., & Bodinier, J.-L. (2021). Phosphate Rocks: A Review of Sedimentary and Igneous Occurrences in Morocco. *Minerals*, *11*(10). https://doi.org/10.3390/min11101137

El Ghorfi, M., Inabi, O., Amar, H., Taha, Y., Elghali, A., Hakkou, R., & Benzaazoua, M. (2024). Design and Implementation of Sampling Wells in Phosphate Mine Waste Rock Piles: Towards an Enhanced Composition Understanding and Sustainable Reclamation. *Minerals*, *14*(3), 286. https://www.mdpi.com/2075-163X/14/3/286

El Machi, A., Mabroum, S., Taha, Y., Tagnit-Hamou, A., Benzaazoua, M., & Hakkou, R. (2021). Use of flint from phosphate mine waste rocks as an alternative aggregates for concrete. *Construction and Building Materials*, *271*. https://doi.org/10.1016/j.conbuildmat.2020.121886

Elghali, A., Benzaazoua, M., Bouzahzah, H., Bussière, B., & Villarraga-Gómez, H. (2018). Determination of the available acid-generating potential of waste rock, part I: Mineralogical approach. *Applied Geochemistry*, *99*, 31-41. https://doi.org/https://doi.org/10.1016/j.apgeochem.2018.10.021

Elghali, A., Benzaazoua, M., Taha, Y., Amar, H., Ait-khouia, Y., Bouzahzah, H., & Hakkou, R. (2023). Prediction of acid mine drainage: Where we are. *Earth-Science Reviews*, *241*, 104421. https://doi.org/https://doi.org/10.1016/j.earscirev.2023.104421

Estabragh, A. R., Javadi, A. A., & Boot, J. C. (2004). Effect of compaction pressure on consolidation behaviour of unsaturated silty soil [Article]. *Canadian Geotechnical Journal*, *41*(3), 540-550. https://doi.org/10.1139/T04-007

Göktepe, F., & Keskin, I. (2018). A Comparison Study between Traditional and Finite Element Methods for Slope Stability Evaluations. *Journal of the Geological Society of India*, *91*(3), 373-379. https://doi.org/10.1007/s12594-018-0864-3

Hakkou, R., Benzaazoua, M., & Bussière, B. (2016). Valorization of Phosphate Waste Rocks and Sludge from the Moroccan Phosphate Mines: Challenges and Perspectives. *Procedia Engineering*, *138*, 110-118. https://doi.org/10.1016/j.proeng.2016.02.068

Inabi, O., Attou, M., Benzaazoua, M., & Qachar, M. (2023). Design of Cost-Effective and Sustainable Treatments of Old Landslides Adapted to the Moroccan Road Network: A Case Study of Regional Road R410 Crossing the Rifan Structural Domain. *Water*, *15*(13), 2423.

Johnston, I., Murphy, W., & Holden, J. (2021). A review of floodwater impacts on the stability of transportation embankments. *Earth-Science Reviews*, *215*, 103553. https://doi.org/https://doi.org/10.1016/j.earscirev.2021.103553

Jong, T., & Parry, D. L. (2005). Evaluation of the stability of arsenic immobilized by microbial sulfate reduction using TCLP extractions and long-term leaching techniques. *Chemosphere*, *60*(2), 254-265. https://doi.org/https://doi.org/10.1016/j.chemosphere.2004.12.046

Kiser, C. D., & Kolay, P. K. (2013). Embankment Slope Stability Analysis of Dwight Mission Mine Site Reclamation Project.

Loutou, M., Hajjaji, M., Mansori, M., Favotto, C., & Hakkou, R. (2013). Phosphate sludge: thermal transformation and use as lightweight aggregate material. *J Environ Manage*, *130*, 354-360. https://doi.org/10.1016/j.jenvman.2013.09.004

Loutou, M., Taha, Y., Benzaazoua, M., Daafi, Y., & Hakkou, R. (2019). Valorization of clay by-product from moroccan phosphate mines for the production of fired bricks. *Journal of Cleaner Production*, *229*, 169-179. https://doi.org/10.1016/j.jclepro.2019.05.003

Malaoui, R., Soltani, M. R., Djellali, A., Soukeur, A., & Kechiched, R. (2023). Geotechnical Characterization of Phosphate Mining Waste Materials for Use in Pavement Construction. *Engineering, Technology & Applied Science Research*, *13*(1), 10005-10013.

Mamat, R. C., Kasa, A., & Razali, S. F. M. (2019). A review of road embankment stability on soft ground: problems and future perspective. *IIUM Engineering Journal*, *20*(2), 32-56.

Memon, Y. (2018). *A Comparison Between Limit Equilibrium and Finite Element Methods for Slope Stability Analysis*. https://doi.org/10.13140/RG.2.2.16932.53124

Miller, S., Jeffery, J., & Wong, J. (1991). Use and misuse of the acid base account for "AMD" prediction. Proceedings of the 2nd International Conference on the Abatement of Acidic Drainage, Montréal, Que,

Mohamed Ali, M., & Yang, H.-S. (2014). A study of some Egyptian carbonate rocks for the building construction industry. *International Journal of Mining Science and Technology*, *24*. https://doi.org/10.1016/j.ijmst.2014.05.008

Mori, T., Tobita, Y., & Okimura, T. (2012). The damage to hillside embankments in Sendai city during the 2011 off the Pacific Coast of Tohoku Earthquake. *Soils and Foundations*, *52*(5), 910-928. https://doi.org/https://doi.org/10.1016/j.sandf.2012.11.011

Morin, K. A., & Hutt, N. M. (2001). *Environmental geochemistry of mine site drainage: Practical theory and case studies, Digital Edition*. MDAG Publishing (www. mdag. com), Surrey, British Columbia.

Mouih, K., Taha, Y., Benzaazoua, M., & Hakkou, R. (2023). Valorization of phosphate waste rocks for the production of compressed stabilized earth bricks using cement stabilizer. *Materials Today: Proceedings*. https://doi.org/https://doi.org/10.1016/j.matpr.2023.03.224

NAVFAC, N. F. E. C. (1982). *Soil mechanics: Design manual 7.1*. Dept. of the Navy Alexandria, VA.

NF-P11-300. (1992). Exécution des Terrassements—Classification des Matériaux Utilisables dans la Construction des Remblais et des Couches de Forme d'infrastructures Routières. In *Association Française de Normalisation: Paris, France.*

NF-P94-051. (1993). Soil: Investigation and Testing. Determination of Atterberg's Limits. Liquid Limit Test Using Cassagrande Apparatus. Plastic Limit Test on Rolled Thread—Sols: Reconnaissance et Essais; Association Française de Normalisation: Paris, France. In.

NF-P94-052-1. (1995). Soil: Investigation and Testing. Atterberg Limit Determination. Part 1: Liquid Limit. Cone Penetrometer Method—Sols: Reconnaissance et essais. In: Association Française de Normalisation Paris, France.

NF EN 1097-1. (2011). Tests for mechanical and physical properties of aggregates - Part 1 : determination of the resistance to wear (micro-Deval). In.

NF EN 12620. (2008). Aggregates for concrete. In.

NF EN ISO 17892-9. (2018). Geotechnical investigation and testing - Laboratory testing of soil - Part 9: consolidated triaxial compression tests on water saturated soils, French standard, AFNOR Editions. France. In.

NF P 94-056. (1996). Soil: Investigation and Testing–Granulometric Analysis–Dry Sieving Method After Washing. *AFNOR, Paris, France*.

NM00.8.095. (2015). Soils: Investigation and Testing. Measuring of the Methylene Blue Adsorption Capacity of à Rocky Soil. Determination of the Methylene Blue of à Soil by Means of the Stain test. In.

NM13.1.008. (1998). Granulometric Analysis. Dry Sieving Method after Washing. In.

NM.10.1.138. (1995). Aggregates: Los Angeles Test. In.

Oberle, B., Bringezu, S., Hatfield-Dodds, S., Hellweg, S., Schandl, H., & Clement, J. (2019). *Global resources outlook: 2019*. International Resource Panel, United Nations Envio, Paris, France.

Oubaha, S., Hakkou, R., Taha, Y., Mghazli, M. O., & Benzaazoua, M. (2022). Elaboration of compressed earth blocks based on phosphogypsum and phosphate mining by-products. *Journal of Building Engineering*, *62*, 105423. https://doi.org/https://doi.org/10.1016/j.jobe.2022.105423

P94-093, N. (1999). Sols: reconnaissance et essais-Détermination des références de compactage d'un matériau-Essai Proctor normal. Essai Proctor modifié. *AFNOR*.

Peyronnard, O., & Benzaazoua, M. (2011). Estimation of the cementitious properties of various industrial by-products for applications requiring low mechanical strength. *Resources, Conservation and Recycling*, *56*(1), 22-33. https://doi.org/https://doi.org/10.1016/j.resconrec.2011.08.008

Rapti, I., Lopez-Caballero, F., Modaressi-Farahmand-Razavi, A., Foucault, A., & Voldoire, F. (2018). Liquefaction analysis and damage evaluation of embankment-type structures. *Acta Geotechnica*, *13*(5), 1041-1059. https://doi.org/10.1007/s11440-018-0631-z

Safhi, A. e. M., Amar, H., El Berdai, Y., El Ghorfi, M., Taha, Y., Hakkou, R., Al-Dahhan, M., & Benzaazoua, M. (2022). Characterizations and potential recovery pathways of phosphate mines waste rocks. *Journal of Cleaner Production*, *374*, 134034. https://doi.org/https://doi.org/10.1016/j.jclepro.2022.134034

Segui, P., Safhi, A. E., Amrani, M., & Benzaazoua, M. (2023). Mining Wastes as Road Construction Material: A Review. *Minerals*, *13*(1).

Setra, & LCPC. (1992). Réalisation des remblais et des couches de forme. *Fascicule I Principes Généraux, 211p*.

Sobek, A. A. (1978). *Field and laboratory methods applicable to overburdens and minesoils*. Industrial Environmental Research Laboratory, Office of Research and ….

Taha, Y., Benzaazoua, M., Hakkou, R., & Mansori, M. (2016). Natural clay substitution by calamine processing wastes to manufacture fired bricks. *Journal of Cleaner Production*, *135*, 847-858. https://doi.org/10.1016/j.jclepro.2016.06.200

Taha, Y., Benzaazoua, M., Hakkou, R., & Mansori, M. (2017). Coal mine wastes recycling for coal recovery and eco-friendly bricks production. *Minerals Engineering*, *107*, 123-138. https://doi.org/https://doi.org/10.1016/j.mineng.2016.09.001

Taha, Y., Elghali, A., Hakkou, R., & Benzaazoua, M. (2021). Towards Zero Solid Waste in the Sedimentary Phosphate Industry: Challenges and Opportunities. *Minerals*, *11*(11). https://doi.org/10.3390/min11111250

USEPA. (1992). Method 1311: toxicity characteristic leaching procedure, SW-846: Test methods for evaluating solid waste - Physical/Chemical Methods. Washington, D.C. In.

Wubalem, A. (2022). Comparison of General Limit Equilibrium Methods for Slope Stability Analysis. *Ethiopian Journal of Natural and Computational Sciences*, *2*(1), 271-290.

Xie, Y., Zhu, W., Xiong, Y., & Ye, G. (2023). Numerical investigation on the effect of initial water content on dynamic responses of unsaturated sandy and clayey embankments. *Soil*

Dynamics and Earthquake Engineering, *173*, 108151. https://doi.org/https://doi.org/10.1016/j.soildyn.2023.108151

Yamaguchi, A., Mori, T., Kazama, M., & Yoshida, N. (2012). Liquefaction in Tohoku district during the 2011 off the Pacific Coast of Tohoku Earthquake. *Soils and Foundations*, *52*(5), 811-829. https://doi.org/https://doi.org/10.1016/j.sandf.2012.11.005

Yang, Y.-Y., Wu, H.-N., Shen, S.-L., Horpibulsuk, S., Xu, Y.-S., & Zhou, Q.-H. (2014). Environmental impacts caused by phosphate mining and ecological restoration: a case history in Kunming, China. *Natural Hazards*, *74*(2), 755-770. https://doi.org/10.1007/s11069-014-1212-6

CHAPTER 7 GENERAL DISCUSSION

7.1 Sampling and characterization

The first objective of this thesis is to thoroughly characterize and analyze each lithological formation upstream in terms of geology, geomechanics, chemistry, mineralogy, and the environment. This comprehensive analysis requires careful selection of the sampling method and the determination of the number of samples to be collected (Annels, 1991; Cao et al., 2018). However, this task was challenging, as it involved coordinating various characterization techniques and dealing with the occasional unavailability of the required quantities for each characterization. As demonstrated by Desharnais (2019), the number of samples to be taken depends on several factors, including the type of deposit, its distribution, direct accessibility to the deposit, and the available budget. Consequently, estimating the sampling step necessitated a consideration of the study's objectives, the level of knowledge about the study site, and the allocated budget (Downing et al., 1999; Marjoribanks, 2010). In our specific case, we opted for a hybrid sampling method combining random and target approaches. This hybrid method allowed us to obtain representative samples and acquire enough quantity of samples for the diverse characterizations.

Non-destructive core drilling is used in this project. As demonstrated by Hussain et al. (2020), the non-destructive core drilling has been able to provide a deeper insight into the variable facies that characterize the study area. The clean and undisturbed state in which the samples were retrieved underscores a critical advantage of non-destructive core drilling. Six core holes were drilled in our case to collect information about the different facies and to obtain cleaner and high-quality samples (Cao et al., 2018). Through the implementation of this technique, we have been able to provide a deeper insight into the variable facies that characterize the study area. By analyzing these core samples, we identified four categories of facies: carbonate, phosphate, siliceous, and clay/marl (Chlahbi et al., 2023). These categories correspond to eight main facies: limestone, dolomite, marly-limestone, indurated phosphate, phosphate flint, flint, silexite, and marly/clay. The number of samples collected depended on the specific characterization techniques employed. Our primary objective was to collect as many samples as possible from the core holes and, if necessary, supplement them with samples from the mining trenches. By carefully observing and logging the various boreholes, we determined 315 samples from the core holes and 185 samples from the

mining trenches. This increases the total number of samples to 500. It is important to note that this sample size was determined based on the characterization techniques employed and the availability of the different facies and required quantities for the analysis (Downing et al., 1999; Elghali et al., 2023).

Analyzing the different lithologies forming the interburdens has proven to be a useful tool in various aspects. Firstly, it allows us to evaluate the potential uses of the identified lithologies (Hakkou et al., 2016; Taha et al., 2021). By understanding the composition and properties of these rock formations, we can determine their suitability for different applications, such as construction materials, industrial processes, or even potential sources of valuable minerals (Idrissi et al., 2021; Taha et al., 2021). This knowledge opens possibilities for economic exploitation and sustainable resource management. Additionally, this analysis demonstrates that some waste rock lithologies are rich in phosphate and trace elements (Amar et al., 2023). This finding is significant as it highlights the potential for resource recovery from what was previously considered waste.

Furthermore, the analysis helps us distinguish between the content of elements in each waste rock and their mineralogical speciation. This distinction is crucial as it allows us to understand how these elements are distributed within the rock formations and their potential for extraction. For example, the mineralogical speciation of phosphate and rare earth elements (REEs) provides insight into the most effective beneficiation techniques and recovery processes (Amar et al., 2023). This knowledge is essential for optimizing resource utilization and minimizing waste generation (Idrissi et al., 2021). Lastly, the analysis of different lithologies contributes to reducing the footprint of the mine site. By understanding the composition and characteristics of the rock formations, we can develop strategies to minimize the disturbance caused by mining activities. This includes implementing selective mining techniques, optimizing the use of resources, and developing efficient waste management practices. Ultimately, this leads to a more sustainable and environmentally friendly mining operation.

7.2 Geomodelling

The 3D modeling carried out in this research project focuses on creating a geological model specifically for the future areas of the Benguerir mine. This model contains crucial information about the lithological discrepancy and thicknesses of the phosphate layers and interburdens (Giraud

et al., 1971; Mallet, 2002). By utilizing this model, we have been able to visualize the distribution of the phosphate series within the mine and make estimations regarding the volumes of the interburdens. Our initial plan also aimed to incorporate all the information collected from the various characterizations (including geomechanical, mineralogical, chemical, and environmental data) into this model. However, due to the significant distance between the boreholes (ranging from 2 to 3 kilometers), we faced challenges in accurately modeling their geominerallurgical behavior (Delgado Vega, 2012) (the geometallurgical approach often used for polymetallic mines has been renamed geominerallurgical, since in our case, we are dealing with a phosphate mineral 'apatite' and not metal). Nevertheless, the geological model has provided valuable insights into the geological composition and distribution of the phosphate series in the Benguerir mine.

In order to establish an effective geominerallurgical model, a sequence of practices is recommended (Bueno et al., 2015; Michaux & O'Connor, 2019). Firstly, adding other drill cores with a closer mesh, typically around 250 m, is recommended (Vermette, 2018). This allows for a more detailed and accurate representation of the deposit's geological features and mineral distribution. By increasing the density of drill cores, a higher level of spatial resolution can be achieved, allowing for a better understanding of the deposit's variability (Lishchuk, 2019; Vermette, 2018). This, in turn, leads to more reliable predictions and estimations. Secondly, the geological logging of the drill cores is of utmost importance in establishing a geominerallurgical model. The logging should be performed based on a standard scale involved in drill core description and sampling. This ensures consistency and comparability of the data collected from different drill cores. Detailed descriptions of lithology, mineralogy, alteration, and other relevant geological characteristics can be recorded through geological logging.

In cases where sufficient numerical data on the parameter of concern are not available, a stochastic process can be utilized (Hammersley & Handscomb, 1964; Niederreiter, 1992). The user must define two continuous independent variables representing the parameter of concern and a categorical variable used to describe the parameters (Toubri et al., 2021). This allows for the generation of synthetic data that can be used to supplement the existing dataset. The stochastic process helps to account for uncertainty and provides a more comprehensive understanding of the geominerallurgical model (Niederreiter, 1992). Finally, constructing a model using variogram and other multi-realization analyses is recommended (Abzalov, 2016b). Variogram analysis is a

statistical tool used to characterize spatial continuity and assess sample correlation (Abzalov, 2016a). It helps to define the range and direction of spatial dependence, which is crucial for accurate resource estimation.

7.3 Guidelines for the valorization of PWR

Phosphate waste rock, a byproduct of phosphate mining, holds significant potential for valorization, contributing to sustainable resource management practices (Chlahbi et al., 2023; Taha et al., 2021). The valorization of PWR plays a crucial role in sustainable resource management by transforming a traditionally discarded byproduct into a valuable resource. Hakkou et al. (2016) emphasize that the valorization of PWR not only helps in mitigating environmental concerns associated with mining activities but also contributes to the efficient utilization of resources. By repurposing waste rock, industries can reduce the ecological footprint of phosphate mining operations and minimize the impact on surrounding ecosystems. In this thesis project, a third objective was to propose a valorization guideline derived from the thorough characterization and analysis of phosphate interburdens. Through detailed examination and evaluation of phosphate interburdens, we aimed to identify and understand the properties and composition of these interburdens to propose potential valorization pathways. According to the findings, including geochemical, mineralogical, and geomechanical aspects, PWR can be used in various applications in different sectors (focusing on the civil engineering sectors), such as road construction, cement industry, phosphate recovery, and acid mine drainage treatment. Figure 7-1 serves as a comprehensive synthesis guideline, offering a structured framework for exploring the potential valorization avenues of PWR.

7.3.1 Phosphate recovery

Indurated phosphate and phosphate flint are notable for their high P_2O_5 contents, typically falling within the range of 14 to 25 wt.%, corresponding to carbonate fluor apatite as demonstrated by Safhi et al. (2022). The results obtained by Amar et al. (2023) showed that indurated phosphate constituted around 50% of the coarse fraction > 30 mm, while phosphate flint (20%) considered mining waste accumulates approximately 70% of the phosphate lithologies from the coarse fraction (> 30 mm) in PWR piles. The process of recovering phosphate from these lithologies involves a

series of post-exploitation steps (Amar et al., 2023). Initially, the material is subjected to crushing and grinding operations until a fine fraction measuring less than 30 mm is obtained. Subsequently, this fine fraction is forwarded to a beneficiation plant for further processing. Recovery of the residual phosphate within this fine fraction can be effectively carried out through multiple techniques including gravity separation serving as a preconcentration phase, flotation, leaching, and calcination (Amar et al., 2023; Guo & Li, 2010; Kawatra & Carlson, 2013; Liu et al., 2016; Zafar & Ashraf, 2007). These methods collectively enable the extraction and concentration of phosphate from indurated phosphate and phosphate flint.

The study conducted by Amar et al. (2023) highlighted challenges in sampling strategies for indurated phosphate and phosphate flint, along with the need for optimization in recovery methods like flotation and gravity separation to enhance P_2O_5 grade. The challenges in sampling strategies for these lithologies primarily revolve around the presence of coarse fractions in the sorted samples. These coarse fractions pose difficulties in achieving homogenization and sample reduction, which are essential for obtaining representative samples. To address these challenges and improve the recovery process, optimization in recovery methods such as flotation and gravity separation is necessary (Safhi et al., 2022). Flotation is a conventional method used in beneficiation plants to separate phosphate minerals from gangue materials (Boujlel et al., 2019; Elgillani & Abouzeid, 1993). By optimizing the flotation process, it is possible to enhance the P_2O_5 grade of the recovered phosphate. Similarly, gravity separation can be employed as a pre-concentration phase to effectively separate gangue minerals from phosphate minerals (Khan et al., 2019). Optimizing the gravity separation process can lead to improved recovery rates and higher P_2O_5 grades in the final product. These optimization efforts are crucial for maximizing the efficiency and effectiveness of the recovery process for indurated phosphate and phosphate flint. The study by Amar et al. (2023) emphasized the significance of accurate sampling for precise assays and the potential of sensor-based sorting for efficient phosphate mineral recovery.

However, the implementation of phosphate recovery should not be taken lightly. Any plans for phosphate recovery must be subject to a thorough technical and economic feasibility study. This study would evaluate the potential benefits and drawbacks of implementing phosphate recovery, considering the technical capabilities, costs, and potential environmental impacts. This will ensure that the implementation of phosphate recovery is truly beneficial and sustainable in the long term.

7.3.2 Cement manufacturing

PWR serves as a valuable source of by-products such as clay and limestone, both of which hold commercial significance. These by-products find application in the construction sector, particularly in the production of clinker, a primary component in various types of cement (Bahhou et al., 2021a). Clinker production involves firing a mix comprising approximately 80% limestone and 20% clay (Taylor, 1997). However, environmental concerns associated with clinker production have prompted a shift toward more sustainable practices. Notably, the production of one ton of clinker results in approximately 0.95 ton of CO_2 emissions (Davidovits, 2015).

To mitigate the environmental impact, there is a growing emphasis on reducing the clinker in cement through the incorporation of supplementary cement materials (SCMs). SCMs are classified into reactive materials (pozzolans) and inactive materials (fillers) (Rahhal et al., 2005). Some pozzolanic materials, such as slag and fly ash, face scarcity issues (Environment et al., 2018). In contrast, clays, due to their availability and pozzolanic reactivity after calcination, emerge as efficient materials for clinker replacement. Marl, as an example of a pozzolan, can be utilized in this context. A key criterion for evaluating the reactivity of clays is the content of Al_2O_3+Fe_2O_3+SiO_2, with ASTM C618 specifying a sum above 70% for Class N pozzolans (He et al., 1995). It's important to note that not meeting this chemical requirement doesn't conclusively determine the pozzolanic reactivity; further analysis is necessary.

The second category of SCMs, fillers, is exemplified by carbonate rocks, with calcite being a prominent example widely available. Calcite is recognized for accelerating the early hydration of cement, and its finer particles offer increased surface area which is crucial for the nucleation of the C-S-H phase (Moon et al., 2017; Scrivener et al., 2015). Dolomite has also emerged as a filler material, as evidenced by a recent study (von Greve-Dierfeld et al., 2020; Zajac et al., 2014).

7.3.3 Road construction materials

A significant volume of geomaterials is extensively utilized in road construction projects worldwide, highlighting the immense demand for such resources (Oberle et al., 2019). Integrating industrial by-products into this sector emerges as a viable solution to address sustainability concerns and reduce waste production. Particularly, PWR are emerging as strong contenders for

serving as alternative secondary raw materials (Ahmed & Abouzeid, 2009; Safhi et al., 2022; Taha et al., 2021). Geotechnical assessments have demonstrated promising physical and mechanical properties of flint, phosphate flint, and limestone, showcasing a density range of 1.9 to 2.8, LA between 25% and 50%, and fragmentability below 7. These findings indicate that PWR can be effectively repurposed as raw materials in road construction activities, offering a sustainable and eco-friendly approach to resource utilization in the industry (Hakkou et al., 2016).

A specific study of the feasibility of using PWR, specifically marly clay and marly limestone, for constructing road embankments was presented in Chapter 6. The geotechnical characterization (LA: 95-98%, fragmentability: 7, optimum moisture content: 22.2 - 23.1%, and maximum dry density 1.352 - 1.518 t/m³, friction angle 18° – 16°, and cohesion 11 - 17 kPa) categorizes these materials as suitable for road embankments. Stability analysis shows that embankments up to 10 m with marly clay are safe, while marly limestone can be used with precautions. This study not only sheds light on the potential of utilizing PWR for road construction but also emphasizes the importance of thorough geotechnical assessments when considering alternative materials for infrastructure projects.

7.3.4 Alternative aggregates

The increasing demand for aggregates from quarries strains natural resources, highlighting the need for alternative sources of aggregate materials. Using PWR local alternative aggregates will help reduce the stress on the primary aggregates. Incorporating PWR as aggregates in concrete not only eases the burden on primary aggregates but also contributes to resource conservation. Limited research has delved into the viability of utilizing PWR aggregates for concrete applications (Ahmed & Abouzeid, 2009; El Machi et al., 2021; Safhi et al., 2022). Findings suggest that various lithologies such as flint, phosphate flint, limestone, and dolomite exhibit good physical and mechanical properties in terms of UCS (up to 104 MPa), LA (25-50%), MD (< 35%), density (2-3) and absorption (0.2-4). These lithologies can be easily crushed for aggregate production and find applications in diverse sectors like concrete production, railroad ballasts, and embankments. Conversely, silexite lithology displays moderate physical and mechanical properties with UCS around 32 MPa, LA approximately 50%, low density of about 1.6, and high absorption exceeding 4%. Due to its lightweight nature, silexite can serve as a suitable lightweight aggregate, ideal for

manufacturing concrete and various construction materials, emphasizing the importance of exploring alternative aggregate sources for sustainable development in the construction industry.

7.3.5 Brick manufacturing

The incorporation of PWR in brick manufacturing presents a promising avenue for sustainable production practices. The clay and marl located at the Int C3/C2 interburden have been thoroughly analyzed in this study, revealing their significant geotechnical attributes. These lithologies exhibit promising characteristics such as a PSD below 2 µm, a plasticity index (PI) ranging from 10 to 35, and a methylene blue value below 10. Understanding the importance of these findings unveils the potential for utilizing these materials as valuable resources, particularly in brick manufacturing applications.

7.3.6 Acid mine drainage treatment

The acid-generating potential assessment detailed in Chapter 5 revealed that PWR exhibits a significant neutralization potential ranging from 38 to 991 kg $CaCO_3$/t, coupled with a low acid potential ranging from 0.31 to 16 kg $CaCO_3$/t. On the other hand, dolomite and limestone showcased significant neutralization potential values ranging from 500 to 991 kg $CaCO_3$/t. These findings indicate that these specific lithologies can serve as effective alkaline materials in managing acid mine drainage issues. A study conducted by Hakkou et al. (2009) supported this notion by demonstrating that incorporating 15 wt% alkaline phosphate waste into Kettara coarse tailings proved highly efficient in neutralizing acidic mine effluents. Moreover, this amendment significantly decreased the concentrations of metals in the leachate compared to the untreated Kettara coarse tailings, highlighting the potential of these materials in mitigating environmental impacts associated with mining activities.

In summary, by implementing these valorization pathways, the phosphate mining industry can revolutionize its waste management and sustainability approach. The potential benefits are twofold: firstly, by adopting these techniques, the industry can significantly reduce environmental hazards associated with phosphate waste. Secondly, transforming waste into a valuable commodity presents a unique opportunity for economic growth and diversification within industry. By strategically planning and applying the insights from this guide, stakeholders can effectively

harness the hidden value of PWR. This process contributes to a more sustainable and efficient mining operation and opens avenues for creating new revenue streams and job opportunities. Ultimately, by embracing these valorization techniques, the phosphate mining industry can pave the way for a more environmentally conscious and economically viable future, setting a positive example for sustainable resource management practices across the globe.

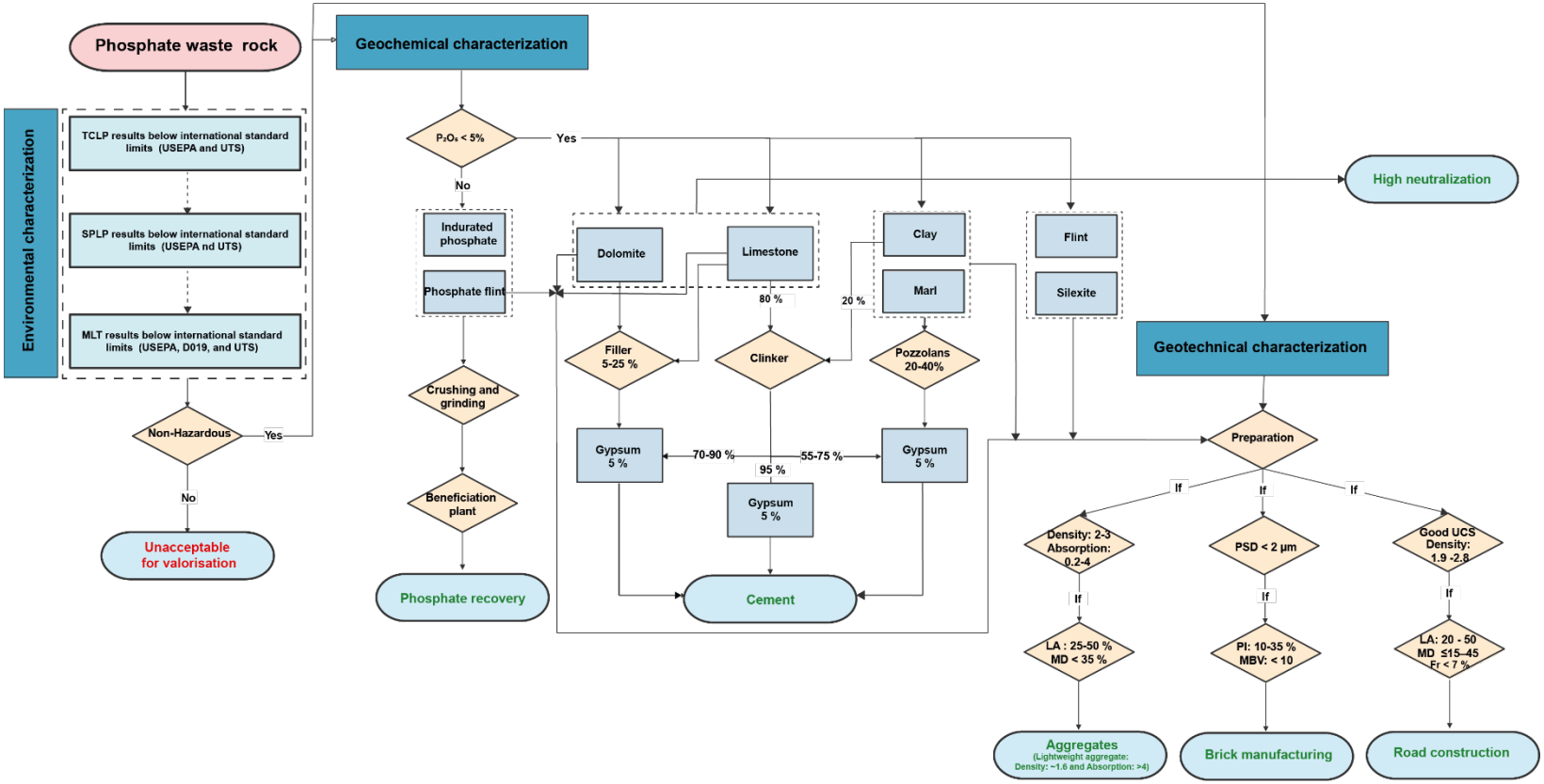

Figure 7-1: Guideline of potential valorization pathways of PWR

CHAPTER 8 CONCLUSIONS AND RECOMMENDATIONS

In conclusion, the mining industry plays an essential role in the economies of many countries, including Morocco. It is a significant source of revenue, job creation, and resource extraction. However, this industry also generates substantial amounts of mining waste that must be effectively managed. Mining waste includes various materials such as tailings, waste rock, sludge, and chemicals left over after the extraction of minerals.

These waste materials can pose significant environmental and health risks if improperly handled. Therefore, countries like Morocco need to prioritize proper management of mining waste to mitigate the negative impacts on ecosystems and local communities. Within this context, the general objective of this thesis was to study phosphate waste rock (PWR) upstream of the mining chain and to characterize each PWR lithology separately.

PWR refers to the residual materials generated during the process of phosphate mining. This thesis project encompassed three specific objectives, each aiming to contribute to a deeper understanding of PWR and its potential applications. Through the characterization of PWR's geological and geomechanical properties, assessment of their geochemistry and environmental behavior, and exploration of their sustainable reuse in road embankments, this project aimed to provide valuable insights and knowledge that could be applied in the fields of civil engineering and phosphate recovery.

8.1 Geological and geomechanical characterization of PWR in view of their potential civil applications

Phosphate waste rock is a byproduct of the phosphate mining industry, and its proper utilization is crucial for minimizing environmental impacts and maximize resource efficiency. The experimental work conducted on the interburdens (soil-like and hard rock samples) collected from the six drill cores and mining trenches at the Benguerir mine site in Morocco has yielded significant conclusions. The main results and conclusions of this study are summarized as follows:

- The Benguerir phosphate series comprised nine phosphate layers, eight interburdens, and an overburden. Additionally, the presence of “phosphate slabs” with either carbonate or siliceous matrix was observed.

- The study identified four types of waste rock, including carbonate (limestone and marly limestone), siliceous (flint and silexite), marly clay, and phosphate (phosphate flint and indurated phosphate).
- The unit sequences of the Benguerir deposit were found to be relatively stable in space, although with varying thickness and occasional interruptions in the units.
- The soil-like samples were classified as A3-A4 (fine soil) and exhibited plastic to very plastic properties. They were also categorized as clayey marl.
- These soil-like samples hold potential as raw materials for various applications, particularly in brick manufacturing, cement production, the field of ceramics, and embankment. Their characteristics ($P_{80\mu m}$ average varied between 100 and 64%, average plasticity index = 50%, average methylene blue value = 7.1, and bulk density = 1886 kg/m^3) make them suitable for these applications, offering a sustainable solution for sourcing raw materials.
- The collected hard rock samples (flint, silexite, phosphate flint, indurated phosphate, limestone, and marly limestone) showed promising geomechanical properties.
- The average compressive strength is 104 MPa for the flint, 35 MPa for the phosphate flint, 32 MPa for the silexite, 26 MPa for the limestone, 11 MPa for the indurated phosphate, and 8 MPa for the marly limestone.
- These hard rock samples could be an excellent alternative secondary raw material for civil engineering and phosphate recovery.

These findings contribute to understanding the Benguerir deposit and offer sustainable alternatives for PWR valorization in various industries.

8.2 Geochemistry and Environmental Assessment of PWR

The present study evaluated the geochemical and environmental behavior of PWR through a comprehensive analysis that included petrographical, chemical, and mineralogical characterizations and leaching tests. The main objective of this study was to provide a complete characterization of PWR samples to understand their composition and potential impact on the environment. The main results and conclusions of this study are summarized as follows:

- PWR mainly comprises calcite, dolomite, apatite, and quartz, with minor phases such as clay minerals and iron oxides.
- Chemically, the major chemical components are CaO (1.2-53.5 %) and MgO (0.2-19.5 %), followed by SiO_2 (2.4-94 %) and P_2O_5 (0.2-25 %). Trace elements can be classified into three groups based on their concentrations: a group with high concentrations composed of Zn and Cr (> 150 ppm), a group with moderate concentrations composed of Ba, V, Ni, Zr, Y, U, Cu, Cd, and Co (10 to 150 ppm), and a group with relatively low concentrations (< 10 ppm) including Rb, Pb, As, Mo, Se, Sc, Ga, Nb, Th, Hf, Sb, and Cs.
- Environmentally, PWR has high neutralizing potential (40 to 740 kg $CaCO_3$/t), neutral to alkaline pH levels (6 ± 0.6 to 9 ± 0.4) in leachates, and the concentration of contaminants (As, Ba, Cd, Cr, Se, U) remains below international standard limits (USEPA, D019, and UTS).
- PWR are classified as nonhazardous waste and could be considered a natural raw material for civil applications.

8.3 Sustainable reuse of PWR in road embankments

This study aimed to assess the feasibility of utilizing PWR in the construction of road embankments, with a specific focus on the lithology of marly clay and marly limestone. These two lithologies were chosen due to their substantial potential volume, estimated at around 27 Mm^3 for marly limestone and 22 Mm^3 for marly clay.

Extensive experimentation was conducted to evaluate the suitability of PWR for road embankments. Stability analysis was performed to determine the safety factor and behavior of the materials under different dispositions. Additionally, a preliminary economic evaluation of the raw material was conducted. This evaluation considered factors such as the operation cost and transportation. The main results and conclusions of this study are summarized as follows:

- Based on chemical, mineralogical, and environmental analyses, it can be concluded that the marly clay and marly limestone do not pose any hazards and can be classified as non-hazardous wastes.

- The stability analysis results indicated that embankments up to a height of 10 m can be constructed using marly clay without any significant risks of physical instability. The safety factors obtained were satisfactory (1.97 and 1.54). On the other hand, the use of marly limestone is restricted to a height of less than 10 m. However, this limitation can be overcome by incorporating a bench of rock fill, which increases the safety factor to 1.64.
- The economic evaluation indicates that PWR can be used as embankment materials within a 28 km radius of the Benguerir mine while maintaining a lower cost compared to conventional materials.

8.4 Guidelines for the Valorization PWR

The valorization of PWR presents a promising avenue for sustainable resource management practices. By repurposing this byproduct of phosphate mining, industries can not only mitigate environmental concerns associated with mining activities but also contribute to the efficient utilization of resources.

The detailed examination and analysis of phosphate interburdens have revealed the diverse potential applications of PWR in sectors such as civil engineering, cement manufacturing, phosphate recovery, road construction materials, brick manufacturing, and acid mine drainage treatment. The recovery of phosphate from indurated phosphate and phosphate flint involves a series of well-defined steps, including crushing, grinding, and beneficiation processes. Moreover, integrating PWR into cement manufacturing can help reduce the environmental impact associated with clinker production by incorporating supplementary cement materials like clay and limestone.

These materials offer sustainable alternatives to traditional pozzolans and fillers, addressing scarcity issues and promoting more eco-friendly practices. Additionally, the utilization of PWR in road construction materials showcases its versatility and potential to meet the demands for sustainable resource utilization. Overall, the valorization of PWR not only transforms a once-discarded byproduct into a valuable resource but also paves the way for more sustainable practices across various industries.

Finally, the valorization of PWR marks a significant shift in how society views and utilizes industrial byproducts. By transforming what was once considered waste into a valuable resource,

this process reduces environmental impacts associated with waste disposal and creates new opportunities for sustainable development. Industries that traditionally generated PWR can now repurpose it for various applications, such as construction materials, cement and brick manufacturing, and recovery of phosphate.

This shift towards valorization minimizes these industries' environmental footprint and contributes to a more circular economy where resources are utilized more efficiently. Embracing the valorization of PWR is a crucial step towards fostering sustainability and innovation across diverse sectors, setting a precedent for how we can rethink our approach to waste management and resource utilization in the future.

8.5 Recommendations

Several recommendations are proposed in this thesis project:

- Adding other drill cores with a closer mesh, typically around 250 m in Benguerir mine, in order to establish an effective geomineralurgical model.
- Extending the upstream geomineralurgical approach in other mine sites of OCP group for better understanding of the composition of interburdens (PWR).
- Implement a sorting protocol to ensure PWR's effective and sustainable valorization before storage.
- Integration of the approach of the PWR’s valorization in the value chain of the phosphate industry.
- Laboratory and pilot tests of the valorization of PWR is recommended to confirm the performance of this approach.

REFERENCES

Abbas, S., Saleem, M. A., Kazmi, S. M. S., & Munir, M. J. (2017). Production of sustainable clay bricks using waste fly ash: Mechanical and durability properties. *Journal of Building Engineering*, *14*, 7-14. https://doi.org/https://doi.org/10.1016/j.jobe.2017.09.008

Abbes, N., Bilal, E., Hermann, L., Steiner, G., & Haneklaus, N. (2020). Thermal Beneficiation of Sra Ouertane (Tunisia) Low-Grade Phosphate Rock. *Minerals*, *10*(11). https://doi.org/10.3390/min10110937

Abzalov, M. (2016a). Introduction to Geostatistics. In (pp. 233-237). https://doi.org/10.1007/978-3-319-39264-6_17

Abzalov, M. (2016b). Methods of the Linear Geostatistics (Kriging).

Adiansyah, J. S., Rosano, M., Vink, S., & Keir, G. (2015). A framework for a sustainable approach to mine tailings management: disposal strategies. *Journal of Cleaner Production*, *108*, 1050-1062. https://doi.org/https://doi.org/10.1016/j.jclepro.2015.07.139

Ahangari Nanehkaran, Y., Pusatli, T., Chengyong, J., Chen, J., Cemiloglu, A., Azarafza, M., & Derakhshani, R. (2022). Application of Machine Learning Techniques for the Estimation of the Safety Factor in Slope Stability Analysis. *Water*, *14*(22), 3743. https://www.mdpi.com/2073-4441/14/22/3743

Ahmari, S. A. L., & Zhang, L. (2012). Production of eco-friendly bricks from copper mine tailings through geopolymerization. *Construction and Building Materials*, *29*, 323-331.

Ahmed, A., & Abouzeid, A.-Z. (2011). An environmental solution for phosphate coarse waste reject-using them as concrete mix aggregates. *JES. Journal of Engineering Sciences*, *39*(1), 207-218.

Ahmed, A. A., & Abouzeid, A. Z. M. (2009). Potential use of phosphate wastes as aggregates in road construction. *Journal of Engineering Sciences*, *37*, 413-422.

Ahmed, A. A. M., Abdel kareem, K. H., Altohamy, A. M., & Rizk, S. A. M. (2014). POTENTIAL USE OF MINES AND QUARRIES SOLID WASTE IN ROAD CONSTRUCTION AND AS REPLACEMENT SOIL UNDRE FOUNDATIONS. *JES. Journal of Engineering Sciences*, *42*(No 4), 1094-1105. https://doi.org/10.21608/jesaun.2014.115043

Aitchison, J. (1982). The statistical analysis of compositional data. *Journal of the Royal Statistical Society: Series B (Methodological)*, *44*(2), 139-160.

Alharshan, G., Eke, C., & Al-Buriahi, M. (2021). Radiation-transmission and self-absorption factors of P2O5 – SrO – Sb2O3 glass system. *Radiation Physics and Chemistry*, *193*, 109938. https://doi.org/10.1016/j.radphyschem.2021.109938

Aliyu, M. M., Shang, J., Murphy, W., Lawrence, J. A., Collier, R., Kong, F., & Zhao, Z. (2019). Assessing the uniaxial compressive strength of extremely hard cryptocrystalline flint. *International Journal of Rock Mechanics and Mining Sciences*, *113*, 310-321. https://doi.org/https://doi.org/10.1016/j.ijrmms.2018.12.002

Alkhraisat, M. H., Rueda, C., Cabrejos-Azama, J., Lucas-Aparicio, J., Mariño, F. T., Torres García-Denche, J., Jerez, L. B., Gbureck, U., & Cabarcos, E. L. (2010). Loading and release of doxycycline hyclate from strontium-substituted calcium phosphate cement. *Acta*

Biomaterialia, *6*(4), 1522-1528. https://doi.org/https://doi.org/10.1016/j.actbio.2009.10.043

Allen, E., & Iano, J. (2019). *Fundamentals of Building Construction: Materials and Methods*. John Wiley & Sons. https://books.google.co.ma/books?id=2HGqDwAAQBAJ&printsec=frontcover&hl=fr#v=onepage&q&f=false

Amar, H., Benzaazoua, M., Elghali, A., Hakkou, R., & Taha, Y. (2022). Waste rock reprocessing to enhance the sustainability of phosphate reserves: A critical review. *Journal of Cleaner Production*, *381*, 135151. https://doi.org/https://doi.org/10.1016/j.jclepro.2022.135151

Amar, H., Benzaazoua, M., Elghali, A., Taha, Y., El Ghorfi, M., Krause, A., & Hakkou, R. (2023). Mine waste rock reprocessing using sensor-based sorting (SBS): Novel approach toward circular economy in phosphate mining. *Minerals Engineering*, *204*, 108415.

Amara, A. (2014). *Pourquoi un nouveau code minier au Maroc? Pour attirer les investisseurs", selon Abdelkader Amara* [Interview]. Usine Nouvelle. https://www.usinenouvelle.com/article/pourquoi-un-nouveau-code-minier-au-maroc-pour-attirer-les-investisseurs-selon-abdelkader-amara.N273731

Amos, R. T., Blowes, D. W., Bailey, B. L., Sego, D. C., Smith, L., & Ritchie, A. I. M. (2015). Waste-rock hydrogeology and geochemistry. *Applied Geochemistry*, *57*, 140-156. https://doi.org/https://doi.org/10.1016/j.apgeochem.2014.06.020

Amrani, M., Taha, Y., El Haloui, Y., Benzaazoua, M., & Hakkou, R. (2020). Sustainable Reuse of Coal Mine Waste: Experimental and Economic Assessments for Embankments and Pavement Layer Applications in Morocco. *Minerals*, *10*(10). https://doi.org/10.3390/min10100851

Amrani, M., Taha, Y., Elghali, A., Benzaazoua, M., Kchikach, A., & Hakkou, R. (2021). An experimental investigation on collapsible behavior of dry compacted phosphate mine waste rock in road embankment. *Transportation Geotechnics*, *26*. https://doi.org/10.1016/j.trgeo.2020.100439

Amrani, M., Taha, Y., Kchikach, A., Benzaazoua, M., & Hakkou, R. (2019). Valorization of Phosphate Mine Waste Rocks as Materials for Road Construction. *Minerals*, *9*(4). https://doi.org/10.3390/min9040237

Annels, A. E. (1991). Mine Sampling. In A. E. Annels (Ed.), *Mineral Deposit Evaluation: A practical approach* (pp. 43-95). Springer Netherlands. https://doi.org/10.1007/978-94-011-9714-4_2

Argane, R., Benzaazoua, M., Hakkou, R., & Bouamrane, A. (2015). Reuse of base-metal tailings as aggregates for rendering mortars: Assessment of immobilization performances and environmental behavior. *Construction and Building Materials*, *96*, 296-306. https://doi.org/https://doi.org/10.1016/j.conbuildmat.2015.08.029

Argane, R., Benzaazoua, M., Hakkou, R., & Bouamrane, A. (2016). A comparative study on the practical use of low sulfide base-metal tailings as aggregates for rendering and masonry

mortars. *Journal of Cleaner Production*, *112*, 914-925. https://doi.org/https://doi.org/10.1016/j.jclepro.2015.06.004

Armstrong, A. (1965). Phosphorus. In Chemical Oceano¬graphy. *Academic Press London and NewYork*, *1*, 323-364.

Aubertin, M. (2013). Waste rock disposal to improve the geotechnical and geochemical stability of piles. World Mining Congress, Montreal, QC, Canada,

Aubertin, M., Bussière, B., Bernier, L., Chapuis, R., Julien, M., Belem, T., Simon, R., Mbonimpa, M., Benzaazoua, M., & Li, L. (2002, 5-8 June). *La gestion des rejets miniers dans un contexte de développement durable et de protection de l'environnement* Congrès annuel de la société canadienne de génie civil, Montréal, Québec, Canada,.

Aubineau, J., Parat, F., Elghali, A., Raji, O., Addou, A., Bonnet, C., Muñoz, M., Mauguin, O., Baron, F., Jouti, M. B., Yazami, O. K., & Bodinier, J.-L. (2022). Highly variable content of fluorapatite-hosted CO32−in the Upper Cretaceous/Paleogene phosphorites (Morocco) and implications for paleodepositional conditions. *Chemical Geology*, *597*, 120818. https://doi.org/https://doi.org/10.1016/j.chemgeo.2022.120818

Azadi, A., Esmatkhah Irani, A., Azarafza, M., Hajialilue Bonab, M., Sarand, F. B., & Derakhshani, R. (2022). Coupled Numerical and Analytical Stability Analysis Charts for an Earth-Fill Dam under Rapid Drawdown Conditions. *Applied Sciences*, *12*(9), 4550. https://www.mdpi.com/2076-3417/12/9/4550

Azarafza, M., Hajialilue Bonab, M., & Akgun, H. (2021). Numerical analysis and stability assessment of complex secondary toppling failures: A case study for the south pars special zone. *Geomechanics and Engineering*, *27*, 481-495. https://doi.org/10.12989/gae.2021.27.5.481

Bahhou, A., Taha, Y., El Khessaimi, Y., Idrissi, H., Hakkou, R., Amalik, J., & Benzaazoua, M. (2021a). Use of phosphate mine by-products as supplementary cementitious materials. *Materials Today: Proceedings*, *37*, 3781-3788. https://doi.org/https://doi.org/10.1016/j.matpr.2020.07.619

Bahhou, A., Taha, Y., Khessaimi, Y. E., Hakkou, R., Tagnit-Hamou, A., & Benzaazoua, M. (2021b). Using Calcined Marls as Non-Common Supplementary Cementitious Materials—A Critical Review. *Minerals*, *11*(5), 517. https://www.mdpi.com/2075-163X/11/5/517

Barcelo-Vidal, C., & Martín-Fernández, J.-A. (2016). The Mathematics of Compositional Analysis. *Austrian Journal of Statistics*, *45*(4), 57-71. https://doi.org/10.17713/ajs.v45i4.142

Bayoussef, A., Loutou, M., Taha, Y., Mansori, M., Benzaazoua, M., Manoun, B., & Hakkou, R. (2021b). Use of clays by-products from phosphate mines for the manufacture of sustainable lightweight aggregates. *Journal of Cleaner Production*, *280*, 124361. https://doi.org/https://doi.org/10.1016/j.jclepro.2020.124361

Bayoussef, A., Oubani, M., Loutou, M., Taha, Y., Benzaazoua, M., Manoun, B., & Hakkou, R. (2021a). Manufacturing of high-performance ceramics using clays by-product from

phosphate mines. *Materials Today: Proceedings*, *37*, 3994-4000. https://doi.org/https://doi.org/10.1016/j.matpr.2020.10.800

Benarchid, Y., Taha, Y., Argane, R., Tagnit-Hamou, A., & Benzaazoua, M. (2019). Concrete containing low-sulphide waste rocks as fine and coarse aggregates: Preliminary assessment of materials. *Journal of Cleaner Production*, *221*, 419-429. https://doi.org/https://doi.org/10.1016/j.jclepro.2019.02.227

Benzaazoua, M., Bussière, B., Dagenais, A. M., & Archambault, M. (2004). Kinetic tests comparison and interpretation for prediction of the Joutel tailings acid generation potential. Environmental Geology,

Bezzi, N., Aïfa, T., Hamoudi, S., & Merabet, D. (2012). Trace Elements of Kef Es Sennoun Natural Phosphate (Djebel Onk, Algeria) and how they Affect the Various Mineralurgic Modes of Treatment. *Procedia Engineering*, *42*, 1915-1927. https://doi.org/10.1016/j.proeng.2012.07.588

Bian, Z., Inyang, H. I., Daniels, J. L., Otto, F., & Struthers, S. (2010). Environmental issues from coal mining and their solutions. *Mining Science and Technology (China)*, *20*(2), 215-223. https://doi.org/https://doi.org/10.1016/S1674-5264(09)60187-3

Bishop, A. W. (1955). The use of the slip circle in the stability analysis of slopes. *Geotechnique*, *5*(1), 7-17.

Bossé, B., Bussière, B., Hakkou, R., Maqsoud, A., & Benzaazoua, M. (2013). Assessment of Phosphate Limestone Wastes as a Component of a Store-and-Release Cover in a Semiarid Climate. *Mine Water and the Environment*, *32*(2), 152-167. https://doi.org/10.1007/s10230-013-0225-9

Boujlel, H., Daldoul, G., Tlil, H., Souissi, R., Chebbi, N., Fattah, N., & Souissi, F. (2019). The beneficiation processes of low-grade sedimentary phosphates of tozeur-nefta deposit (Gafsa-metlaoui basin: South of Tunisia) [Article]. *Minerals*, *9*(1), Article 2. https://doi.org/10.3390/min9010002

Boujo, A. (1976). *Contribution à l'étude géologique du gisement de phosphate crétacé-éocène des Ganntour (Maroc occidental)* (Publication Number 43) Université Louis-Pasteur]. www.persee.fr. Strasbourg : Institut de Géologie https://www.persee.fr/doc/sgeol_0302-2684_1976_mon_43_1

Boumaza, B., Chekushina, T. V., Kechiched, R., Benabdeslam, N., Brahmi, L., Kucher, D. E., & Rebouh, N. Y. (2023). Environmental Geochemistry of Potentially Toxic Metals in Phosphate Rocks, Products, and Their Wastes in the Algerian Phosphate Mining Area (Tébessa, NE Algeria). *Minerals*, *13*(7), 853. https://www.mdpi.com/2075-163X/13/7/853

Boumaza, B., Chekushina, T. V., Vorobyev, K. A., & Schesnyak, L. E. (2021b). The heavy metal pollution in groundwater, surface and spring water in phosphorite mining area of Tebessa (Algeria). *Environmental Nanotechnology, Monitoring & Management*, *16*, 100591. https://doi.org/https://doi.org/10.1016/j.enmm.2021.100591

Boumaza, B., Kechiched, R., & Chekushina, T. V. (2021a). Trace metal elements in phosphate rock wastes from the Djebel Onk mining area (Tébessa, eastern Algeria): A geochemical study and environmental implications. *Applied Geochemistry*, *127*. https://doi.org/10.1016/j.apgeochem.2021.104910

Boumaza, B., Kechiched, R., Chekushina, T. V., Benabdeslam, N., Senouci, K., Hamitouche, A. y.-e., Merzeg, F. A., Rezgui, W., Rebouh, N. Y., & Harizi, K. (2024). Geochemical distribution and environmental assessment of potentially toxic elements in farmland soils, sediments, and tailings from phosphate industrial area (NE Algeria). *Journal of Hazardous Materials*, *465*, 133110. https://doi.org/https://doi.org/10.1016/j.jhazmat.2023.133110

Bouza, P. J., Simón, M., Aguilar, J., del Valle, H., & Rostagno, M. (2007). Fibrous-clay mineral formation and soil evolution in Aridisols of northeastern Patagonia, Argentina. *Geoderma*, *139*(1-2), 38-50. https://doi.org/10.1016/j.geoderma.2007.01.001

Bouzahzah, H., Benzaazoua, M., Plante, B., & Bussiere, B. (2015). A quantitative approach for the estimation of the "fizz rating" parameter in the acid-base accounting tests: A new adaptations of the Sobek test. *Journal of Geochemical Exploration*, *153*, 53-65. https://doi.org/https://doi.org/10.1016/j.gexplo.2015.03.003

Buccione, R., Kechiched, R., Mongelli, G., & Sinisi, R. (2021). REEs in the North Africa P-Bearing Deposits, Paleoenvironments, and Economic Perspectives: A Review. *Minerals*, *11*(2), 214. https://www.mdpi.com/2075-163X/11/2/214

Bueno, M., Foggiatto, B., & Lane, G. (2015). *Geometallurgy Applied in Comminution to Minimize Design Risks*.

Cai, F., & Ugai, K. (2001). Discussion: Slope stability analysis by finite elements. *Geotechnique*, *51*(7), 653-654. https://doi.org/10.1680/geot.2001.51.7.653

Cao, P., Chen, Y., Liu, M., & Chen, B. (2018). Optimal Design of Novel Drill Bit to Control Dust in Down-the-Hole Hammer Reverse Circulation Drilling. *Arabian Journal for Science and Engineering*, *43*(3), 1313-1324. https://doi.org/10.1007/s13369-017-2884-5

Chahi, A., Duplay, J., & Lucas, J. (1993). Analyses of palygorskites and associated clays from the jbel Rhassoul (Morocco) : chemical characteristics and origin of formation. *Clays clay miner*, *41*, 401-411.

Chlahbi, S., Belem, T., Elghali, A., Rochdane, S., Zerouali, E., Inabi, O., & Benzaazoua, M. (2023). Geological and Geomechanical Characterization of Phosphate Mine Waste Rock in View of Their Potential Civil Applications: A Case Study of the Benguerir Mine Site, Morocco. *Minerals*, *13*(10), 1291. https://www.mdpi.com/2075-163X/13/10/1291

Cissé, L., & Mrabet, T. (2004). Vol.World Phosphate Production: Overview and Prospects. *Phosphorus Research Bulletin 15* 21-25.

Collin, J. G., Leshchinsky, D., Hung, C. J. J., Parsons, B., Quade, Douglas, Institute, N. H., & Administration, U. S. F. H. (2005). *Soil Slope and Embankment Design: Reference Manual*. United States Department of Transportation, Federal Highway Administration, National Highway Institute. https://books.google.co.ma/books?id=ZfD1jgEACAAJ

da Silva, E. F., Mlayah, A., Gomes, C., Noronha, F., Charef, A., Sequeira, C., Esteves, V., & Marques, A. R. (2010). Heavy elements in the phosphorite from Kalaat Khasba mine (North-western Tunisia): potential implications on the environment and human health. *J Hazard Mater*, *182*(1-3), 232-245. https://doi.org/10.1016/j.jhazmat.2010.06.020

Dassamiour, M. (2012). *Eléments en traces et valorisation des minerais de phosphate du gisement de Kef Essennoun - Dj. Onk (Algérie Orientale)* [Thèse en Sciences, Université Badji Mokhtar Annaba].

Datamine. (2004). *Studio Wireframing : User Guide*

Davidovits, J. (2015). False values on CO2 emission for geopolymer cement/concrete published in scientific papers. *Technical paper*, *24*, 1-9.

Day, R. W. (2010). *Foundation engineering handbook: design and construction with the 2009 international building code*. McGraw-Hill Education.

Deconinck, J.-F., Brigaud, B., & Pellenard, P. (2016). *Pétrographie et environnements sédimentaires*. https://international-scholarvox-com.eressources.um6p.ma/reader/docid/88875313/page/55?searchterm=p%C3%A9trographie%20et%20environnements%20s%C3%A9dimentaires

Deere, D. U. (1964). Technical description of rock cores for engineering purpose. *Rock Mechanics and Engineering Geology*, *1*(1), 17-22.

Deere, D. U., Hendron, A. J., Patton, F. D., & Cording, E. J. (1967). Design of surface and near-surface construction in rock

in Failure and breakage of rock, C. Fairhurst, Ed, So-ciety of Mining Engineers of AIME, New York, 237-302. .

Delgado Vega, J. M. (2012). *Apport des modèles géo-métallurgiques et de la catégorisation des ressources à la définition de la fosse ultime d'une mine à ciel ouvert : Application à la mine de cuivre de Mantos de la Luna au Chili* [Thèse, École nationale supérieure des mines de Paris]. https://pastel.archives-ouvertes.fr/pastel-00858806

Derakhshanalavijeh, R., & Teixeira, J. M. C. (2017). Cost overrun in construction projects in developing countries, gas-oil industry of Iran as a case study. *Journal of Civil Engineering and Management*, *23*(1), 125-136.

Desharnais, G. (2019). Manuel Bustillo Revuelta: Mineral resources, from exploration to sustainability assessment, first edition. Earth sciences, textbook geography and environment Springer, (2019), 653 p. *Mineralium Deposita*, *54*(8), 1281-1283. https://doi.org/10.1007/s00126-019-00901-8

Dixon, D. E., Prestrera, J. R., Burg, G., Chairman, S. A., Abdun-Nur, E. A., Barton, S. G., Bell, L. W., Blas Jr, S. J., Carrasquillo, R. L., & Carrasquillo, P. M. (1991). Standard practice for selecting proportions for normal, heavyweight, and mass concrete (ACI 211.1-91). *Farmington Hills: ACI*.

Djellal, S., Guendouzen, S., & Malek, N. (2015). *Valorisation de rejet de minerai de phosphate noir de gisement de kef Es Sennoun de la mine de Djebel Onk (Tebéssa-Algérie) dans l'élaboration d'une biocéramique*.

Downing, B., Sc, M., & Geo, P. (1999). ARD sampling and sample preparation. In: Enviromine website, http://www. enviromine. com/ard.

Dunham, R. J. (1962). Classification of Carbonate Rocks According to Depositional Texture in Classification of Carbonate Rockes. . *Sympo AAPG.*

Durante Ingunza, M. d. P., dos Santos Júnior, O. F., & Gerab, A. T. F. d. S. C. (2020). Potential Use of Sandy Mining Wastes as Raw Material in Road Construction. *Geotechnical and Geological Engineering*, *38*(5), 5681-5691. https://doi.org/10.1007/s10706-020-01382-7

EFMA. (2000). Phosphorus: essential element for food production. *European Fertilizer Manufacturers Association (EFMA), Brussels*, 9-10.

Egozcue, J. J., Gozzi, C., Buccianti, A., & Pawlowsky-Glahn, V. (2024). Exploring geochemical data using compositional techniques: A practical guide. *Journal of Geochemical Exploration*, *258*, 107385. https://doi.org/https://doi.org/10.1016/j.gexplo.2024.107385

El Bamiki, R. (2020a). *Étude géologique des occurrences phosphatées du Haut-Atlas marocain : Compréhension des contrôles géologiques sur l'accumulation du phosphate* Université de Montpellier].

El Bamiki, R. (2020b). *Étude géologique des occurrences phosphatées du Haut-Atlas Marocain: Compréhension des contrôles géologiques sur l'accumulation du phosphate* Université Montpellier; Université Cadi Ayyad (Marrakech, Maroc)].

El Bamiki, R., Raji, O., Ouabid, M., Elghali, A., Khadiri Yazami, O., & Bodinier, J.-L. (2021). Phosphate Rocks: A Review of Sedimentary and Igneous Occurrences in Morocco. *Minerals*, *11*(10). https://doi.org/10.3390/min11101137

El Bamiki, R., Séranne, M., Parat, F., Aubineau, J., Chellaï, E. H., Marzoqi, M., & Bodinier, J.-L. (2023). Post-phosphogenesis processes and the natural beneficiation of phosphates: Geochemical evidence from the Moroccan High Atlas phosphate-rich sediments. *Chemical Geology*, *631*, 121523. https://doi.org/https://doi.org/10.1016/j.chemgeo.2023.121523

El Ghorfi, M., Inabi, O., Amar, H., Taha, Y., Elghali, A., Hakkou, R., & Benzaazoua, M. (2024). Design and Implementation of Sampling Wells in Phosphate Mine Waste Rock Piles: Towards an Enhanced Composition Understanding and Sustainable Reclamation. *Minerals*, *14*(3), 286. https://www.mdpi.com/2075-163X/14/3/286

El Haddi, H. (2014). *Les silicifications de la série phosphatée des Ouled Abdoun (Maastrichtien-Lutétien, Maroc) : Sédimentologie, Minéralogie, Géochimie et Contexte Génétique*

(Publication Number CED/101/14) [Thèse de Doctorat en Géologie, Université Hassan II de Casablanca, Faculté des Sciences Ben M'Sik].

El Machi, A., Mabroum, S., Taha, Y., Tagnit-Hamou, A., Benzaazoua, M., & Hakkou, R. (2021). Use of flint from phosphate mine waste rocks as an alternative aggregates for concrete.

Construction and Building Materials, *271*, 121886. https://doi.org/https://doi.org/10.1016/j.conbuildmat.2020.121886

El Machi, A., Mabroum, S., Taha, Y., Tagnit-Hamou, A., Benzaazoua, M., & Hakkou, R. (2021a). Use of flint from phosphate mine waste rocks as an alternative aggregates for concrete. *Construction and Building Materials*, *271*. https://doi.org/10.1016/j.conbuildmat.2020.121886

El Machi, A., Mabroum, S., Taha, Y., Tagnit-Hamou, A., Benzaazoua, M., & Hakkou, R. (2021b). Valorization of phosphate mine waste rocks as aggregates for concrete. *Materials Today: Proceedings*, *37*, 3840-3846.

Elghali, A., Benzaazoua, M., Bouzahzah, H., Bussière, B., & Villarraga-Gómez, H. (2018). Determination of the available acid-generating potential of waste rock, part I: Mineralogical approach. *Applied Geochemistry*, *99*, 31-41. https://doi.org/https://doi.org/10.1016/j.apgeochem.2018.10.021

Elghali, A., Benzaazoua, M., Bussière, B., & Bouzahzah, H. (2019). Determination of the available acid-generating potential of waste rock, part II: Waste management involvement. *Applied Geochemistry*, *100*, 316-325. https://doi.org/https://doi.org/10.1016/j.apgeochem.2018.12.010

Elghali, A., Benzaazoua, M., Couvidat, J., Taha, Y., Darricau, L., Neculita, C. M., & Chatain, V. (2022). Chapter 7 - Stabilization/solidification of sediments: challenges and novelties. In D. C. W. Tsang & L. Wang (Eds.), *Low Carbon Stabilization and Solidification of Hazardous Wastes* (pp. 93-112). Elsevier. https://doi.org/https://doi.org/10.1016/B978-0-12-824004-5.00023-2

Elghali, A., Benzaazoua, M., Taha, Y., Amar, H., Ait-khouia, Y., Bouzahzah, H., & Hakkou, R. (2023). Prediction of acid mine drainage: Where we are. *Earth-Science Reviews*, *241*, 104421. https://doi.org/https://doi.org/10.1016/j.earscirev.2023.104421

Elgillani, D. A., & Abouzeid, A. Z. M. (1993). Flotation of carbonates from phosphate ores in acidic media. *International Journal of Mineral Processing*, *38*(3), 235-256. https://doi.org/https://doi.org/10.1016/0301-7516(93)90077-N

Eliche-Quesada, D., Azevedo-Da Cunha, R., & Corpas-Iglesias, F. A. (2015). Effect of sludge from oil refining industry or sludge from pomace oil extraction industry addition to clay ceramics. *Applied Clay Science*, *114*, 202-211. https://doi.org/https://doi.org/10.1016/j.clay.2015.06.009

Embry, A. F., & Klovan, J. E. (1971). A Late Devonian reef tract on northeastern Banks Island, NWT. *Bulletin of Canadian petroleum geology*, *19*(4), 730-781.

Environment, U., Scrivener, K. L., John, V. M., & Gartner, E. M. (2018). Eco-efficient cements: Potential economically viable solutions for a low-CO2 cement-based materials industry. *Cement and concrete research*, *114*, 2-26.

Estabragh, A. R., Javadi, A. A., & Boot, J. C. (2004). Effect of compaction pressure on consolidation behaviour of unsaturated silty soil [Article]. *Canadian Geotechnical Journal*, *41*(3), 540-550. https://doi.org/10.1139/T04-007

Ettoumi, M. (2020). *Les boues phosphatées rejetées par les laveries de la compagnie de phosphate Gafsa : Récupération et recyclage des eaux et essais de valorisation* [Thèse de Doctorat en Géologie, Unoversité de Tunis El Manar, Faculté des Sciences de Tunis].

Farid, A. T. M. (2013). Modified Value of Rock Quality Designation Index RQD in Rock Formation. International Conference on Case Histories in Geotechnical Engineering. 1, Chicago, Illinois.

Filzmoser, P., Hron, K., & Reimann, C. (2010). The bivariate statistical analysis of environmental (compositional) data. *Science of The Total Environment*, *408*(19), 4230-4238. https://doi.org/https://doi.org/10.1016/j.scitotenv.2010.05.011

Garnit, H., Bouhlel, S., & Jarvis, I. (2017). Geochemistry and depositional environments of Paleocene–Eocene phosphorites: Metlaoui Group, Tunisia. *Journal of African Earth Sciences*, *134*, 704-736. https://doi.org/https://doi.org/10.1016/j.jafrearsci.2017.07.021

Giraud, J., Pamart, P., & Riverain, J. (1971). *Les mots «dans le vent»* (Vol. 5).

GMTR. (2002). *Guide Marocain pour les Terrassements Routier. Direction des Routes et de la Circulation Routière. Fasci-cule 1; Ministère de l'Equipement: Rabat, Royaume du Maroc*.

Göktepe, F., & Keskin, I. (2018). A Comparison Study between Traditional and Finite Element Methods for Slope Stability Evaluations. *Journal of the Geological Society of India*, *91*(3), 373-379. https://doi.org/10.1007/s12594-018-0864-3

Guo, F., & Li, J. (2010). Separation strategies for Jordanian phosphate rock with siliceous and calcareous gangues. *International Journal of Mineral Processing*, *97*(1), 74-78. https://doi.org/https://doi.org/10.1016/j.minpro.2010.08.006

Guo, Y., Zhang, Y., Huang, H., Meng, K., Hu, K., Hu, P., Wang, X., Zhang, Z., & Meng, X. (2014). Novel glass ceramic foams materials based on red mud. *Ceramics International*, *40*(5), 6677-6683. https://doi.org/https://doi.org/10.1016/j.ceramint.2013.11.128

Hakkou, R., Benzaazoua, M., & Bussière, B. (2008). Acid Mine Drainage at the Abandoned Kettara Mine (Morocco): 1. Environmental Characterization. *Mine Water and the Environment*, *27*(3), 145-159. https://doi.org/10.1007/s10230-008-0036-6

Hakkou, R., Benzaazoua, M., & Bussière, B. (2009). Laboratory Evaluation of the Use of Alkaline Phosphate Wastes for the Control of Acidic Mine Drainage. *Mine Water and the Environment*, *28*(3), 206-218. https://doi.org/10.1007/s10230-009-0081-9

Hakkou, R., Benzaazoua, M., & Bussière, B. (2016). Valorization of Phosphate Waste Rocks and Sludge from the Moroccan Phosphate Mines: Challenges and Perspectives. *Procedia Engineering*, *138*, 110-118. https://doi.org/10.1016/j.proeng.2016.02.068

Hammersley, J. M., & Handscomb, D. (1964). Monte Carlo Methods.

Hanein, T., Thienel, K.-C., Zunino, F., Marsh, A. T. M., Maier, M., Wang, B., Canut, M., Juenger, M. C. G., Ben Haha, M., Avet, F., Parashar, A., Al-Jaberi, L. A., Almenares-Reyes, R. S., Alujas-Diaz, A., Scrivener, K. L., Bernal, S. A., Provis, J. L., Sui, T., Bishnoi, S., & Martirena-Hernández, F. (2021). Clay calcination technology: state-of-the-art review by the

RILEM TC 282-CCL. *Materials and Structures*, *55*(1), 3. https://doi.org/10.1617/s11527-021-01807-6

Hasan, B. M. S., & Abdulazeez, A. M. (2021). A review of principal component analysis algorithm for dimensionality reduction. *Journal of Soft Computing and Data Mining*, *2*(1), 20-30.

Hazen, A. (1914). Storage to be provided in impounding municipal water supply. *Transactions of the American society of civil engineers*, *77*(1), 1539-1640.

He, C., Osbaeck, B., & Makovicky, E. (1995). Pozzolanic reactions of six principal clay minerals: activation, reactivity assessments and technological effects. *Cement and concrete research*, *25*(8), 1691-1702.

Hussain, M., Amao, A. O., Al-Ramadan, K., Negara, A., & Saleh, T. A. (2020). Non-destructive techniques for linking methodology of geochemical and mechanical properties of rock samples. *Journal of Petroleum Science and Engineering*, *195*. https://doi.org/10.1016/j.petrol.2020.107804

Idrissi, H., Taha, Y., Elghali, A., El Khessaimi, Y., Aboulayt, A., Amalik, J., Hakkou, R., & Benzaazoua, M. (2021). Sustainable use of phosphate waste rocks: From characterization to potential applications. *Materials Chemistry and Physics*, *260*. https://doi.org/10.1016/j.matchemphys.2020.124119

Inabi, O., Attou, M., Benzaazoua, M., & Qachar, M. (2023). Design of Cost-Effective and Sustainable Treatments of Old Landslides Adapted to the Moroccan Road Network: A Case Study of Regional Road R410 Crossing the Rifan Structural Domain. *Water*, *15*(13), 2423.

Jacob, H. L., Paré, C., & Hébert, Y. (1990). *Les phosphates au Québec* (MB 90 - 22, Issue. http://gq.mines.gouv.qc.ca/documents/examine/MB9022/MB9022.pdf

Jarvis, I. (1994). Phosphorite geochemistry: state-of-the-art and environmental concerns. *Eclogae Geologicae Helvetiae*, *87*, 643-700.

Jasinski, S. M. (2020). Mineral commodity summaries: Phosphate Rock. *U.S. Geol. Surv.*, *705*, 122–123.

Jasinski, S. M. (2022). Mineral commodity summaries: Phosphate Rock. *U.S. Geological Survey*.

Jiang, L.-g., Liang, B., Xue, Q., & Yin, C.-w. (2016). Characterization of phosphorus leaching from phosphate waste rock in the Xiangxi River watershed, Three Gorges Reservoir, China. *Chemosphere*, *150*, 130-138. https://doi.org/https://doi.org/10.1016/j.chemosphere.2016.02.008

Johnston, I., Murphy, W., & Holden, J. (2021). A review of floodwater impacts on the stability of transportation embankments. *Earth-Science Reviews*, *215*, 103553. https://doi.org/https://doi.org/10.1016/j.earscirev.2021.103553

Jong, T., & Parry, D. L. (2005). Evaluation of the stability of arsenic immobilized by microbial sulfate reduction using TCLP extractions and long-term leaching techniques. *Chemosphere*, *60*(2), 254-265. https://doi.org/https://doi.org/10.1016/j.chemosphere.2004.12.046

Joosu, L., Lepland, A., Kirsimäe, K., Romashkin, A. E., Roberts, N. M. W., Martin, A. P., & Črne, A. E. (2015). The REE-composition and petrography of apatite in 2Ga Zaonega Formation,

Russia: The environmental setting for phosphogenesis. *Chemical Geology*, *395*, 88-107. https://doi.org/10.1016/j.chemgeo.2014.11.013

Jouini, M., Benzaazoua, M., Neculita, C. M., & Genty, T. (2020). Performances of stabilization/solidification process of acid mine drainage passive treatment residues: Assessment of the environmental and mechanical behaviors. *Journal of Environmental Management*, *269*, 110764. https://doi.org/https://doi.org/10.1016/j.jenvman.2020.110764

Jouini, M., Rakotonimaro, T. V., Neculita, C. M., Genty, T., & Benzaazoua, M. (2019). Prediction of the environmental behavior of residues from the passive treatment of acid mine drainage. *Applied Geochemistry*, *110*, 104421. https://doi.org/https://doi.org/10.1016/j.apgeochem.2019.104421

Kawatra, S. K., & Carlson, J. T. (2013). *Beneficiation of Phosphate Ore*. Society for Mining, Metallurgy, and Exploration. https://books.google.co.ma/books?id=f_BIAgAAQBAJ

Kazakov, A. V. (1937). *The phosphate facies: origin of the phosphorite and the geologic factors of formation of the deposits* (Vol. 145).

Kechiched, R., Laouar, R., Bruguier, O., Salmi-Laouar, S., Kocsis, L., Bosch, D., Foufou, A., Ameur-Zaimeche, O., & Larit, H. (2018). Glauconite-bearing sedimentary phosphorites from the Tébessa region (eastern Algeria): Evidence of REE enrichment and geochemical constraints on their origin. *Journal of African Earth Sciences*, *145*, 190-200. https://doi.org/10.1016/j.jafrearsci.2018.05.018

Keyser, F., & Cook, P. J. (1972). Geology of the Middle Cambrian Phosphorites and Associated Sediments of Northwestern Queensland. *Dep. of Nation. Development, Bur. Minera. Res. Geol. Geophys. Bull. Canberra*, *138*.

Khalil, A., Hanich, L., Bannari, A., Zouhri, L., Pourret, O., & Hakkou, R. (2013). Assessment of soil contamination around an abandoned mine in a semi-arid environment using geochemistry and geostatistics: Pre-work of geochemical process modeling with numerical models. *Journal of Geochemical Exploration*, *125*, 117-129. https://doi.org/10.1016/j.gexplo.2012.11.018

Khan, N. M., Ali, I., & Ullah, H. (2019). Phosphate rock upgradation by combination of shaking table and high intensity magnetic separator: Ghari Habibullah, Pakistan. *Journal of Applied and Emerging Sciences*, *8*(2), pp118-123.

Khelifi, F., Besser, H., Ayadi, Y., Liu, G., Yousaf, B., Harabi, S., Bedoui, S., Zighmi, K., & Hamed, Y. (2019). Evaluation of potentially toxic elements' (PTEs) vertical distribution in sediments of Gafsa–Metlaoui mining basin (Southwestern Tunisia) using geochemical and multivariate statistical analysis approaches. *Environmental Earth Sciences*, *78*(2), 53. https://doi.org/10.1007/s12665-019-8048-z

Khelifi, F., Caporale, A. G., Hamed, Y., & Adamo, P. (2021). Bioaccessibility of potentially toxic metals in soil, sediments and tailings from a north Africa phosphate-mining area: Insight into human health risk assessment. *Journal of Environmental Management*, *279*, 111634. https://doi.org/https://doi.org/10.1016/j.jenvman.2020.111634

Khelifi, F., Melki, A., Hamed, Y., Adamo, P., & Caporale, A. G. (2020). Environmental and human health risk assessment of potentially toxic elements in soil, sediments, and ore-processing wastes from a mining area of southwestern Tunisia. *Environmental Geochemistry and Health*, *42*(12), 4125-4139. https://doi.org/10.1007/s10653-019-00434-z

Kiser, C. D., & Kolay, P. K. (2013). Embankment Slope Stability Analysis of Dwight Mission Mine Site Reclamation Project.

Knidiri, J., Bussière, B., Hakkou, R., Benzaazoua, M., Parent, E., & Maqsoud, A. (2015). Design, construction and preliminary results for an inclined store-and-release cover experimental cell built on an abandoned mine site in Morocco. Proceeding for the 10th ICARD, International Conference on Acid Rock Drainage, and IMWA, International Mine Water Association,

Kocsis, L., Gheerbrant, E., Mouflih, M., Cappetta, H., Ulianov, A., Chiaradia, M., & Bardet, N. (2016). Gradual changes in upwelled seawater conditions (redox, pH) from the late Cretaceous through early Paleogene at the northwest coast of Africa: Negative Ce anomaly trend recorded in fossil bio-apatite. *Chemical Geology*, *421*, 44-54. https://doi.org/https://doi.org/10.1016/j.chemgeo.2015.12.001

Kocsis, L., Ulianov, A., Mouflih, M., Khaldoune, F., & Gheerbrant, E. (2021). Geochemical investigation of the taphonomy, stratigraphy, and palaeoecology of the mammals from the Ouled Abdoun Basin (Paleocene-Eocene of Morocco). *Palaeogeography, Palaeoclimatology, Palaeoecology*, *577*, 110523. https://doi.org/https://doi.org/10.1016/j.palaeo.2021.110523

Kosson, D. S., van der Sloot, H. A., Sanchez, F., & Garrabrants, A. C. (2002). An integrated framework for evaluating leaching in waste management and utilization of secondary materials. *Environmental engineering science*, *19*(3), 159-204.

Krishna, R. S., Mishra, J., Meher, S., Das, S. K., Mustakim, S. M., & Singh, S. K. (2020). Industrial solid waste management through sustainable green technology: Case study insights from steel and mining industry in Keonjhar, India. *Materials Today: Proceedings*, *33*, 5243-5249. https://doi.org/10.1016/j.matpr.2020.02.949

Król, A., Mizerna, K., & Bożym, M. (2020). An assessment of pH-dependent release and mobility of heavy metals from metallurgical slag. *Journal of Hazardous Materials*, *384*, 121502. https://doi.org/https://doi.org/10.1016/j.jhazmat.2019.121502

Kynčlová, P., Hron, K., & Filzmoser, P. (2017). Correlation Between Compositional Parts Based on Symmetric Balances. *Mathematical Geosciences*, *49*(6), 777-796. https://doi.org/10.1007/s11004-016-9669-3

Labaronne, D. (2015). Chapitre 3. La place d'OCP dans l'économie marocaine et son rôle dans la sécurité alimentaire mondiale. In *Donner du sens à la recherche de performances* (pp. 65-90). EMS Editions. https://www.cairn.info/donner-du-sens-a-la-recherche-de-performances--9782847696981-page-65.htm

https://www.cairn.info/load_pdf.php?ID_ARTICLE=EMS_LABAR_2015_01_0065

Lahmira, B., Lefebvre, R., Aubertin, M., & Bussière, B. (2016). Effect of heterogeneity and anisotropy related to the construction method on transfer processes in waste rock piles. *Journal of Contaminant Hydrology*, *184*, 35-49. https://doi.org/https://doi.org/10.1016/j.jconhyd.2015.12.002

Lèbre, É., & Corder, G. (2015). Integrating Industrial Ecology Thinking into the Management of Mining Waste. *Resources*, *4*(4), 765-786. https://www.mdpi.com/2079-9276/4/4/765

Ledin, M., & Pedersen, K. (1996). The environmental impact of mine wastes — Roles of microorganisms and their significance in treatment of mine wastes. *Earth-Science Reviews*, *41*(1), 67-108. https://doi.org/https://doi.org/10.1016/0012-8252(96)00016-5

Lee, C., & Gu, F. (2017, 11-13 October). *Co-disposal of waste rock with backfill* UMT 2017: Proceedings of the First International Conference on Underground Mining Technology, Sudbury. https://papers.acg.uwa.edu.au/p/1710_27_Lee/

Li, Y., Richardson, J. B., Walker, A. K., & Yuan, P.-C. (2006). TCLP Heavy Metal Leaching of Personal Computer Components. *Journal of Environmental Engineering*, *132*(4), 497-504. https://doi.org/doi:10.1061/(ASCE)0733-9372(2006)132:4(497)

Lishchuk, V. (2019). *Bringing predictability into a geometallurgical program : An iron ore case study* [Doctoral thesis, comprehensive summary, Luleå University of Technology]. DiVA. Luleå. http://urn.kb.se/resolve?urn=urn:nbn:se:ltu:diva-71580

Liu, G., Li, L., Yao, M., Landry, D., Malek, F., Yang, X., & Guo, L. (2017). An Investigation of the Uniaxial Compressive Strength of a Cemented Hydraulic Backfill Made of Alluvial Sand. *Minerals*, *7*(1), 4. https://www.mdpi.com/2075-163X/7/1/4

Liu, Q., Wang, X., Gao, M., Guan, Y., Wu, C., Wang, Q., Rao, Y., & Liu, S. (2022). Heavy metal leaching behaviour and long-term environmental risk assessment of cement-solidified municipal solid waste incineration fly ash in sanitary landfill. *Chemosphere*, *300*, 134571. https://doi.org/https://doi.org/10.1016/j.chemosphere.2022.134571

Liu, X., Zhang, Y., Liu, T., Cai, Z., Chen, T., & Sun, K. (2016). Beneficiation of a Sedimentary Phosphate Ore by a Combination of Spiral Gravity and Direct-Reverse Flotation. *Minerals*, *6*(2), 38. https://www.mdpi.com/2075-163X/6/2/38

Loutou, M., Hajjaji, M., Mansori, M., Favotto, C., & Hakkou, R. (2013). Phosphate sludge: thermal transformation and use as lightweight aggregate material. *J Environ Manage*, *130*, 354-360. https://doi.org/10.1016/j.jenvman.2013.09.004

Loutou, M., Hajjaji, M., Mansori, M., Favotto, C., & Hakkou, R. (2016). Heated blends of phosphate waste: Microstructure characterization, effects of processing factors and use as a phosphorus source for alfalfa growth. *J Environ Manage*, *177*, 169-176. https://doi.org/10.1016/j.jenvman.2016.04.030

Loutou, M., Taha, Y., Benzaazoua, M., Daafi, Y., & Hakkou, R. (2019). Valorization of clay by-product from moroccan phosphate mines for the production of fired bricks. *Journal of Cleaner Production*, *229*, 169-179. https://doi.org/10.1016/j.jclepro.2019.05.003

Mabroum, S., Aboulayt, A., Taha, Y., Benzaazoua, M., Semlal, N., & Hakkou, R. (2020). Elaboration of geopolymers based on clays by-products from phosphate mines for

construction applications. *Journal of Cleaner Production*, *261*. https://doi.org/10.1016/j.jclepro.2020.121317

Maknoon, M., & Aubertin, M. (2021). On the Use of Bench Construction to Improve the Stability of Unsaturated Waste Rock Piles. *Geotechnical and Geological Engineering*, *39*, 1-25. https://doi.org/10.1007/s10706-020-01567-0

Malaoui, R., Soltani, M. R., Djellali, A., Soukeur, A., & Kechiched, R. (2023). Geotechnical Characterization of Phosphate Mining Waste Materials for Use in Pavement Construction. *Engineering, Technology & Applied Science Research*, *13*(1), 10005-10013.

Mallet, J. L. (2002). *Geomodeling*.

Mamat, R. C., Kasa, A., & Razali, S. F. M. (2019). A review of road embankment stability on soft ground: problems and future perspective. *IIUM Engineering Journal*, *20*(2), 32-56.

Mar, S. S., & Okazaki, M. (2012). Investigation of Cd contents in several phosphate rocks used for the production of fertilizer. *Microchemical Journal*, *104*, 17-21. https://doi.org/https://doi.org/10.1016/j.microc.2012.03.020

Marjoribanks, R. (2010). Drilling: A General Discussion the Importance of Drilling. In R. Marjoribanks (Ed.), *Geological Methods in Mineral Exploration and Mining* (pp. 75-84). Springer Berlin Heidelberg. https://doi.org/10.1007/978-3-540-74375-0_5

MDDELCC, M. d. D. D., de l'Environnement et Lutte Contre les Changements Climatiques. (2013). *Ministère du Développement Durable, de l'Environnement et Lutte Contre les Changements*

Climatiques. Critère de qualité de l'eau de surface. Direction de suivi de l'état de l'environnement. Bibliothèque et Archives Nationales du Québec, QC, Canada, 510p.

Mehahad, M. S., & Bounar, A. (2020). Phosphate mining, corporate social responsibility and community development in the Gantour Basin, Morocco. *The Extractive Industries and Society*, *7*(1), 170-180. https://doi.org/10.1016/j.exis.2019.11.016

loi n°33-13 relative aux mines, 3275-3286 (2015).

Memon, Y. (2018). *A Comparison Between Limit Equilibrium and Finite Element Methods for Slope Stability Analysis*. https://doi.org/10.13140/RG.2.2.16932.53124

Merchichi, A., Hamou, M. O., Edahbi, M., Bobocioiu, E., Neculita, C. M., & Benzaazoua, M. (2021). Passive treatment of acid mine drainage from the Sidi-Kamber mine wastes (Mediterranean coastline, Algeria) using neighbouring phosphate material from the Djbel Onk mine. *Sci Total Environ*, 151002. https://doi.org/10.1016/j.scitotenv.2021.151002

Michard, A. (1976). *Eléments de géologie marocaine*.

Michaux, S., & O'Connor, L. (2019). *How to Set Up and Develop a Geometallurgical Program* (Geologian tutkimuskeskus, Issue.

Miller, S., Jeffery, J., & Wong, J. (1991). Use and misuse of the acid base account for "AMD" prediction. Proceedings of the 2nd International Conference on the Abatement of Acidic Drainage, Montréal, Que,

Ministère de l'Environnement. (2002). *Guide de valorisation des matières résiduelles inorganiques non dangereuses de source industrielle comme matériau de construction.* Québec, Canada Retrieved from https://www.environnement.gouv.qc.ca/matieres/mat_res/inorganique/index.htm

Ministre de la Transition Energétique et du Développement Durable. (2021). *Mines*. https://www.mem.gov.ma/Pages/secteur.aspx?e=7

Mohamed Ali, M., & Yang, H.-S. (2014). A study of some Egyptian carbonate rocks for the building construction industry. *International Journal of Mining Science and Technology*, *24*. https://doi.org/10.1016/j.ijmst.2014.05.008

Moody, R. T. J. (2002). PIQUÉ, A. 2001. Geology of Northwest Africa. Beiträge zur Regionalen Geologie der Erde, Vol. 29. Translated by M. S. N. Carpenter. xiv+310 pp. Berlin, Stuttgart: Gebrüder Borntraeger. Price Euros 86.00 (hard covers). ISBN 3 443 11029 0. *Geological Magazine*, *139*(5), 595-598. https://doi.org/10.1017/S0016756802257118

Moon, G. D., Oh, S., Jung, S. H., & Choi, Y. C. (2017). Effects of the fineness of limestone powder and cement on the hydration and strength development of PLC concrete. *Construction and Building Materials*, *135*, 129-136.

Mori, T., Tobita, Y., & Okimura, T. (2012). The damage to hillside embankments in Sendai city during The 2011 off the Pacific Coast of Tohoku Earthquake. *Soils and Foundations*, *52*(5), 910-928. https://doi.org/https://doi.org/10.1016/j.sandf.2012.11.011

Morin, K. A., & Hutt, N. M. (2001). *Environmental geochemistry of minesite drainage: Practical theory and case studies, Digital Edition*. MDAG Publishing (www. mdag. com), Surrey, British Columbia.

Mouflih, M. (2015). *Les phosphates du maroc central et du moyen atlas (maastrichtien-lutetien, maroc) : Sedimentologie, stratigraphie sequentielle, contexte genetique et valorisation* Universite Cadi Ayyad].

Mouih, K., Hakkou, R., Taha, Y., & Benzaazoua, M. (2023b). Performances of compressed stabilized bricks using phosphate waste rock for sustainable construction. *Construction and Building Materials*, *388*, 131577. https://doi.org/https://doi.org/10.1016/j.conbuildmat.2023.131577

Mouih, K., Taha, Y., Benzaazoua, M., & Hakkou, R. (2023a). Valorization of phosphate waste rocks for the production of compressed stabilized earth bricks using cement stabilizer. *Materials Today: Proceedings*. https://doi.org/https://doi.org/10.1016/j.matpr.2023.03.224

NAVFAC, N. F. E. C. (1982). *Soil mechanics: Design manual 7.1*. Dept. of the Navy Alexandria, VA.

Negm, A. A., & Abouzeid, A. Z. M. (2008). UTILIZATION OF SOLID WASTES FROM PHOSPHATE PROCESSING PLANTS. *Physicochemical Problems of Mineral Processing*, *42*, 5-16.

Nen, E., . 7375:2004 (2004). Leaching characteristics of moulded or monolithic building and waste materials. Determination of leaching of inorganic

components with the diffusion test, NNIS (Netherlands Normalisation Institute Standard). In.

NF-P11-300. (1992). Exécution des Terrassements—Classification des Matériaux Utilisables dans la Construction des Remblais et des Couches de Forme d'infrastructures Routières. In *Association Française de Normalisation: Paris, France.*

NF-P94-051. (1993). Soil: Investigation and Testing. Determination of Atterberg's Limits. Liquid Limit Test Using Cassagrande Apparatus. Plastic Limit Test on Rolled Thread—Sols: Reconnaissance et Essais; Association Française de Normalisation: Paris, France. In.

NF-P94-052-1. (1995). Soil: Investigation and Testing. Atterberg Limit Determination. Part 1: Liquid Limit. Cone Penetrometer Method—Sols: Reconnaissance et essais. In: Association Française de Normalisation Paris, France.

NF EN 933–8+A1. (2015). Tests for geometrical properties of aggregates - Part 8 : assessment of fines - Sand equivalent test. In.

NF EN 1097-1. (2011). Tests for mechanical and physical properties of aggregates - Part 1 : determination of the resistance to wear (micro-Deval). In.

NF EN 12620. (2008). Aggregates for concrete. In.

NF EN ISO 17892-9. (2018). Geotechnical investigation and testing - Laboratory testing of soil - Part 9: consolidated triaxial compression tests on water saturated soils, French standard, AFNOR Editions. France. In.

NF P94-066. (1992). Soils: Investigation and Tests. Fragmentability Coefficient of Rocky Material—Sols: Reconnaissance et

essais; Association Française de Normalisation: Paris, France. In.

NF P94-067. (1992). Soils: Investigation and Tests. Degradability Coefficient of ROCKY material—Sols: Reconnaissance et

essais; Association Française de Normalisation: Paris, France. In.

NF P94-410-1. (2001). Rock - Test for physical properties of rock - Part 1 : determination of water content of rock - Oven-drying method. In.

NF P94-410-2. (2001). Rock - Tests for physical properties of rock - Part 2 : determination of density - Cutting curb - Water immersion methods. In.

NF P94-410-3. (2001). Rock - Tests for physical properties of rock - Part 3 : determination of porosity. In.

NF P94-420. (2000). Rock - Determination of the uniaxial compressive strength. In.

NF P 94-056. (1996). Soil: Investigation and Testing–Granulometric Analysis–Dry Sieving Method After Washing. *AFNOR, Paris, France*.

Niederreiter, H. (1992). *Random number generation and quasi-Monte Carlo methods*. SIAM.

NM00.8.083. (2015). Soils: recognition and test of granulometric analysis of soils sedimentation method. In: IMANOR.

NM00.8.095. (2015). Soils: Investigation and Testing. Measuring of the Methylene Blue Adsorption Capacity of à Rocky Soil. Determination of the Methylene Blue of à Soil by Means of the Stain test. In.

NM13.1.008. (1998). Granulometric Analysis. Dry Sieving Method after Washing. In.

NM13.1.119. (2009). Soils - Recognition and Testing - Laboratory Density Determination of Fine Soils - Cutting Kit, Mold and Water Immersion Methods. In: IMANOR.

NM13.1.152. (2011). Soils: Investigation and testing - Determination of the water content by weight of materials - Oven Drying Method. In.

NM.10.1.138. (1995). Aggregates: Los Angeles Test. In.

Notholt, A. J. G. (1985). Phosphorite resources in the Mediterranean (Tethyan) phosphogenic province : a progress report. *Sciences Géologiques, bulletins et mémoires*, 9-17. https://www.persee.fr/doc/sgeol_0302-2684_1985_sem_77_1_2044

Nwaila, G. T., Ghorbani, Y., Zhang, S. E., Frimmel, H. E., Tolmay, L. C. K., Rose, D. H., Nwaila, P. C., & Bourdeau, J. E. (2021). Valorisation of mine waste - Part I: Characteristics of, and sampling methodology for, consolidated mineralised tailings by using Witwatersrand gold mines (South Africa) as an example. *Journal of Environmental Management*, *295*, 113013. https://doi.org/https://doi.org/10.1016/j.jenvman.2021.113013

Oberle, B., Bringezu, S., Hatfield-Dodds, S., Hellweg, S., Schandl, H., & Clement, J. (2019). *Global resources outlook: 2019*. International Resource Panel, United Nations Envio, Paris, France.

Ouakibi, O., Loqman, S., Hakkou, R., & Benzaazoua, M. (2013). The Potential Use of Phosphatic Limestone Wastes in the Passive Treatment of AMD: A Laboratory Study. *Mine Water and the Environment*, *32*(4), 266-277. https://doi.org/10.1007/s10230-013-0226-8

Oubaha, S., Hakkou, R., Taha, Y., Mghazli, M. O., & Benzaazoua, M. (2022). Elaboration of compressed earth blocks based on phosphogypsum and phosphate mining by-products. *Journal of Building Engineering*, *62*, 105423. https://doi.org/https://doi.org/10.1016/j.jobe.2022.105423

P94-074, N. (1994). Sols : reconnaissance et essais - Essais à l'appareil triaxial de révolution - Appareillage - Préparation des éprouvettes - Essai (UU) non consolidé non drainé - Essai (Cu+U) consolidé non drainé avec mesure de pression interstitielle - Essai (CD) consolidé drainé. MO. In.

P94-093, N. (1999). Sols: reconnaissance et essais-Détermination des références de compactage d'un matériau-Essai Proctor normal. Essai Proctor modifié. *AFNOR*.

Pagé, P., Li, L., Yang, P., & Simon, R. (2019). Numerical investigation of the stability of a base-exposed sill mat made of cemented backfill. *International Journal of Rock Mechanics and Mining Sciences*, *114*, 195-207. https://doi.org/https://doi.org/10.1016/j.ijrmms.2018.10.008

Peaver, D. R. (1966). The estuarine formation of United States Atlantic coastal plain phospho-rite. *Econ. Geol. 61*, *2*, 251-256.

Pesenson, M. Z., Suram, S. K., & Gregoire, J. M. (2015). Statistical analysis and interpolation of compositional data in materials science. *ACS combinatorial science*, *17*(2), 130-136.

Peyronnard, O., & Benzaazoua, M. (2011). Estimation of the cementitious properties of various industrial by-products for applications requiring low mechanical strength. *Resources, Conservation and Recycling*, *56*(1), 22-33. https://doi.org/https://doi.org/10.1016/j.resconrec.2011.08.008

Plante, B., Benzaazoua, M., & Bussière, B. (2011). Predicting Geochemical Behaviour of Waste Rock with Low Acid Generating Potential Using Laboratory Kinetic Tests. *Mine Water and the Environment*, *30*, 2-21. https://doi.org/10.1007/s10230-010-0127-z

Prévôt, L. (1988). *Geochimie et petrographie de la formation a phosphate des ganntour (maroc) : utilisation pour une explication de la genese des phosphorites cretace-eocenes*

Prévôt, L. (1990). Geochemistry, petrography, genesis of Cretaceous-Eocene phosphorites: the Ganntour deposit (Morocco)-A type example. *Soc. Geol. France, Memoire*, *158*, 232.

Prothero, D. R., & Schwab, F. L. (2013). *Sedimentary geology: an introduction to sedimentary rocks and stratigraphy, Third edition.* .

Pufahl, P. K., & Groat, L. A. (2017). Sedimentary and Igneous Phosphate Deposits: Formation and Exploration: An Invited Paper. *Economic Geology*, *112*(3), 483-516. https://doi.org/10.2113/econgeo.112.3.483

Rahhal, V. F., Bonavetti, V. L., & Talero, R. (2005). Hidratación temprana de cementos con mediano y alto contenido de adiciones minerales cristalinas. *Revista de la Construcción*, *4*(2), 13-24.

Ramsey, D., & Davis, R. (1975). Fabrication of ceramic articles from mining waste materials. *American Ceramic Society Bulletin*, *54*(3).

Rapti, I., Lopez-Caballero, F., Modaressi-Farahmand-Razavi, A., Foucault, A., & Voldoire, F. (2018). Liquefaction analysis and damage evaluation of embankment-type structures. *Acta Geotechnica*, *13*(5), 1041-1059. https://doi.org/10.1007/s11440-018-0631-z

Redclift, M. (2005). Sustainable development (1987–2005): an oxymoron comes of age. *Sustainable Development*, *13*(4), 212-227. https://doi.org/https://doi.org/10.1002/sd.281

Reimann, C., Fabian, K., Flem, B., Schilling, J., Roberts, D., & Englmaier, P. (2016). Pb concentrations and isotope ratios of soil O and C horizons in Nord-Trøndelag, central Norway: Anthropogenic or natural sources? *Applied Geochemistry*, *74*, 56-66. https://doi.org/https://doi.org/10.1016/j.apgeochem.2016.09.002

Reimann, C., & Filzmoser, P. (2000). Normal and lognormal data distribution in geochemistry: death of a myth. Consequences for the statistical treatment of geochemical and environmental data. *Environmental Geology*, *39*(9), 1001-1014. https://doi.org/10.1007/s002549900081

Reimann, C., Schilling, J., Roberts, D., & Fabian, K. (2015). A regional-scale geochemical survey of soil O and C horizon samples in Nord-Trøndelag, Central Norway: Geology and mineral

potential. *Applied Geochemistry*, *61*, 192-205. https://doi.org/https://doi.org/10.1016/j.apgeochem.2015.05.019

Sabiha, J., Mehmood, T., Chaudhry, M. M., Tufail, M., & Irfan, N. (2009). Heavy metal pollution from phosphate rock used for the production of fertilizer in Pakistan. *Microchemical Journal*, *91*(1), 94-99. https://doi.org/https://doi.org/10.1016/j.microc.2008.08.009

Safhi, A. e. M., Amar, H., El Berdai, Y., El Ghorfi, M., Taha, Y., Hakkou, R., Al-Dahhan, M., & Benzaazoua, M. (2022). Characterizations and potential recovery pathways of phosphate mines waste rocks. *Journal of Cleaner Production*, *374*, 134034. https://doi.org/https://doi.org/10.1016/j.jclepro.2022.134034

Safhi, A. E. M. E., (1st ed.). CRC Press. . (2022). *Valorization of Dredged Sediments as Sustainable Construction Resources* ((1st ed.) ed.). CRC Press. https://doi.org/https://doi.org/10.1201/9781003315551

Sapsford, D. J., Bowell, R. J., Dey, M., & Williams, K. P. (2009). Humidity cell tests for the prediction of acid rock drainage. *Minerals Engineering*, *22*(1), 25-36. https://doi.org/https://doi.org/10.1016/j.mineng.2008.03.008

Scoble, M., Klein, B., & Dunbar, W. S. (2003). Mining Waste: Transforming Mining Systems for Waste Management. *International Journal of Surface Mining, Reclamation and Environment*, *17*(2), 123-135. https://doi.org/10.1076/ijsm.17.2.123.14129

Scrivener, K. L., Lothenbach, B., De Belie, N., Gruyaert, E., Skibsted, J., Snellings, R., & Vollpracht, A. (2015). TC 238-SCM: hydration and microstructure of concrete with SCMs: State of the art on methods to determine degree of reaction of SCMs. *Materials and Structures*, *48*, 835-862.

Segui, P., Safhi, A. E., Amrani, M., & Benzaazoua, M. (2023). Mining Wastes as Road Construction Material: A Review. *Minerals*, *13*(1).

Setra, & LCPC. (1992). Réalisation des remblais et des couches de forme. *Fascicule I Principes Généraux, 211p*.

Shapiro, S. S., & Wilk, M. B. (1965). An Analysis of Variance Test for Normality (Complete Samples). *Biometrika*, *52*(3/4), 591-611. https://doi.org/10.2307/2333709

Sidibé, M. (1995). *Etude de l'utilisation des granulats de type silexlte en géotechnique routière (notamment en couches de base et revêtement des couches de chaussées).* Ecole Polytechnique de Thiès.].

Singer, A., Kirsten, W., & Bühmann, C. (1995). Fibrous clay minerals in the soils of Namaqualand, South Africa: characteristics and formation. *Geoderma 66*, 43-70.

Skierszkan, E. K., Mayer, K. U., Weis, D., & Beckie, R. D. (2016). Molybdenum and zinc stable isotope variation in mining waste rock drainage and waste rock at the Antamina mine, Peru. *Sci Total Environ*, *550*, 103-113. https://doi.org/10.1016/j.scitotenv.2016.01.053

Slansky, M. (1980). *Géologie des phosphates*

sédimentaires.

Slimane, S., Nouna, K., & Malek, N. (2017). *Valorisation de rejet de broyage de minerai phosphate de gisement de Kef Es Sennoun de la mine de Djebel Onk (Tébessa) dans le mortier.* [Mémoire de master,

Sobek, A. A. (1978). *Field and laboratory methods applicable to overburdens and minesoils*. Industrial Environmental Research Laboratory, Office of Research and ….

Somasundaran, P., & Wang, D. (2006). Chapter 3 Mineral–solution equilibria. In D. Wang (Ed.), *Developments in Mineral Processing* (Vol. 17, pp. 45-72). Elsevier. https://doi.org/https://doi.org/10.1016/S0167-4528(06)17003-9

Stöber, W., Fink, A., & Bohn, E. (1968). Controlled growth of monodisperse silica spheres in the micron size range. *Journal of Colloid and Interface Science*, *26*(1), 62-69. https://doi.org/https://doi.org/10.1016/0021-9797(68)90272-5

Taha, Y., Benzaazoua, M., Hakkou, R., & Mansori, M. (2016b). Natural clay substitution by calamine processing wastes to manufacture fired bricks. *Journal of Cleaner Production*, *135*, 847-858. https://doi.org/10.1016/j.jclepro.2016.06.200

Taha, Y., Benzaazoua, M., Hakkou, R., & Mansori, M. (2017b). Coal mine wastes recycling for coal recovery and eco-friendly bricks production. *Minerals Engineering*, *107*, 123-138. https://doi.org/https://doi.org/10.1016/j.mineng.2016.09.001

Taha, Y., Benzaazoua, M., Mansori, M., Yvon, J., Kanari, N., & Hakkou, R. (2016a). Manufacturing of ceramic products using calamine hydrometallurgical processing wastes. *Journal of Cleaner Production*, *127*, 500-510. https://doi.org/https://doi.org/10.1016/j.jclepro.2016.04.056

Taha, Y., Elghali, A., Hakkou, R., & Benzaazoua, M. (2021). Towards Zero Solid Waste in the Sedimentary Phosphate Industry: Challenges and Opportunities. *Minerals*, *11*(11). https://doi.org/10.3390/min11111250

Tayebi-Khorami, M., Edraki, M., Corder, G., & Golev, A. (2019). Re-Thinking Mining Waste through an Integrative Approach Led by Circular Economy Aspirations. *Minerals*, *9*(5). https://doi.org/10.3390/min9050286

Taylor, H. F. (1997). *Cement chemistry* (Vol. 2). Thomas Telford London.

Torres, J., Pintos, V., Gonzatto, L., Domínguez, S., Kremer, C., & Kremer, E. (2011). Selenium chemical speciation in natural waters: Protonation and complexation behavior of selenite and selenate in the presence of environmentally relevant cations. *Chemical Geology*, *288*(1), 32-38. https://doi.org/https://doi.org/10.1016/j.chemgeo.2011.06.015

Toubri, Y., Demers, I., Poirier, A., Pépin, G., Gosselin, M.-C., & Beier, N. A. (2021). Merging 3D geological modeling and stochastic simulation to foster waste rock upstream management. *Journal of Geochemical Exploration*, *224*, 106739. https://doi.org/https://doi.org/10.1016/j.gexplo.2021.106739

Tucker, M. E. (2001). *Sedimentary Petrology : An Introduction to the Origin of Sedimentary Rocks*.

Ukaogo, P. O., Ewuzie, U., & Onwuka, C. V. (2020). 21 - Environmental pollution: causes, effects, and the remedies. In P. Chowdhary, A. Raj, D. Verma, & Y. Akhter (Eds.), *Microorganisms*

for Sustainable Environment and Health (pp. 419-429). Elsevier. https://doi.org/https://doi.org/10.1016/B978-0-12-819001-2.00021-8

Urien, P., N., C., R., G., & D., G. (2017). Sondages miniers In C. L. m. e. F. » (Ed.), (Collection « La mine en France », Tome 11 ed., Vol. Tome 11, pp. 42).

USEPA. (1992). Method 1311: toxicity characteristic leaching procedure, SW-846: Test methods for evaluating solid waste - Physical/Chemical Methods. Washington, D.C. In.

USEPA. (1994). Method 1312: synthetic precipitation leaching procedure, SW-846: part of test methods for evaluating solid waste, physical/chemical methods. In.

USEPA. (2017). Method 1315 : mass transfer rates of constituents in monolithic or compacted granular materials using a semi-dynamic tank leaching procedure. In.

USEPA. (2009). HazardousWaste Characteristics. In *AUser-Friendly Reference Document; EPA:Washington, DC, USA*.

USGS, U. S. G. S. (2018). *Mineral commodity summaries 2018. U.S. Geological*

Survey.

USGS, U. S. G. S. (2021). *Mineral Commodity Summaries 2021. U.S. Geological Survey*.

UTS, U. (2017). Land disposal restrictions, rules and regulations. In *https://www.epa.gov/hw/land-disposal-restrictions-hazardous-waste*.

Vassilev, N., & Vassileva, M. (2003). Biotechnological solubilization of rock phosphate on media containing agro-industrial wastes. *Applied Microbiology and Biotechnology*, *61*(5), 435-440. https://doi.org/10.1007/s00253-003-1318-3

Vermette, D. (2018). *Approche de caractérisation géoenvironnementale axée sur l'utilisation des concepts géométallurgiques.* [Maitrise en Sciences Appliquées Université de Montréal, Ecole Polytechnique de Montréal]. http://depositum.uqat.ca/765/1/Memoire_DVermette.pdf.

von Greve-Dierfeld, S., Lothenbach, B., Vollpracht, A., Wu, B., Huet, B., Andrade, C., Medina, C., Thiel, C., Gruyaert, E., & Vanoutrive, H. (2020). Understanding the carbonation of concrete with supplementary cementitious materials: a critical review by RILEM TC 281-CCC. *Materials and Structures*, *53*(6), 136.

Wadjinny, A. (1979). *Milieu de sédimentation et mécanismes de dépôt des «couches inférieures» de la série phosphatée de Ben Guerir (Ganntour, Maroc), une étude séquentielle*. Univ L Pasteur Strasbourg.

Weber, P. A., Thomas, J. E., Skinner, W. M., & Smart, R. S. C. (2004). Improved acid neutralisation capacity assessment of iron carbonates by titration and theoretical calculation. *Applied Geochemistry*, *19*(5), 687-694. https://doi.org/https://doi.org/10.1016/j.apgeochem.2003.09.002

Wubalem, A. (2022). Comparison of General Limit Equilibrium Methods for Slope Stability Analysis. *Ethiopian Journal of Natural and Computational Sciences*, *2*(1), 271-290.

Xie, Y., Zhu, W., Xiong, Y., & Ye, G. (2023). Numerical investigation on the effect of initial water content on dynamic responses of unsaturated sandy and clayey embankments. *Soil Dynamics and Earthquake Engineering*, *173*, 108151. https://doi.org/https://doi.org/10.1016/j.soildyn.2023.108151

XP P 94-429. (2002). Rock - Point load strength test - Franklin test. In.

XPP94-202. (1995). Soil : investigation and testing. Soil sampling. Methodology and procedures. In.

Yamaguchi, A., Mori, T., Kazama, M., & Yoshida, N. (2012). Liquefaction in Tohoku district during the 2011 off the Pacific Coast of Tohoku Earthquake. *Soils and Foundations*, *52*(5), 811-829. https://doi.org/https://doi.org/10.1016/j.sandf.2012.11.005

Yang, Y.-Y., Wu, H.-N., Shen, S.-L., Horpibulsuk, S., Xu, Y.-S., & Zhou, Q.-H. (2014). Environmental impacts caused by phosphate mining and ecological restoration: a case history in Kunming, China. *Natural Hazards*, *74*(2), 755-770. https://doi.org/10.1007/s11069-014-1212-6

Yang, Z., lin, Q., Xia, J., He, Y., Liao, G., & Ke, Y. (2013). Preparation and crystallization of glass–ceramics derived from iron-rich copper slag. *Journal of Alloys and Compounds*, *574*, 354-360. https://doi.org/https://doi.org/10.1016/j.jallcom.2013.05.091

Zafar, Z. I., & Ashraf, M. (2007). Selective leaching kinetics of calcareous phosphate rock in lactic acid. *Chemical Engineering Journal*, *131*(1), 41-48. https://doi.org/https://doi.org/10.1016/j.cej.2006.12.002

Zajac, M., Bremseth, S. K., Whitehead, M., & Haha, M. B. (2014). Effect of CaMg (CO3) 2 on hydrate assemblages and mechanical properties of hydrated cement pastes at 40 C and 60 C. *Cement and concrete research*, *65*, 21-29.

Zargouni, F. U. L. P. (1985). *Tectonique de l'atlas méridional de Tunisie : évolution géométrique et cinématique des structures en zone de cisaillement* [s.n.]]. /z-wcorg/. [S.l.].

Zhang, L. (2013). Production of bricks from waste materials – A review. *Construction and Building Materials*, *47*, 643-655. https://doi.org/https://doi.org/10.1016/j.conbuildmat.2013.05.043

APPENDIX A CORE DRILLING

1. Photographs of core boxes (Example SC06)

Figure A. 1: Photographs of core boxes (Example SC06)

Figure A. 2: Photographs of core boxes (Example SC06) (Continued)

2. Litho-stratigraphic section for the six drill cores

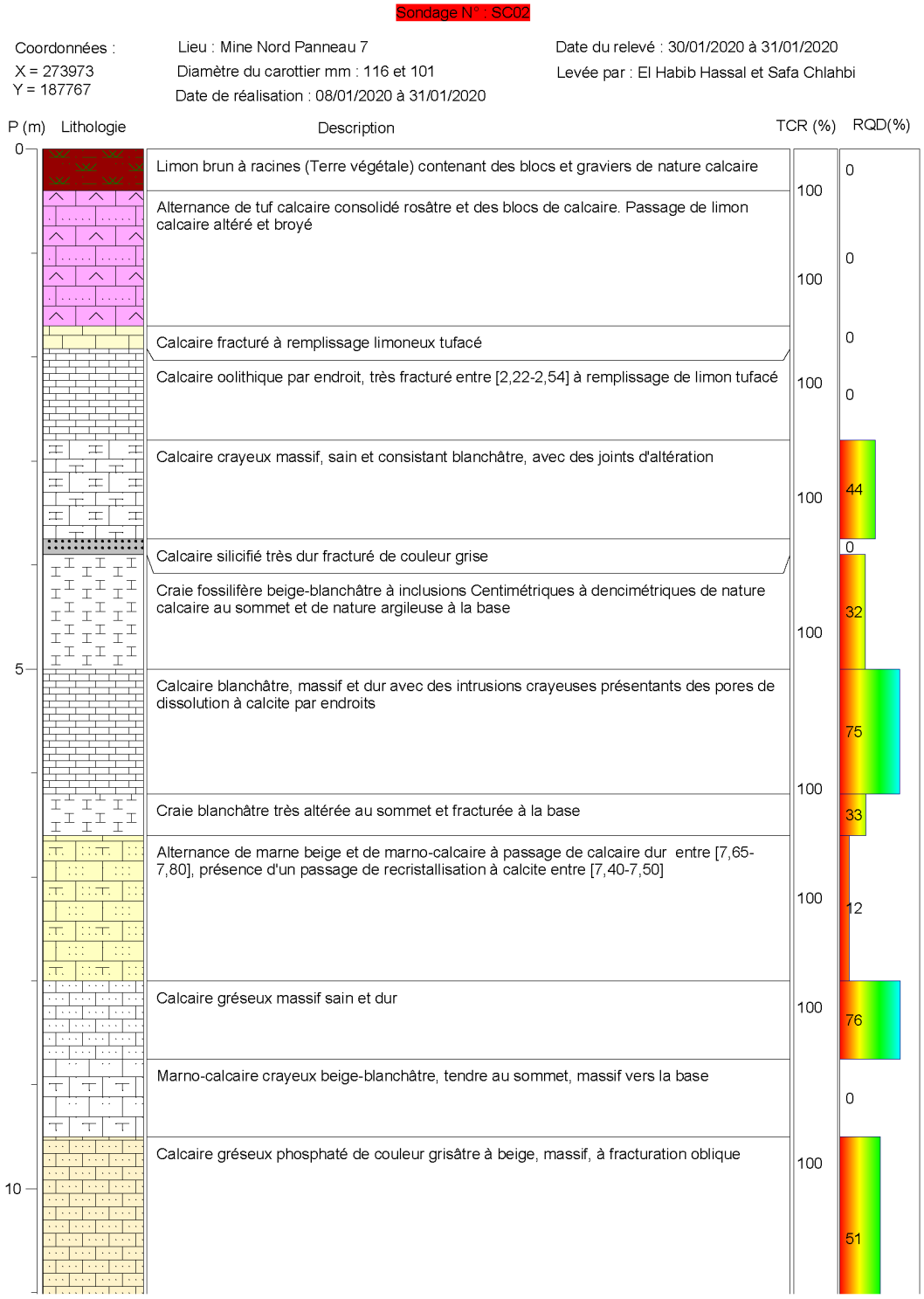

Figure A. 3: Litho-stratigraphic section for the SC02 drill core

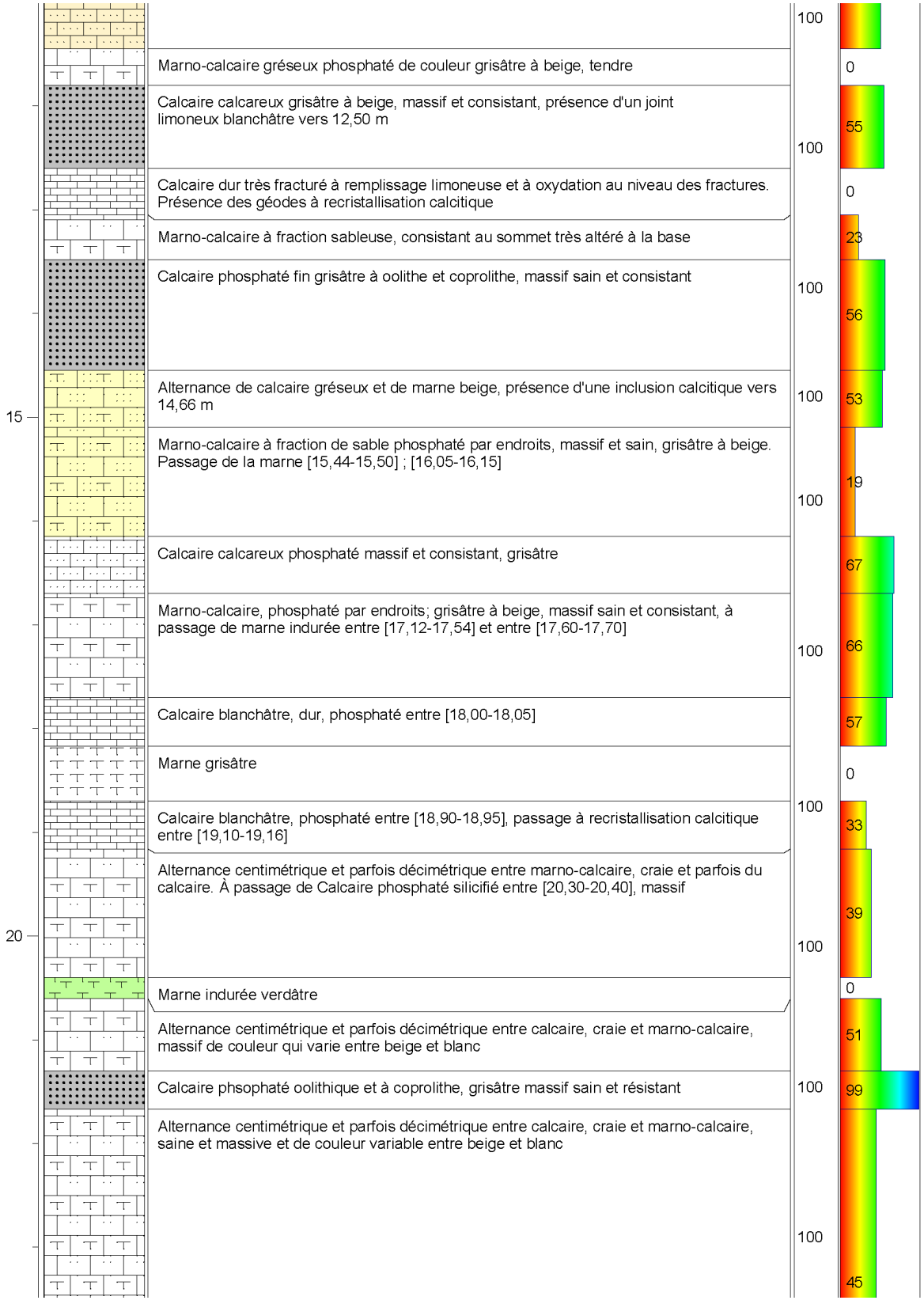

Figure A. 4: Litho-stratigraphic section for the SC02 drill core (Continued)

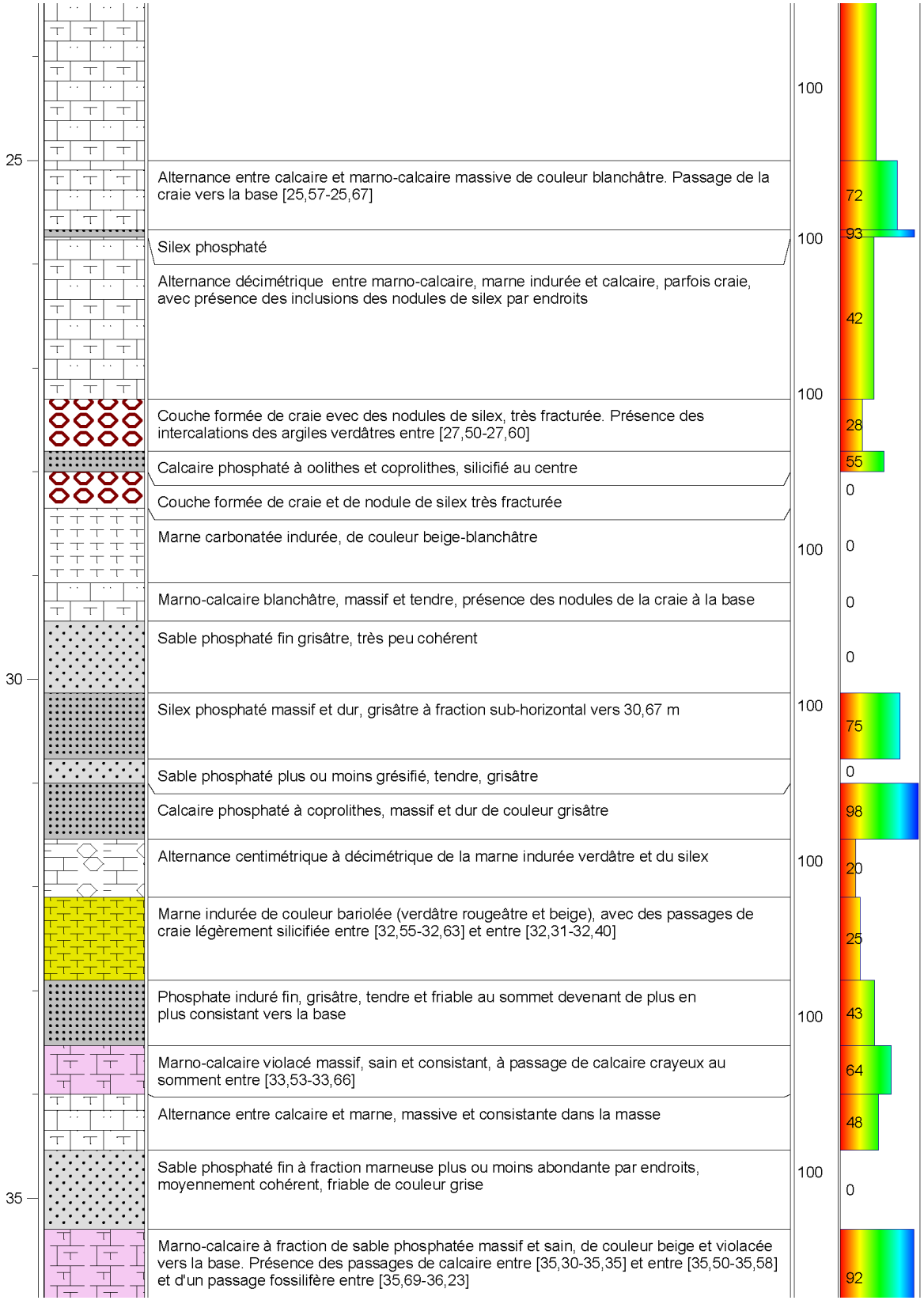

Figure A. 5: Litho-stratigraphic section for the SC02 drill core (Continued)

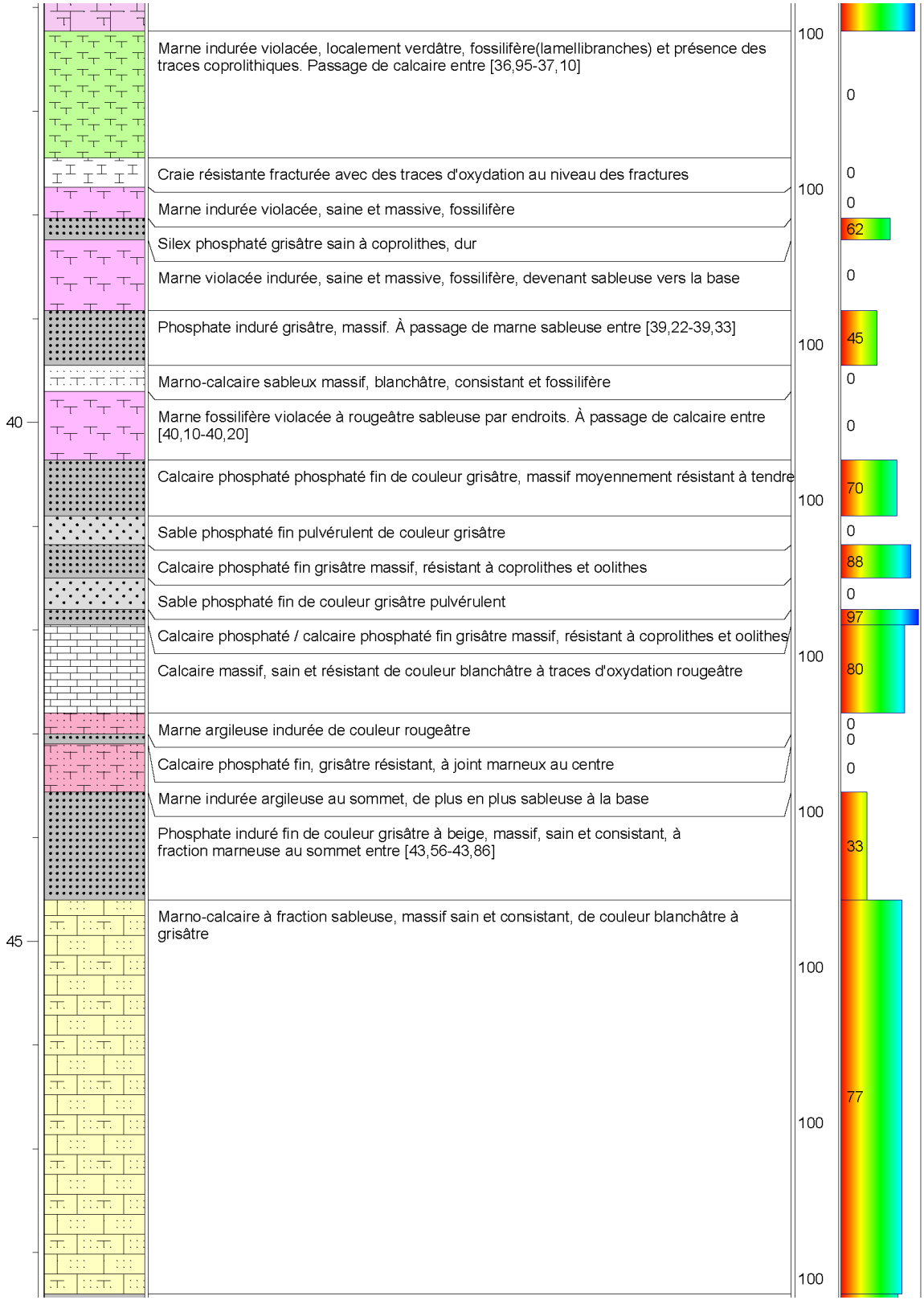

Figure A. 6: Litho-stratigraphic section for the SC02 drill core (Continued)

Figure A. 7: Litho-stratigraphic section for the SC02 drill core (Continued)

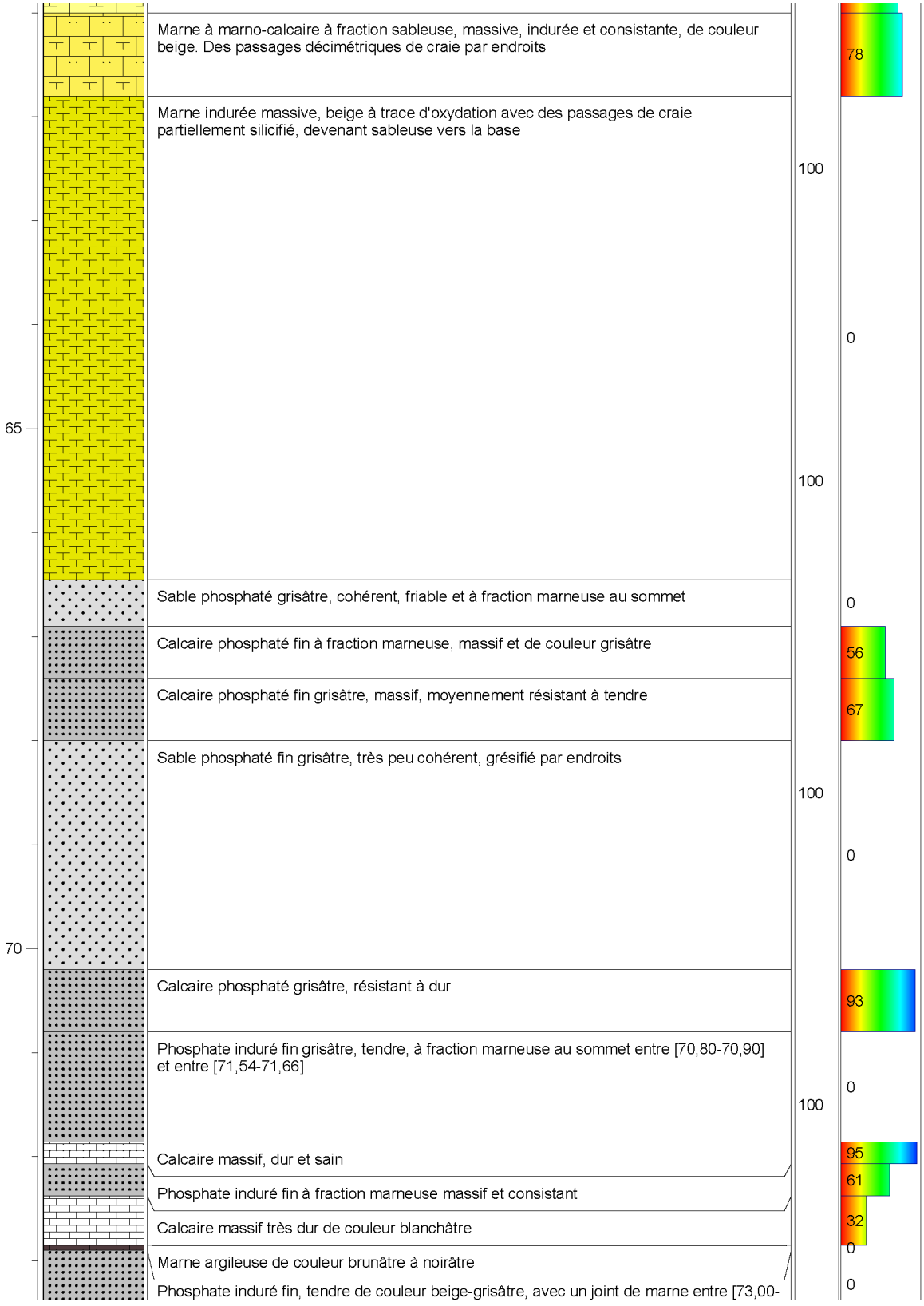

Figure A. 8: Litho-stratigraphic section for the SC02 drill core (Continued)

Figure A. 9: Litho-stratigraphic section for the SC02 drill core (Continued)

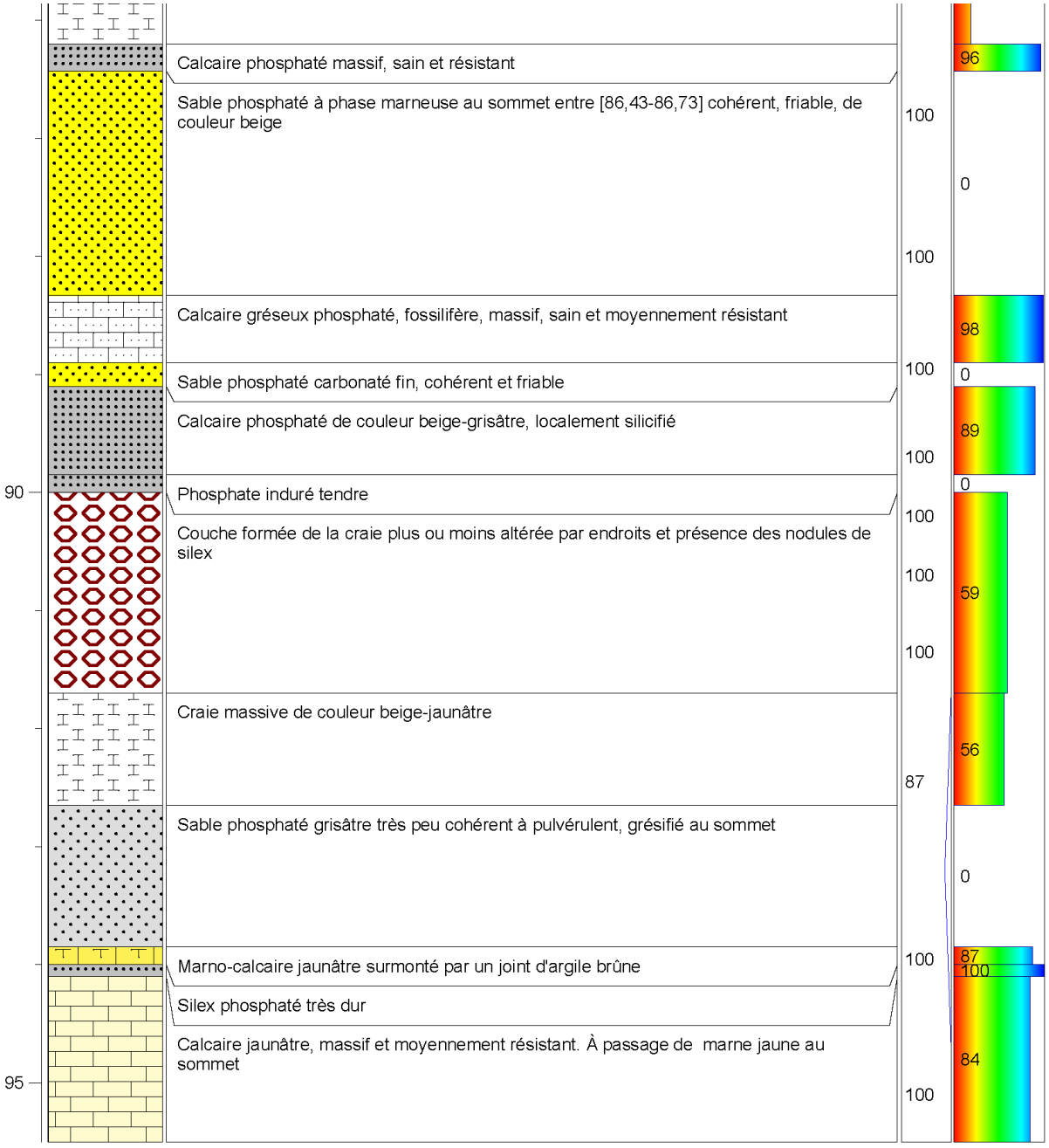

Figure A. 10: Litho-stratigraphic section for the SC02 drill core (Continued)

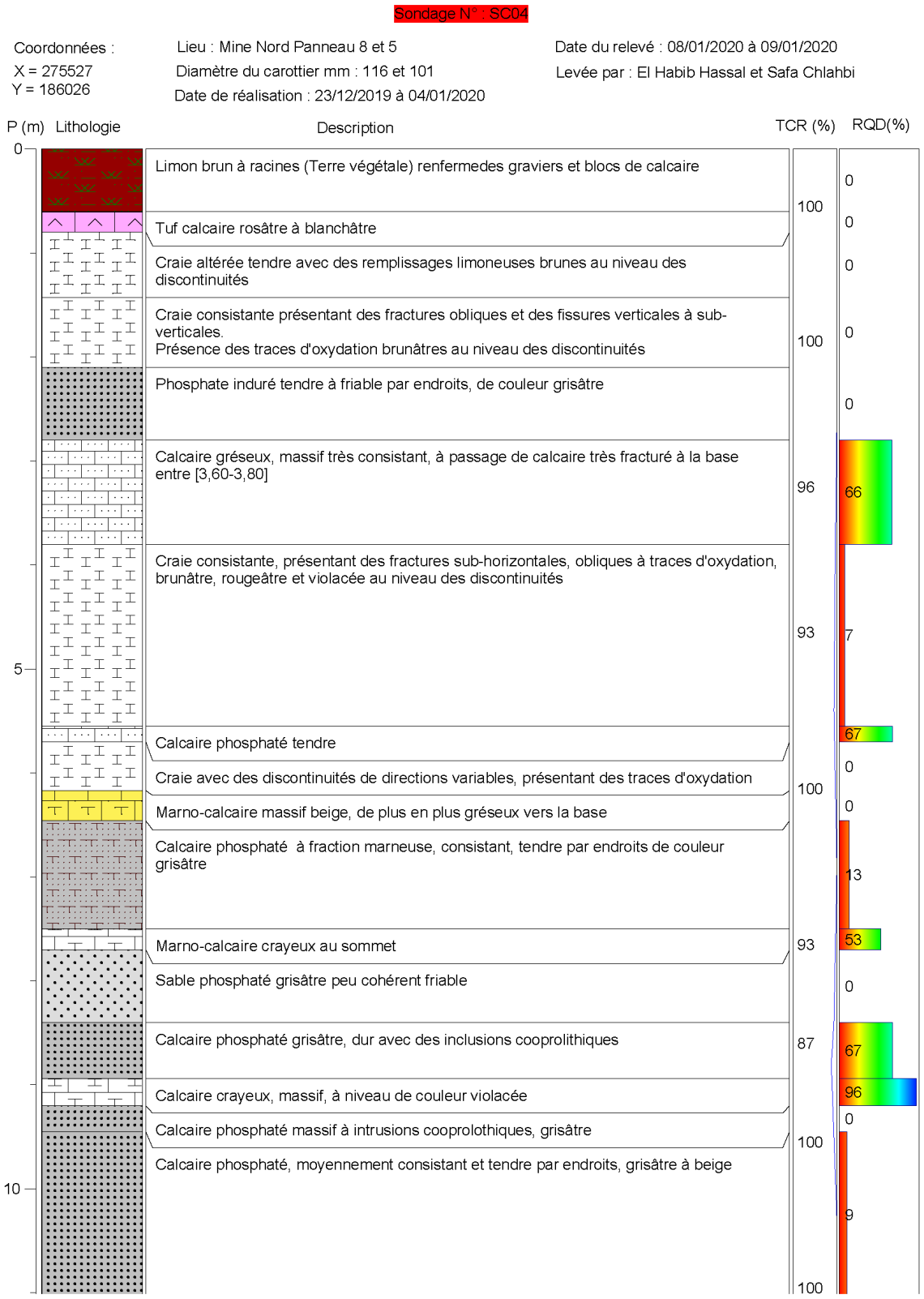

Figure A. 11: Litho-stratigraphic section for the SC04 drill core

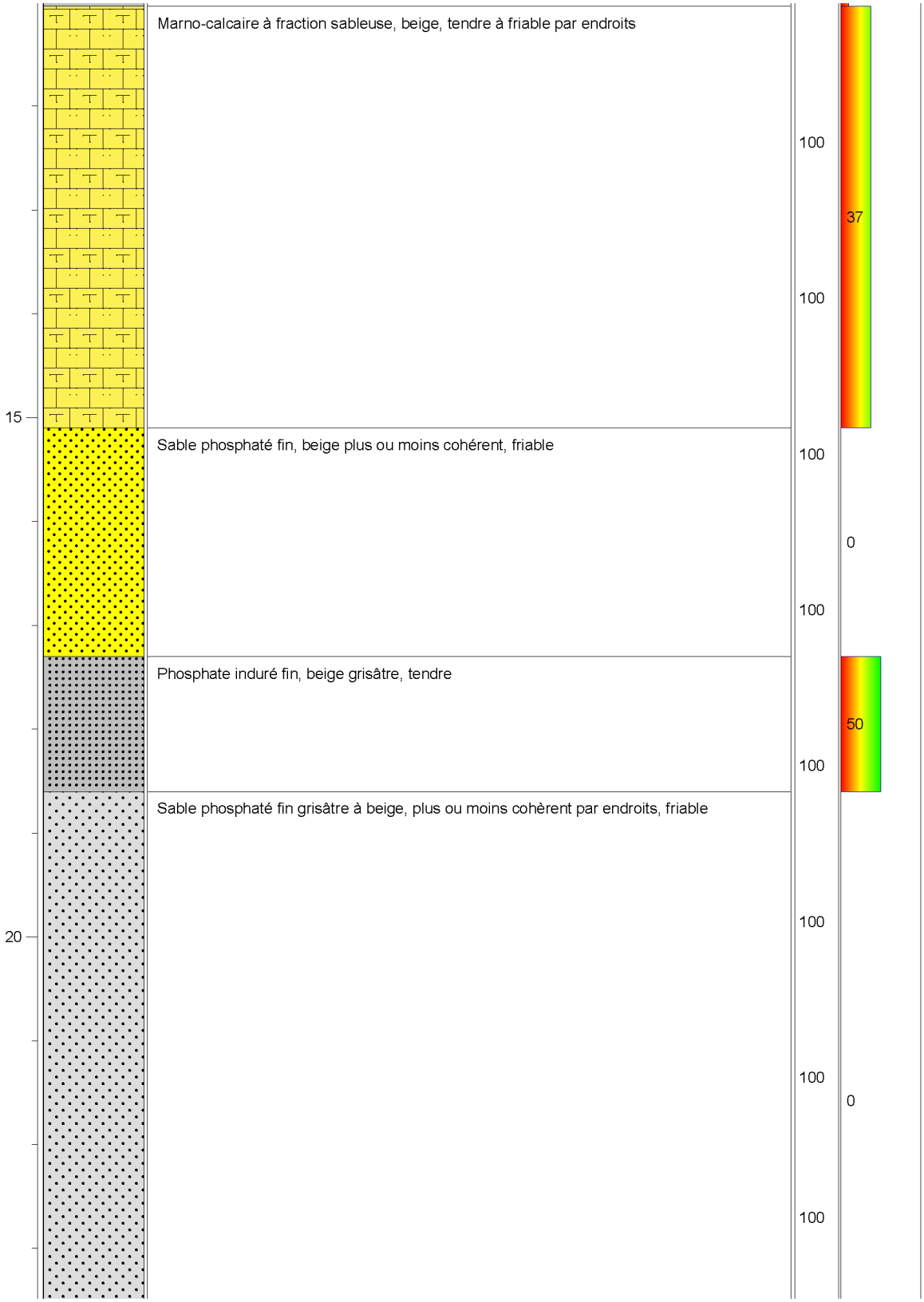

Figure A. 12: Litho-stratigraphic section for the SC04 drill core (Continued)

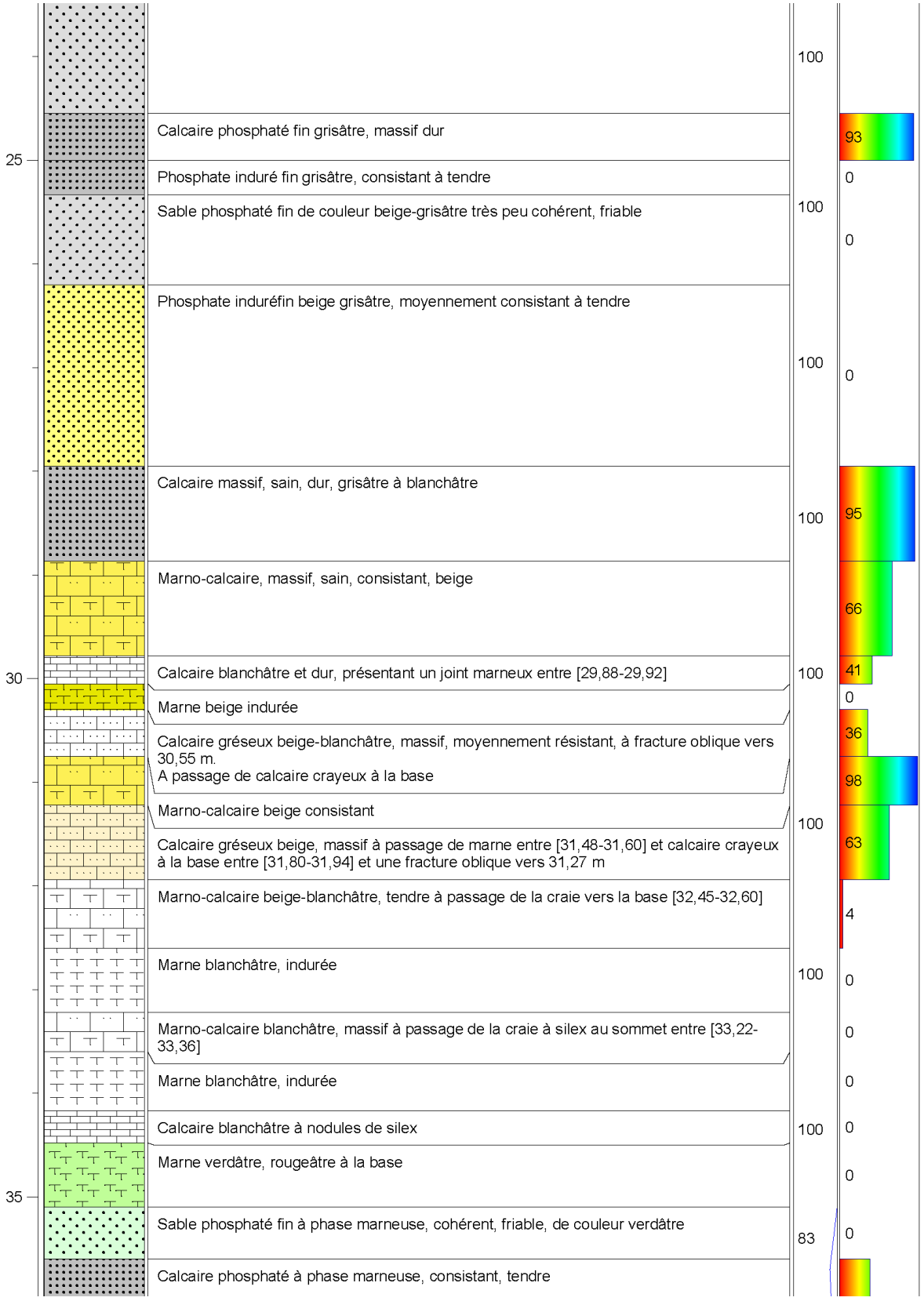

Figure A. 13: Litho-stratigraphic section for the SC04 drill core (Continued)

Figure A. 14: Litho-stratigraphic section for the SC04 drill core (Continued)

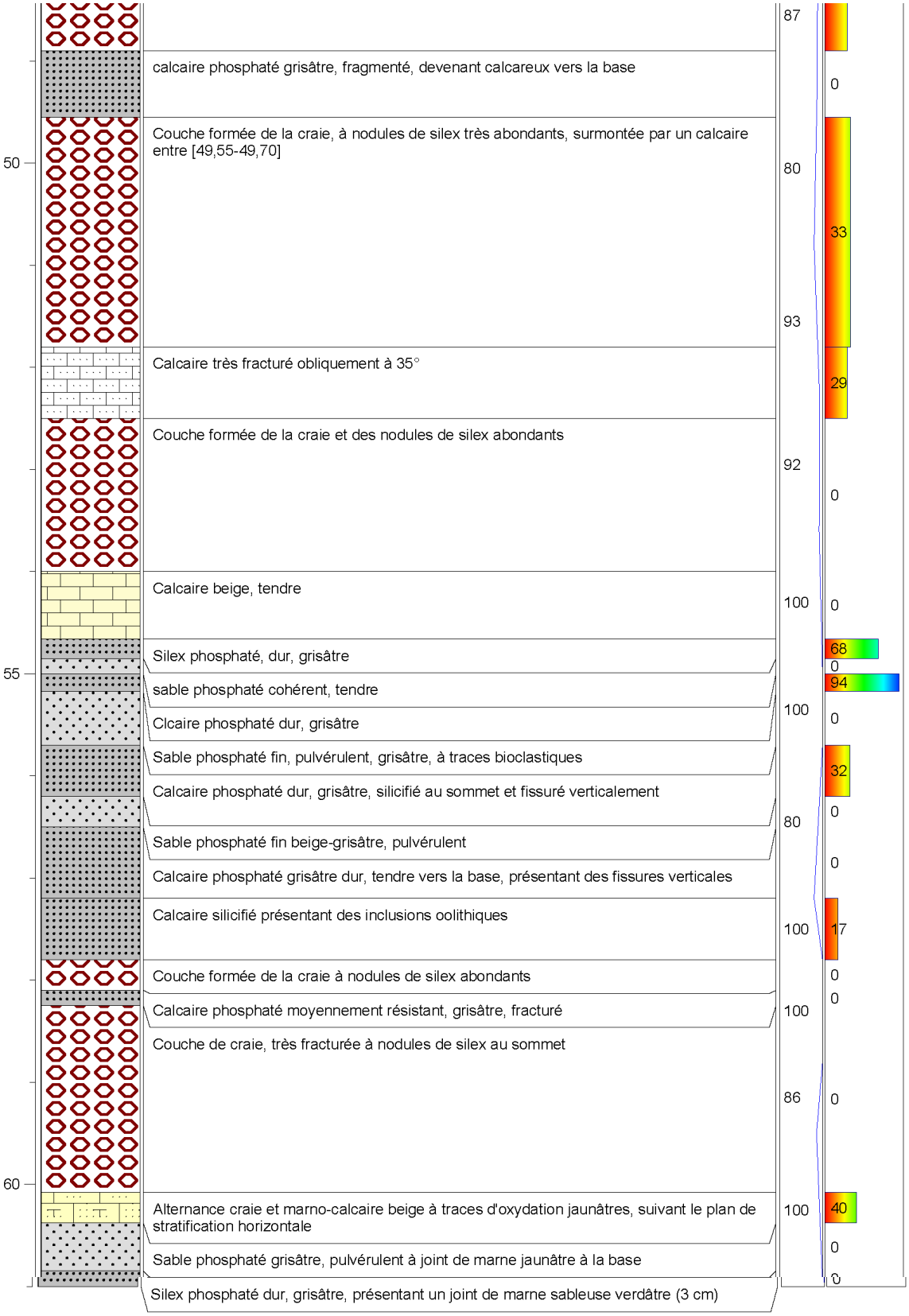

Figure A. 15: Litho-stratigraphic section for the SC04 drill core (Continued)

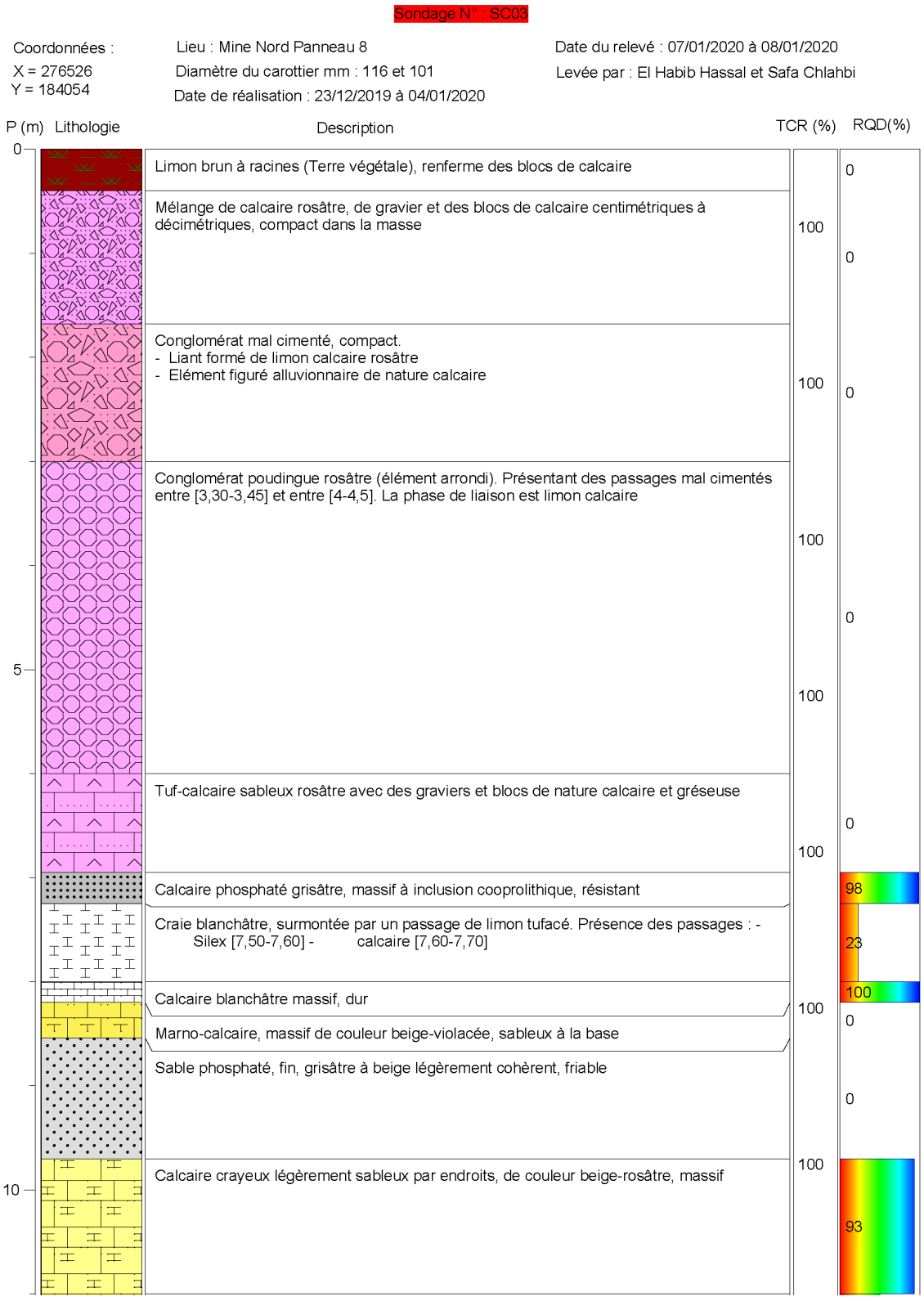

Figure A. 16: Litho-stratigraphic section for the SC03 drill core

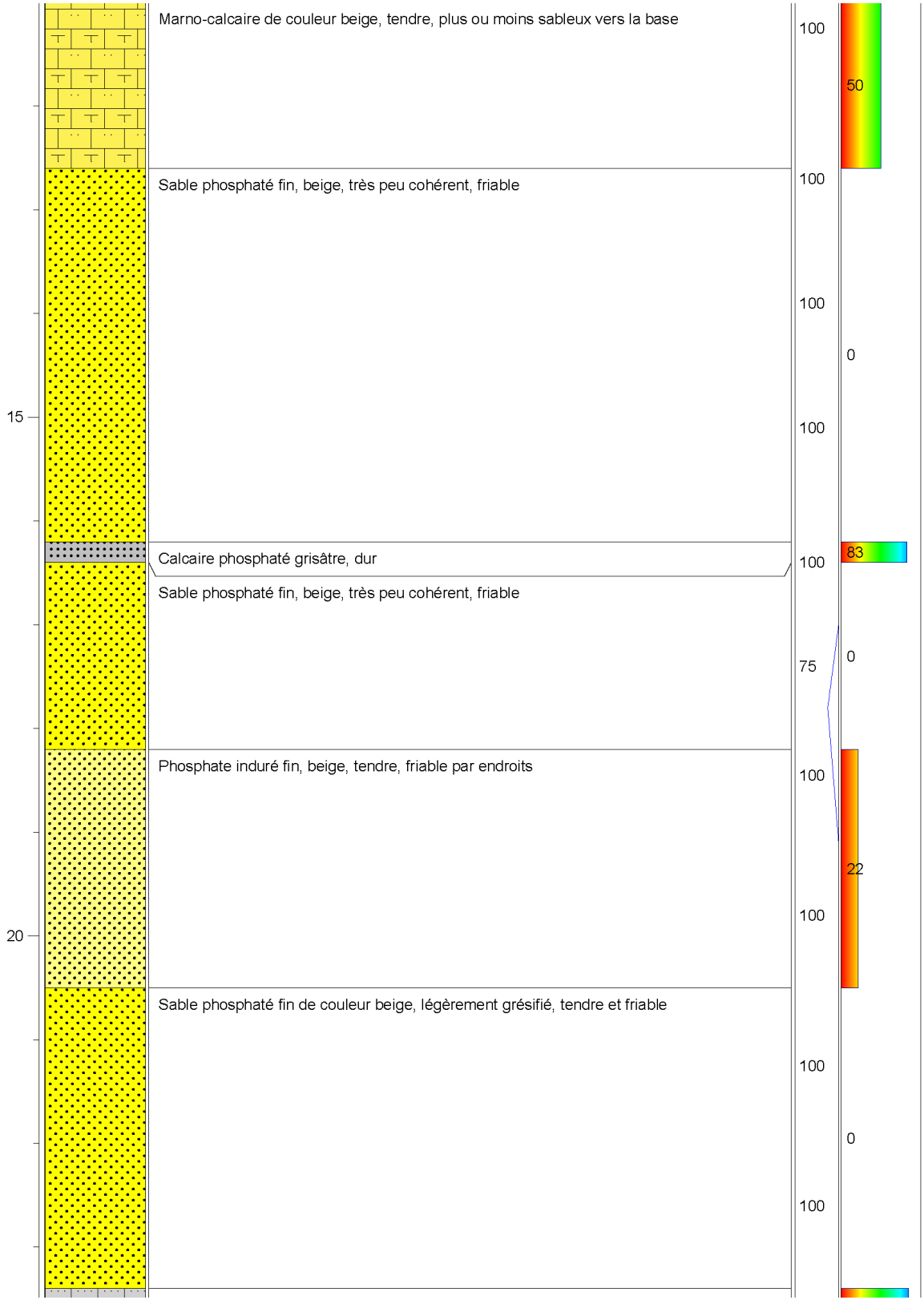

Figure A. 17: Litho-stratigraphic section for the SC03 drill core (Continued)

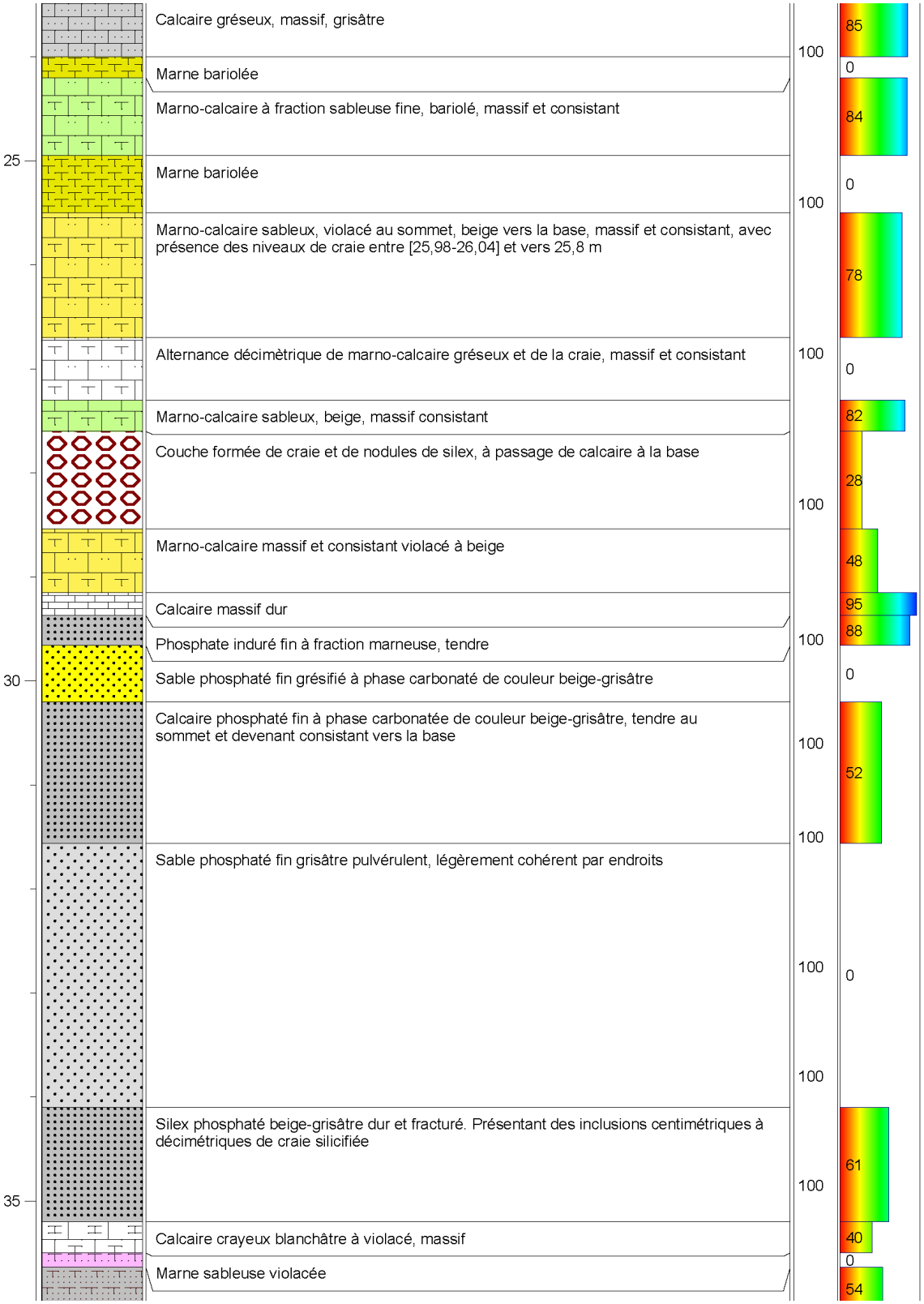

Figure A. 18: Litho-stratigraphic section for the SC03 drill core (Continued)

Figure A. 19: Litho-stratigraphic section for the SC03 drill core (Continued)

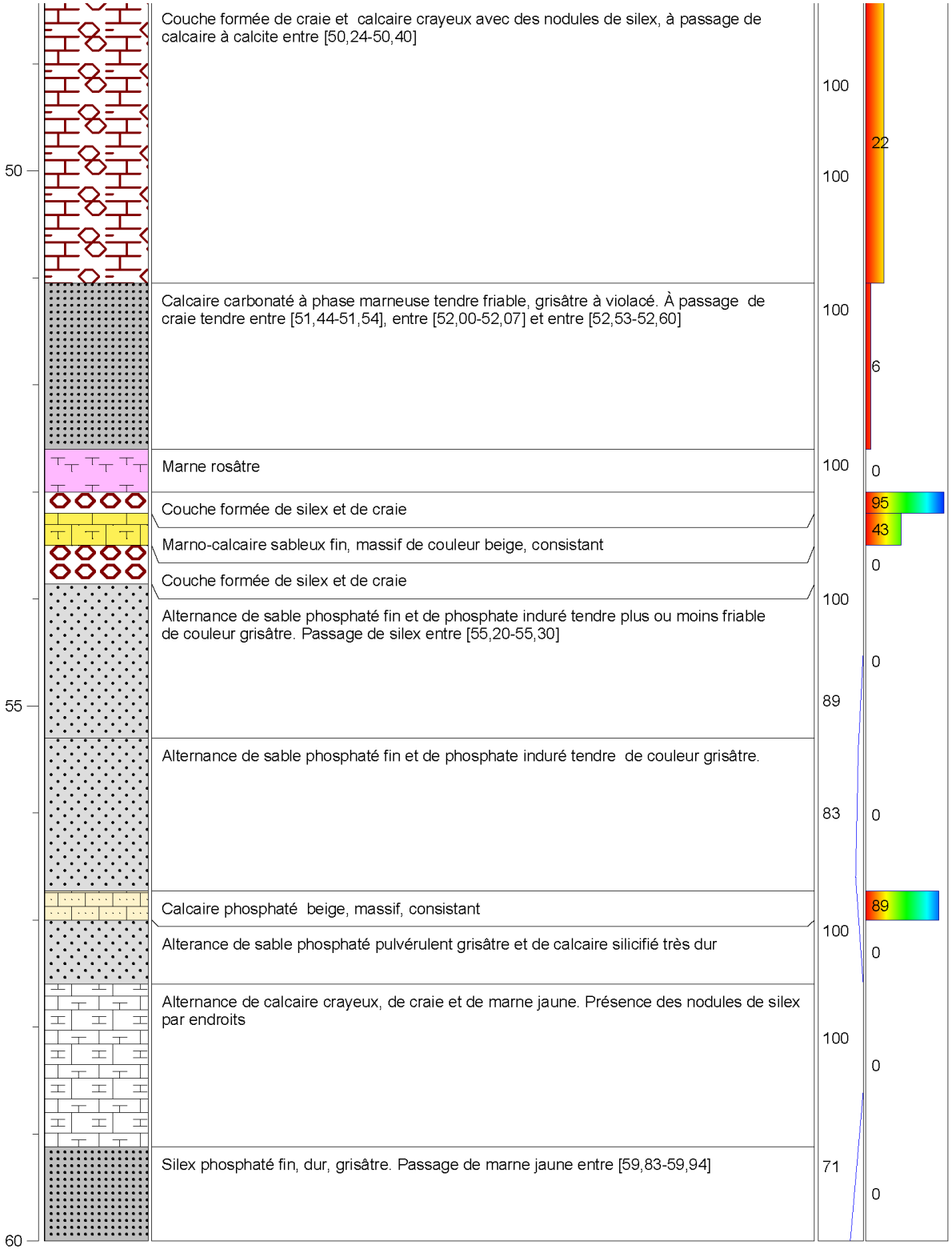

Figure A. 20: Litho-stratigraphic section for the SC03 drill core (Continued)

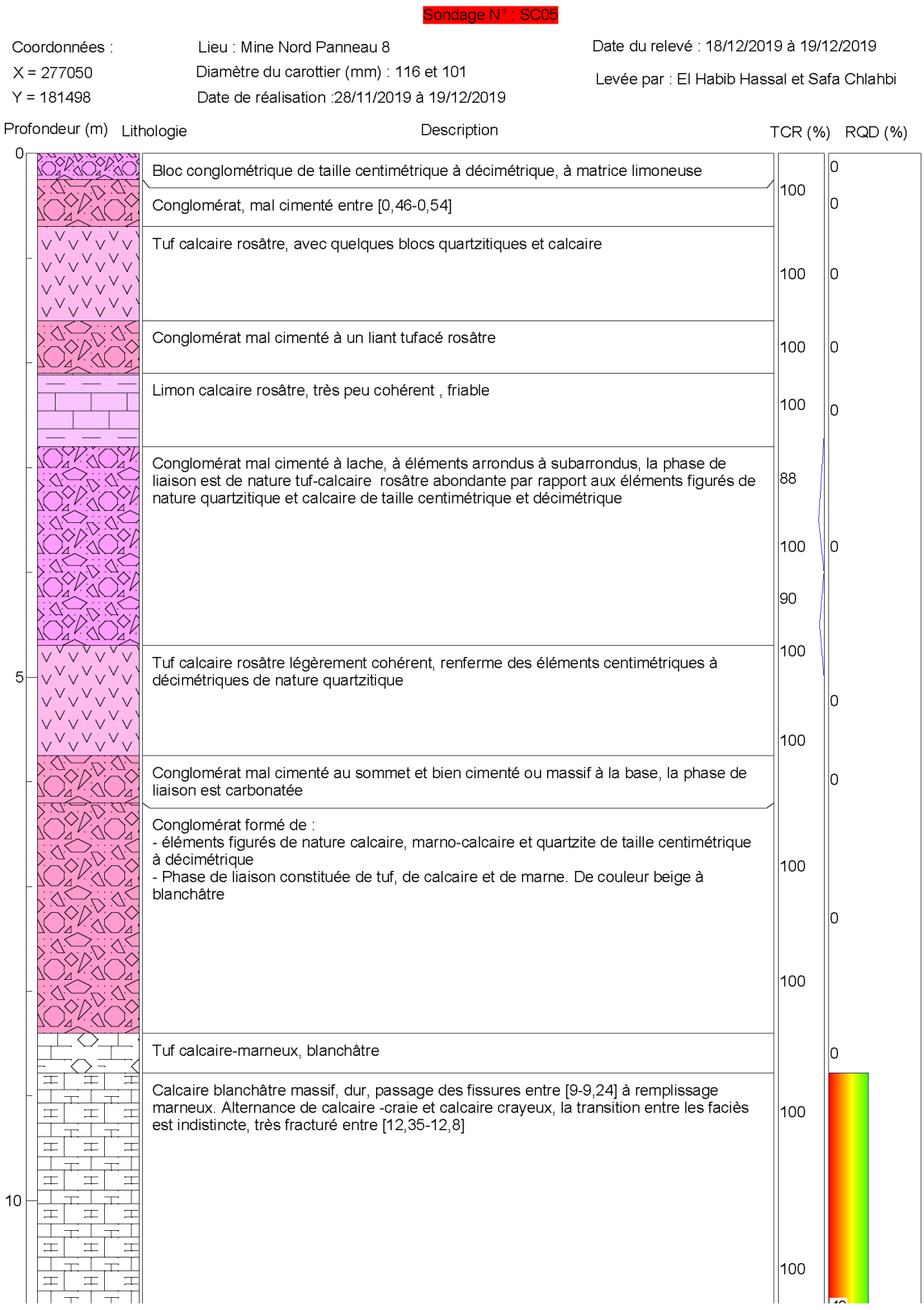

Figure A. 21: Litho-stratigraphic section for the SC05 drill core

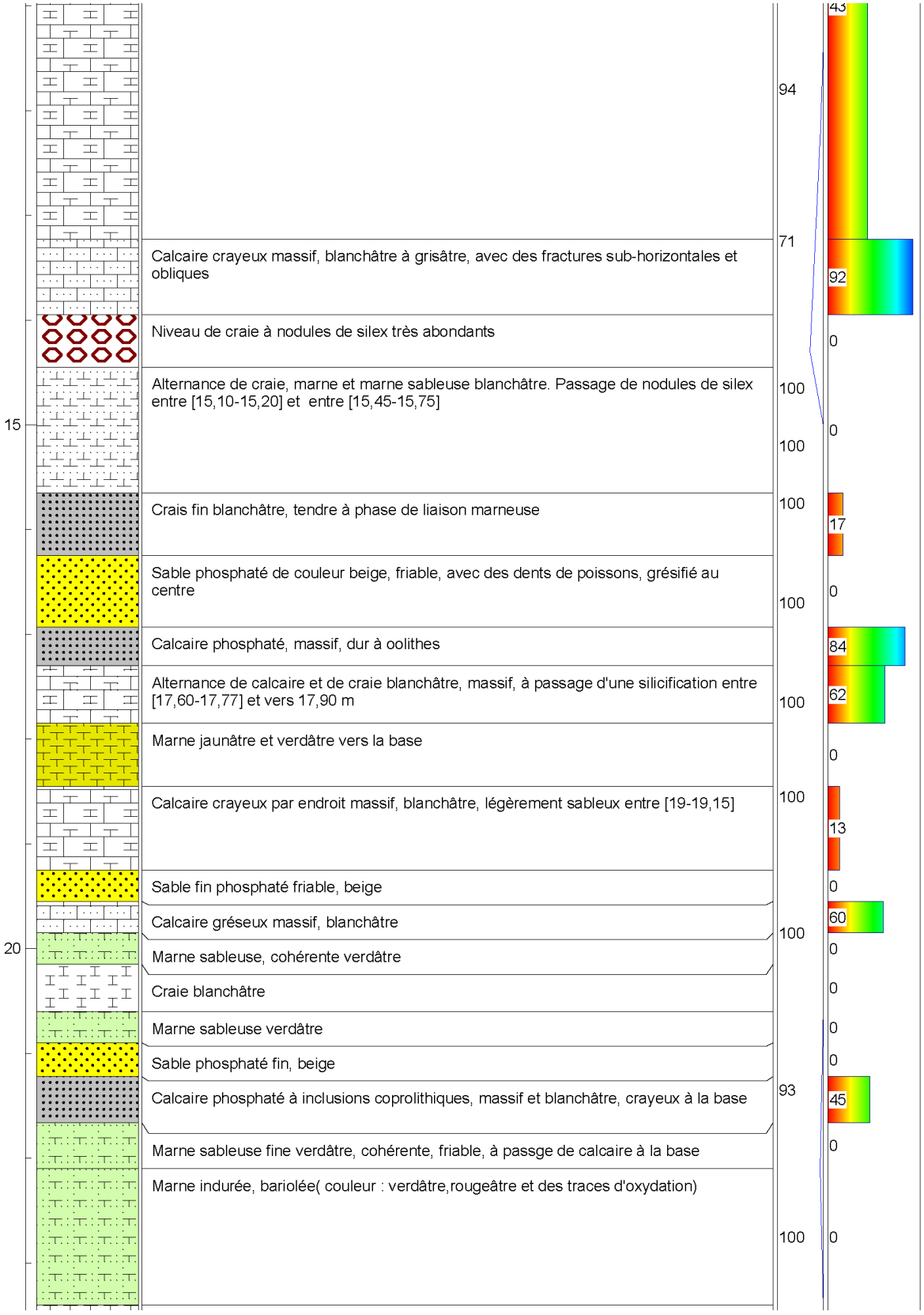

Figure A. 22: Litho-stratigraphic section for the SC05 drill core (Continued)

Figure A. 23: Litho-stratigraphic section for the SC05 drill core (Continued)

Figure A. 24: Litho-stratigraphic section for the SC05 drill core (Continued)

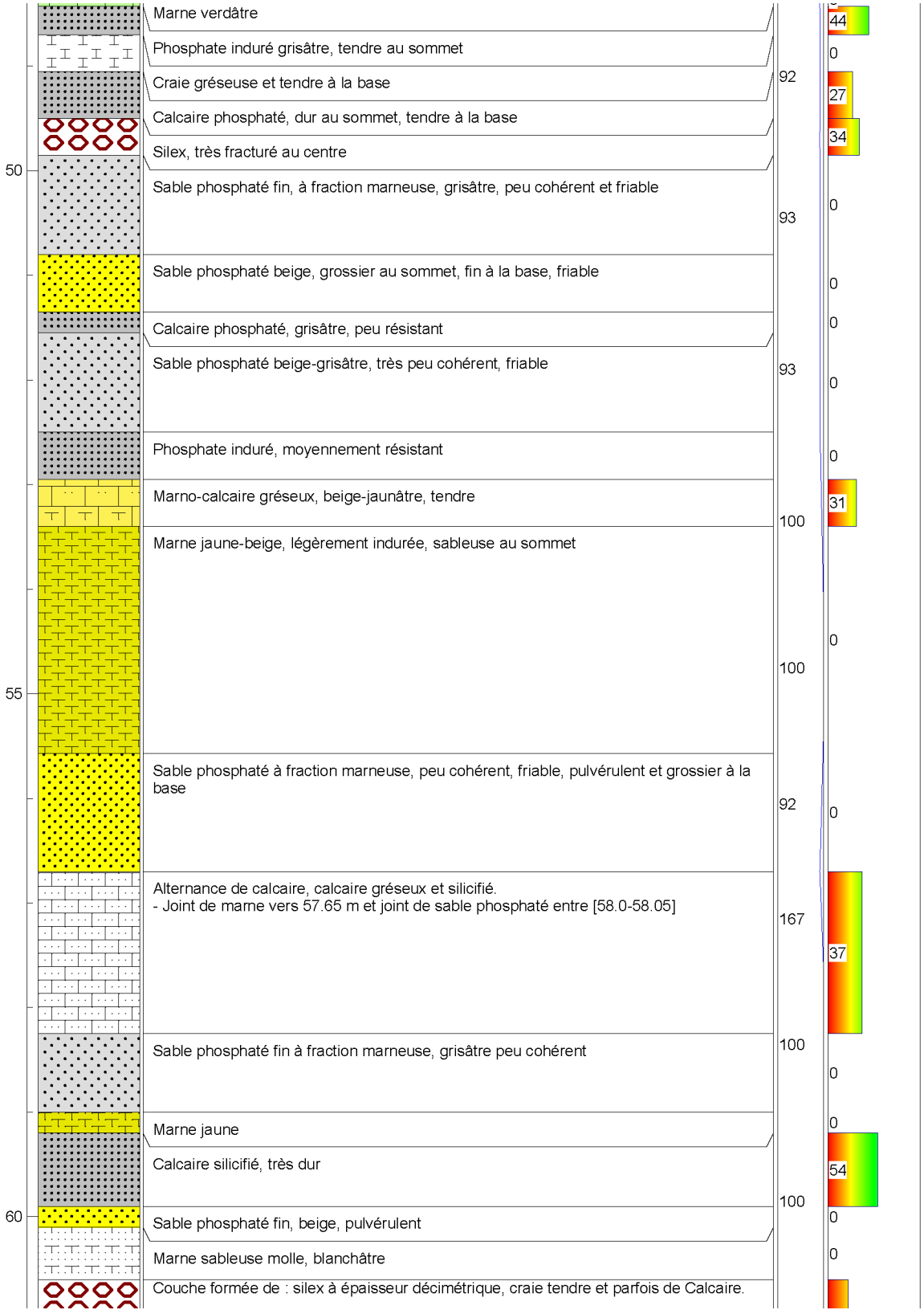

Figure A. 25: Litho-stratigraphic section for the SC05 drill core (Continued)

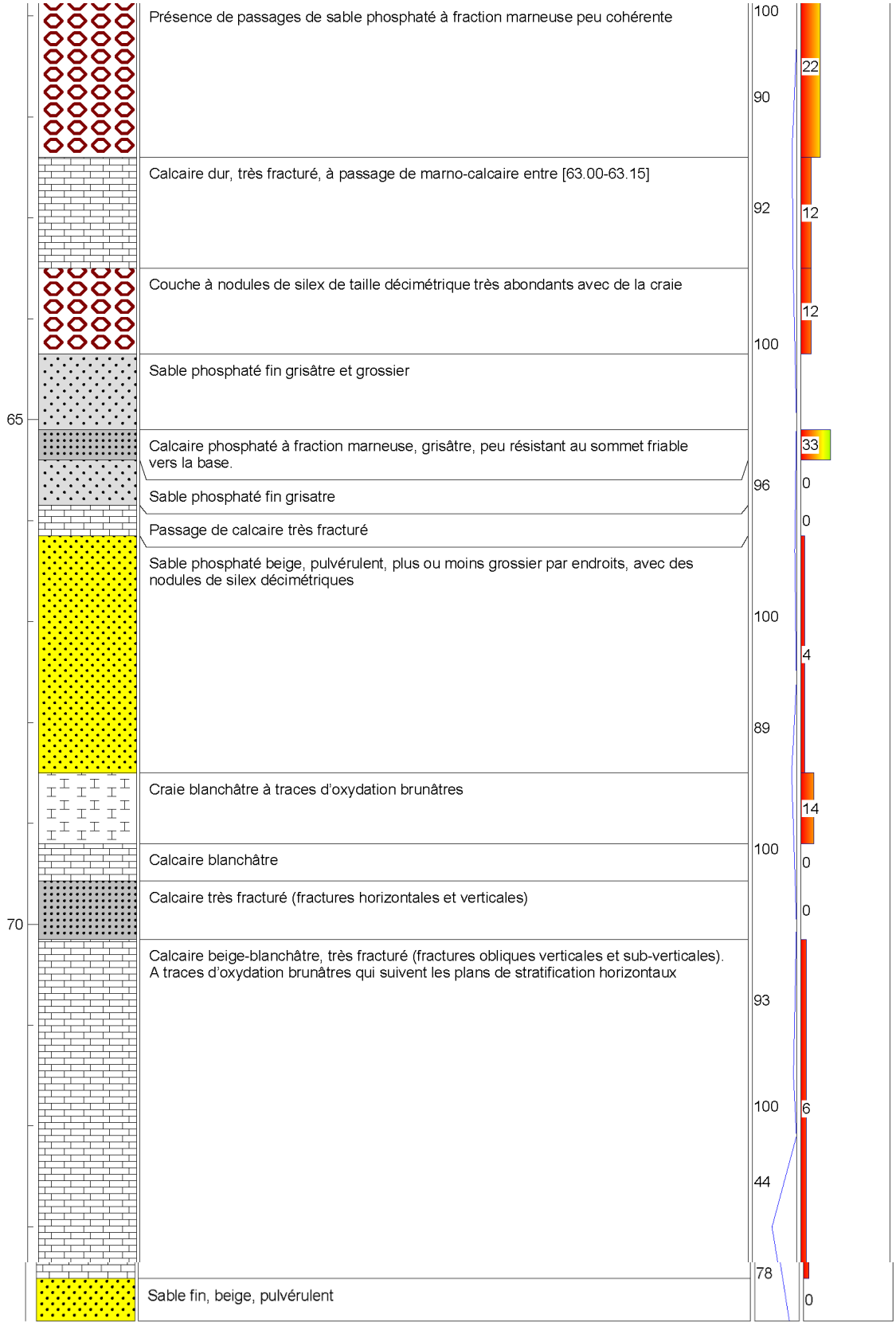

Figure A. 26: Litho-stratigraphic section for the SC05 drill core (Continued)

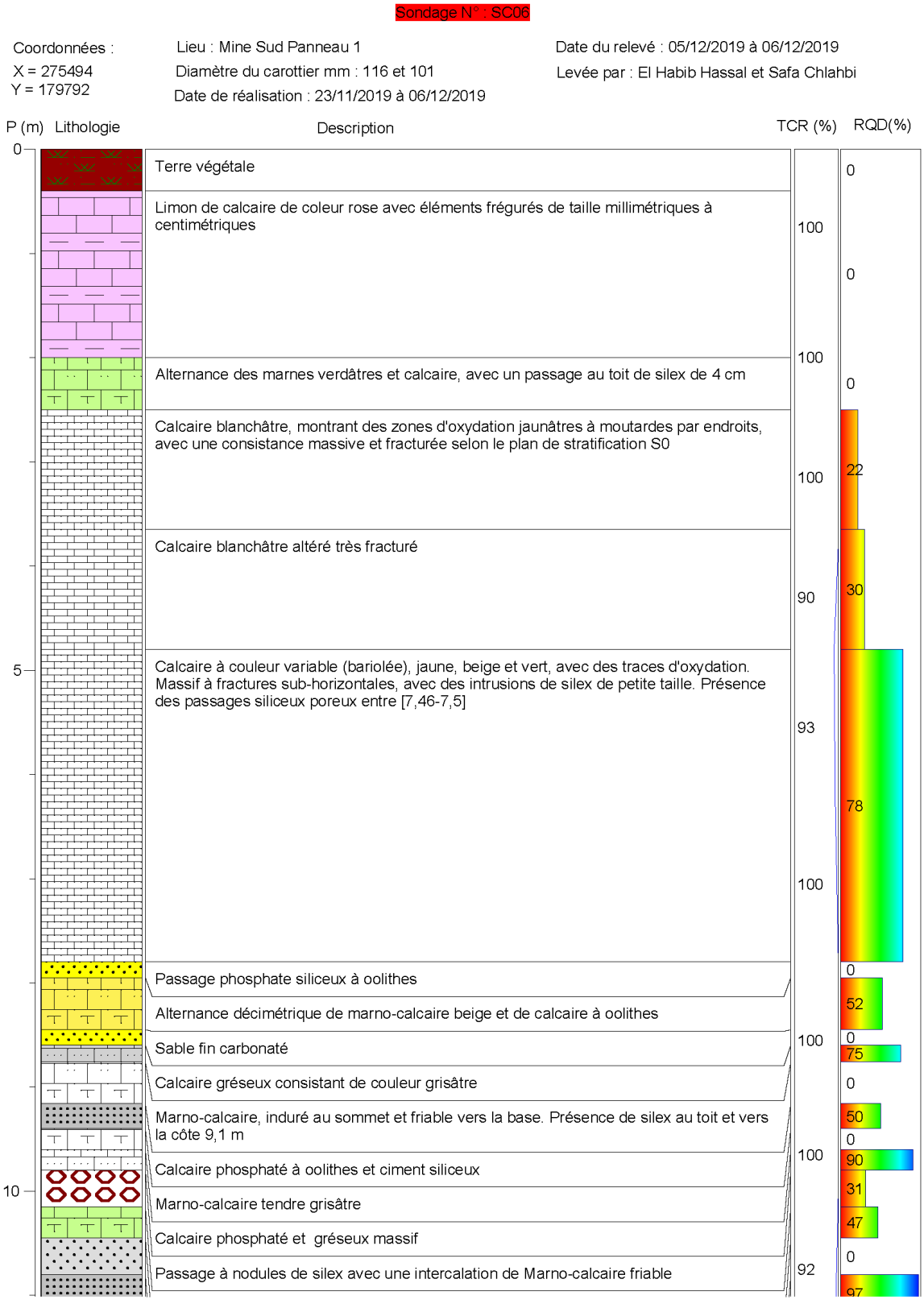

Figure A. 27: Litho-stratigraphic section for the SC06 drill core

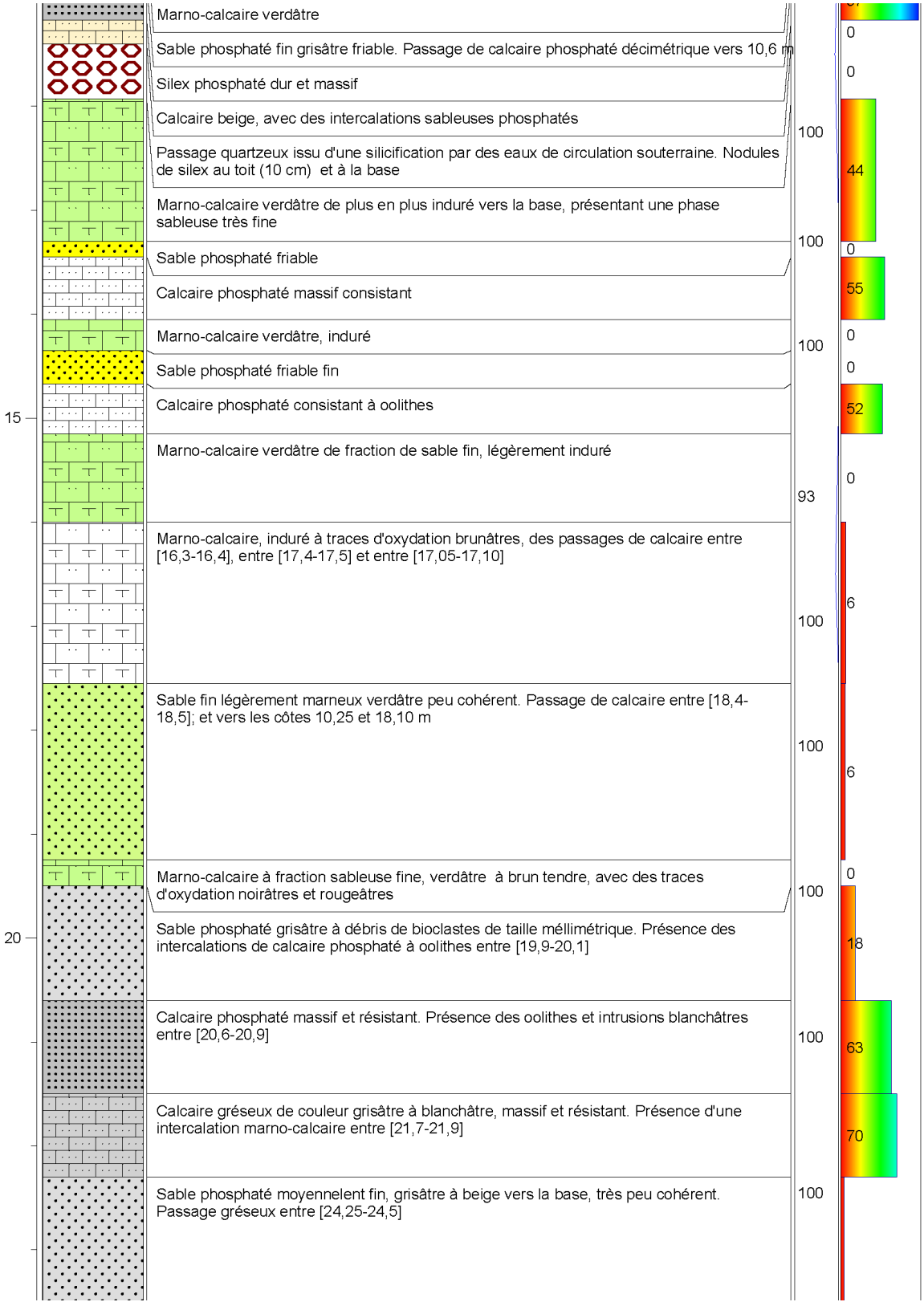

Figure A. 28: Litho-stratigraphic section for the SC06 drill core (Continued)

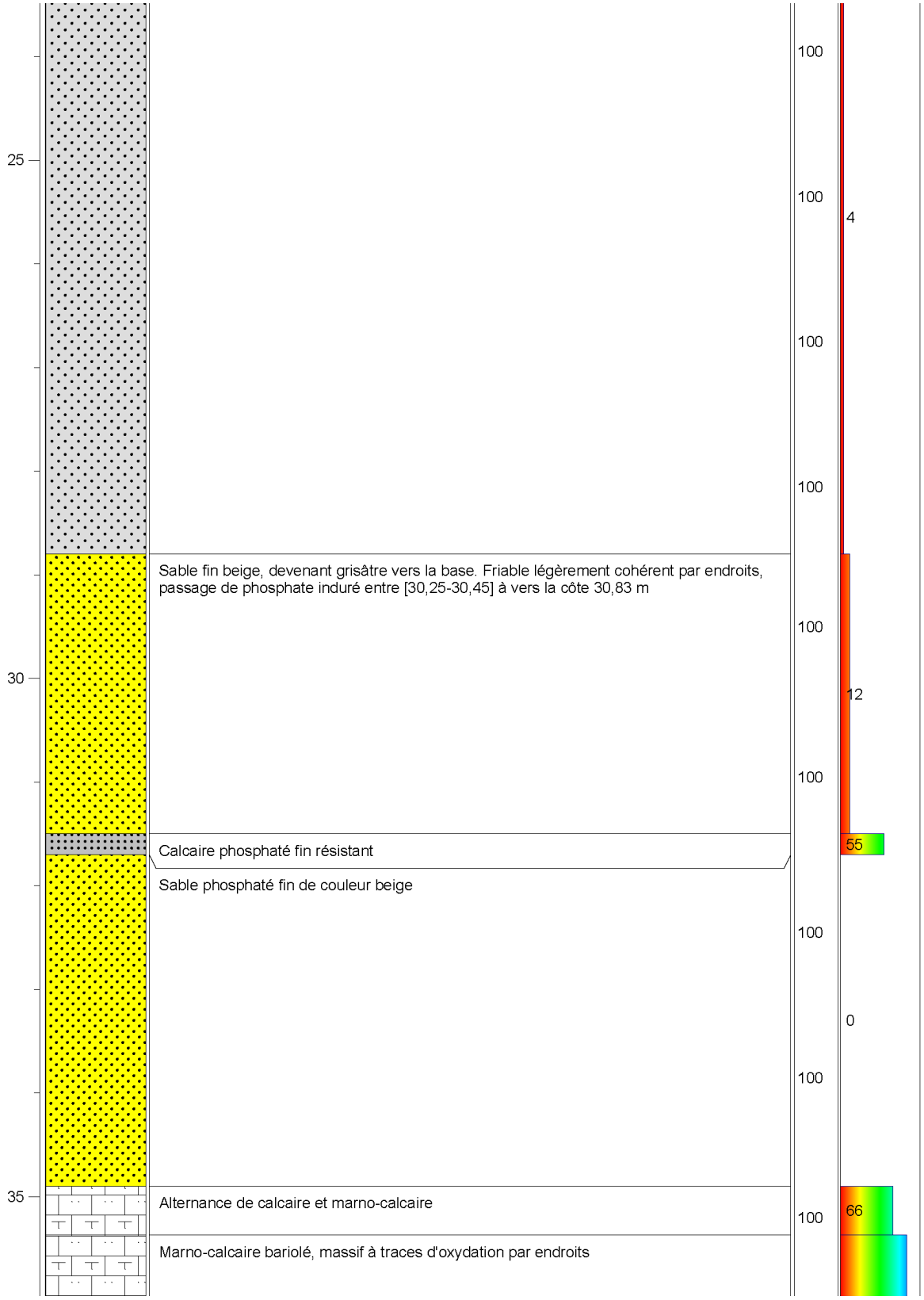

Figure A. 29: Litho-stratigraphic section for the SC06 drill core (Continued)

Figure A. 30: Litho-stratigraphic section for the SC06 drill core (Continued)

Figure A. 31: Litho-stratigraphic section for the SC06 drill core (Continued)

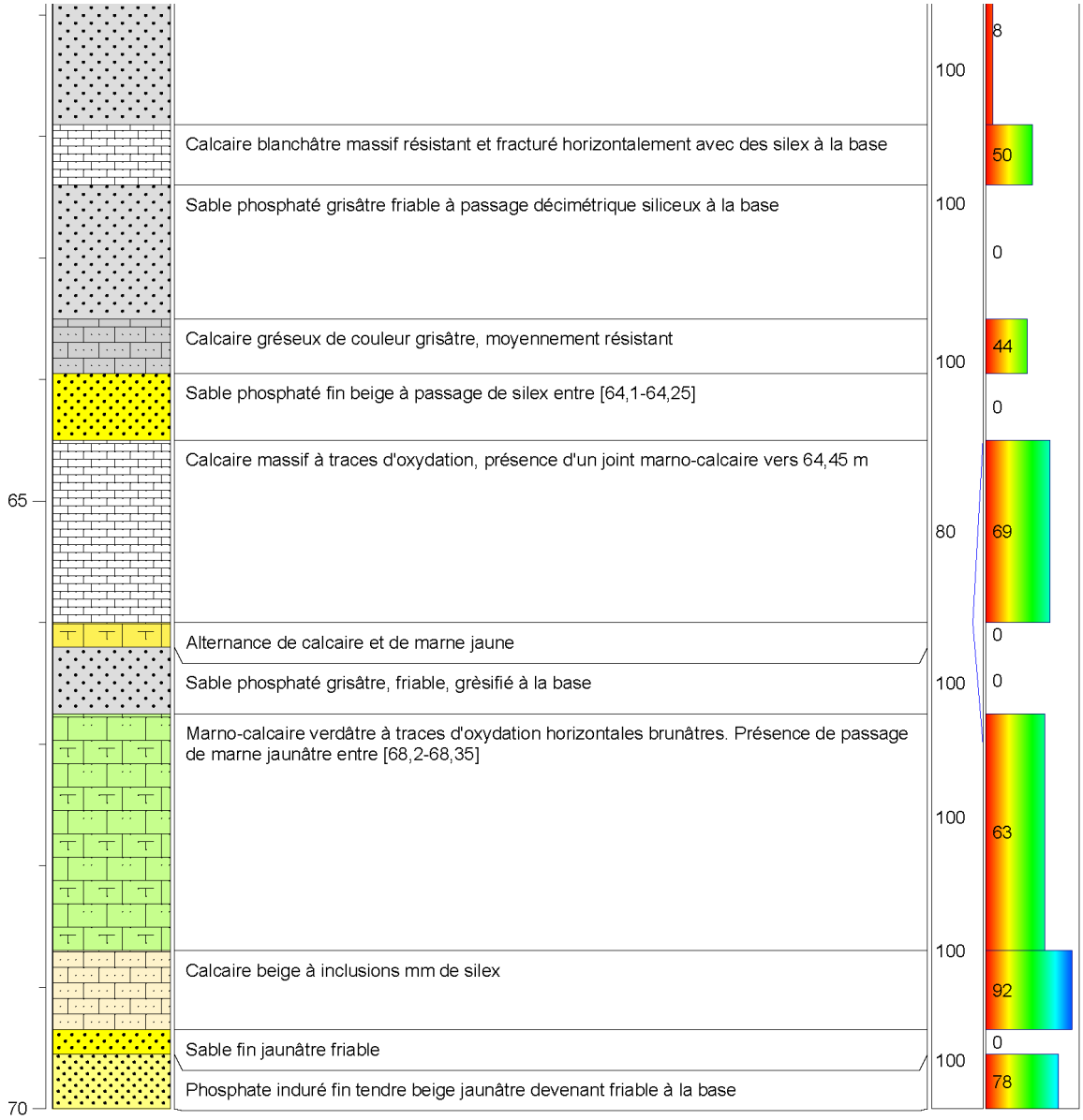

Figure A. 32: Litho-stratigraphic section for the SC06 drill core (Continued)

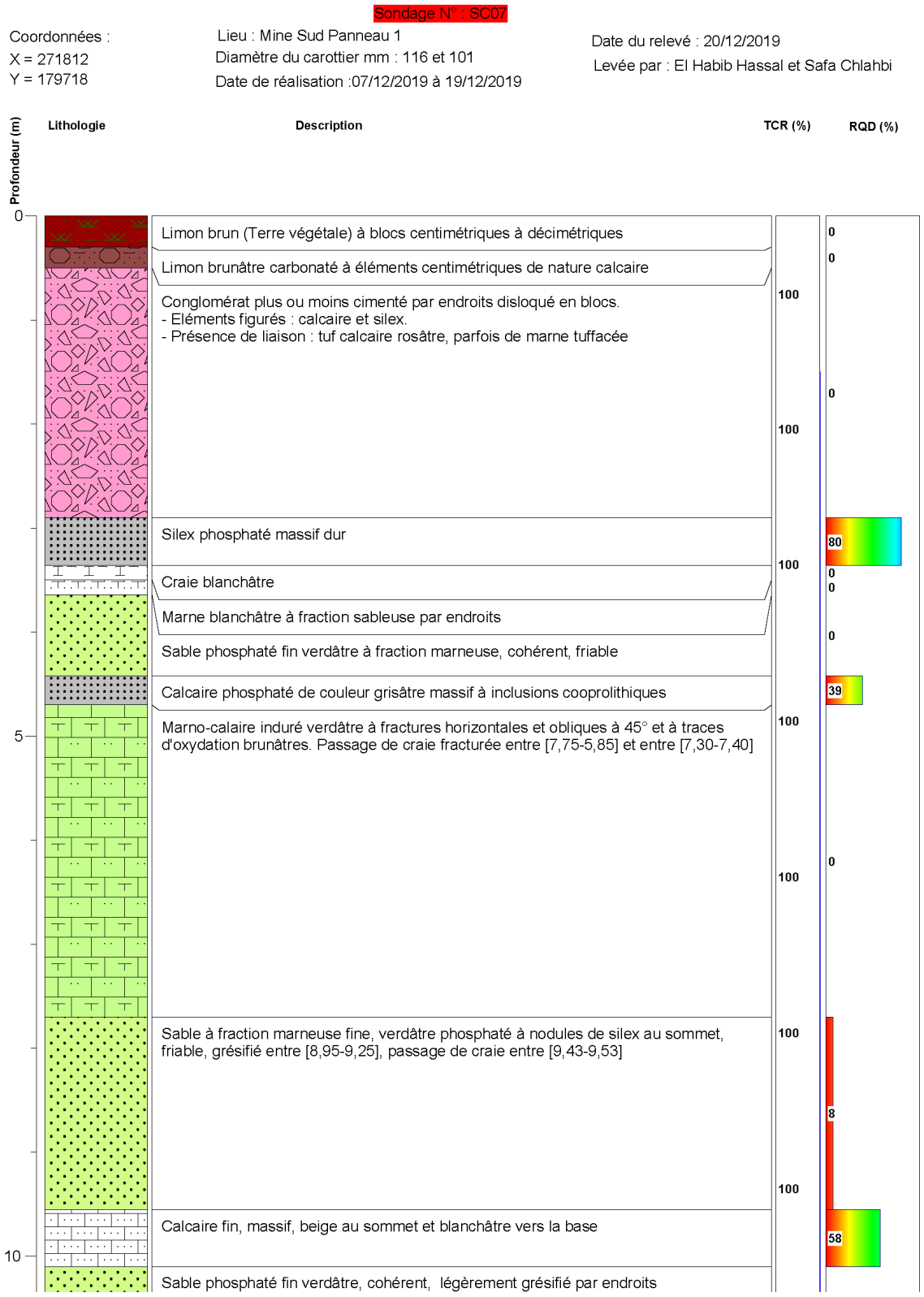

Figure A. 33: Litho-stratigraphic section for the SC07 drill core

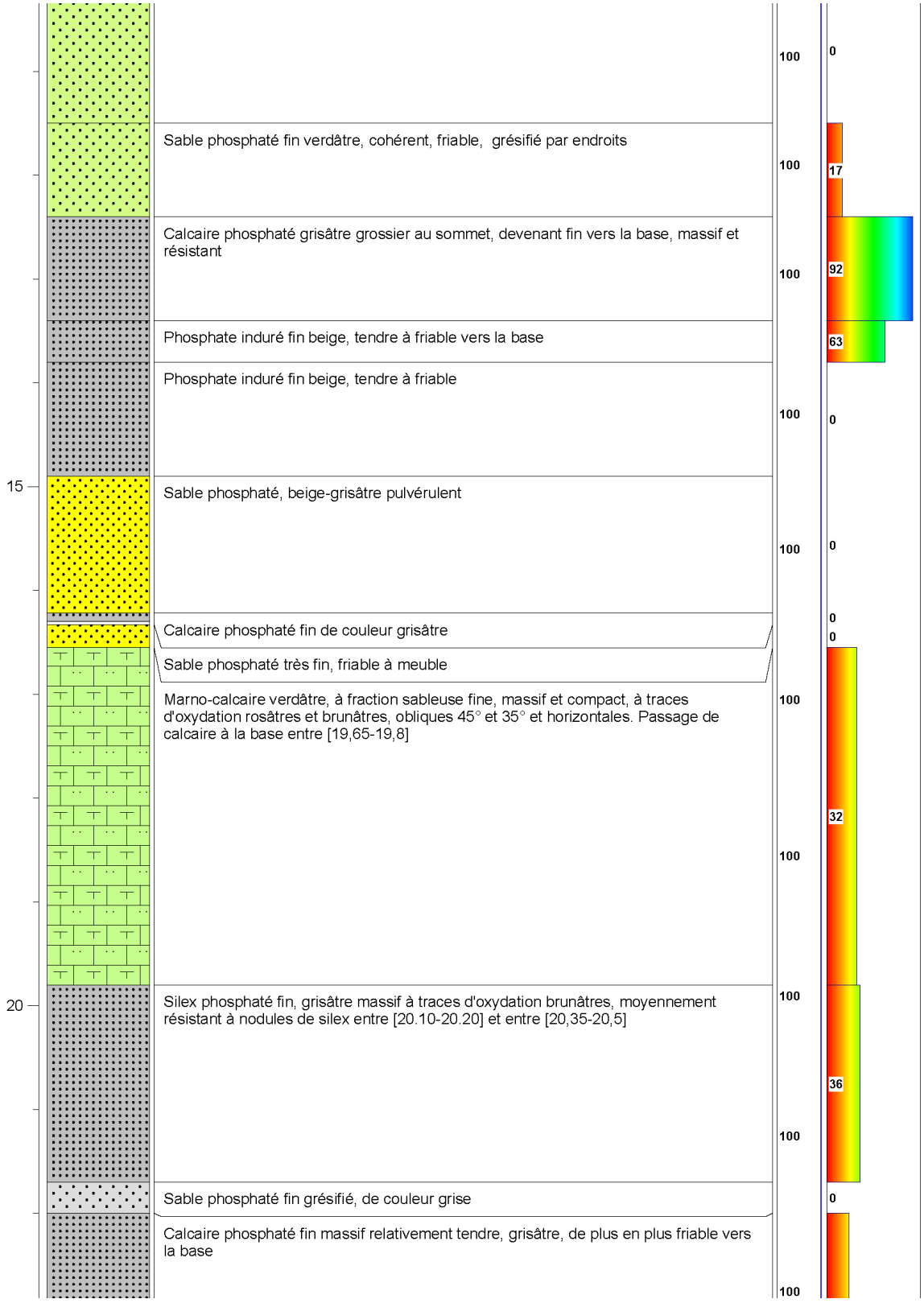

Figure A. 34: Litho-stratigraphic section for the SC07 drill core (Continued)

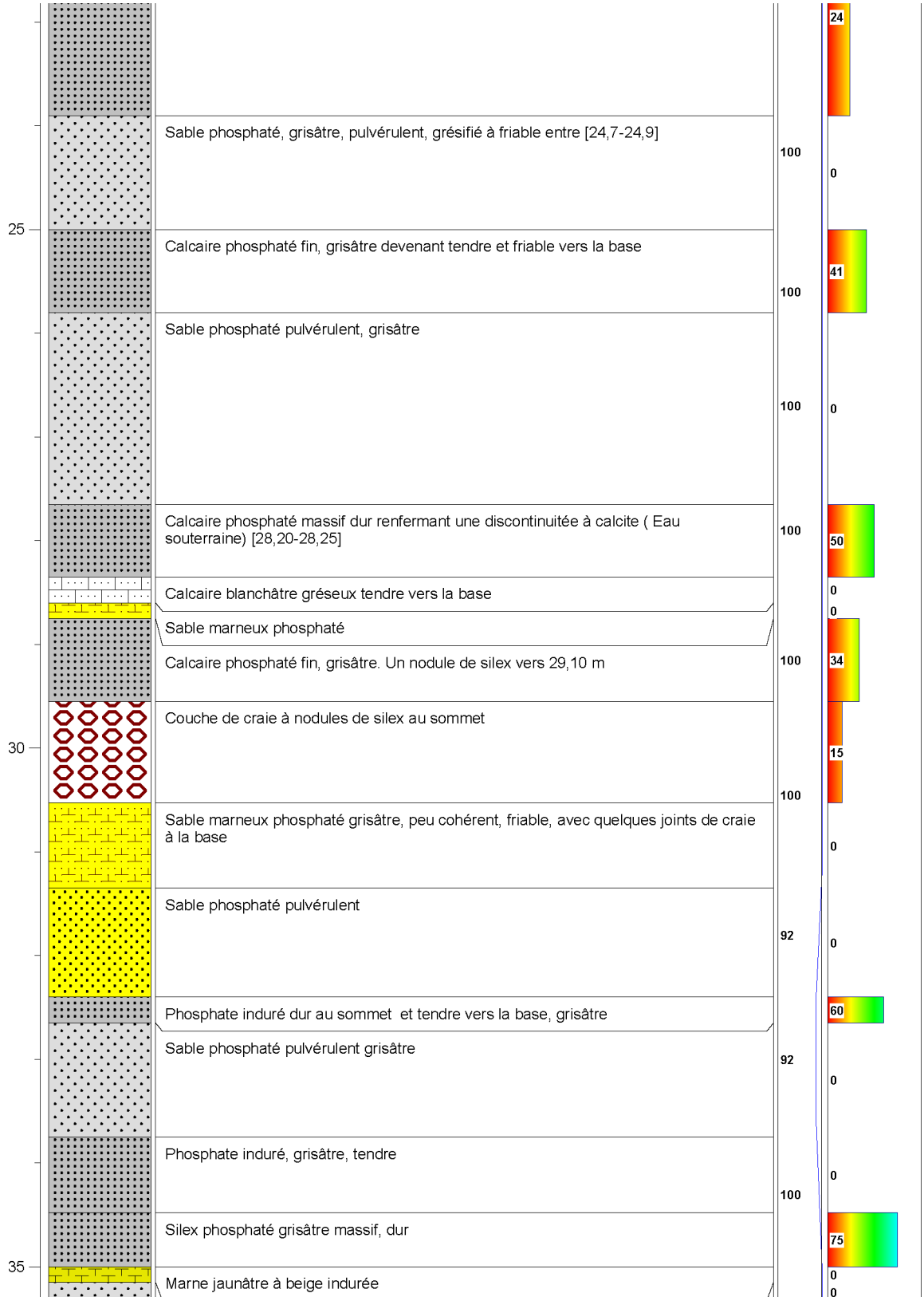

Figure A. 35: Litho-stratigraphic section for the SC07 drill core (Continued)

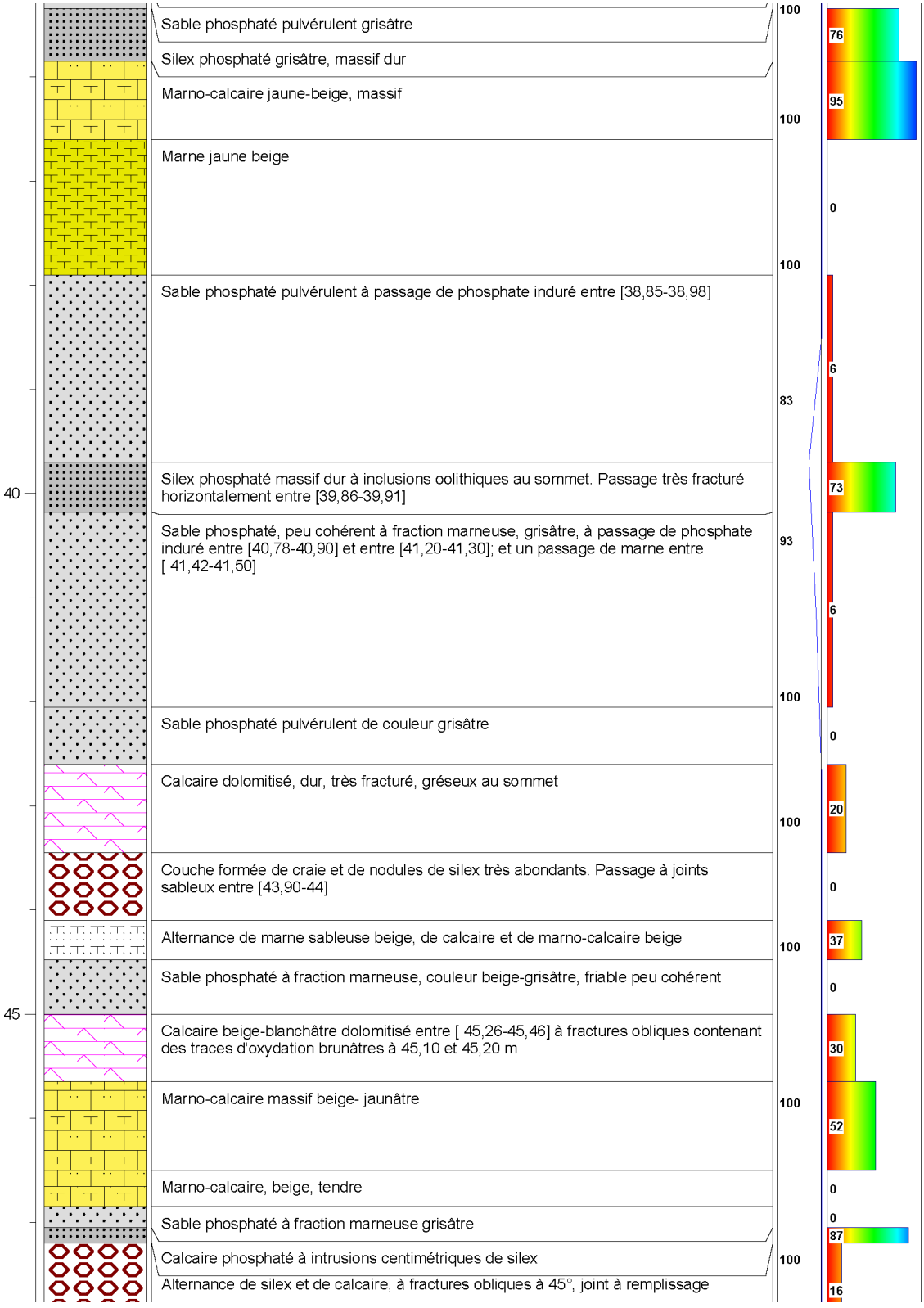

Figure A. 36: Litho-stratigraphic section for the SC07 drill core (Continued)

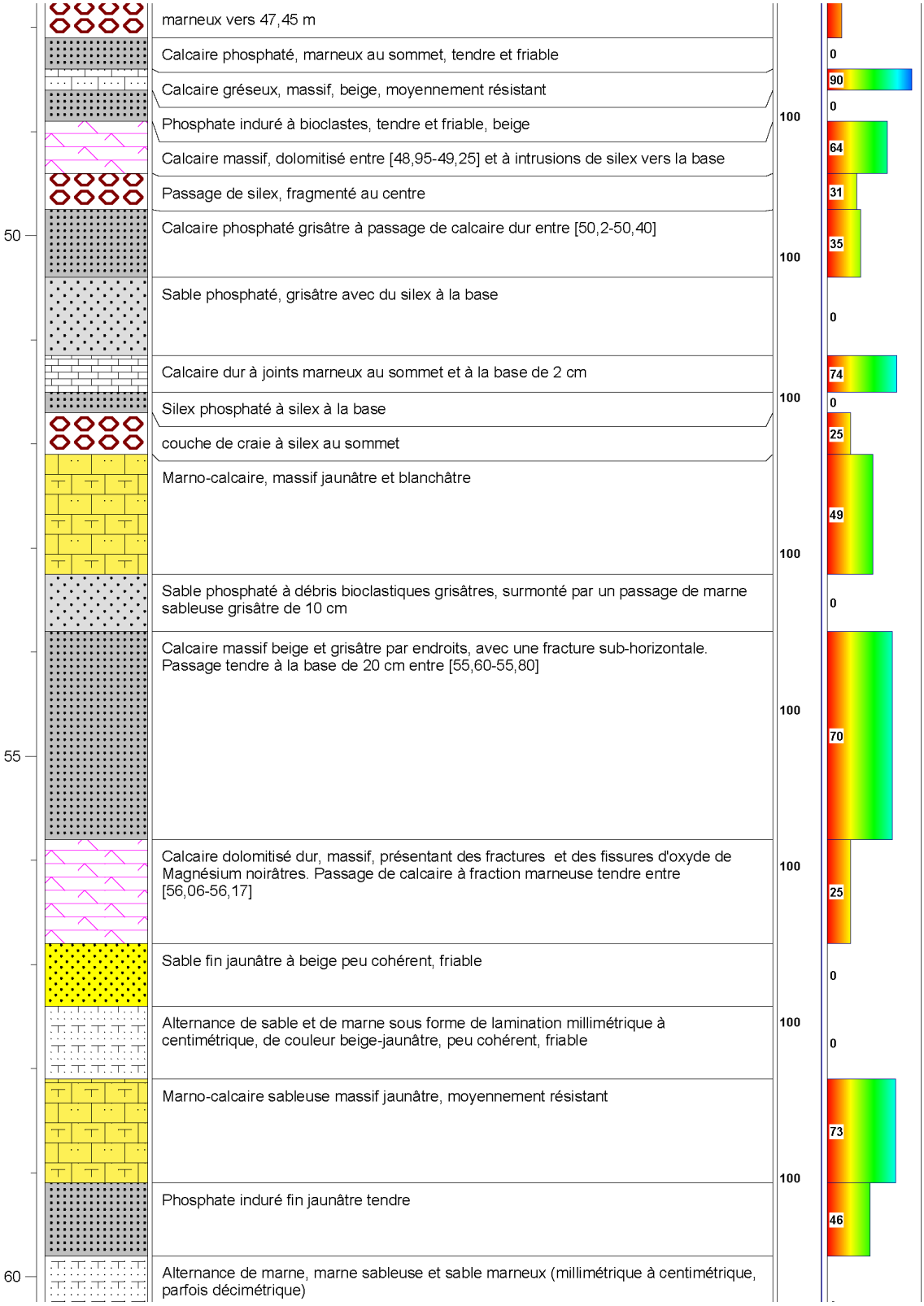

Figure A. 37: Litho-stratigraphic section for the SC07 drill core (Continued)

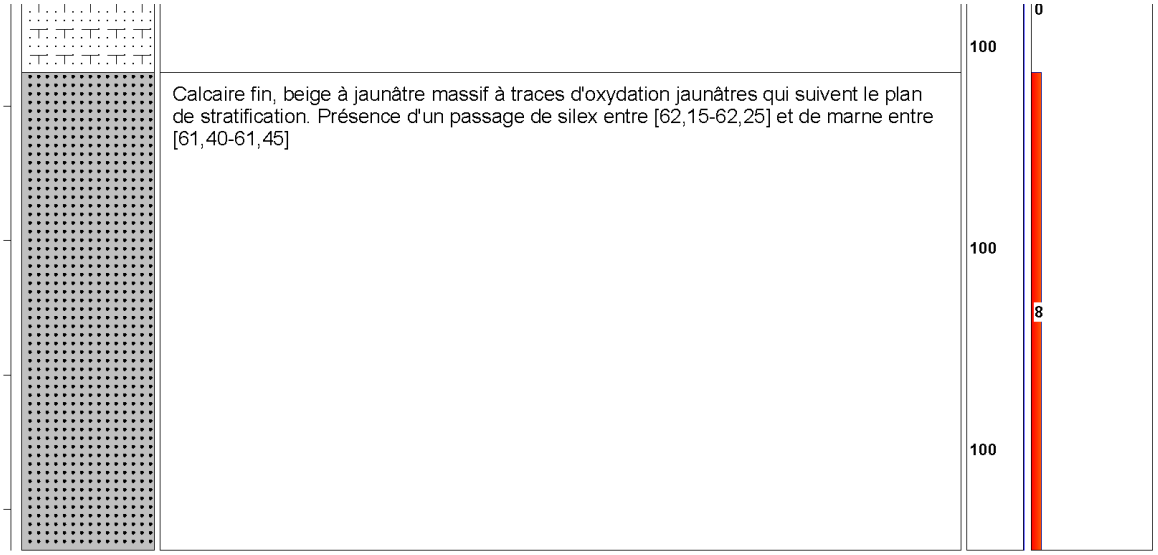

Figure A. 38: Litho-stratigraphic section for the SC07 drill core (Continued)

3. Some photographs of the sampling mission (core drilling and mining trenches)

Figure A. 39: Collecting and preparing samples from core drills

Figure A. 40: Sampling from mining trenches

APPENDIX B Supplementary material of article 1: Geological and geomechanical characterizations of phosphate mine waste rocks in view of their potential civil applications: a case study of the benguerir mine site, morocco

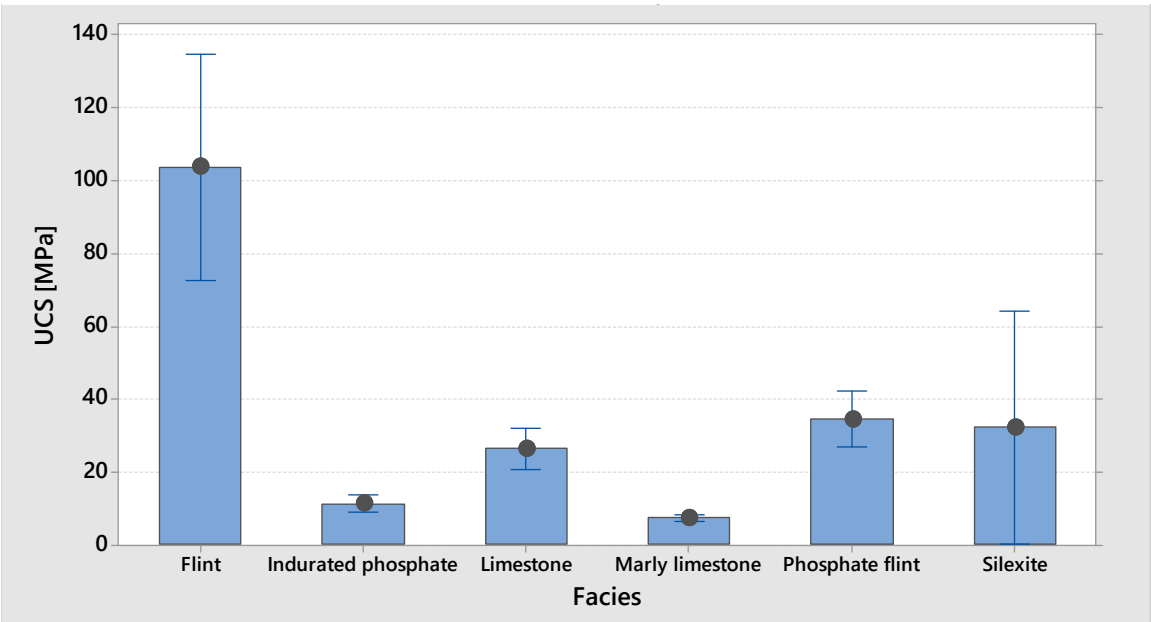

Figure B. 1: The UCS intervals for the six facies.

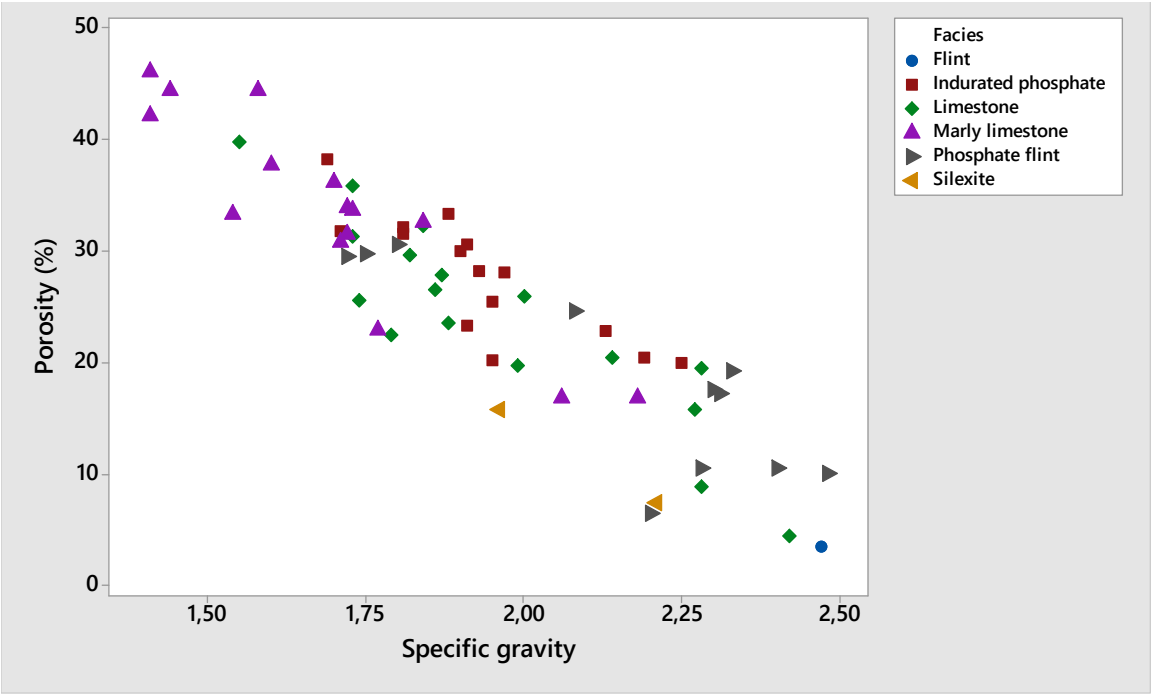

Figure B. 2: Variation of specific gravity with porosity for the six facies

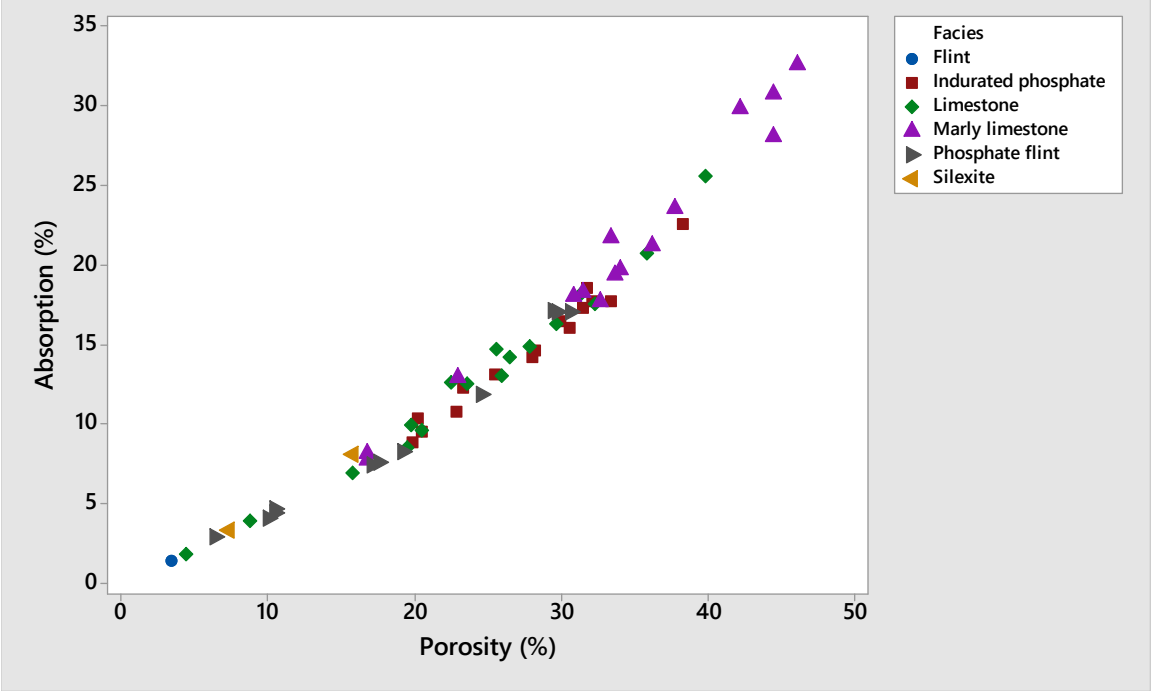

Figure B. 3: Variation of porosity with absorption for the five facies

APPENDIX C Supplementary material of article 2: An upstream geo-environmental assessment of sedimentary phosphate waste rock

1. The results of major elements, trace elements (TEs), and rare-earth elements (REE)

Table C. 1: The results of major elements, trace elements (TEs), and rare-earth elements (REE) of samples S2-I1 to S2-I10

Samples		**S2-I1**	**S2-I2**	**S2-I3**	**S2-I4**	**S2-I5**	**S2-I6**	**S2-I7**	**S2-I8**	**S2-I9**	**S2-I10**
Major oxides (wt.%)	D.L (%)										
SiO_2	0.01	7.86	4.81	7.13	4.06	9.76	15.15	10.55	24.2	20.4	50.14
Al_2O_3	0.01	0.51	0.52	1.26	0.38	0.57	0.43	2.3	1.38	1.42	1.71
Fe_2O_3	0.01	0.18	0.23	0.37	0.21	0.27	0.17	0.99	0.47	0.49	0.86
CaO	0.01	49.6	50.87	31.9	53.5	47.08	47.7	26.9	33.7	36.2	22.33
MgO	0.01	0.51	0.62	17.75	0.61	0.77	0.62	17.6	6.73	6.96	2.08
Na_2O	0.01	0.52	0.57	0.05	0.13	0.24	0.33	0.03	0.17	0.16	0.13
K_2O	0.01	0.07	0.08	0.13	0.05	0.11	0.13	0.12	0.35	0.35	0.31
TiO2	0.001	0.03	0.029	0.08	0.02	0.039	0.06	0.14	0.16	0.19	0.172
P_2O_5	0.01	20.7	21.43	0.38	2.92	7.98	13.75	0.42	5.62	6.03	3.37
LOI		18.35	19.1	42.5	39.1	31.19	23.1	40.7	27.6	29	18.51
Total		98.49	98.25	101.58	101.08	98	101.55	99.79	100.5	101.29	99.61
Trace elements (ppm)	D. L (ppm)										
Ba	2	119.5	168	28.4	155.5	77	96.2	25.3	81.8	80.8	65
Cr	20	280	180	40	70	120	160	50	200	170	220
Cs	0.1	0.21	0.2	0.39	0.14	0.2	0.14	0.49	0.49	0.49	0.8
Ga	1	1.2	2	1.6	0.6	2	0.7	3.2	2	2	3
Hf	0.1	0.6	0.4	0.6	0.2	1.1	1.4	0.8	3.1	3.8	0.8
Nb	0.2	0.6	0.5	1.4	0.4	0.7	1.2	2.2	3.1	4	3.1

Table C. 2: The results of major elements, trace elements (TEs), and rare-earth elements (REE) of samples S2-I1 to S2-I10 (continued)

Samples		**S2-I1**	**S2-I2**	**S2-I3**	**S2-I4**	**S2-I5**	**S2-I6**	**S2-I7**	**S2-I8**	**S2-I9**	**S2-I10**
Trace elements (ppm)	D.L (ppm)										
Rb	1	3.7	4	5.9	2.4	4	4	6.3	11.3	11.8	13
Sr	2	912	937	177.5	653	592	675	86.8	365	346	278
Th	0.05	1.84	1	0.99	0.6	1.98	1.34	1.58	1.94	1.79	1.31
U	0.01	85.6	87.1	2.01	19.1	37.8	40.6	1.84	13.4	11.55	7.52
V	5	130	146	25	41	61	86	154	57	37	60
Zr	1	37	21	25	12	49	66	32	143	169	35
As	5	8.6	6	1.5	2.3	6	2.7	5.1	2.7	2.8	5
Sb	0.2	0.65	0.7	0.55	0.54	1.2	0.88	0.33	0.79	0.69	1.6
Se	0.1	2.6	0.9	0.8	2	1.7	1.8	0.4	1.5	1.2	0.5
Cd	0.5	18	7	0.6	12.4	14.2	30.7	10.6	16.9	19.1	48.7
Cu	10	26	30	7	14	30	11	7	16	13	30
Mo	5	10	3	6	13	11	6	<1	2	1	3
Ni	20	202	30	47	22	40	40	66	76	72	70
Pb	5	2	< 5	3	3	< 5	4	5	6	5	< 5
Sc	1	4	3	1	2	4	3	2	3	3	3
Zn	30	204	170	102	91	110	148	194	241	240	230
Y	0.5	184	106	9.5	49.5	117	73.9	4.2	37	35.4	20

Table C. 3: The results of major elements, trace elements (TEs), and rare-earth elements (REE) of samples S2-I1 to S2-I10 (continued)

Samples		**S2-I1**	**S2-I2**	**S2-I3**	**S2-I4**	**S2-I5**	**S2-I6**	**S2-I7**	**S2-I8**	**S2-I9**	**S2-I10**
Rare earth element (ppm)	D. L (ppm)										
La	0.05	68.8	50.3	6.2	22.1	61.3	32.1	5.1	19	18.2	12.4
Ce	0.05	28	20	5.1	9.5	29	20.8	10.2	18.9	18.1	11.6
Pr	0.01	10.05	6.58	1.03	3.45	10.1	5.11	1.16	3.5	3.27	2.12
Nd	0.05	43.5	28.2	4.2	15.1	43.3	21.7	4.5	14.5	13.2	8.21
Sm	0.01	8.82	5.4	0.74	3.09	9.21	4.44	0.97	3	2.82	1.67
Eu	0.005	2.18	1.39	0.19	0.76	2.26	1.12	0.23	0.69	0.68	0.404
Gd	0.01	12.45	7.15	0.89	4.02	10.9	5.8	0.77	3.41	3.1	1.78
Tb	0.01	1.75	1.12	0.1	0.55	1.71	0.81	0.14	0.48	0.45	0.29
Dy	0.01	12.4	7.91	0.87	4.05	11.5	5.76	0.72	3.34	3.17	1.86
Ho	0.01	3.07	2.01	0.18	0.95	2.65	1.34	0.15	0.72	0.7	0.44
Er	0.01	10.05	6.48	0.57	3.08	8.14	4.52	0.47	2.47	2.29	1.36
Tm	0.005	1.42	0.929	0.07	0.4	1.1	0.62	0.06	0.36	0.32	0.196
Yb	0.01	9.39	6.36	0.52	2.88	7.15	4.2	0.4	2.41	2.29	1.29
Lu	0.002	1.57	1.11	0.07	0.46	1.54	0.68	0.07	0.36	0.36	0.249
SLREE	-	159.17	110.5	17.27	53.24	152.9	84.15	21.93	58.9	55.59	36
SHREE	-	54.28	34.46	3.46	17.15	46.95	24.85	3.01	14.24	13.36	7.869
SREE	-	213.45	144.9	20.73	70.39	199.9	109	24.94	73.14	68.95	43.87

Table C. 4: The results of major elements, trace elements (TEs), and rare-earth elements (REE) of samples S2-I11 to S2-I20

Samples		**S2-I11**	**S2-I12**	**S2-I13**	**S2-I14**	**S2-I15**	**S2-I16**	**S2-I17**	**S2-I18**	**S2-I19**	**S2-I20**
Major oxides (wt.%)	D.L (%)										
SiO_2	0.01	22.4	17.3	4.51	12.23	2.38	2.87	65.7	10.68	23.57	37.6
Al_2O_3	0.01	1.88	1.98	0.93	1.24	0.42	0.41	1.78	1.46	5.15	8.94
Fe_2O_3	0.01	0.69	0.77	0.37	0.47	0.2	0.3	0.72	0.63	2.15	3.59
CaO	0.01	32.1	30.3	50.8	44.24	36.1	51.14	10.15	26.69	19.32	12.05
MgO	0.01	6.81	12.75	1.54	1.7	16.2	0.45	5.23	19.5	14.02	8.83
Na_2O	0.01	0.19	0.13	0.11	0.28	0.12	0.58	0.1	0.03	0.08	0.08
K_2O	0.01	0.37	0.38	0.11	0.23	0.04	0.04	0.34	0.07	0.34	0.47
TiO2	0.001	0.21	0.22	0.06	0.117	0.03	0.032	0.12	0.083	0.291	0.5
P_2O_5	0.01	7.18	3.65	2.61	9.78	4.43	24.77	1.21	0.16	0.42	0.63
LOI		26.2	33.5	39.1	28.37	40.7	17.17	14	41.59	33.75	25.4
Total		98.14	101.1	100.3	98.67	100.7	97.77	99.41	100.9	99.11	98.14

Table C. 5: The results of major elements, trace elements (TEs), and rare-earth elements (REE) of samples S2-I11 to S2-I20 (continued)

Samples		**S2-I11**	**S2-I12**	**S2-I13**	**S2-I14**	**S2-I15**	**S2-I16**	**S2-I17**	**S2-I18**	**S2-I19**	**S2-I20**
Trace elements (ppm)	D. L (ppm)										
Ba	2	82.6	62.4	40.7	90	27.1	114	60.8	17	39	67.7
Cr	20	320	290	380	270	100	170	180	30	131	170
Cs	0.1	0.83	0.83	0.36	0.4	0.12	0.1	0.79	0.3	1.5	2.1
Ga	1	3.3	3.2	2.1	2	0.7	2	2.1	2	7.4	11.1
Hf	0.1	2.2	2.6	0.5	2.3	0.1	0.8	1.3	0.3	2	2.1
Nb	0.2	4.4	4.8	1.4	2.4	0.5	0.5	2.2	1.3	< 0.1	8.7
Rb	1	15.1	15.2	5.1	8	2	2	12.3	4	20.4	25.6
Sr	2	476	283	976	661	318	1122	122.5	86	103	110
Th	0.05	1.87	1.88	0.8	3.25	0.57	1.77	1.46	0.9	3.7	6.03
U	0.01	16.5	9.05	11.15	46.4	20.7	77.5	7.11	1.03	1.8	3.27
V	5	75	67	83	281	93	96	148	127	180	283
Zr	1	97	106	25	103	9	43	55	14	14	80
As	5	2.3	1.9	4.3	5	1.1	5	3.2	5	8.7	8
Sb	0.2	0.38	0.56	1.6	1.1	0.3	1.1	0.58	0.2	0.9	0.56
Se	0.1	1.1	1.1	2.4	0.3	1.3	1	0.3	0.4	0.5	31.2
Cd	0.5	18.7	12.4	52.2	51.1	18.4	58	8	9.9	4.2	7.6
Cu	10	36	29	43	30	7	30	15	< 10	9.5	13
Mo	5	1	2	5	< 2	1	7	2	< 2	4.46	<1
Ni	20	82	93	110	140	39	50	78	30	79.5	147
Pb	5	5	5	4	< 5	2	< 5	5	< 5	4.9	9
Sc	1	4	4	3	8	1	6	2	1	5.1	9
Zn	30	300	293	279	370	229	290	254	90	308	382
Y	0.5	39.4	28.5	26.3	128	18.8	62.6	13	1.9	7.5	11

Table C. 6: The results of major elements, trace elements (TEs), and rare-earth elements (REE) of samples S2-I11 to S2-I20 (continued)

Samples		**S2-I11**	**S2-I12**	**S2-I13**	**S2-I14**	**S2-I15**	**S2-I16**	**S2-I17**	**S2-I18**	**S2-I19**	**S2-I20**
Rare earth element (ppm)	D. L (ppm)										
La	0.05	20.5	15.6	11.8	63	7.4	27.6	7.8	2.77	11.5	16.9
Ce	0.05	18.6	16.4	6.9	34.7	5.6	20.9	10.5	5.41	23.4	36
Pr	0.01	3.51	2.85	1.94	10.5	1.15	4.25	1.58	0.64	2.7	4.07
Nd	0.05	14.4	11.9	8.3	44.9	4.9	18.1	6.4	2.25	10.5	15.5
Sm	0.01	2.95	2.41	1.68	9.57	1.03	3.8	1.34	0.46	2.2	3.09
Eu	0.005	0.7	0.55	0.37	2.39	0.26	0.973	0.3	0.103	0.43	0.64
Gd	0.01	3.24	2.6	2.06	11.7	1.41	4.74	1.33	0.38	1.7	2.49
Tb	0.01	0.44	0.39	0.29	1.85	0.17	0.73	0.18	0.05	1.3	0.33
Dy	0.01	3.41	2.72	2.19	12.5	1.4	5.06	1.27	0.32	0.2	2.06
Ho	0.01	0.76	0.57	0.52	2.92	0.3	1.21	0.25	0.06	0.3	0.34
Er	0.01	2.58	1.98	1.64	8.94	1.09	3.87	0.91	0.19	0.8	1.05
Tm	0.005	0.37	0.27	0.24	1.25	0.16	0.581	0.12	0.027	0.1	0.15
Yb	0.01	2.54	1.84	1.67	8.44	1.17	4.04	0.82	0.21	0.7	1.02
Lu	0.002	0.39	0.31	0.26	1.41	0.16	0.725	0.15	0.048	0.1	0.14
SLREE	-	59.96	49.16	30.62	162.67	20.08	74.65	27.62	11.53	50.3	75.56
SHREE	-	14.43	11.23	9.24	51.4	6.12	21.929	5.33	1.388	5.63	8.22
SREE	-	74.39	60.39	39.86	214.07	26.2	96.579	32.95	12.92	55.93	83.78

Table C. 7: The results of major elements, trace elements (TEs), and rare-earth elements (REE) of samples S2-I21 to S2-I30

Samples		**S2-I21**	**S2-I22**	**S2-I23**	**S2-I24**	**S2-I25**	**S2-I26**	**S2-I27**	**S2-I28**	**S2-I29**	**S2-I30**
Major oxides (wt.%)	D.L (%)										
SiO_2	0.01	47.53	84.8	49.3	68.8	5.22	5.01	54.08	94	29.5	17.85
Al_2O_3	0.01	10.84	0.28	0.42	0.64	0.98	0.66	0.34	0.42	1.06	1.51
Fe_2O_3	0.01	4.69	0.2	0.32	0.36	0.33	0.37	0.41	0.14	0.37	0.79
CaO	0.01	7.61	4.25	26	8.47	32.2	51.5	23.3	1.24	22	26.7
MgO	0.01	5.65	1.92	1.32	5.57	15.8	0.72	0.23	0.64	14.55	16
Na_2O	0.01	0.14	0.07	0.49	0.08	0.15	0.57	0.46	0.08	0.06	0.1
K_2O	0.01	0.8	0.05	0.1	0.12	0.16	0.11	0.07	0.11	0.21	0.31
TiO2	0.001	0.647	0.02	0.03	0.034	0.06	0.04	0.02	0.02	0.08	0.12
P_2O_5	0.01	1.31	0.72	15.05	0.52	5.65	23.1	14.56	0.16	0.58	2.23
LOI		20.35	6.04	7.64	13.65	37.5	17.15	5.7	2.91	32.4	35.4
Total		99.58	98.37	100.78	98.25	98.09	99.36	99.18	99.87	100.84	101.1

Table C. 8: The results of major elements, trace elements (TEs), and rare-earth elements (REE) of samples S2-I21 to S2-I30 (continued)

Samples		**S2-I21**	**S2-I22**	**S2-I23**	**S2-I24**	**S2-I25**	**S2-I26**	**S2-I27**	**S2-I28**	**S2-I29**	**S2-I30**
Trace elements (ppm)	D. L (ppm)										
Ba	2	80	62.5	77.8	74	24.2	65.5	301	1150	28.3	42.8
Cr	20	282	30	110	50	80	120	70	30	60	130
Cs	0.1	3.11	0.1	0.22	0.3	0.41	0.25	0.1	0.14	0.47	0.58
Ga	1	15.5	0.5	0.9	1	1.4	1.3	1	0.5	1.4	2.3
Hf	0.1	3	0.1	0.4	0.3	1	0.8	0.3	0.2	1	1.9
Nb	0.2	< 0.1	0.3	0.5	0.2	0.9	0.7	< 0.2	0.4	1.2	1.8
Rb	1	44	1.8	3.3	5	6.7	4.5	2	2.7	7.9	11.3
Sr	2	136	45.5	697	60	241	863	675	43.5	87	166
Th	0.05	8.1	0.19	1.35	0.43	1.22	1.94	1.07	0.3	0.96	1.63
U	0.01	5	3.58	62.8	3.07	24.3	120.5	85	1.8	3.39	12.4
V	5	269	61	266	110	54	124	124	27	65	132
Zr	1	3	8	29	15	45	43	22	8	46	86
As	5	14.8	1	3.4	< 5	1.8	9.5	5	0.8	0.9	3
Sb	0.2	2.4	0.4	0.9	0.2	0.26	0.57	1	0.13	0.25	1.65
Se	0.1	< 0.1	1.1	6.1	2.4	0.9	3	1.7	0.3	0.5	0.8
Cd	0.5	3.7	4.4	25.5	6	10.7	32.2	8.1	1.1	5.3	10.1
Cu	10	15.9	6	27	10	17	19	20	8	10	20
Mo	5	3.06	2	1	< 2	<1	1	< 2	2	<1	1
Ni	20	148	22	32	30	38	49	30	15	26	47
Pb	5	10.6	<2	6	< 5	2	6	< 5	<2	3	5
Sc	1	10.8	<1	4	< 1	3	3	2	<1	1	2
Zn	30	618	78	445	100	166	585	250	37	78	166
Y	0.5	17.9	2.4	69.7	2.8	29	69.4	35	1.4	5	17.7

Table C. 9: The results of major elements, trace elements (TEs), and rare-earth elements (REE) of samples S2-I21 to S2-I30 (continued)

Samples		**S2-I21**	**S2-I22**	**S2-I23**	**S2-I24**	**S2-I25**	**S2-I26**	**S2-I27**	**S2-I28**	**S2-I29**	**S2-I30**
Rare earth element (ppm)	D. L (ppm)										
La	0.05	25.1	1.2	25.8	2.05	12.4	28.8	17	1	3.8	9.3
Ce	0.05	51.6	1.4	17	2.91	12.4	24.5	13.8	1.6	6.5	13
Pr	0.01	6	0.21	3.62	0.4	2.04	4.89	2.65	0.19	0.87	1.94
Nd	0.05	22.7	0.9	15.8	1.59	8.9	20.6	11.5	0.8	3.4	7.8
Sm	0.01	4.3	0.15	3.31	0.32	1.93	4.4	2.35	0.26	0.69	1.79
Eu	0.005	0.96	0.05	0.83	0.071	0.48	1.12	0.607	0.02	0.15	0.35
Gd	0.01	3.4	0.14	4.46	0.31	2.53	5.55	2.76	0.12	0.6	1.85
Tb	0.01	3.1	<0.01	0.64	0.05	0.38	0.78	0.44	<0.01	0.07	0.25
Dy	0.01	0.5	0.16	4.74	0.31	2.51	5.49	3.01	0.11	0.56	1.86
Ho	0.01	0.6	0.01	1.17	0.07	0.62	1.24	0.67	<0.01	0.1	0.39
Er	0.01	1.8	0.12	4.11	0.22	2.02	4.13	2.02	0.09	0.36	1.26
Tm	0.005	0.2	0.01	0.55	0.033	0.29	0.55	0.296	<0.01	0.05	0.18
Yb	0.01	1.6	0.16	3.92	0.23	1.94	3.87	2.04	0.09	0.39	1.24
Lu	0.002	0.3	0.01	0.72	0.047	0.36	0.66	0.36	<0.01	0.06	0.2
SLREE	-	109.7	3.86	65.53	7.27	37.67	83.19	47.3	3.85	15.26	33.83
SHREE	-	12.46	0.66	21.14	1.341	11.13	23.39	12.203	0.43	2.34	7.58
SREE	-	122.16	4.52	86.67	8.611	48.8	106.58	59.503	4.28	17.6	41.41

2. Descriptive statistics (Quantitative data)

Table C. 10: Descriptive statistics (Quantitative data)

Variable	Observations	Minimum	Maximum	Average	Standard deviation
SiO2	30	2.400	94.000	26.985	25.769
Al2O3	30	0.300	10.800	1.728	2.419
Fe2O3	30	0.140	4.690	0.738	1.012
CaO	30	1.200	53.500	30.533	15.659
MgO	30	0.200	19.500	6.790	6.673
Na2O	30	0.030	0.580	0.207	0.179
K2O	30	0.040	0.800	0.204	0.169
TiO2	30	0.020	0.650	0.123	0.144
P2O5	30	0.160	24.800	6.712	7.642
LOI	30	3.000	43.000	25.640	11.837
Ba	30	17.000	1150.000	113.497	203.508
Cr	30	30.000	380.000	149.767	96.201
Cs	30	0.100	3.110	0.552	0.650
Ga	30	0.500	15.500	2.667	3.225
Hf	30	0.100	3.800	1.200	1.014
Nb	30	0.100	8.700	1.660	1.871
Rb	30	1.800	44.000	8.843	8.846
Sr	30	43.500	1122.000	409.793	331.158
Th	30	0.190	8.100	1.793	1.646
U	30	1.030	120.500	27.429	33.109
V	30	25.000	283.000	115.400	75.062
Zr	30	3.000	169.000	48.000	41.595
As	30	0.800	14.800	4.413	3.117
Sb	30	0.130	2.400	0.766	0.522
Se	30	0.100	31.200	2.330	5.578
Cd	30	0.600	58.000	17.527	16.014
Cu	30	6.000	43.000	18.647	10.062
Mo	30	1.000	13.000	3.317	3.212
Ni	30	15.000	202.000	65.017	45.171
Pb	30	2.000	10.600	4.650	1.909
Sc	30	1.000	10.800	3.330	2.421
Zn	30	37.000	618.000	234.933	141.113
Y	30	1.400	184.000	40.793	44.091
La	30	1.000	68.800	20.227	18.501
Ce	30	1.400	51.600	16.477	11.433
Pr	30	0.190	10.500	3.412	2.843
Nd	30	0.800	44.900	14.252	12.201

Table C. 11: Descriptive statistics (Quantitative data) (continued)

Variable	Observations	Minimum	Maximum	Average	Standard deviation
Sm	30	0.150	9.570	2.940	2.531
Eu	30	0.020	2.390	0.709	0.636
Gd	30	0.120	12.450	3.455	3.304
Tb	30	0.010	3.100	0.629	0.699
Dy	30	0.110	12.500	3.399	3.540
Ho	30	0.010	3.070	0.811	0.841
Er	30	0.090	10.050	2.620	2.665
Tm	30	0.010	1.420	0.364	0.373
Yb	30	0.090	9.390	2.494	2.482
Lu	30	0.010	1.570	0.430	0.447

3. Correlation matrix (Pearson (n))

See Excel file.

4. Summary of Shapiro-Wilk test

Table C. 12: Summary of Shapiro-Wilk test

Variable\Test	Shapiro-Wilk
SiO2	**0.000**
Al2O3	**<0,0001**
Fe2O3	**<0,0001**
CaO	0.104
MgO	**0.000**
Na2O	**<0,0001**
K2O	**0.000**
TiO2	**<0,0001**
P2O5	**<0,0001**
LOI	0.190
Ba	**<0,0001**
Cr	0.055
Cs	**<0,0001**
Ga	**<0,0001**
Hf	**0.003**
Nb	**<0,0001**
Rb	**<0,0001**
Sr	**0.004**
Th	**<0,0001**

Table C. 13: Summary of Shapiro-Wilk test (Continued)

Variable\Test	Shapiro-Wilk
U	**<0,0001**
V	**0.001**
Zr	**0.001**
As	**0.002**
Sb	**0.004**
Se	**<0,0001**
Cd	**0.000**
Cu	**0.018**
Mo	**<0,0001**
Ni	**0.001**
Pb	**0.000**
Sc	**0.000**
Zn	**0.015**
Y	**<0,0001**
La	**0.000**
Ce	**0.037**
Pr	**0.001**
Nd	**0.001**
Sm	**0.000**
Eu	**0.000**
Gd	**0.000**
Tb	**<0,0001**
Dy	**<0,0001**
Ho	**<0,0001**
Er	**0.000**
Tm	**0.000**
Yb	**0.000**
Lu	**<0,0001**

5. Kaiser-Meyer-Olkin measure of sampling adequacy (raw data)

Table C. 14: Kaiser-Meyer-Olkin measure of sampling adequacy (raw data)

SiO2	0.417
Al2O3	0.524
Fe2O3	0.779
CaO	0.518
MgO	0.527
Na2O	0.533
K2O	0.624

Table C. 15: Kaiser-Meyer-Olkin measure of sampling adequacy (raw data) (Continued)

TiO2	0.712
P2O5	0.552
LOI	0.340
Ba	0.294
Cr	0.503
Cs	0.635
Ga	0.545
Hf	0.393
Nb	0.377
Rb	0.570
Sr	0.556
Th	0.618
U	0.551
V	0.642
Zr	0.206
As	0.467
Sb	0.517
Se	0.362
Cd	0.383
Cu	0.515
Mo	0.359
Ni	0.424
Pb	0.529
Sc	0.817
Zn	0.541
Y	0.709
La	0.684
Ce	0.770
Pr	0.761
Nd	0.609
Sm	0.614
Eu	0.644
Gd	0.863
Tb	0.697
Dy	0.634
Ho	0.660
Er	0.687
Tm	0.679
Yb	0.602
Lu	0.848
KMO	0.594

6. Normal Q-Q plots

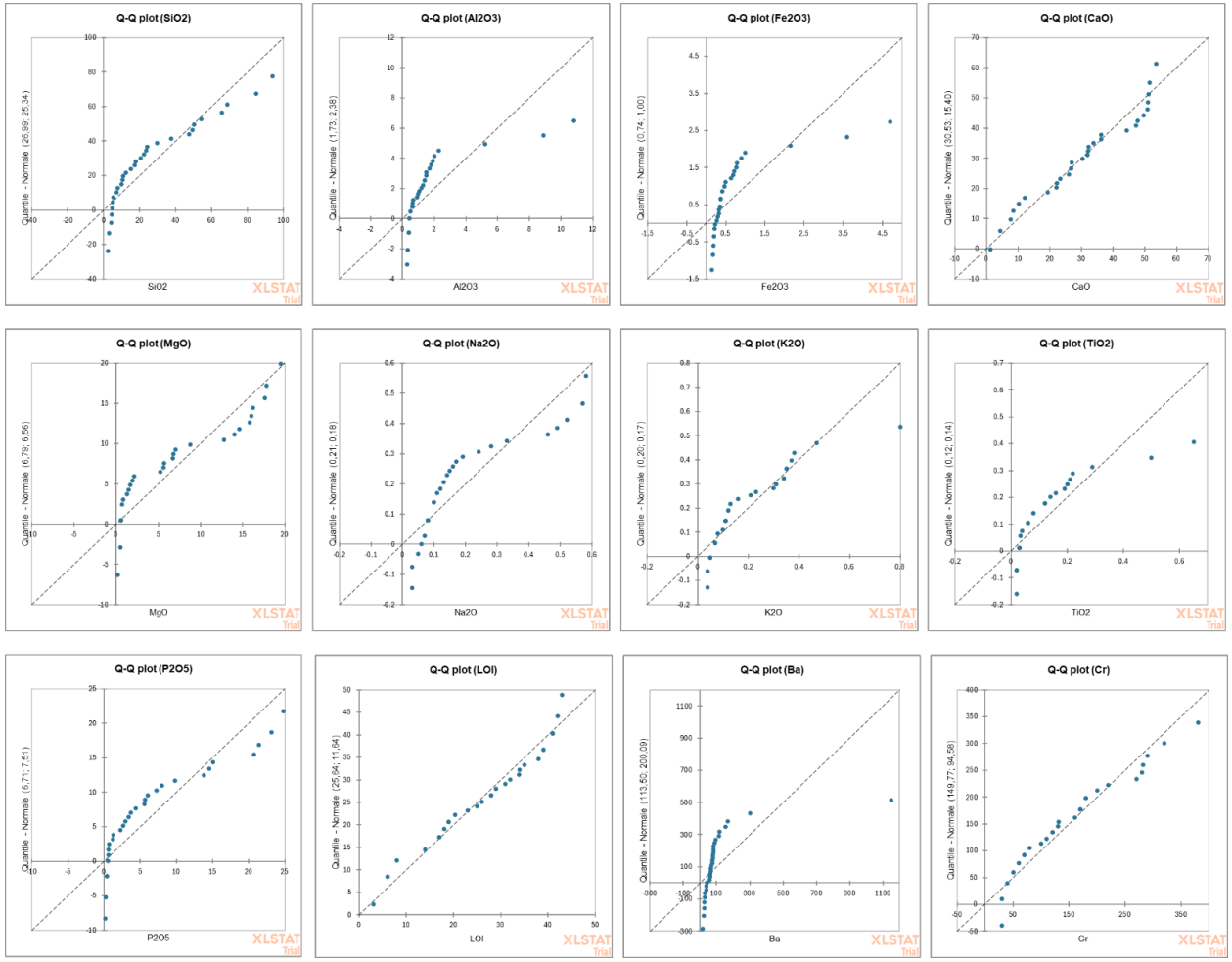

Figure C. 1: Normal Q-Q plots

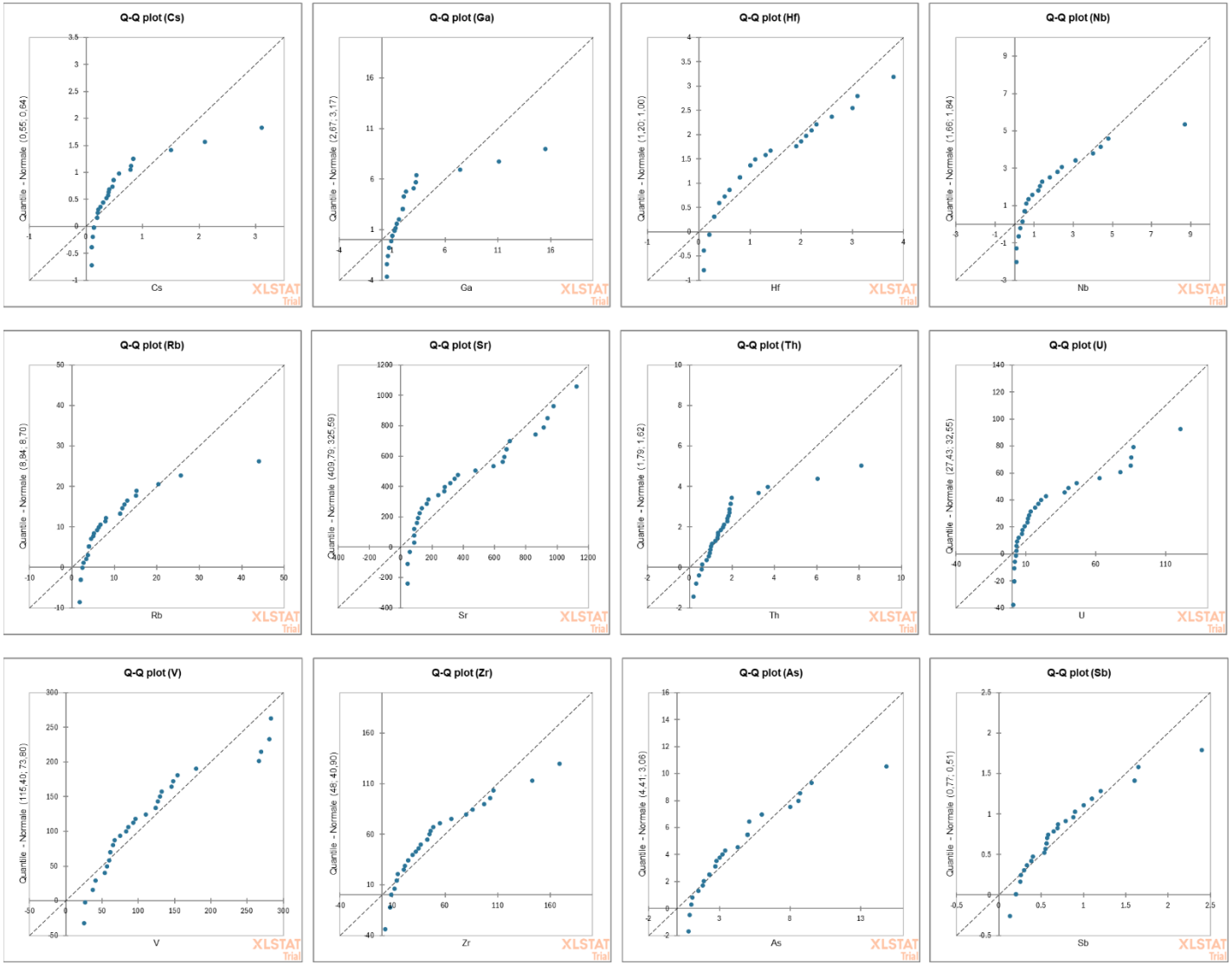

Figure C. 2: Normal Q-Q plots (continued)

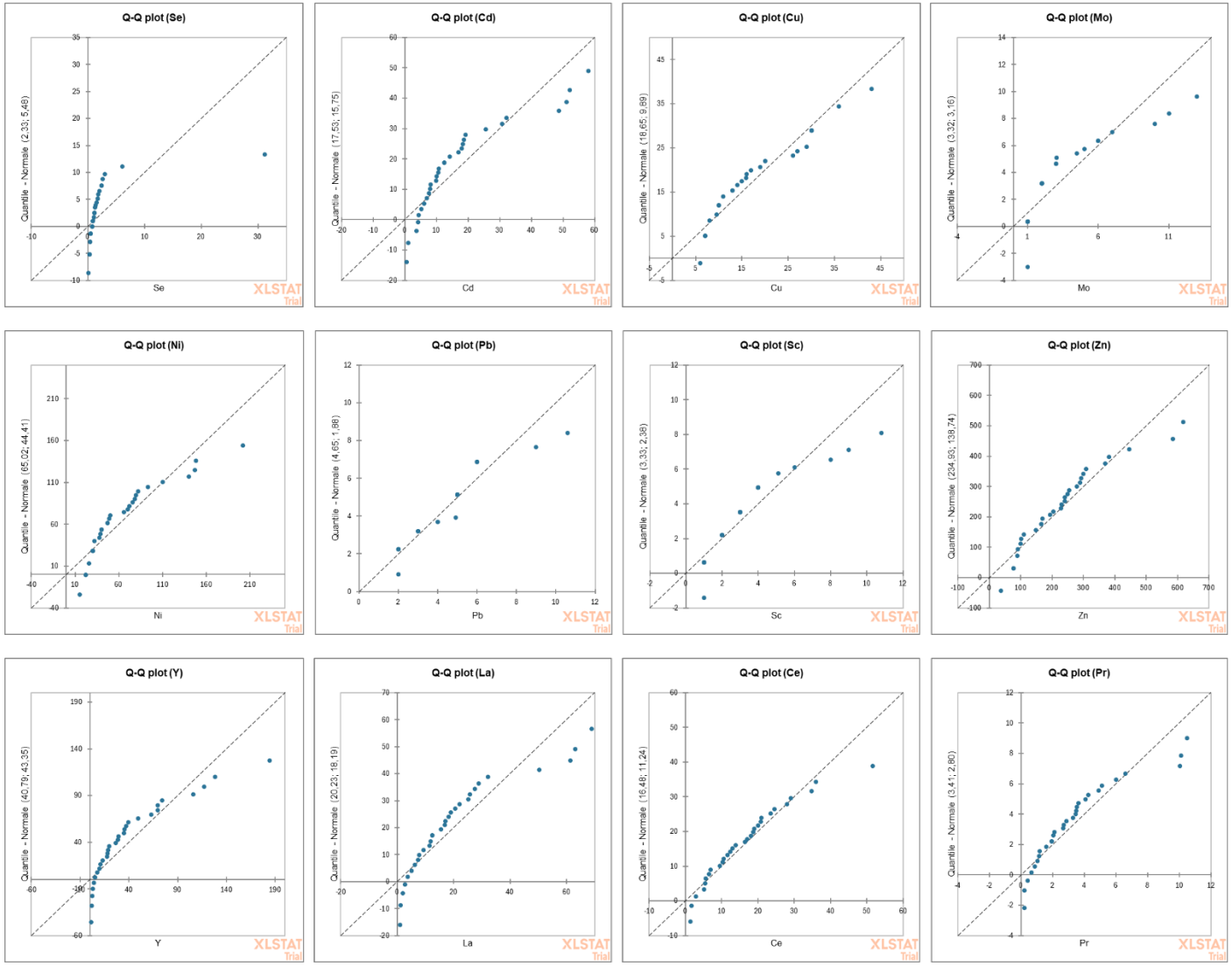

Figure C. 3: Normal Q-Q plots (continued)

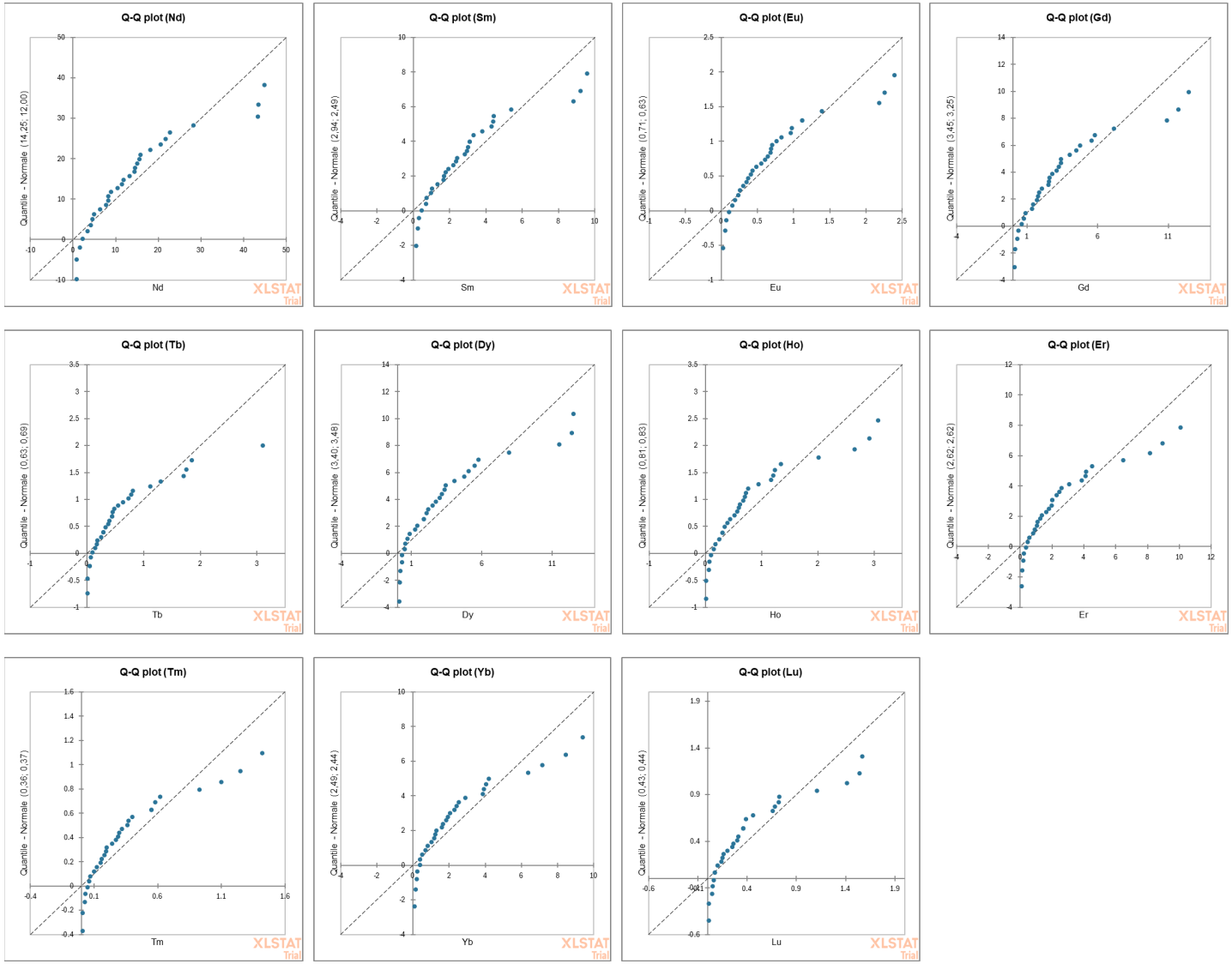

Figure C. 4: Normal Q-Q plots (continued)

7. Results of the CLR transformation of the initial dataset

Table C. 16: Results of the CLR transformation of the initial dataset (samples S2-I1 to S2-I10)

Samples	S2-I1	S2-I2	S2-I3	S2-I4	S2-I5	S2-I6	S2-I7	S2-I8	S2-I9	S2-I10
clr.SiO2	-0.00906	-0.23953	1.215537	0.125933	0.290249	0.982722	1.448897	1.43501	1.312055	2.405569
clr.Al2O3	-2.76907	-2.50129	-0.48219	-2.20134	-2.50296	-2.65486	-0.07905	-1.41487	-1.36701	-0.97782
clr.Fe2O3	-3.79073	-3.27782	-1.73881	-2.8457	-3.30147	-3.51053	-0.92201	-2.50637	-2.41683	-1.61381
clr.CaO	1.828064	2.12172	2.718048	2.694627	1.860139	2.126358	2.380169	1.766155	1.885579	1.596135
clr.MgO	-2.76907	-2.31897	2.134641	-1.79588	-2.21528	-2.2494	1.955942	0.150764	0.24243	-0.76651
clr.Na2O	-2.72985	-2.37026	-3.74029	-3.32528	-3.41925	-2.84724	-4.41852	-3.5233	-3.53606	-3.81104
clr.K2O	-4.73519	-4.33387	-2.78478	-4.28079	-4.19941	-3.77879	-3.03222	-2.80117	-2.7533	-2.71242
clr.TiO2	-5.58248	-5.3147	-3.27029	-5.19708	-5.21101	-4.55198	-2.87807	-3.58392	-3.36421	-3.11789
clr.P2O5	0.954207	1.255248	-1.66085	-0.22034	0.087308	0.886095	-1.82825	-0.02858	0.088279	-0.28468
clr.LOI	0.814445	1.136296	3.016642	2.378507	1.441853	1.396921	2.801615	1.580861	1.663816	1.435987
clr.Ba	2.707389	3.315821	2.601831	3.761591	2.351672	2.827856	2.318847	2.652934	2.688497	2.665935
clr.Cr	3.558863	3.384814	2.944322	2.963441	2.795358	3.336601	3.000066	3.546974	3.432318	3.885175
clr.Cs	-3.63657	-3.41758	-1.68617	-3.25117	-3.60157	-3.70469	-1.62531	-2.46469	-2.41683	-1.7316
clr.Ga	-1.89361	-1.115	-0.27455	-1.79588	-1.29899	-2.09525	0.251194	-1.0582	-1.01033	-0.40984
clr.Hf	-2.58675	-2.72443	-1.25538	-2.89449	-1.89682	-1.4021	-1.1351	-0.61994	-0.36848	-1.7316
clr.Nb	-2.58675	-2.50129	-0.40809	-2.20134	-2.34881	-1.55625	-0.1235	-0.61994	-0.31719	-0.37705
clr.Rb	-0.76759	-0.42185	1.030395	-0.40959	-0.60584	-0.35228	0.928592	0.67346	0.764619	1.056497
clr.Sr	4.739713	5.03454	4.434413	5.196523	4.391373	4.776139	3.551649	4.148554	4.142959	4.119169
clr.Th	-1.46616	-1.80814	-0.75461	-1.79588	-1.30904	-1.4459	-0.45453	-1.08866	-1.12126	-1.23842
clr.U	2.373758	2.658914	-0.04642	1.664634	1.640175	1.965195	-0.30219	0.843912	0.743205	0.509114
clr.V	2.791607	3.175464	2.474318	2.428518	2.11874	2.715774	4.124995	2.291708	1.907438	2.585892
clr.Zr	1.534991	1.236379	2.474318	1.199852	1.899686	2.451081	2.553779	3.211502	3.426418	2.046896
clr.As	0.075835	-0.01638	-0.33909	-0.45215	-0.20037	-0.74532	0.717283	-0.75809	-0.67386	0.100986
clr.Sb	-2.50671	-2.16482	-1.34239	-1.90124	-1.80981	-1.86641	-2.02062	-1.98707	-2.07454	-1.03845

Table C. 17: Results of the CLR transformation of the initial dataset (samples S2-I1 to S2-I10) (Continued)

Samples	S2-I1	S2-I2	S2-I3	S2-I4	S2-I5	S2-I6	S2-I7	S2-I8	S2-I9	S2-I10
clr.Se	-1.12042	-1.9135	-0.9677	-0.59191	-1.46151	-1.15079	-1.82825	-1.34588	-1.52116	-2.2016
clr.Cd	0.814445	0.137767	-1.25538	1.232642	0.661108	1.685689	1.448897	1.075971	1.246208	2.377227
clr.Cu	1.18217	1.593054	1.201352	1.354003	1.409064	0.659322	1.033953	1.021246	0.861469	1.892745
clr.Mo	0.226658	-0.70953	1.047202	1.279895	0.405761	0.053186	-0.91196	-1.0582	-1.70348	-0.40984
clr.Ni	3.232341	1.593054	3.10559	1.805988	1.696746	1.950306	3.277697	2.57939	2.573186	2.740043
clr.Pb	-1.38278	-0.19871	0.354055	-0.18644	-0.3827	-0.35228	0.697481	0.040416	-0.09404	0.100986
clr.Sc	-0.68963	-0.70953	-0.74456	-0.59191	-0.60584	-0.63996	-0.21881	-0.65273	-0.60487	-0.40984
clr.Zn	3.242193	3.327655	3.880415	3.225805	2.708346	3.258639	4.355901	3.733454	3.777159	3.929627
clr.Y	3.139009	2.855296	1.506734	2.616918	2.77004	2.56414	0.523127	1.859575	1.863232	1.48728
clr.La	2.155277	2.109862	1.079992	1.810523	2.123646	1.730283	0.717283	1.193096	1.197941	1.009244
clr.Ce	1.256278	1.187589	0.884683	0.966238	1.375162	1.29638	1.41043	1.187819	1.192432	0.942553
clr.Pr	0.231646	0.075892	-0.715	-0.04668	0.320402	-0.10737	-0.76354	-0.49858	-0.51869	-0.75704
clr.Nd	1.696834	1.531179	0.690527	1.42964	1.776019	1.338739	0.59212	0.922806	0.876737	0.596901
clr.Sm	0.101095	-0.12174	-1.04566	-0.15688	0.228156	-0.24792	-0.94242	-0.65273	-0.66674	-0.99563
clr.Eu	-1.2966	-1.47884	-2.40529	-1.55949	-1.17677	-1.62524	-2.38163	-2.12241	-2.08914	-2.41479
clr.Gd	0.445794	0.158969	-0.86109	0.106228	0.396629	0.019285	-1.17332	-0.52463	-0.57208	-0.93184
clr.Tb	-1.51631	-1.69481	-3.04714	-1.88289	-1.45564	-1.94929	-2.87807	-2.48531	-2.50199	-2.74633
clr.Dy	0.441769	0.259985	-0.88382	0.113663	0.450213	0.012364	-1.24046	-0.54537	-0.54975	-0.88788
clr.Ho	-0.95425	-1.11001	-2.45936	-1.33635	-1.01757	-1.4459	-2.80908	-2.07985	-2.06016	-2.32943
clr.Er	0.231646	0.060578	-1.30668	-0.16012	0.104656	-0.23006	-1.66698	-0.84712	-0.87493	-1.20097
clr.Tm	-1.72527	-1.88179	-3.40382	-2.20134	-1.89682	-2.21661	-3.72537	-2.77299	-2.84291	-3.13809
clr.Yb	0.163718	0.041885	-1.39848	-0.22726	-0.02502	-0.30349	-1.82825	-0.87172	-0.87493	-1.25381
clr.Lu	-1.62485	-1.70378	-3.40382	-2.06158	-1.56035	-2.12424	-3.57122	-2.77299	-2.72513	-2.89875
clr.åLREE	2.994046	2.896691	2.104413	2.689756	3.037716	2.694028	2.175898	2.324498	2.314523	2.075067
clr.åHREE	1.918229	1.731627	0.496711	1.556944	1.856949	1.474284	0.189983	0.904712	0.888785	0.554479
clr.åREE	3.28771	3.167901	2.285576	2.969139	3.305683	2.952775	2.302911	2.540485	2.530626	2.273462

Table C. 18: Results of the CLR transformation of the initial dataset (samples S2-I11 to S2-I20)

Samples	S2-I11	S2-I12	S2-I13	S2-I14	S2-I15	S2-I16	S2-I17	S2-I18	S2-I19	S2-I20
clr.SiO2	1.296833	1.145653	0.072548	0.235312	0.027733	-0.66364	2.938682	1.927724	1.783536	1.789769
clr.Al2O3	-1.17037	-1.01191	-1.53689	-2.0838	-1.76403	-2.64464	-0.65863	-0.03705	0.270948	0.348816
clr.Fe2O3	-2.18329	-1.96642	-2.42578	-3.02115	-2.45717	-2.93233	-1.57492	-0.90456	-0.61224	-0.55908
clr.CaO	1.656628	1.706094	2.496367	1.522601	2.738557	2.205431	1.07597	2.842144	1.582394	0.65597
clr.MgO	0.104694	0.844392	-1.02606	-1.7355	1.937276	-2.4215	0.402241	2.527895	1.261347	0.337516
clr.Na2O	-3.47296	-3.74527	-3.6388	-3.53909	-2.968	-2.27308	-3.549	-3.94908	-3.90344	-4.36296
clr.K2O	-2.80648	-2.67264	-3.6388	-3.7358	-4.06661	-4.94723	-2.32523	-3.10178	-2.45652	-2.59226
clr.TiO2	-3.37288	-3.21918	-4.24494	-4.38639	-4.35429	-5.23491	-3.36668	-2.96825	-2.61559	-2.53038
clr.P2O5	0.161853	-0.39672	-0.47602	0.016259	0.633869	1.48249	-1.0641	-2.05196	-2.294	-2.34806
clr.LOI	1.445868	1.821307	2.232033	1.066081	2.865837	1.10486	1.39264	3.29515	2.14275	1.38164
clr.Ba	2.601781	2.428512	2.274699	2.233686	2.451798	3.007845	2.861172	2.390694	2.285851	2.377851
clr.Cr	3.956093	3.964828	4.508642	3.332298	3.757435	3.407445	3.946539	2.958678	3.497487	3.298563
clr.Cs	-1.99856	-1.89138	-2.45318	-3.18241	-2.968	-4.03094	-1.48214	-1.64649	-0.97225	-1.0953
clr.Ga	-0.61831	-0.5419	-0.68959	-1.57298	-1.20441	-1.03521	-0.50448	0.250627	0.623769	0.56971
clr.Hf	-1.02377	-0.74954	-2.12468	-1.43321	-3.15032	-1.9515	-0.98405	-1.64649	-0.68456	-1.0953
clr.Nb	-0.33062	-0.13644	-1.09506	-1.39065	-1.54088	-2.4215	-0.45796	-0.18016	-3.6803	0.326088
clr.Rb	0.902466	1.016242	0.197711	-0.18668	-0.15459	-1.03521	1.263182	0.943775	1.637824	1.405357
clr.Sr	4.35319	3.940394	5.451933	4.22763	4.914316	5.294514	3.561694	4.011828	3.257018	2.863245
clr.Th	-1.18629	-1.07378	-1.65467	-1.08747	-1.40985	-1.15737	-0.86798	-0.54788	-0.06938	-0.04049
clr.U	0.991132	0.497712	0.97991	1.571176	2.182398	2.621924	0.715085	-0.41296	-0.78992	-0.65245
clr.V	2.50526	2.499639	2.987312	3.372231	3.684864	2.835995	3.750795	4.401667	3.815246	3.808212
clr.Zr	2.762483	2.958386	1.787347	2.368605	1.349489	2.032846	2.760916	2.196538	1.261347	2.544791
clr.As	-0.97932	-1.0632	0.027086	-0.65669	-0.75243	-0.11892	-0.08327	1.166918	0.785612	0.242206
clr.Sb	-2.77981	-2.28487	-0.96153	-2.17081	-2.05171	-1.63304	-1.79114	-2.05196	-1.48307	-2.41705
clr.Se	-1.71692	-1.60974	-0.55606	-3.4701	-0.58537	-1.72835	-2.45039	-1.35881	-2.07086	1.603183

Table C. 19: Results of the CLR transformation of the initial dataset (samples S2-I11 to S2-I20) (Continued)

Samples	S2-I11	S2-I12	S2-I13	S2-I14	S2-I15	S2-I16	S2-I17	S2-I18	S2-I19	S2-I20
clr.Cd	1.116295	0.812643	2.523553	1.667661	2.064615	2.332089	0.833024	1.850015	0.057374	0.190913
clr.Cu	1.771291	1.662243	2.329671	1.135074	1.098175	1.672844	1.461633	1.860065	0.873581	0.727714
clr.Mo	-1.81223	-1.01191	0.177909	-1.57298	-0.84774	0.217556	-0.55327	0.250627	0.117438	-1.83724
clr.Ni	2.594491	2.827546	3.268951	2.675519	2.815826	2.183669	3.110291	2.958678	2.998046	3.153197
clr.Pb	-0.20279	-0.09562	-0.04523	-0.65669	-0.15459	-0.11892	0.363021	1.166918	0.211524	0.359989
clr.Sc	-0.42593	-0.31876	-0.33292	-0.18668	-0.84774	0.063406	-0.55327	-0.44252	0.25153	0.359989
clr.Zn	3.891554	3.975119	4.199683	3.647379	4.585987	3.941527	4.290917	4.05729	4.352389	4.108185
clr.Y	1.861538	1.644851	1.83804	2.585907	2.086121	2.408412	1.318532	0.199334	0.637192	0.56066
clr.La	1.208197	1.042218	1.03657	1.877011	1.153745	1.589462	0.807706	0.576328	1.064636	0.990078
clr.Ce	1.110933	1.092228	0.499992	1.280616	0.875031	1.311395	1.104958	1.245729	1.775025	1.746284
clr.Pr	-0.55661	-0.65773	-0.76884	0.085252	-0.70797	-0.28143	-0.78899	-0.88881	-0.38446	-0.43359
clr.Nd	0.855	0.771485	0.684726	1.538314	0.7415	1.167558	0.609881	0.36841	0.973664	0.903605
clr.Sm	-0.73042	-0.82543	-0.91274	-0.00749	-0.81818	-0.39335	-0.95375	-1.21905	-0.58925	-0.70906
clr.Eu	-2.1689	-2.30289	-2.42578	-1.39483	-2.19481	-1.75572	-2.45039	-2.71555	-2.22168	-2.28352
clr.Gd	-0.63665	-0.74954	-0.70882	0.193465	-0.50415	-0.17232	-0.96124	-1.4101	-0.84708	-0.92495
clr.Tb	-2.63321	-2.64666	-2.6694	-1.65094	-2.61969	-2.04306	-2.96122	-3.43825	-1.11535	-2.9459
clr.Dy	-0.58552	-0.70442	-0.64763	0.259605	-0.51126	-0.10699	-1.0074	-1.58195	-2.98715	-1.11453
clr.Ho	-2.08667	-2.26717	-2.08546	-1.19454	-2.05171	-1.53773	-2.63271	-3.25593	-2.58168	-2.91605
clr.Er	-0.86444	-1.02196	-0.93683	-0.07559	-0.76156	-0.3751	-1.34073	-2.10325	-1.60085	-1.78845
clr.Tm	-2.80648	-3.01439	-2.85865	-2.04298	-2.68032	-2.27136	-3.36668	-4.05444	-3.6803	-3.73436
clr.Yb	-0.88006	-1.09529	-0.91871	-0.13314	-0.69073	-0.33211	-1.44487	-2.00317	-1.73439	-1.81743
clr.Lu	-2.75384	-2.87624	-2.7786	-1.92253	-2.68032	-2.04994	-3.14354	-3.47907	-3.6803	-3.80335
clr.åLREE	2.281449	2.190027	1.990124	2.8256	2.151989	2.584457	2.072123	2.002433	2.540294	2.487692
clr.åHREE	0.857081	0.713536	0.792013	1.673514	0.963827	1.359456	0.426934	-0.11466	0.350399	0.269335
clr.åREE	2.497228	2.395936	2.254847	3.100319	2.418024	2.842225	2.25009	2.114708	2.64639	2.591198

Table C. 20: Results of the CLR transformation of the initial dataset (samples S2-I21 to S2-I30)

Samples	S2-I21	S2-I22	S2-I23	S2-I24	S2-I25	S2-I26	S2-I27	S2-I28	S2-I29	S2-I30
clr.SiO2	1.972169	4.65572	2.2072	3.851028	0.320452	-0.19028	2.638491	4.917979	2.706223	1.460643
clr.Al2O3	0.490985	-0.98855	-2.55822	-0.82646	-1.35225	-2.21723	-2.43078	-0.49282	-0.6199	-1.00925
clr.Fe2O3	-0.34313	-1.39401	-2.83016	-1.40183	-2.44071	-2.79597	-2.24357	-1.59143	-1.67242	-1.65708
clr.CaO	0.139587	1.674039	1.567372	1.75989	2.139921	2.139864	1.79648	0.557006	2.412875	1.863303
clr.MgO	-0.14809	0.857278	-1.42836	1.342591	1.427964	-2.15839	-2.96141	-0.13614	2.002855	1.351228
clr.Na2O	-3.85467	-2.44384	-2.40407	-2.9059	-3.22917	-2.36384	-2.1285	-2.15104	-3.49158	-3.72395
clr.K2O	-2.1117	-2.78031	-3.99331	-2.50044	-3.16463	-4.00899	-4.01123	-1.83259	-2.23881	-2.59254
clr.TiO2	-2.31934	-3.6966	-5.19728	-3.76157	-4.14546	-5.02059	-5.264	-3.53734	-3.2039	-3.54162
clr.P2O5	-1.6262	-0.14125	1.020654	-1.0341	0.39961	1.338115	1.326305	-1.4579	-1.22289	-0.61936
clr.LOI	1.126974	2.007184	0.388717	2.258881	2.305541	1.031496	0.439786	1.473296	2.787569	2.133988
clr.Ba	2.493466	4.350591	2.663417	3.923889	1.854307	2.380333	4.355137	7.422201	2.664695	2.335178
clr.Cr	3.753346	3.616622	3.009756	3.531847	3.049981	2.985774	2.896522	3.775881	3.416178	3.446174
clr.Cs	-0.75394	-2.08716	-3.20485	-1.58415	-2.22364	-3.18801	-3.65456	-1.59143	-1.43319	-1.96609
clr.Ga	0.852279	-0.47772	-1.79608	-0.38018	-0.99557	-1.53935	-1.35197	-0.31846	-0.34169	-0.58845
clr.Hf	-0.78995	-2.08716	-2.60701	-1.58415	-1.33205	-2.02486	-2.55595	-1.23475	-0.67817	-0.77951
clr.Nb	-4.19115	-0.98855	-2.38387	-1.98961	-1.43741	-2.15839	-2.96141	-0.54161	-0.49585	-0.83357
clr.Rb	1.895629	0.803211	-0.4968	1.229262	0.570062	-0.29764	-0.65883	1.367936	1.388696	1.003442
clr.Sr	3.024094	4.033137	4.856061	3.714169	4.152751	4.958697	5.162739	4.147445	3.787741	3.690627
clr.Th	0.203303	-1.44531	-1.39062	-1.22415	-1.13319	-1.13903	-1.28431	-0.82929	-0.71899	-0.93278
clr.U	-0.27912	1.490787	2.449231	0.741502	1.858431	2.989932	3.090678	0.962471	0.542663	1.096336
clr.V	3.70615	4.326298	3.892772	4.320304	2.656939	3.018564	3.468308	3.670521	3.49622	3.461441
clr.Zr	-0.78995	2.294866	1.676572	2.327874	2.474617	1.959483	1.739069	2.454126	3.150474	3.032987
clr.As	0.806066	0.215424	-0.46695	1.229262	-0.74426	0.449574	0.257465	0.15154	-0.78353	-0.32275
clr.Sb	-1.01309	-0.70087	-1.79608	-1.98961	-2.67912	-2.36384	-1.35197	-1.66554	-2.06446	-0.92059
clr.Se	-4.19115	0.310735	0.117565	0.495293	-1.43741	-0.70311	-0.82134	-0.82929	-1.37131	-1.6445
clr.Cd	-0.58023	1.697029	1.547954	1.411584	1.038198	1.670249	0.739891	0.469994	0.98954	0.891175
clr.Cu	0.877758	2.007184	1.605113	1.922409	1.501168	1.142721	1.643759	2.454126	1.624418	1.574372

Table C. 21: Results of the CLR transformation of the initial dataset (samples S2-I21 to S2-I30) (Continued)

Samples	S2-I21	S2-I22	S2-I23	S2-I24	S2-I25	S2-I26	S2-I27	S2-I28	S2-I29	S2-I30
clr.Mo	-0.77015	0.908572	-1.69072	0.312971	-1.33205	-1.80172	-0.65883	1.067831	-0.67817	-1.42136
clr.Ni	3.108651	3.306467	1.775012	3.021021	2.305541	2.090103	2.049224	3.082734	2.57993	2.428787
clr.Pb	0.472293	0.908572	0.101035	1.229262	-0.6389	-0.00996	0.257465	1.067831	0.420445	0.188077
clr.Sc	0.490985	0.215424	-0.30443	-0.38018	-0.23343	-0.70311	-0.65883	0.374684	-0.67817	-0.72821
clr.Zn	4.537927	4.572133	4.40735	4.224994	3.779942	4.569894	4.169488	3.985602	3.678542	3.690627
clr.Y	0.99624	1.090893	2.553476	0.649444	2.03525	2.438169	2.203375	0.711156	0.931271	1.452204
clr.La	1.334307	0.397746	1.55965	0.337664	1.185651	1.558658	1.48124	0.374684	0.656834	0.808654
clr.Ce	2.054961	0.551897	1.142489	0.687977	1.185651	1.396956	1.272695	0.844688	1.193635	1.143589
clr.Pr	-0.0968	-1.34522	-0.40425	-1.29647	-0.6191	-0.21453	-0.37741	-1.28605	-0.81743	-0.75867
clr.Nd	1.233804	0.110064	1.069286	0.083558	0.854006	1.223574	1.090374	0.15154	0.545608	0.632763
clr.Sm	-0.42995	-1.6817	-0.49378	-1.51961	-0.67453	-0.32011	-0.49756	-0.97239	-1.04923	-0.83914
clr.Eu	-1.92938	-2.78031	-1.87705	-3.02525	-2.06601	-1.68839	-1.8512	-3.53734	-2.57529	-2.47118
clr.Gd	-0.66479	-1.75069	-0.19558	-1.55136	-0.40383	-0.08792	-0.33674	-1.74558	-1.18899	-0.80617
clr.Tb	-0.75716	-4.38975	-2.13701	-3.37591	-2.29963	-2.05018	-2.17295	-4.23049	-3.33743	-2.80765
clr.Dy	-2.58171	-1.61716	-0.13469	-1.55136	-0.41176	-0.09879	-0.25003	-1.83259	-1.25799	-0.80078
clr.Ho	-2.39939	-4.38975	-1.53372	-3.03944	-1.81008	-1.58661	-1.75245	-4.23049	-2.98075	-2.36297
clr.Er	-1.30077	-1.90484	-0.2773	-1.8943	-0.62895	-0.38344	-0.64888	-2.03326	-1.69982	-1.19025
clr.Tm	-3.498	-4.38975	-2.28856	-3.79142	-2.56992	-2.39955	-2.56937	-4.23049	-3.6739	-3.13616
clr.Yb	-1.41856	-1.61716	-0.32463	-1.84985	-0.66936	-0.44846	-0.63902	-2.03326	-1.61978	-1.20625
clr.Lu	-3.09253	-4.38975	-2.01923	-3.43778	-2.3537	-2.21723	-2.37362	-4.23049	-3.49158	-3.0308
clr.åLREE	2.809188	1.566092	2.491784	1.60358	2.296819	2.61941	2.504537	1.722757	2.047068	2.099987
clr.åHREE	0.633962	-0.20009	1.360443	-0.08676	1.077599	1.350591	1.149709	-0.46929	0.171984	0.604153
clr.åREE	2.916771	1.719502	2.77173	1.771586	2.555685	2.867366	2.734003	1.833299	2.189732	2.30192

8. CLR Correlation matrix (Pearson (n))

See Excel file.

9. Kaiser-Meyer-Olkin measure of sampling adequacy

Table C. 22: Kaiser-Meyer-Olkin measure of sampling adequacy

clr.SiO2	0.547
clr.Al2O3	0.617
clr.Fe2O3	0.667
clr.CaO	0.452
clr.MgO	0.795
clr.Na2O	0.523
clr.K2O	0.601
clr.TiO2	0.738
clr.P2O5	0.657
clr.LOI	0.382
clr.Ba	0.581
clr.Cr	0.182
clr.Cs	0.865
clr.Ga	0.884
clr.Hf	0.414
clr.Nb	0.474
clr.Rb	0.719
clr.Sr	0.740
clr.Th	0.615
clr.U	0.817
clr.V	0.687
clr.Zr	0.252

Table C. 23: 9. Kaiser-Meyer-Olkin measure of sampling adequacy (Continued)

clr.As	0.323
clr.Sb	0.298
clr.Se	0.385
clr.Cd	0.331
clr.Cu	0.562
clr.Mo	0.217
clr.Ni	0.491
clr.Pb	0.565
clr.Sc	0.569
clr.Zn	0.561
clr.Y	0.630
clr.La	0.848
clr.Ce	0.354
clr.Pr	0.733
clr.Nd	0.569
clr.Sm	0.620
clr.Eu	0.632
clr.Gd	0.681
clr.Tb	0.535
clr.Dy	0.828
clr.Ho	0.648
clr.Er	0.734
clr.Tm	0.615
clr.Yb	0.718
clr.Lu	0.759
KMO	**0.619**

10. Varimax rotation (Kaiser normalization)

Table C. 24: Varimax rotation (Kaiser normalization)

	D1	D2	F3	F4	F5	F6	F7	F8	F9	F10	F11	F12	F13	F14	F15
Variability (%)	37.098	31.059	8.361	4.909	3.637	3.615	2.009	1.628	1.343	1.127	1.027	0.820	0.777	0.612	0.434
% cumulative	37.098	68.157	76.518	81.427	85.064	88.679	90.688	92.316	93.659	94.786	95.813	96.634	97.410	98.022	98.456

Table C. 25: 10. Varimax rotation (Kaiser normalization) (Continued)

	F16	F17	F18	F19	F20	F21	F22	F23	F24	F25	F26	F27	F28	F29
Variability (%)	0.330	0.260	0.257	0.184	0.148	0.106	0.097	0.074	0.030	0.020	0.017	0.011	0.006	0.003
% cumulative	98.786	99.047	99.304	99.488	99.636	99.742	99.838	99.913	99.943	99.963	99.980	99.991	99.997	100.000

11. Factor loadings after Varimax rotation

Table C. 26: Factor loadings after Varimax rotation

	D1	D2
clr.SiO2	-0.404	-0.668
clr.Al2O3	-0.945	-0.287
clr.Fe2O3	-0.895	-0.341
clr.CaO	0.476	-0.142
clr.MgO	-0.634	-0.486
clr.Na2O	0.702	-0.165
clr.K2O	-0.795	-0.412
clr.TiO2	-0.922	-0.247
clr.P2O5	0.874	0.238
clr.LOI	-0.315	-0.437
clr.Ba	0.146	-0.525
clr.Cr	-0.138	-0.285
clr.Cs	-0.907	-0.326
clr.Ga	-0.911	-0.224
clr.Hf	-0.719	0.003
clr.Nb	-0.163	-0.510
clr.Rb	-0.889	-0.338
clr.Sr	0.913	0.021
clr.Th	-0.933	0.136
clr.U	0.897	0.141
clr.V	-0.379	-0.412
clr.Zr	0.049	-0.407
clr.As	-0.401	-0.159
clr.Sb	-0.138	-0.296
clr.Se	0.249	-0.475

Table C. 27: Factor loadings after Varimax rotation (Continued)

	D1	D2
clr.Cd	0.474	-0.304
clr.Cu	0.259	-0.690
clr.Mo	0.121	-0.336
clr.Ni	-0.609	-0.408
clr.Pb	-0.498	-0.685
clr.Sc	-0.559	-0.066
clr.Zn	-0.387	-0.405
clr.Y	0.823	0.526
clr.La	0.541	0.822
clr.Ce	-0.498	0.754
clr.Pr	0.296	0.936
clr.Nd	0.379	0.909
clr.Sm	0.384	0.877
clr.Eu	0.455	0.862
clr.Gd	0.576	0.812
clr.Tb	0.089	0.931
clr.Dy	0.839	0.355
clr.Ho	0.564	0.777
clr.Er	0.726	0.672
clr.Tm	0.720	0.670
clr.Yb	0.780	0.608
clr.Lu	0.697	0.673
clr.åLREE	0.234	0.951
clr.åHREE	0.657	0.746
clr.åREE	0.346	0.927

12. Factor scores after Varimax rotation

Table C. 28: Factor scores after Varimax rotation

	D1	D2
S2-I1	1.169	1.335
S2-I2	1.202	0.948
S2-I3	-0.501	-0.381
S2-I4	1.204	0.478
S2-I5	0.758	1.552
S2-I6	0.956	0.692
S2-I7	-1.245	-0.193
S2-I8	-0.035	0.170
S2-I9	-0.106	0.224
S2-I10	-0.129	-0.532
S2-I11	-0.025	0.024
S2-I12	-0.311	-0.098
S2-I13	0.780	-0.990
S2-I14	0.296	1.375
S2-I15	0.864	-0.535
S2-I16	1.184	0.309
S2-I17	-0.648	-0.400
S2-I18	-0.884	-1.011
S2-I19	-2.118	0.991
S2-I20	-1.856	0.535
S2-I21	-2.565	1.884
S2-I22	0.217	-2.405
S2-I23	1.093	0.132
S2-I24	-0.183	-1.818
S2-I25	0.183	0.270
S2-I26	0.850	0.555

Table C. 29: Factor scores after Varimax rotation (Continued)

	D1	D2
S2-I27	1.086	-0.019
S2-I28	-0.307	-2.074
S2-I29	-0.589	-0.719
S2-I30	-0.343	-0.301